

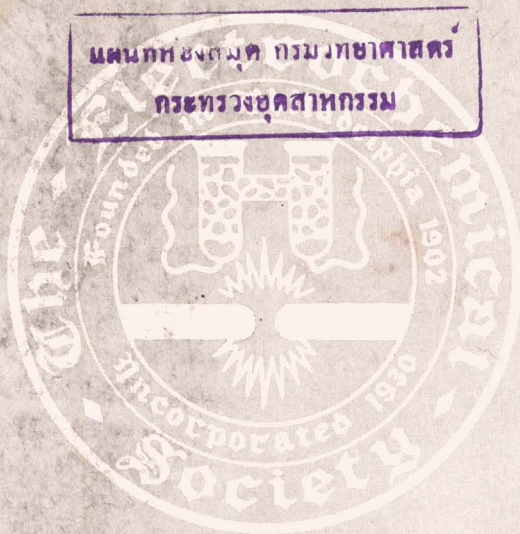
JOURNAL OF THE

Electrochemical Society

Vol. 106, No. 2

February 1959

มหาวิทยาลัยเทคโนโลยีพระจอมเกล้าธนบุรี
คณะวิทยาศาสตร์และเทคโนโลยี
ภาควิชาเคมี



NOW YOU WILL KNOW THEY ARE FROM GREAT LAKES CARBON



This New Emblem is your assurance of carbon and graphite products—production engineered to the highest standards of quality.

The emblem is being introduced in all of our packaging—in electrode end protectors, nipple cartons, palletized anodes, palletized carbon brick, and drums of carbonaceous materials.

Watch for this emblem—it identifies products made to give you matchless performance.



GREAT LAKES CARBON CORPORATION

18 EAST 48TH STREET, NEW YORK 17, N.Y. OFFICES IN PRINCIPAL CITIES

GRAPHITE ELECTRODES • ANODES • AND SPECIALTIES

EDITORIAL STAFF

H. H. Uhlig, Chairman, Publication Committee
Cecil V. King, Editor
Norman Hackerman, Technical Editor
Ruth G. Sterns, Managing Editor
U. B. Thomas, News Editor
H. W. Salzberg, Book Review Editor
Natalie Michalski, Assistant Editor

DIVISIONAL EDITORS

W. C. Vosburgh, Battery
Milton Stern, Corrosion, I
R. T. Foley, Corrosion, II
T. D. Collinson, Electric Insulation
Abner Brenner, Electrodeposition
H. C. Froelich, Electronics
Ernest Paskell, Electronics—Semiconductors
Sherlock Swann, Jr., Electro-Organic, I
Stanley Wawzonek, Electro-Organic, II
John M. Blocher, Jr., Electrothermics and Metallurgy, I
A. U. Seybolt, Electrothermics and Metallurgy, II
N. J. Johnson, Industrial Electrolytic
C. W. Tobias, Theoretical Electrochemistry, I
A. J. deBethune, Theoretical Electrochemistry, II

REGIONAL EDITORS

Howard T. Francis, Chicago
Joseph Schulein, Pacific Northwest
J. C. Schumacher, Los Angeles
G. W. Heise, Cleveland
G. H. Fetterley, Niagara Falls
Oliver Osborn, Houston
Earl A. Gulbransen, Pittsburgh
A. C. Holm, Canada
J. W. Cuthbertson, Great Britain
T. L. Rama Char, India

ADVERTISING OFFICE

ECS

1860 Broadway, New York 23, N. Y.

ECS OFFICERS

Sherlock Swann, Jr., President
University of Illinois, Urbana, Ill.
W. C. Gardiner, Vice-President
Olin Mathieson Chemical Corp., Niagara Falls, N. Y.
R. A. Schaefer, Vice-President
Cleveland Graphite Bronze Div., Clevite Corp., Cleveland, Ohio
Henry B. Linford, Vice-President
Columbia University, New York, N. Y.
Lyle I. Gilbertson, Treasurer
Air Reduction Co., Murray Hill, N. J.
I. E. Campbell, Secretary
National Steel Corp., Weirton, W. Va.
Robert K. Shannon, Executive Secretary
National Headquarters, The ECS, 1860 Broadway, New York 23, N. Y.

Journal of the Electrochemical Society

FEBRUARY 1959

VOL. 106 • NO. 2

CONTENTS

Editorial

Wisdom 24C

Technical Papers

Zinc-Mercuric Dioxysulfate Dry Cell. S. Ruben 77
The Potential of the Manganese Dioxide Electrode and the Surface Composition of the Oxide. A. Kozawa 79
Anodic Dissolution of Magnesium Alloys in Aqueous Salt Solutions. R. Glicksman 83
Electrolytic Transition of Ag₂O to AgO in Alkaline Solutions. T. P. Dirkse and G. J. Werkema 88
Strain Electrometry and Corrosion, IV. Film Properties and Strain Potential. J. C. Giddings, A. G. Funk, C. J. Christensen, and H. Eyring 91
Oriented Dioxide Films on Uranium. J. T. Waber, J. A. O'Rourke, and R. Kleinberg 96
Kinetics of the Uranium-Steam Reaction. B. E. Hopkinson 102
Tarnishing Reactions of Silver in Iodine Atmospheres. D. M. Smyth and M. Cutler 107
Potential Studies on Passivity to Corrosion Induced by Pretreatment Processes for Metals, I. Aluminum. K. S. Rajagopalan 113
Mechanism of Electrodeposition of Nickel from Liquid Ammonia Solutions of Spin-Free Nickel(II) Complexes. G. W. Watt and D. A. Hazlehurst 117
Electrodeposition of Molybdenum. T. T. Campbell 119
Microfurnace for Thermal Microscopy and Studies at High Temperatures. W. A. Lambertson and G. Lewis 124
Zirconium Coating of Uranium by the Iodide Process. W. L. Robb 126
Transport Numbers and Ionic Mobilities in the System Potassium Chloride-Lead Chloride. F. R. Duke and R. A. Fleming 130
Galvanic Behavior in Fused Electrolytes, I. The Nominal System Mg/LiCl-KCl/Ni. S. M. Selis, G. R. B. Elliott, and L. P. McGinnis 134
Enhanced Surface Reactions, III. Adsorption of Gases on Prepared Ruthenium Surfaces. M. J. D. Low and H. A. Taylor 138

Technical Notes

Electrolytic Preparation of Titanium from Fused Salts, II. Design of Laboratory Cells. M. B. Alpert, J. A. Hamilton, F. J. Schultz, and W. F. Sullivan 142
Process for Electrolytic Extraction of Titanium Metal from Titanium Carbide Anodes. G. Ervin, Jr., H. F. G. Ueltz, and M. E. Washburn 144
Comparison of the Life of Linings in Rotating and Stationary Phosphorus Furnaces. M. M. Striplin, Jr., J. M. Potts, and E. C. Marks 146

Technical Feature

Electrolysis of Organic Solvents with Reference to the Electrodeposition of Metals. A. Brenner 148

Brief Communication

Composition and Properties of Saturated Solutions of ZnO in KOH. T. P. Dirkse 154

Current Affairs 30C-38C

Index (Vol. 105, 1958) i-viii

Published monthly by The Electrochemical Society, Inc., from Manchester, N. H., Executive Offices, Editorial Office and Circulation Dept., and Advertising Office at 1860 Broadway, New York 23, N. Y., combining the JOURNAL and TRANSACTIONS OF THE ELECTROCHEMICAL SOCIETY. Statements and opinions given in articles and papers in the JOURNAL OF THE ELECTROCHEMICAL SOCIETY are those of the contributors, and The Electrochemical Society assumes no responsibility for them. Nondefectible subscription to members \$5.00; subscription to nonmembers \$18.00. Single copies \$1.25 to members, \$1.75 to nonmembers. Copyright 1959 by The Electrochemical Society, Inc. Entered as second-class matter at the Post Office at Manchester, N. H., under the act of August 24, 1912.

แผนกหนังสือพิมพ์ กองบรรณาธิการ
21C

กองบรรณาธิการหนังสือพิมพ์



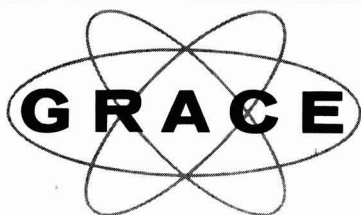
GRACE

Si

For

low boron

content . . .



SILICON

(ultra-high-purity)

"For want of a nail the battle was lost" becomes painfully true when translated to lack of purity in the semi-conductor material you choose for your transistors, diodes or other silicon devices.

The Pechiney process, used in the manufacture of Grace Silicon, is noted for a product with low

boron content as well as overall high purity.

May we suggest that whenever top quality silicon is desired—silicon combining both high purity and uniform quality—you get in touch with GRACE ELECTRONIC CHEMICALS, INC., at PLaza 2-7699, 101 N. Charles Street in Baltimore.

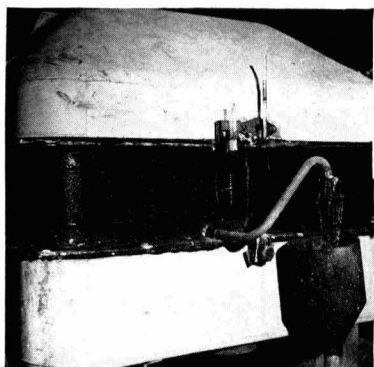
GRACE ELECTRONIC CHEMICALS, INC.



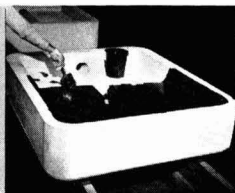
101 N. Charles St., Baltimore, Maryland
Subsidiary of W. R. GRACE & CO.

Cut Chlor-Alkali Production Costs

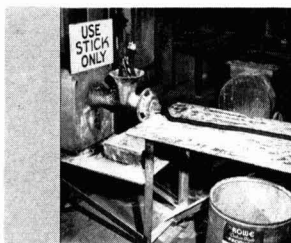
with
**ROWE'S
CELL ROOM
PRODUCTS**



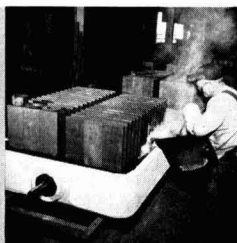
ELECTROLYTIC CELLS in a chlor-alkali plant maintain peak efficiency through the use of Rowe custom-made products. Rowe #35 Cell Putty is clearly visible between a cathode and cell top and cathode and cell bottom.



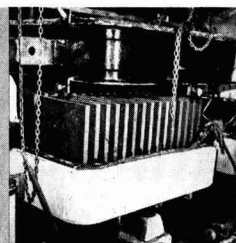
#738 ENAMEL being applied in a thin coat to bottom of concrete cell eliminating possible solvent entrapment, a common cause of heaving during the operation of the cell.



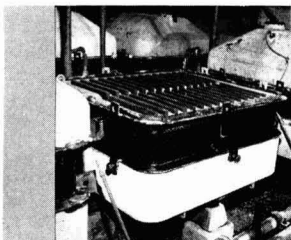
#35 CELL PUTTY is extruded from the extrusion machine in a cell make-up room in long, narrow rolls. Putty is now ready for direct application to the cell itself and the cathode.



#47 MASTIC being poured into cell to form a lower final mass thickness, allowing for an increase in circulation of brine in cell. Only one pour is necessary for consistent quality.



#35 CELL PUTTY now applied to bottom of cell block in even mass. This unusually pliable and adhesive material completely fills up cracks and crevices — keeps cells tight.



#35 CELL PUTTY now increases the adhesive quality as cathode is placed on cell. Putty around the top of a cathode assures greater strength, and gaskets may be eliminated.



#10 MINROX CEMENT now applied to dog legs attached to cell and a chlorine header line for complete gas leakage protection. Precautions like these mean longer cell life and higher production.



#5-E-84 MASTIC prevents caustic soda corrosion of cell pedestals and their surrounding concrete areas. Applied clear to pedestals, or with sand added, as a mastic in any thickness on floors or other concrete surfaces. Lasts six or more years.

ONE LOOK at Rowe's cell room products in action will tell you why electrolytic cell performance is increased while production costs are cut way down. Rowe's cell room products are specifically made for this job. Ask for case histories.

ROWE PRODUCTS INC.

COLLEGE AVENUE AND HYDE PARK BOULEVARD
NIAGARA FALLS, N. Y.—PHONE: BUTLER 5-9348

Specialists in protective coatings to the chemical process and allied industries since 1921.



Wisdom

FOR a mere \$15 per year, or \$250 for a lifetime, you may become a member of *The Wisdom Society for the Advancement of Knowledge, Learning and Research in Education*. Among the benefits you will receive the monthly magazine *Wisdom*, and with life membership you will also receive a hand-carved American walnut statuette, a copy of Rodin's *The Thinker*. The membership fee is tax-deductible, since *The Wisdom Society* is a nonprofit educational and literary organization. There is, however, no promise of a higher IQ or of a better position.

If you are a college student in good standing but without funds to continue, or an intelligent but impecunious high school student with yearnings for a college education, you can almost certainly borrow Federal funds up to \$1000 per year. The National Defense Education Act, signed by the President last September, provides \$46,500,000 for such loans in the current year, and a total of \$294,000,000 has been authorized through June 1962. It is reported that even U. S. Office of Education officials doubt that all these funds will be used. Many schools report that they have sufficient private endowment loan funds to cover all requests. Many students are reluctant to borrow in this way, prefer to search out fellowships and scholarships, and to supplement the money their families can provide with part-time and summer employment.

The National Science Foundation has for several years provided a program of graduate, postdoctoral, and science faculty fellowships. For the coming year, it is able to offer an additional 1000 "cooperative graduate fellowships" in science and engineering, available at some 115 institutions which award the doctorate. Applications were due in December, recipients will be announced in April. Fellows will receive a stipend of \$2200 and the institution will receive a sum to cover tuition and fees. Graduate students who act as teaching assistants during the academic year are eligible for summer fellowships, so that they may spend their time in study and research rather than in extra employment.

Not so many years ago a postdoctoral fellowship was both an honor and an opportunity, and accepting it entailed no great financial loss. In recent years the funds have been insufficient compared to the salaries offered by industry. The National Academy of Sciences and the National Research Council now offer postdoctoral research associateships for work in various Government Laboratories, with stipends of \$6000 to \$7500 per year. It is hoped that these will attract young scientists of unusual ability, and give them advanced training in basic research.

The roads to Wisdom and Knowledge are many and devious, but some road is open to almost everyone who is able and willing to follow it. We have mentioned only a portion of the new and greatly enlarged Federal Aid-to-Education program. It is hoped that this program, coupled with the augmented efforts of foundations, industry, and individuals, will provide a powerful incentive to our capable young men and women. We need a bigger pool of educated, trained manpower, in science and in other fields too. It will take several years to learn the effect of present efforts.

—CVK

NEROFIL

*A Family of
Specially-Processed
Carbon-Based Filteraids*

**BASIC CAUSTIC PRODUCERS
USE NEROFIL FOR:**

**PARTICULAR PROPERTIES
OF NEROFIL PRODUCTS**



1. Filtering caustic production particularly where high purity is required, such as for the rayon industry, etc.

2. Nerofil filtration of brine over and above ordinary clarification methods more than justifies itself through increased efficiency of the DeNora and other type mercury cell operations. Nerofil's low vanadium content makes it the preferred filteraid for this new approach to brine preparation.

Fast Flowrates, Excellent Clarity—On these points, Nerofil filteraids are comparable to many grades of diatomite filteraids.

Lower Cake Density—Because of its lower cake density and high porosity, Nerofil affords filteraid savings of up to 20%.

Full Range of Grades—Six grades of Nerofil filteraids are now available to cover a wide range of process liquors.

Physical and Chemical Stability—Tests show no silicon solubility in 30 minutes in 50% sodium hydroxide at 125°F.

Compatibility with Process Liquors—Being practically pure carbon, Nerofil is unaffected by either acids or alkalis, and is readily wettable to either aqueous or non-aqueous solutions.

Combustible Filtercake—A Nerofil filtercake has a fuel value of 13,000 BTU per pound. Disposal thus presents no problem and metal values recovery in metallurgical filtration is made easy.

Uniform Quality—Exact quality control maintains particle size range and distribution constant in every grade.

NERO-PRODUCTS DEPT., Great Lakes Carbon Corp.
333 No. Michigan Ave. Chicago 1, Ill.

Please send me further information on Nerofil

NAME _____
POSITION _____
COMPANY _____
ADDRESS _____
CITY _____ ZONE _____ STATE _____



NOW!

... Greatly Reduced Clogging
of Diaphragms

... Lower
Cell Maintenance Costs

... Longer Anode Life

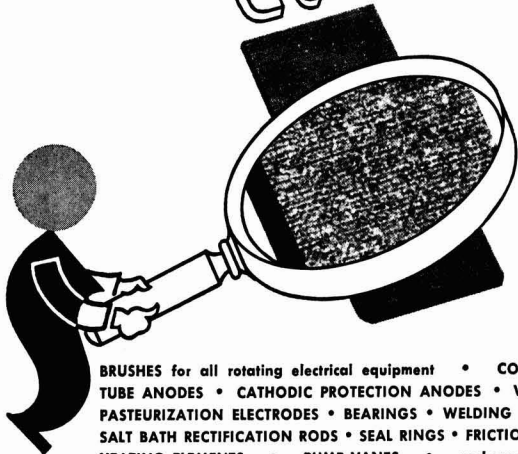
Costly, troublesome clogging of diaphragms due to the oil impregnant in conventional anodes, is materially lessened by the new Stackpole "GraphAnodes." Cell maintenance costs are reduced accordingly.

Better results are achieved because Stackpole *GraphAnodes* present a uniform, low-porosity surface to the electrolyte. The graphite is consumed slowly and evenly. It does not slough off to clog the diaphragm or contaminate the cell.

Let Stackpole arrange for a convincing demonstration of these new anodes on your own equipment. You be the judge—and, by way of convincing proof we suggest that you pay particular attention to the reduced frequency of diaphragm renewals.

STACKPOLE CARBON COMPANY
St. Marys, Pa.

STACKPOLE GraphAnodes



MAGNIFIED, UNRETOUCHED PHOTO ... shows uniform structure of Stackpole GraphAnodes. The low-porosity surface assures that electrolyte will act on the surface, not below to cause premature anode deterioration and cell contamination by droppings of unconsumed graphite particles.

BRUSHES for all rotating electrical equipment • CONTACTS (carbon-graphite and metal powder types)
TUBE ANODES • CATHODIC PROTECTION ANODES • VOLTAGE REGULATOR DISCS • WATER HEATER and
PASTEURIZATION ELECTRODES • BEARINGS • WELDING CARBONS • MOLDS AND DIES • POROUS CARBON
SALT BATH RECTIFICATION RODS • SEAL RINGS • FRICTION SEGMENTS • CLUTCH RINGS • ELECTRIC FURNACE
HEATING ELEMENTS • PUMP VANES • and many other carbon, graphite, and electronic components.

Zinc-Mercuric Dioxysulfate Dry Cell

Samuel Ruben

Ruben Laboratories, New Rochelle, New York

ABSTRACT

A dry cell is described which provides some of the desirable characteristics of the mercuric oxide alkaline cell while allowing the use of inexpensive conventional dry cell construction. The system is $\text{Zn}/\text{ZnSO}_4/\text{HgSO}_4 \cdot 2\text{HgO} + \text{C}$ and has an over-all reaction of $3\text{Zn} + \text{HgSO}_4 \cdot 2\text{HgO} \rightarrow \text{ZnSO}_4 + 2\text{ZnO} + 3\text{Hg}$. A relatively flat discharge characteristic is obtained within the proper limits of current density. The cell capacity is directly referable to the $\text{HgSO}_4 \cdot 2\text{HgO}$ or $3\text{HgO} \cdot \text{SO}_3$ content.

The alkaline mercuric oxide cell (1-3) possesses a number of characteristics, particularly for specialized use such as military applications where compactness, long shelf life, and storage at high ambient temperatures are necessary. It is used in commercial applications requiring cells of high capacity in small dimensions such as in hearing aids and other miniaturized electronic devices. One specific characteristic of this system, the maintenance of a flat discharge voltage and low impedance during discharge, has been of particular advantage in transistor applications.

An electrochemical system has been developed which is suitable for many applications and which combines some of the desirable discharge characteristics of the mercuric oxide cell with the low cost structure of the Leclanché zinc-carbon cell.

In the past, attempts have apparently been made (4) to use mercury compounds in the cathode of a nonalkaline dry cell, but these have failed because of inherent limitations of the materials used.

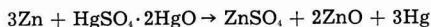
Zinc-Mercuric Dioxysulfate Cell

In the new cell, which might be termed the Mercury-Zinc Carbon Cell, the cathode reactant is a basic mercurial compound, such as mercuric dioxysulfate, and the electrolyte is a zinc sulfate solution in which the cathode is stable. The anode is zinc. The combination permits conventional zinc carbon cylindrical and flat cell constructions.

The electrochemical system in the presence of an aqueous solution of zinc sulfate can be expressed as



with an over-all reaction on the discharge as



In addition to the reactive components it is desirable to add a buffer agent to raise and maintain the pH of the electrolyte in the desired range to reduce the solubility of the mercuric dioxysulfate to a minimum. Various buffers have been used, such as the addition of calcium carbonate to the cathode mix or the addition of acetate to the electrolyte, to maintain the pH in the range of 5 to 6.

An inhibitor such as potassium dichromate is added to the electrolyte to inhibit continued amalga-

mation of anode by the slight amount of active cathode material in solution. The cathode is spaced from the anode by a paper cellophane laminate processed to provide barrier action and control of electrolyte transfer.

Construction of the Cell

The dry mix is composed of 8 parts mercuric dioxysulfate and 1 part acetylene black.

The electrolyte consists of a 20% solution of $\text{ZnSO}_4 \cdot 7\text{H}_2\text{O}$ to which 1% of $\text{K}_2\text{Cr}_2\text{O}_7$ is added. The electrolyte is added to the dry mix in the proportions of 1 part electrolyte to 2 parts dry mix.

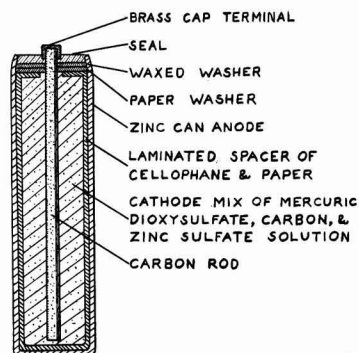


Fig. 1. Construction and components of the zinc-mercuric dioxysulfate cell.

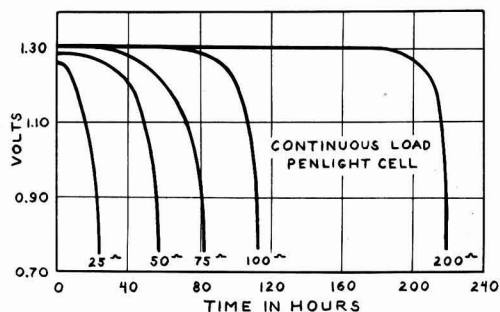


Fig. 2. Discharge characteristics of an AA-size cell discharged continuously at loads of 25, 50, 75, 100, and 200 ohm.

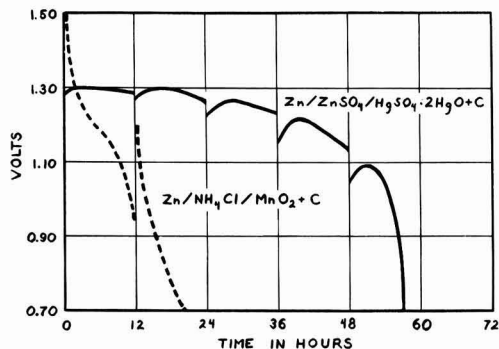


Fig. 3. Discharge characteristics of an AA-size cell discharged at 50 ohms 12 hr/day.

The zinc can is lined with a spacer which consists of a laminate of 0.004 in. paper and 0.0009 in. cellophane cemented together and coated with an aqueous glycerine gum arabic solution. The paper side of the laminate contacts the zinc can.

No free space is incorporated in the cell since there is negligible expansion of the bobbin during use. The top edge of the zinc can is rolled over and the space between the rolled edge and waxed washer on top of the bobbin filled with sealing compound. This gives a secure top seal and holds the bobbin in intimate contact with the lined can. The can thickness is about 0.004 in. greater than used in standard zinc-carbon cells to allow higher capacity without puncture at end of life.

Freshly made cells have an open-circuit voltage of 1.45 v. This stabilizes with initial use or on shelf to 1.36 v. The closed circuit potential has 1.3 v for loads within the rated current density.

Due to the high efficiency of the cathode mix, the capacity per unit volume exceeds that of the conventional zinc-carbon cell and is directly referable to the $\text{HgSO}_4 \cdot 2\text{HgO}$ content. The theoretical capacity of the $\text{HgSO}_4 \cdot 2\text{HgO}$ is approximately 0.22 amp-hr/g and the practical capacity, 0.21 amp-hr/g. Cells connected to a gas collecting apparatus and maintained at 45°C (113°F) have shown negligible gas evolution over several months tests.

Electrical Characteristics

Figure 1 illustrates the construction and components of the cell.

Figure 2 illustrates the discharge characteristic of AA (penlight) size cells discharged continuously through resistances of 25, 50, 75, 100, and 200 ohms.

Figure 3 illustrates the discharge characteristics of AA (penlight) size cells discharged intermittently 12 hr per day through a resistance of 50 ohms. Similar discharge of a commercial Leclanché cell of the same size is included for comparison.

Figure 4 illustrates the discharge characteristics of AA cells after 8 months' casual storage.

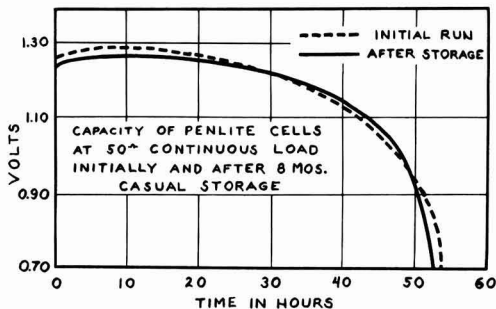


Fig. 4. Discharge characteristics of AA cells after 8 months' casual storage.

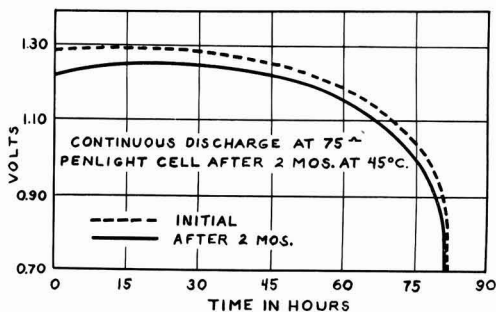


Fig. 5. Discharge characteristics of AA-size cells after 2 months' storage at 45°C (113°F).

Figure 5 illustrates the discharge characteristics of AA-size cells after two months' storage at 45°C (113°F).

The initial impedance of an AA-size cell at 1000 cycles is eight-tenths ohms and the impedance after continuous discharge is one ohm. On intermittent loads the impedance is higher at the start of each cycle and decreases to the normal value.

The weight of an AA-size cell constructed with a capacity of 1360 ma-hr is 20 g.

In summary, the new cell described has some desirable characteristics where a low current discharge is required over long periods of time with a flat voltage output. One such application has been for electronic clocks where D-size cells have been operating for a year with a total capacity of 8.0 amp-hr.

Manuscript received June 9, 1958. This paper was prepared for delivery before the Ottawa Meeting, Sept. 28-Oct. 2, 1958.

Any discussion of this paper will appear in a Discussion Section to be published in the December 1959 JOURNAL.

REFERENCES

1. S. Ruben, U. S. Pat. 2,814,664 (1957).
2. M. Friedman and C. E. McCawley, *Trans. Electrochem. Soc.*, **92**, 195 (1947).
3. S. Ruben, *ibid.*, **92**, 183 (1947).
4. A. Heil, German Pat. 212,468 (1908).

The Potential of the Manganese Dioxide Electrode and the Surface Composition of the Oxide

Akiya Kozawa¹

Department of Applied Chemistry, Faculty of Engineering, Nagoya University, Nagoya, Japan

ABSTRACT

When manganese dioxide is heated, the electrode potential decreases with the heating temperature. This potential decrease cannot be explained as a phase transformation nor as an ordinary decomposition of MnO_2 to Mn_2O_3 . A lower oxide film is formed on the surface of MnO_2 when it is heated at temperatures up to 450°C . The potential decrease on heating can be explained as the result of the lower oxide film formation, the potential of manganese dioxide depending on the surface oxidation state. The reaction of Mn^{++} in slightly alkaline electrolyte with MnO_2 gives a similar decrease in potential explainable as a surface effect.

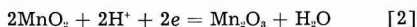
When a MnO_2 electrode is discharged the potential decreases gradually as reduction takes place to a lower oxide such as Mn_2O_3 (or MnOOH) or to Mn^{++} ion. To understand the potential decrease, we must know what factors determine the electrode potential.

The potential of the MnO_2 electrode in neutral or alkaline solution free from manganese(II) ion may be expressed by

$$E = E^\circ - 0.059 \text{ pH} - \frac{RT}{2F} \ln \frac{a_{\text{MnO}_2}}{(a_{\text{MnO}_2})^2} \quad [1]$$

$$E^\circ_{\text{red}} = 1.014$$

corresponding to the reaction



However, the potential seems to be dependent on the composition of the oxide surface rather than on the activities of two separate phases in neutral electrolyte (2). In this paper the effect on the potential of alteration of the surface composition of MnO_2 by heating at moderate temperatures and by the adsorption of Mn(II) ion is considered. Heating at $100^\circ\text{--}450^\circ\text{C}$ affects the potential, the discharge capacity, and the water content (2-5) although the decomposition temperature is higher than this, $480^\circ\text{--}580^\circ\text{C}$ for different kinds of manganese dioxide. The decrease in potential on heating has been ascribed to a change in crystal form (5).² The experiments to be described lead to a different explanation, namely, that the change in potential is the result of loss of oxygen at the surface.

¹ Present address: Department of Chemistry, Western Reserve University, Cleveland, Ohio.

² The idea that different phases of manganese dioxide may have different potentials can be tested by calculating the approximate free energy difference between $\gamma\text{-MnO}_2$ and $\beta\text{-MnO}_2$ using the decomposition temperature of MnO_2 to Mn_2O_3 at 1 atm pressure. The decomposition temperature is measured as 480°C for $\gamma\text{-MnO}_2$ and 580°C for $\beta\text{-MnO}_2$ from the author's thermal balance experiments, which can be seen to be the starting point of the decomposition in Fig. 1. From the Nerst approximation formula $\log P_{\text{O}_2} = \Delta H/4.573T + 1.75 \log T + 2.3$, ΔH is calculated for each MnO_2 , then the potential difference $\Delta E = (\Delta H_{\text{iso}} - \Delta H_{\text{iso}})/4F + T(\Delta S_{\text{iso}} - \Delta S_{\text{iso}})/4F$ is obtained, where the second term is neglected. The results shows $\gamma\text{-MnO}_2$ should be 44 mv higher than $\beta\text{-MnO}_2$ in potential. The 44 mv is too small to explain the potential decrease (about 250 mv) on heating.

Experimental

Preparation of oxides.—An electrolytic oxide, presumably $\gamma\text{-MnO}_2$, was prepared by electrodeposition from an acid bath at $97^\circ\text{--}98^\circ\text{C}$ with a current density of 1.74 amp/dm^2 . Initially the bath was $0.85 \text{ mole/l MnSO}_4$ and $0.03 \text{ mole/l H}_2\text{SO}_4$, and at the end $0.48 \text{ mole/l MnSO}_4$ and $0.51 \text{ mole/l H}_2\text{SO}_4$.

Figure 1 gives the result of a differential thermal analysis of this MnO_2 along with one of natural pyrolusite. The electrolytic oxide was ground to pass through a 100-mesh sieve. The powdered sample was washed with hot $2N \text{ H}_2\text{SO}_4$, several times, then several times with water, and finally with very dilute ammonia solution. It was dried at 80°C for 10 hr. Samples of this oxide, of the oxide before washing, and of a natural pyrolusite were heated at various temperatures from 160° to 438°C for 1 hr in an electric furnace in air.

Some of the $\gamma\text{-MnO}_2$ was heated to constant weight at 800°C . The resulting oxide was shown by analysis to be Mn_2O_3 .

Potential of heated MnO_2 .—The potentials of the heated oxides were measured as follows. A 1.00-g sample of each oxide was placed in 50 ml of $2M \text{ NH}_4\text{Cl}$ and NH_3 , pH 8.35, in an Erlenmeyer flask, shaken occasionally for 3 hr, and then digested overnight at room temperature. The mixture was cen-

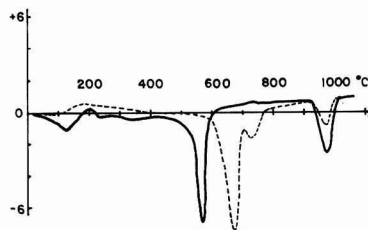


Fig. 1. Differential thermal analysis of manganese dioxides. The temperature was raised at a rate of 2°C/min . — electrolytic MnO_2 ($\gamma\text{-MnO}_2$), - - - pyrolusite ($\beta\text{-MnO}_2$).

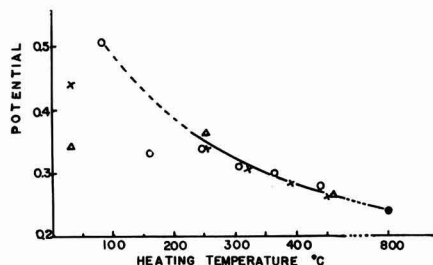


Fig. 2. Potentials, corrected to pH8, vs. saturated calomel electrode of heated manganese dioxides. O, electrolytic MnO_2 washed with H_2SO_4 ; X, electrolytic MnO_2 not washed; Δ , natural pyrolusite ($\beta\text{-MnO}_2$); \bullet , Mn_2O_3 made from the electrolytic MnO_2 by heating at 800°C .

trifuged in a 15-ml centrifuge tube with a narrow bottom. A platinum foil electrode was inserted in the manganese dioxide layer at the bottom of the centrifuge tube. The potential then was measured against a saturated calomel electrode and the pH of the solution was measured by a glass electrode pH meter.

Results are shown in Fig. 2 for all potentials which were corrected to pH 8.0 assuming a change of -60 mv per pH unit. It is clear that the potential decreases with heating temperature between 250° and 450°C regardless of the kind of manganese dioxide and of acid washing. Although three different unheated samples gave very different potentials, they came to agreement on heating above 250°C . The potential after heating to 450°C was fairly close to that of Mn_2O_3 , although the composition was not much different from that of the original unheated sample, as shown in Fig. 3.

Analysis of the heated MnO_2 was carried out by the FeSO_4 method for available oxygen and by the NaBiO_3 method for total Mn. The calculated x values in MnO_x , as shown in Fig. 3, decrease with heating temperature from 1.977 to 1.946.

According to Fig. 1 no extensive decomposition takes place below 450°C , and the small change in x -value (in MnO_x) confirms this. Heating at 250°C did not give a continuous change; after 1 hr the x -value (in MnO_x) was 1.965, after 4 hr, 1.963, and after 6 hr, 1.964. Previously (2) heating at 450°C gave a similar result. Maxwell and Thirsk observed

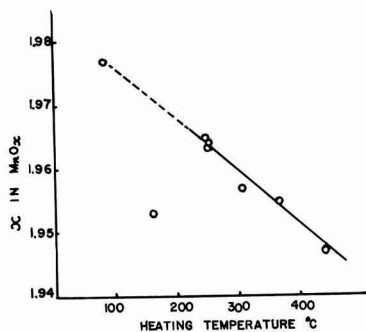


Fig. 3. Results of analysis of electrolytic MnO_2 heated at various temperatures; values of x in MnO_x . Three points around 250°C are for different heating times, 1, 4, and 6 hr.

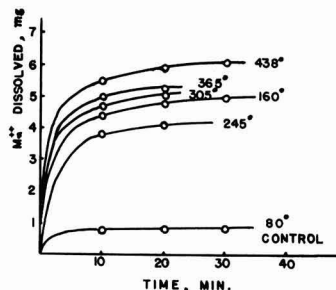


Fig. 4. Manganese (II) ion dissolution from heated manganese dioxide (0.5 g) by 1N H_2SO_4 stirring at room temperature. After 10 min stirring, it was allowed to stand for 5 min which was not counted in the abscissa of this figure. Heating temperatures of MnO_2 are indicated in the figure.

a similar decrease in x value of MnO_2 heated under O_2 atmosphere (6).

The sample of $\gamma\text{-MnO}_2$ heated at 160° differed in x value, potential, and also in dissolution of Mn^{2+} (as shown in Fig. 4) from what would be expected on the basis of the data for the other heated oxides. A similar deviation was observed previously (2). That the deviation is real and not the result of an error is suggested.

Changes on heating can be shown to be the result of the MnO_2 surface. Samples of the heated oxides (of electrolytic origin) of 0.50 g each were mixed with 50 ml of 1N H_2SO_4 , the mixtures being stirred at room temperature for exactly 10 min. After 5 min, a 5-ml sample of the supernatant solution was taken for Mn^{2+} ion determination. The sample was added to 5 ml of 0.01M E.D.T.A. solution and buffer ($\text{NH}_4\text{Cl} + \text{NH}_3$) added to adjust the pH at 9 to 9.5. Then the excess E.D.T.A. was titrated with a standard ZnSO_4 solution (0.0100M) using Eriochrom Black T as indicator. In this method, small particles of manganese dioxide, if any are present, do not interfere. Then the mixture of MnO_2 and H_2SO_4 solution was stirred again for 10 min and, after 5 minutes' standing, another sample was analyzed, and the whole procedure repeated a third time.

Results are shown in Fig. 4. The unheated original MnO_2 (control in Fig. 4) was washed with 2N H_2SO_4 , previous to the experiment and gave only a little Mn(II) ion dissolved. Most of the Mn(II) ion dissolves in 10 min.

The larger amount of Mn(II) dissolved from heated MnO_2 may be considered as the result of lower oxide formation on the surface of manganese dioxide by heating. Increase of heating temperature gives an increase in Mn(II) ion dissolved, except that the 160°C curve is out of place, as mentioned above.

The decrease in x -value of the various samples can be compared with the Mn(II) ion dissolved by acid. A decrease in x from 1.977 for the original sample to 1.947 for the sample heated at 438°C corresponds to the reduction of about 3% of the total Mn from Mn(IV) to Mn(II) . In the 0.5-g sample treated with acid, 3% of the total Mn, or 8.6 mg, should have been Mn(II) according to the analysis and calculation. The acid treatment extracted 5.9

mg of Mn(II) according to Fig. 4, but this should be corrected by 0.8 mg extracted from the unheated sample, leaving 5.1 mg additional extractable Mn(II) as the result of heating. This is 59% of the total estimated from the analysis.

Another experiment was carried out to confirm the lower oxide formation on the surface of MnO_2 using three kinds of MnO_2 : $\gamma\text{-MnO}_2$ or electrolytic MnO_2 , $\alpha\text{-MnO}_2$ or cryptomelane made from the electrolytic MnO_2 by autoclaving with NH_4Cl solution at 170°C (7), and $\beta\text{-MnO}_2$ or natural pyrolusite. Two grams of each sample heated at various temperatures for 3 hr were shaken with a MnSO_4 solution buffered with acetic acid-sodium acetate (pH, 5.4), then the supernatant solution was analyzed to determine the adsorption of the divalent manganese ion on the manganese dioxide. Results are shown in Fig. 5. The absolute value of the Mn(II) ion adsorption should be affected by the surface area and the original surface oxidation state of the manganese dioxides. However, the results show that the higher the heating temperature the smaller is the adsorption. This means the more of the lower oxide on the surface the less of a reaction between MnO_2 and Mn(II) ion to form the lower oxide, $\text{MnO}_2 + \text{Mn}^{++} \rightarrow \text{Mn}_2\text{O}_3$.

From the above results it seems possible to conclude that the potential decrease of heated manganese dioxide is the result of lower oxide formation on the surface, and also that the potential of manganese dioxide depends mainly on the surface oxidation state.

In an electron diffraction study of manganese dioxide, Butler and Thirsk (8) found a lower oxide on the surface of manganese dioxide, but they pointed out that it may have been formed there by the bombardment with electrons.

Potential change on heating various MnO_2 samples.—Samples of four oxides: B, electrolytic MnO_2 or $\gamma\text{-MnO}_2$; A, sample B treated by Na_2CO_3 solution for dry-cell use; C, natural ore, probably $\alpha\text{-MnO}_2$; D, natural pyrolusite or $\beta\text{-MnO}_2$, were heated at various temperatures for 3-4 hr. Then 5.00 g of each sample was digested with 25 ml of 0.5M NH_4Cl solution for 5 days at 25°C with occasional shaking. The potentials and pH values of the

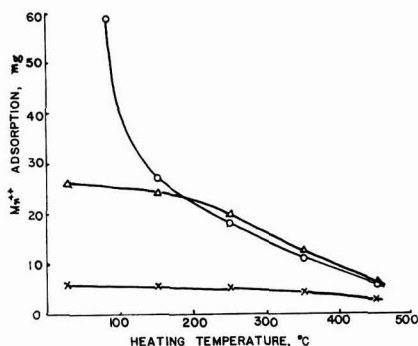


Fig. 5. Adsorption of Mn^{++} on MnO_2 heated. o, $\gamma\text{-MnO}_2$; Δ , $\alpha\text{-MnO}_2$; x, $\beta\text{-MnO}_2$. 2-g sample was shaken with 50 ml of NaAc-HAc buffered solution containing MnSO_4 (100 mg as Mn^{++}), pH 5.4.

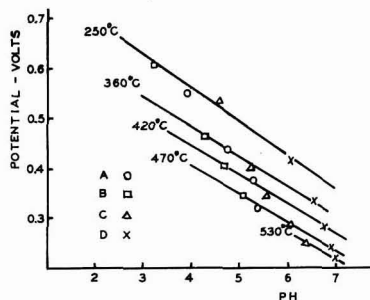
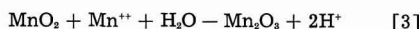


Fig. 6. Potentials of various MnO_2 samples after heating. Potentials were measured against a 0.1N calomel electrode. A, B, $\gamma\text{-MnO}_2$; C, probably $\alpha\text{-MnO}_2$; D, $\beta\text{-MnO}_2$.

solutions were measured as described before. Results are shown in Fig. 6. On heating below 250°C no regularity was found between the pH and the potential, and those points are omitted from Fig. 6. However, above 250°C a straight line relationship for each temperature was obtained between pH and potential irrespective of the kind of manganese dioxide, and the slope was near the theoretical 0.059 v per pH unit.

This result can be interpreted in terms of a surface layer of lower oxide. Originally each of the four samples had its individual surface oxidation state, so there was no consistent relation between the potentials of different samples and the pH. However, on heating at 250°C or higher the surface attains the same oxidation state for all, determined only by the temperature and irrespective of the original surface oxidation state, crystal structure, and chemical composition of the interior of the crystals.

Potential of MnO_2 with a known amount of lower oxide on the surface.— MnO_2 reacts with Mn(II) ion in a solution of suitable pH as follows:



and the lower oxide (Mn_2O_3 or MnOOH) will remain on the surface of the MnO_2 . When MnO_2 having a known surface area reacts with a known amount of Mn(II) ion, we can calculate the percentage of surface covered by the lower oxide. Therefore, a quantitative relation between the electrode potential and the surface oxidation state can be established. Some experiments were carried out to examine this point of view.

Powdered MnO_2 made by electrodeposition was washed with 2N H_2SO_4 several times to remove lower oxide and then washed with water and dried at 80°C . The sample had a surface area of $60 \text{ m}^2/\text{g}$ as measured by the B.E.T. method by N_2 adsorption at liquid nitrogen temperature. Samples of 1.50 g were treated with 50 ml of 0.5M NH_4Cl containing varying amounts of manganese sulfate (0-180 mg of Mn^{++}). The pH of the solution was adjusted to around 8 by addition of NH_3 . The mixtures were heated at about 70°C for 1 hr with occasional shaking and allowed to stand overnight at room temperature. Then the potential and pH of the solution were measured. Colorimetric tests showed that the

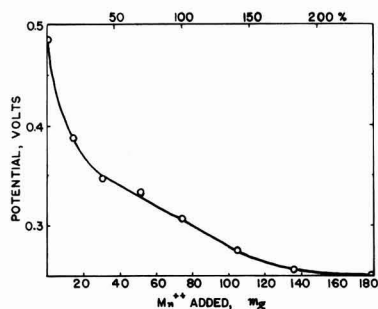


Fig. 7. Potential (vs. saturated calomel electrode) of manganese dioxide with known amount of lower oxide on the surface. The upper abscissa scale represents the percentage of the surface covered by lower oxide.

supernatant solution contained no detectable Mn(II) ion; that is, all Mn^{++} added had reacted with the manganese dioxide. Figure 7 shows the potentials corrected to pH 8 using a theoretical coefficient, -60 mv/pH. The lower scale of abscissas represents divalent manganese added to 1.50 g of the manganese dioxide. The upper scale represents the percentage of the surface covered by lower oxide assuming that all Mn(II) ion added remains on the surface of MnO_2 .

The number of manganese atoms on the MnO_2

surface can be calculated from $n = \left(\frac{d \times N}{MnO_2} \right)^{2/3} \times$

$100^2 \times S$, in which d is the density of MnO_2 taken as 4.020 found from pycnometer measurements for this sample, N is Avogadro's number, MnO_2 represents the formula weight, and S is the surface area (m^2/g). Let it be assumed that for each atom of Mn(IV) on the surface one Mn^{++} ion from the solution is added to form Mn_2O_3 as indicated in Eq. [3]. Then 75.4 mg of Mn^{++} is necessary to cover the total surface of 1.5 g of this MnO_2 by Mn_2O_3 .

The results in Fig. 7 show that one and half layer or two layer coverage of the MnO_2 surface by Mn_2O_3 gives nearly the same potential as that of Mn_2O_3 , which is shown in Fig. 2.

From the data in Fig. 7, E^0 in Eq. [1] can be calculated, if the ratio $a_{Mn_2O_3}/a_{MnO_2}$ is taken to be the ratio in the surface. When 50% of the surface is covered in Mn_2O_3 , E is 0.342 v (from Fig. 7). If activity coefficients can be neglected, Eq. [1] becomes:

$$0.342 = E^0 - (0.059 \times 8) - 0$$

Then, E^0 is 0.814 v referred to the calomel electrode or 1.056 v referred to the hydrogen electrode. This is near enough to the calculated value 1.014 v from thermal data to support the assumption that the potential is determined by the composition of the surface.

Discussion

When a MnO_2 electrode is discharged the potential decreases and on interruption of the discharge the

potential is recovered. As one of the factors to explain the potential recovering process, the following mechanism has been considered (9). On the discharge of MnO_2 , lower oxides (Mn_2O_3 or $MnOOH$) may be formed on the surface of MnO_2 , and on interruption the lower oxides may start to diffuse into the interior of the MnO_2 , namely, a rearrangement between the surface and the inside may take place in such a way that only electrons and protons are moving (10).

The results given in the present paper have shown that the lower oxide on the surface of MnO_2 is fairly stable (from experiments shown in Fig. 5-7) even for electrolytic MnO_2 containing water (about 8%) which may help to move proton. The potential of the MnO_2 electrode, therefore, is dependent mainly on the surface oxidation state of the dioxide instead of the activity of the whole oxide.

Therefore it seems that the rate of the rearrangement process would be very slow if there is any contribution of it to the potential recovery process.

Acknowledgment

The author wishes to express his appreciation to Professor W. C. Vosburgh, Duke University, who has given much helpful advice in preparation of this paper and particularly under whom the experiments of Fig. 7 have been carried out. The author is indebted to Dr. K. Nagasawa, Nagoya University of Japan, for the differential thermal analysis. This portion of the work was supported in part by the Office of Naval Research.

Thanks are also due Professor E. Yeager and Professor F. Hovorka, Western Reserve University, and Professor K. Sasaki, Nagoya University, Japan, for their encouragement and valuable comments.

Manuscript received July 28, 1958. This paper was presented at the Cleveland Local Section meeting of The Electrochemical Society on April 8, 1958.

Any discussion of this paper will appear in a Discussion Section to be published in the December 1959 JOURNAL.

REFERENCES

1. A. M. Moussard, J. Brenet, F. Jolas, M. Pourbaix, and J. Van Muylder, *Proceeding of the Sixth Meeting of the International Committee for Electrochemical Thermodynamics and Kinetics*, p. 190 (1954).
2. A. Kozawa and K. Sasaki, *J. Electrochem. Soc. Japan*, **22**, 569 (1954).
3. K. Sasaki and A. Kozawa, *ibid.*, **25**, 273 (1957).
4. K. Sasaki and A. Kozawa, *ibid.*, **25**, 115 (1957).
5. J. Brenet and A. M. Briot, *Compt. rend.*, **232**, 1300, 2021 (1951).
6. K. H. Maxwell and H. R. Thirsk, *J. Chem. Soc.*, **1955**, 4057.
7. H. F. McMurdie, *Trans. Electrochem. Soc.*, **86**, 313 (1944).
8. G. Butler and H. R. Thirsk, *This Journal*, **100**, 297 (1953).
9. J. J. Coleman, *Trans. Electrochem. Soc.*, **90**, 545 (1946).
10. D. T. Ferrell and W. C. Vosburgh, *This Journal*, **98**, 334 (1951).

Anodic Dissolution of Magnesium Alloys in Aqueous Salt Solutions

R. Glicksman

RCA Laboratories, Radio Corporation of America, Princeton, New Jersey

ABSTRACT

The anodic dissolution of a magnesium AZ10A alloy has been studied by measuring corrosion rates and electrode potentials as functions of current density, pH, and electrolyte concentration. Results are interpreted in terms of a rate-controlling proton transfer step through a surface film of magnesium oxide and/or hydroxide.

The effect of different alloy compositions and soluble metal additives to the electrolyte on the anodic corrosion rate and electrode potential also has been measured.

Although the theoretical advantages of magnesium as an anode for primary batteries have been recognized for well over fifty years (1), nothing significant had been reported on a Mg dry cell until the recent work of Kirk, George, and Fry (2,3). Their cell, which is patterned after the conventional Leclanché cell, contains a magnesium alloy anode, a manganese dioxide cathode, and a magnesium bromide electrolyte. More recently, magnesium dry cells containing a magnesium bromide electrolyte and organic cathode materials have been reported (4,5).

These developments indicate that magnesium may find extensive use in primary cells. However, some basic problems present themselves. One of these is the poor electrode efficiency of the magnesium alloys. Information on the mechanism of anodic dissolution should help to explain these low electrode efficiencies and could indicate new approaches that might be taken to improve anode performance. In the present investigation the anodic dissolution of an AZ10A magnesium alloy has been studied by measuring corrosion rates and electrode potentials as functions of current density, pH, and electrolyte concentration. The effect of different alloy compositions and soluble metal additives to the electrolyte on the anodic corrosion rate and electrode potential also has been measured.

Experimental

Corrosion rates were obtained by measuring the amount of hydrogen liberated at a magnesium anode while it was undergoing anodic dissolution. The apparatus used in making these measurements is shown in Fig. 1. A carbon rod was used as the cathode, while the anode consisted of cylinders of magnesium approximately 2.5 cm in diameter and 2.5 cm long. These were mounted on a steel shaft with ends protected by plastic washers. The remainder of the shaft was protected by a close fitting Bakelite sleeve, which is set tightly on a ground glass male joint.

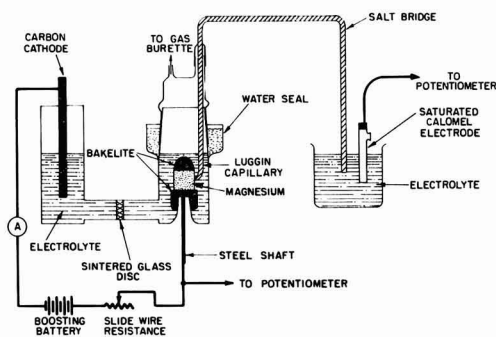


Fig. 1. Apparatus used to investigate magnesium corrosion rates and anode potentials.

The current flow in the circuit was maintained constant by means of a variable resistance and booster battery, and the hydrogen was collected in a gas buret in the usual manner. The procedure and apparatus were checked by measuring the volume of hydrogen liberated at a platinum electrode in 2N HCl solution, which corresponded to within 1% of the theoretical amount of hydrogen expected, based on calculations using Faraday's law.

The magnesium specimens, compositions of which are shown in Table I, were prepared by etching them in dilute acetic acid for 1-2 min and washing them in distilled water. Solutions were prepared with Fisher purified magnesium bromide and certified sodium bromide reagents using doubly distilled water. All solutions were saturated with Fisher N. F. magnesium hydroxide reagent.

The duration of each run was 3 hr except in the more corrosive solutions where quantities of hydrogen in excess of 100 cc were evolved in shorter time intervals. With but few exceptions all reported measurements represent the average of two or three runs, and each result was obtained with fresh electrolyte and a newly prepared magnesium cylinder. Duplicate runs varied from 1 to 3% for most of the

Table I. Local corrosion rates, electrode potentials, and anode efficiencies of various commercial magnesium alloys dissolving anodically in 2N MgBr₂ electrolyte [st'd with Mg(OH)₂] at a current density of 2.0 ma/cm²

Alloy*	Composition, %†					Maximum† impurities, %		Anode efficiency, %	Anode potential, v	Corrosion rate × 10 ⁻² mdd
	Al	Zn	Mn	Ca	Zr	Ni	Fe			
Commercially pure magnesium	—	—	0.15 Max.	—	—	0.001	—	63.5	1.327	12.5
AZ10A	0.8-1.2	0.3-0.5	0.15 Max.	0.1-0.25	—	0.001	0.002	68.3	1.287	10.2
AZ31B	2.5-3.5	0.7-1.3	0.20 Min.	0.04 Max.	—	0.005	0.005	67.0	1.232	10.7
AZ80A	7.9-9.2	0.2-0.8	0.15 Min.	—	—	0.005	0.005	68.9	1.227	9.8
ZK60A†	—	4.8-6.5	—	—	0.45 Min.	—	—	58.3	1.233	15.6
M1A	—	—	1.20 Min.	0.08-0.14	—	0.01	—	52.6	1.328	19.6

* Alloys obtained from Dow Chemical Co. and White Metal Rolling and Stamping Corp.

† Data supplied by the Dow Chemical Co.

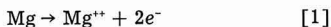
measurements, while a variation of 5-6% was obtained with the more corrosive solutions. Average values in terms of mg/dm²/day (mdd) are reported for the dissolution rates.

All runs were made at room temperature which varied from 24°-30°C during the course of this investigation. The effect of temperature on the corrosion rate over this temperature range has been shown to be negligible (6), and duplicate runs made at varying temperatures indicate no correction for this factor was necessary. Measurements of the effect of dissolved oxygen on the corrosion of magnesium in magnesium bromide solution (7) showed it has little or no effect on the corrosion rate, a result in agreement with previously reported data (8). Therefore, this factor was not controlled either.

The magnesium potentials were measured with a L&N type K potentiometer at the completion of each run using a Luggin capillary and a saturated calomel reference electrode as shown in Fig. 1. The reported potentials are all steady-state values and represent the average of two or three measurements. The individual measurements had a reproducibility of ±0.001 v for the majority of the runs.

Effect of Current Density

The effect of a polarizing current on the dissolution rate of a magnesium AZ10A alloy¹ in 2N MgBr₂ solution is shown in Fig. 2. When the specimen is made anodic, the observed dissolution rate is the sum of the rate due to the external current as defined by



and the rate due to local action as defined by



It is seen that the local corrosion rate increases with increasing anodic current density. This is known in the theory of corrosion as the negative difference effect. For magnesium, the magnitude of this effect has been found by Robinson (9) to be dependent on

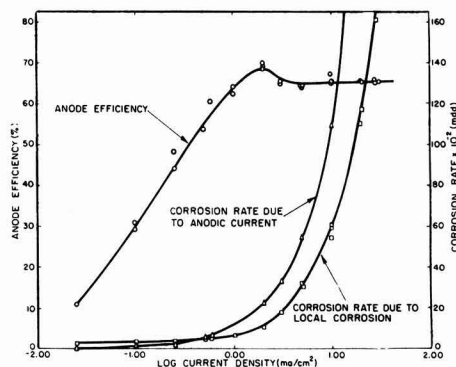


Fig. 2. Effect of current density on the local corrosion rate and anode efficiency of a magnesium AZ10A alloy dissolving in 2N MgBr₂ electrolyte [st'd with Mg(OH)₂].

both the electrolyte and anode composition including alloy ingredients and level of impurities.

For such an anode, the electrode efficiency is given by the following relationship:

Electrode efficiency =

$$\frac{\text{number of Faradays passed through the circuit}}{\text{number of equivalents of magnesium dissolved}} \times 100 \quad [3]$$

i.e., by the rate of useful corrosion over the total dissolution rate. For many anodes the electrode efficiencies would approach 100% as a limit. However, if the rate of local corrosion were to increase with the rate of useful corrosion, efficiencies would tend to approach a limiting value of less than 100%. This is indicated by the anode efficiency curve for the magnesium AZ10A alloy which reaches a limiting efficiency of 65% at current densities above 1 ma/cm² in the 2N MgBr₂ electrolyte, although efficiency values as high as 68-69% are attained at a current density of 2 ma/cm².

Figure 3 is a plot of the negative difference effect obtained on a magnesium AZ10A alloy in 2N MgBr₂ vs. the anodic current density. It is seen that the

¹ This alloy, which was furnished by the Dow Chemical Co., consists principally of magnesium, but contains in addition 1% aluminum and 0.5% zinc.

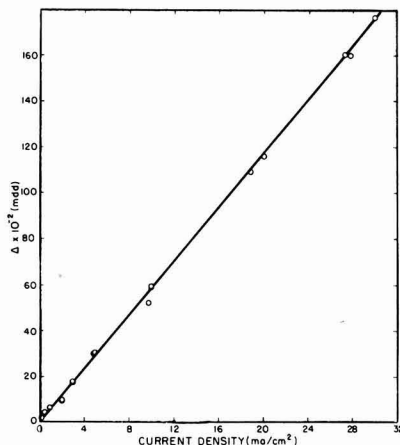
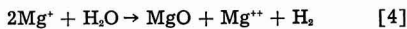


Fig. 3. Effect of current density on the negative difference effect obtained from a magnesium AZ10A alloy in 2N MgBr₂ electrolyte [st'd with Mg(OH)₂].

difference effect is directly proportional to the galvanic current up to 30 mA/cm². This type of effect has also been observed on magnesium corroding in a 3% NaCl solution (10) and is usually found with very active anodic metals covered by a protective layer. The positive effect is found in the absence of a protective layer as in the case of magnesium dissolving in HCl (11). Similarly, aluminum anodes show positive difference effects in certain corrosive electrolytes such as NaOH (12) and HF (13) which can dissolve the protective film, while the negative effect shows up in HCl (13) because of the presence of a film on the metal. The work of Kroenig and Uspenskaja (10) indicates that the magnitude of the negative difference effect increases with the thickness of the oxide layer.

There are two hypotheses which explain the negative difference effect. The first of these attributes the increased corrosion of magnesium to the destruction of the anodic films with increased current density, resulting in continuous exposure of impurity particles which serve as sites for cathode reactions (13, 14). The second hypothesis explains the experimental results by assuming that unipositive magnesium is formed as an unstable intermediate. Oxidation of this species to the common dispositive state by water



was held responsible for hydrogen evolution (15, 16). All efforts to isolate and identify a compound containing unipositive magnesium thus far have been unsuccessful. Although the various experimental observations on the magnesium anode can be explained by either of these hypotheses, the experimental evidence available at the present time cannot serve as a convincing demonstration of the correctness of one or the other of these hypotheses.

It is proposed that a more appropriate model with which to consider the anodic corrosion of magnesium is one in which the over-all rate is controlled by the rate of either proton or magnesium ion transport through a surface film of magnesium oxide and/or

hydroxide. (Control by proton transfer appears more likely because of the apparent ease with which magnesium ions penetrate the film during anodic dissolution.) This model, suggested by Casey and Bergeron (17) to explain the dissolution rates of magnesium in acidic salt solutions, is used to explain the experimental data in the present study. Thus, the negative difference effect could be attributed to the action of the polarizing current in breaking down the protective film. This would manifest itself as an increased rate of local corrosion, since changes in the structure of the film due to the anodic current would be reflected by changes in the rate of passage of any particle through the film.

Effect of Soluble Metal Additives to the Electrolyte

In the corrosion of metals, where the cathode process is hydrogen evolution, the nature of the cathode material, specifically its hydrogen overvoltage, plays an important role in the corrosion reaction (18). Thus the galvanic currents observed when magnesium anodes were coupled with various other metals in a 3% NaCl solution bore no relationship to the reversible electrode potentials of these metals, but were governed by their hydrogen overvoltages, the metals of lowest overvoltage permitting the greatest galvanic currents. In regard to promoting corrosion, the elements arranged in an increasing order of effect, were found by Kroenig and Kostylev (19) to be Hg, Zn, Mn, Pb, Cu, Ni, Fe, Al, and Pt.

In order to study the effect of impurities on the anodic dissolution rate of the magnesium AZ10A alloy, corrosion rates and electrode potentials were measured in a 2N MgBr₂ electrolyte containing various soluble metal additives in the form of their bromide salts. Solutions were made up by adding 1 g of the metallic bromide to a liter of 2N MgBr₂ electrolyte and saturating the resultant solution with magnesium hydroxide to maintain the pH constant. Experimental measurements were made with solutions containing the following salts: ZnBr₂, PbBr₂, TlBr, AlBr₃, MnBr₂, Hg₂Br₂, CdBr₂, CuBr₂, AgBr, and PtBr₄.

In Fig. 4, the local corrosion rates are plotted against the logarithm of the exchange current for the hydrogen evolution reaction on the corresponding metal. The exchange currents, which provide a standard state at which the velocities of the reaction $2\text{H}^+ + 2e^- \rightarrow \text{H}_2$ on various metals can be com-

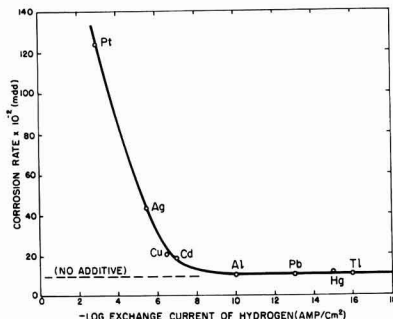


Fig. 4. Effect of various soluble metal bromide additives on the corrosion rate of a magnesium AZ10A alloy dissolving anodically in a 2N MgBr₂ electrolyte [st'd with Mg(OH)₂] at a current density of 2.0 mA/cm².

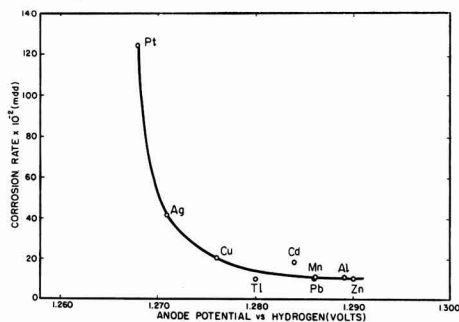


Fig. 5. Relationship between the corrosion rate and anode potential of a magnesium AZ10A alloy dissolving anodically in a 2N MgBr_2 electrolyte [st'd with $\text{Mg}(\text{OH})_2$] containing various soluble metal bromide additives at a current density of 2.0 ma/cm^2 .

pared, were estimated from the data available in the literature (20-22). For the corrosion of magnesium in a neutral or slightly alkaline aqueous salt solution, it is seen that a small quantity of low overpotential metal in the solution greatly accelerates the corrosion reaction. Apparently these metals are deposited on or in the oxide film and form centers on which hydrogen can come off more easily. Metals having hydrogen exchange currents of 10^{-6} or less appear to have little effect on the local corrosion rate as measured under these experimental conditions.²

The effect of the various additives on the anode potential is illustrated in Fig. 5, where the corrosion rate is plotted vs. magnesium potential. It is seen that, with the metal additives which cause little or no change in the corrosion rate, the anode potentials range from 1.280 to 1.290 v as compared to a potential of 1.287 v in solutions containing no additives. The low overpotential metal additives, such as Cu, Ag, and Pt, which cause a marked increase in the corrosion rates, lower the magnesium potential by 0.01-0.02 v, the greatest effect occurring with the Pt additive.

Assuming the anodic polarization curve of magnesium is the same for all these solutions, any differences in the corrosion currents and potentials would be dependent on the cathodic polarization curve. If the cathodic areas possess a low overpotential, the cathodic polarization curve slopes down less than if the overpotential is high. Thus the current is greater, and the potential more noble, in agreement with the experimental data.

The effect of the Hg additive on the potential was quite marked, resulting in an anode potential of 1.376 v, a value too high to be shown in Fig. 5. The high potential encountered with this additive is believed due to the partial removal of the magnesium oxide film by amalgamation. This type of behavior is similar to that found for amalgamated aluminum anodes. The effectiveness of the Hg additive in maintaining a low corrosion rate, despite the absence of a

controlling oxide film, is attributed to the difficulty of proton discharge on this high overvoltage metal.

Effect of Electrolyte

The effect of electrolyte concentration and pH on the local corrosion rate and electrode potential of a magnesium AZ10A alloy dissolving anodically in various magnesium and sodium bromide solutions is shown in Fig. 6.

It is seen that the corrosion rate of magnesium in the magnesium bromide solutions increases approximately linearly with decreasing electrolyte pH over the range of 6.3-8.1 pH units. At pH values greater than 8.1, the corrosion rate approaches a constant value of $12.7 \times 10^{-7} \text{ mdd}$, which corresponds to an anode efficiency of 63%. The minimum in the corrosion rate occurs at a pH of 8.1, corresponding to an anode efficiency of 68%.

In contrast to the marked change in electrolyte pH with magnesium bromide concentration, which is a consequence of the common ion effect, the sodium bromide electrolyte shows only a 0.7 variation in pH over a concentration range of 1.0-6.0 N. Over this small range of pH 9-10 the corrosion rate is essentially constant at a value of $11.5-12.1 \times 10^{-7} \text{ mdd}$. This result is comparable to those obtained in magnesium bromide electrolytes having pH values of 8 or higher.

The effect of electrolyte pH on the anode potential of the magnesium AZ10A alloy also is illustrated in Fig. 6. For the magnesium bromide electrolyte it is seen that the anode potential falls rapidly with increasing pH in the basic pH range. For the weakly acidic solutions the potential varies only slightly with pH, approaching a constant value of 1.36 v. In contrast to the marked drop in potential observed in the weakly basic magnesium bromide solutions, the anode potential in the sodium bromide electrolytes decreases only 0.04 v in the pH range 9.3-10.0.

The data in Fig. 6 can be explained in terms of the effect of these electrolytes on the structure of a surface film which must be magnesium oxide and/or magnesium hydroxide. This film is more easily penetrable at low pH values because the OH^- ion concentration is too low to maintain an effective magnesium hydroxide film. Thus at low pH values,

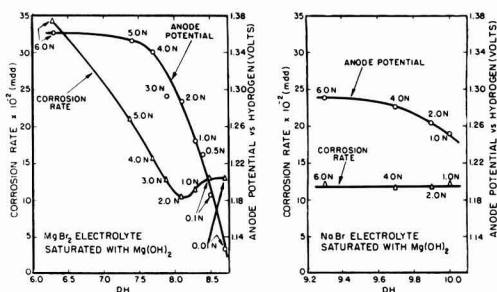


Fig. 6. Effect of pH on the corrosion rate and anode potential of a magnesium AZ10A alloy dissolving anodically in various MgBr_2 and NaBr electrolytes [st'd with $\text{Mg}(\text{OH})_2$] at a current density of 2.0 ma/cm^2 .

² The corrosion rates of the magnesium AZ10A alloy in solutions containing ZnBr_2 and MnBr_2 were 10.0 and $10.8 \times 10^{-7} \text{ mdd}$, respectively. These results were not included in Fig. 4 because their hydrogen exchange currents were not known.

high corrosion rates and high anode potentials are observed.

At high pH values the OH^- ion concentration of the electrolyte controls the precipitation of the Mg^{++} ions produced at the anode, which, according to Robinson (9), are precipitated so close to the anode as to stifle the anodic reaction. This results in more cathodic potentials, a decrease in local corrosion, and excessive polarization of the anode.

In an intermediate pH range, precipitation of magnesium hydroxide occurs at a sufficient distance from the active anodic areas to permit the anodes to function normally. It is in this pH range that other properties of the electrolyte exert a greater influence over such factors as local corrosion and anode potential. Since the magnesium bromide and sodium bromide electrolytes appear to operate in this intermediate pH range, the similar corrosion rates in the 1.0-6.0N NaBr and 0.01-3.0N MgBr_2 electrolytes are to be expected, despite the differences in electrolyte pH. At the higher magnesium bromide electrolyte concentrations, pH becomes the dominant factor, and the corrosion rates in the magnesium bromide solutions are much greater than in the sodium bromide electrolyte.

The slightly lower corrosion rates found in the 1.0-3.0N MgBr_2 electrolytes as compared to the more basic sodium bromide electrolytes are similar to the type of results obtained by Casey and Bergeron (17), who found that the dissolution rates of magnesium in acidified potassium chloride solutions are greater than those in comparable magnesium chloride solutions of the same pH. Their results were explained on the basis of a thicker or less porous oxide film on magnesium in the magnesium chloride electrolyte, formed as a result of the lower solubility of magnesium hydroxide in the magnesium chloride solutions. The lower solubility in this electrolyte is a consequence of the common ion effect. Thus, if the rate of dissolution of magnesium in aqueous salt solution depends on the solubility of the magnesium hydroxide film, as was first suggested by Whitby (23, 24), it follows that corrosion rates would be greatest in those electrolytes where a thinner or more porous oxide film on magnesium is obtained.

The electrode potential data in Fig. 6 can be explained in the following way. Because of the higher pH of the sodium bromide solutions, the potential of magnesium, when measured at a current density of 2.0 ma/cm², is more anodic for the concentrated (3.0-6.0N) MgBr_2 solutions. However, for the more dilute magnesium bromide solutions the anode potential decreases rapidly with increasing pH, becoming more cathodic than the potentials measured in the sodium bromide electrolytes. These lower potentials are attributed in part to the effect of the Mg^{++} ions in stifling the anode reaction with increasing pH. In addition a significant portion of the potential ennoblement at the low magnesium bromide concentrations is due to the decreased bromide ion concentration of the electrolyte.

Effect of Anode Composition

It has been shown by Hannawalt, Nelson, and Peloubet (25) that the presence of certain impuri-

ties and alloying metals has a marked effect on the corrosion characteristics of magnesium alloys in an aqueous salt solution. They determined tolerance limits of impurities such as Fe and Ni, for magnesium and some of its alloys. When the amount of the element present exceeds this tolerance limit, there results a large increase in corrosion rate. These findings point to the importance of knowing the concentration of deleterious impurities and their tolerance limits when investigating alloy effects. In addition, it must be realized that the corrosion behavior of magnesium alloys in other electrolytes will be different from that in the 3% NaCl solution of Hanawalt, *et al.* and care should be exercised in extending their results to other electrolyte systems.

In Table I are presented corrosion rates and anode efficiencies of six different commercial magnesium alloys along with their compositions and significant metal impurities. It is seen that magnesium alloys containing aluminum and manganese operate at higher anode efficiencies than commercially pure magnesium, as well as the ZK60A and M1A magnesium alloys. Alloying the magnesium with aluminum permits removing most of the major cathodic impurity, iron, by precipitation with manganese. The corrosion resistance of such high-purity alloys is very good and, as anodes, they perform more efficiently than any of the magnesium compositions tested to date (9).

Also presented in Table I are anode potentials of these alloys, when measured in a 2N MgBr_2 electrolyte at a current density of 2.0 ma/cm². It is seen that the alloys containing Al or Zn are 0.04-0.10 v more cathodic than commercially pure magnesium. The pure magnesium has a potential of 1.33 v on the normal hydrogen scale, as compared to values of 1.23-1.29 v for the Mg-Al alloys, whose potential is more anodic with decreasing amounts of Al. This type of behavior has been found by other investigators with other electrolytes (9, 26).

Conclusions

It is proposed that the most appropriate model with which to consider the anodic corrosion of magnesium in aqueous salt solutions is one in which the over-all rate is controlled by the rate of proton transport through a surface film of magnesium oxide and/or hydroxide. The anodic corrosion rates and potentials of a magnesium AZ10A alloy in various magnesium bromide and sodium bromide electrolytes can be explained in terms of the effect of these electrolytes on the structure of this film.

It has also been shown that the presence of certain low overvoltage metal impurities, such as Cu, Ag, and Pt, with hydrogen exchange currents greater than 10⁻⁴ amp/cm², have a deleterious effect on the corrosion characteristics of magnesium alloys in an aqueous salt solution.

Acknowledgments

The author wishes to express his appreciation to G. S. Lozier and C. K. Morehouse for their many helpful suggestions during the course of this investigation.

Manuscript received May 5, 1958. This paper was prepared for delivery before the New York Meeting, April 27-May 1, 1958.

Any discussion of this paper will appear in a Discussion Section to be published in the December 1959 JOURNAL.

REFERENCES

1. C. K. Morehouse, *This Journal*, **99**, 187C (1952).
2. R. C. Kirk and A. B. Fry, *J. (and Trans.) Electrochem. Soc.*, **94**, 277 (1948).
3. R. C. Kirk, P. F. George, and A. B. Fry, *This Journal*, **99**, 323 (1952).
4. C. K. Morehouse and R. Glicksman, *ibid.*, **105**, 306 (1958).
5. C. K. Morehouse and R. Glicksman, *ibid.*, **105**, 619 (1958).
6. H. H. Uhlig, Editor, "Corrosion Handbook," pp. 218-222, John Wiley & Sons, Inc., New York (1948).
7. R. Laity, Unpublished work.
8. Ref. (6), p. 218.
9. H. A. Robinson, *Trans. Electrochem. Soc.*, **90**, 485 (1946).
10. W. O. Kroenig and V. N. Uspenskaja, *Korrosion u. Metallschutz*, **11**, 10 (1935).
11. B. Roald and W. Beck, *This Journal*, **98**, 277 (1951).
12. M. A. Streicher, *J. (and Trans.) Electrochem. Soc.*, **93**, 285 (1948).
13. M. E. Straumanis and Y. N. Wang, *This Journal*, **102**, 304 (1955).
14. R. E. McNulty and J. D. Hanawalt, *Trans. Electrochem. Soc.*, **81**, 423 (1942).
15. R. L. Petty, A. W. Davidson, and J. Kleinberg, *J. Am. Chem. Soc.*, **76**, 363 (1954).
16. J. H. Greenblatt, *This Journal*, **103**, 539 (1956).
17. E. J. Casey and R. E. Bergeron, *Can. J. Chem.*, **31**, 849 (1953).
18. Ref. (6), p. 490.
19. W. Kroenig and G. Kostylev, *Z. Metallk.*, **25**, 144 (1933).
20. J. O. 'M. Bockris, "Modern Aspects of Electrochemistry," p. 199, Academic Press Inc., New York (1954).
21. J. O. 'M. Bockris, "Electrochemical Constants," pp. 252-257, National Bureau of Standards Circular 524 (1953).
22. J. A. V. Butler, "Electrical Phenomena at Interfaces," pp. 164-165, Macmillan Co., New York (1951).
23. L. Whitby, *Trans. Faraday Soc.*, **31**, 638 (1935).
24. L. Whitby, *ibid.*, **29**, 1318 (1933).
25. J. D. Hanawalt, C. E. Nelson, and J. A. Peloubet, *Trans. Am. Inst. Min. Met. Eng.*, **147**, 273 (1943).
26. J. A. Boyer, Aeronautics, 12th Ann. Rep. Nat. Adv. Comm. 445 (1926).

Electrolytic Transition of Ag_2O to AgO in Alkaline Solutions

Thedford P. Dirkse and George J. Werkema

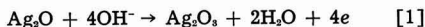
Department of Chemistry, Calvin College, Grand Rapids, Michigan

ABSTRACT

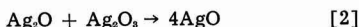
An interrupted current technique was used to study the electrolytic oxidation of silver in alkaline solutions. The short voltage peak just preceding the stage corresponding to the production of AgO in the voltage-time curves is interpreted as being due to the high electrical resistance to the Ag_2O layer.

During the anodic treatment of silver in alkaline solutions a two level curve is obtained when voltage is plotted against time. Such a curve, obtained by a constant current oxidation, is shown on Fig. 1. Part a corresponds to the formation of Ag_2O , part c to the formation of AgO , and d to the evolution of oxygen. The work reported here deals with the peak represented by b. Such a peak may or may not be present also at the beginning of stage a, but is usually present during the transition from stage a to stage c. It is found whether a constant current or a constant potential process is used. It is also found in the charging curves for commercial silver-zinc batteries.

Although very little has been written about this peak, two different explanations for it appear in the literature. The first was given by Hickling and Taylor (1) who suggested that the peak corresponds to the change



and the Ag_2O_3 , being unstable, quickly decomposes as follows:



As soon as this latter reaction begins the voltage begins to decline from the peak. This mechanism, whereby the oxidation of Ag^+ to Ag^{++} proceeds through the formation of Ag^{+++} , has been proposed also for acid solutions by others.

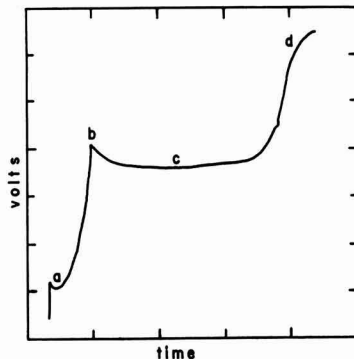


Fig. 1. Typical voltage-time curve for constant current oxidation of silver in KOH solution.

Yost (2) studied the catalytic effect of Ag^+ on the oxidation of Cr^{+++} by persulfuric acid. He suggested a mechanism for this action in which the persulfate first oxidized the Ag^+ to Ag^{+++} and the latter, in turn, oxidized the Cr^{+++} to dichromate. This mechanism is consistent with the kinetic data obtained for this process. Later Noyes, *et al.* (3) studied the rate of oxidation of AgNO_3 by ozone in acid solution and interpreted their kinetic data in a way similar to that of Yost. A study of the rate of reduction of Ag^{+++} by water in acid solution showed this process to be fairly complex, but it was suggested that Ag^{+++} was an intermediate in this reaction also (4). Gordon and Wahl (5) used a similar mechanism to explain their data on the rate of the exchange reaction between Ag^+ and Ag^{++} .

This interpretation has, however, not gone unchallenged. Bawn and Margerison (6) studied the oxidation of a hydrazyl using Ag^+ and persulfuric acid. They suggest that their results can be interpreted in a manner similar to that proposed by Yost (2). However, they contend also that such results can be interpreted just as well without assuming the formation of Ag^{+++} as an intermediate. They prefer a mechanism involving the formation of free radicals and Ag^{++} .

Aside from the fact of the existence or nonexistence of tripositive silver, it is doubtful whether peak b in Fig. 1 is due to its formation. This peak is obtained even when the potential of the silver electrode is kept 100–150 mv above the reversible potential of the Ag_2O – AgO couple in alkaline solution, and such a potential is not of sufficient magnitude to result in the formation of Ag^{+++} from Ag^+ or Ag^{++} . This value is lower than that generally accepted as the potential of Ag^{+++} – Ag^{++} in alkaline solutions (7).

Another explanation of this peak has been given by Jones, *et al.* (8). They suggest that the transition from Ag_2O to AgO proceeds with difficulty and the peak represents the difficulty of forming centers of AgO in the lattice of Ag_2O . They also suggest that some Ag_2O_3 may be formed, but at the end rather than at the beginning of stage c.

Because of this divergence of opinions, and because of the possibility that a proper understanding of the meaning of this peak may afford a clue to the unravelling of the kinetics of these particular electrode reactions, a special effort was made to study this phenomenon further.

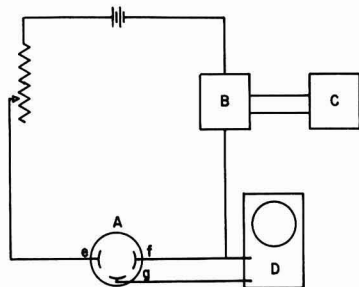


Fig. 2. Schematic diagram of interrupter apparatus. A, cell; B, Western Electric 275 Relay; C, sine wave generator; D, oscilloscope; e, auxiliary silver electrode; f, working electrode; g, reference electrode.

Experimental

The method used in this study involved the passage of interrupted current through the electrode. The voltage changes were observed on an oscilloscope both during passage of the current and during decay (open-circuit condition). A schematic diagram of the apparatus is shown on Fig. 2. The Western Electric 275 relay served as a current interrupter, and frequency of interruption was governed by the frequency delivered by the sine wave generator. The working electrode was a silver wire with about 0.5 cm^2 surface area. Constant current processes were used in all this work. The auxiliary and reference electrodes were relatively large pieces of silver screen. The traces on the oscilloscope were recorded photographically. All runs were made at room temperature. The variables studied were: concentration of KOH , current density, and effect of oxygen. The last of these was studied by bubbling air through the solution and then making an identical run except for the fact that purified nitrogen was bubbled through the solution during the run.

Results

The nature and shape of the traces obtained were the same whether air or nitrogen was bubbled through the electrolyte during the run. Consequently, the phenomena observed were not due to the presence or absence of oxygen in the electrolyte.

In all cases the electrolyte was a solution of KOH . A change in the concentration of the electrolyte did not give rise to any changes in the traces that were obtained. When the more concentrated KOH solutions were used the electrolyte gradually became discolored due to the presence of finely divided particles of silver oxides. Furthermore, since the silver oxides are slightly soluble in KOH solutions, it was possible that the nature of the decay curve could be affected by the solubility of the oxides produced during passage of current. For these reasons, the results used here are those obtained when 1N KOH was the electrolyte.

Types of the traces that were obtained are shown on Fig. 3. These were all traced from photographs taken during the runs. Similar traces were obtained

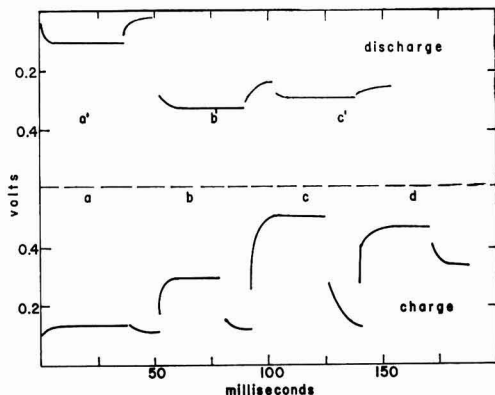


Fig. 3. Voltage-time traces for anodic and cathodic treatment of silver electrode in N KOH solution. Current density, 7 ma/cm^2 .

over an apparent current density range of 1-10 ma/cm². The voltages are expressed as the difference between that of the working electrode and of the reference electrode. A base line was recorded before beginning each charge or discharge. The charge curves on Fig. 3 are given in the order in which they appear. At the beginning of the charge the traces are of the type shown in panel a. As the treatment continues the amplitude of this curve increases slightly. This is followed by a rapid transition from type a to type c. Panel b represents an intermediate in this transition. In each case the decay curve shows that Ag₂O is the oxide still on the surface. The curve in panel c represents the peak referred to in Fig. 1. Curve d is of the type that follows the transition from a to c. It should be noted that the decay curve now shows the presence of AgO on the electrode, and at the same time the charging voltage is lower than that in panel c. Traces of the type shown in panel d continue for a while, and then the voltage levels become higher as gassing begins.

During discharge a similar sequence takes place, see the upper set of curves in Fig. 3. Here the top border of the graph represents the base line obtained before the discharge was begun. Panel a' represents the kind of trace obtained at the beginning of discharge. The decay curve shows the presence of AgO. Then there follows a rapid transition to traces such as shown in panel c'. Panel b' shows an intermediate trace. Here again the voltage during passage of current (discharge) is lower in panel b' than in panel c'. This is similar to the peak obtained on charge.

Discussion

It is suggested here that these phenomena can be interpreted in terms of the resistance of the Ag₂O layer that is formed on the electrode. It has been pointed out (9) that the electrical resistance of Ag₂O is considerably greater than that of AgO. According to this interpretation, then, as the oxidation of silver proceeds, a film of Ag₂O is formed on the surface of the electrode. As this film builds up, the electrical resistance at the electrode-electrolyte interface increases. When this film completely covers the surface, the resistance, and consequently the IR drop also, increases giving rise to the peak represented by b in Fig. 1. The traces on Fig. 3 also show a relatively large IR drop at this point (panel c). As soon as some of this Ag₂O is changed to AgO, the resistance of the surface film decreases, the IR drop decreases, and the open-circuit voltage (on decay) rises to that of AgO. As more AgO is formed the resistance of the surface film and the voltage decrease slightly.

This explanation also accounts for the phenomena observed on discharge. As the discharge progresses, AgO is changed to Ag₂O and the resistance of the surface layer increases. When all the surface AgO has been changed to Ag₂O this resistance is at its maximum and there is the greatest voltage loss on discharge. The open-circuit voltage is that of Ag₂O, Fig. 3 b'. This trace also shows a large IR drop. On further discharge the Ag₂O changes to Ag and the resistance of the surface layer decreases. Consequently, the discharge voltage is a little higher, Fig. 3 c'.

It is believed that this interpretation is more consistent with the data obtained than are the other interpretations that have been offered. The existence of Ag₂O₂ is doubtful, particularly in alkaline solutions. Moreover, if Ag₂O₂ were an intermediate in the formation of AgO from Ag₂O, this might account for peak b in Fig. 1 but would not account for a corresponding dip in the discharge curve when the AgO is gone.

Similar reasoning tends to eliminate the idea that the peak on charge is due to the difficulty of forming AgO nuclei in an Ag₂O lattice. Again, this suggestion can be used to account for the charge phenomenon, but it does not account for a similar event on discharge.

Acknowledgment

The authors wish to express their appreciation and thanks to the Office of Naval Research for sponsoring the work reported here under Contract No. Nonr-1682(01), and to Mr. S. Schuldiner for his suggestions with respect to the experimental procedures.

Manuscript received July 16, 1958.

Any discussion of this paper will appear in a Discussion Section to be published in the December 1959 JOURNAL.

REFERENCES

1. A. Hickling and D. Taylor, *Disc. Faraday Soc.*, **1**, 277 (1947).
2. D. M. Yost, *J. Am. Chem. Soc.*, **48**, 152 (1926).
3. A. A. Noyes, J. L. Hoard, and K. S. Pitzer, *ibid.*, **57**, 1221 (1935).
4. A. A. Noyes, C. D. Coryell, F. Stitt, and A. Kosciakoff, *ibid.*, **59**, 1316 (1937).
5. B. M. Gordon and A. C. Wahl, *ibid.*, **80**, 273 (1958).
6. C. E. H. Bawn and D. Margerison, *Trans. Faraday Soc.*, **51**, 925 (1955).
7. R. Luther and F. Pokorny, *Z. anorg. u. allgem. Chem.*, **57**, 290 (1908).
8. P. Jones, H. Thirsk, and W. F. K. Wynne-Jones, *Trans. Faraday Soc.*, **52**, 1003 (1956).
9. M. Le Blanc and H. Sachse, *Physik. Z.*, **32**, 887 (1931).

Strain Electrometry and Corrosion, IV

Film Properties and Strain Potential

J. Calvin Giddings, Albert G. Funk, Carl J. Christensen, and Henry Eyring

University of Utah, Salt Lake City, Utah

ABSTRACT

Measurements of the strain transients have been recorded here for several metal electrodes including copper, aluminum, zinc, nickel, silver, and iron. The magnitude of the transients as a function of the percentage strain are treated by an extension of previous theoretical results. It is found that the transients depend on the position of an electrode in the emf series and on the protective nature of the film as predicted by the theoretical considerations. In addition, several experiments have been reported concerning the effect of corrosion inhibitors and organic coatings on strain transients. Some possible theoretical interpretations are made on these preliminary results.

It has been shown that the magnitude of the strain transient for a metallic wire is related to the chemical and physical nature of the protective film along with the chemical nature of the surrounding solution (1-3). In order to extend this study of rapid interface reactions we have measured and compared strain transients for a group of metals possessing films of greatly differing nature. It has been found possible to correlate approximately the relative values of these transients with the position of the metal in the electromotive series, for the same per cent strain, of the metals used (Cu, Al, Zn, Ni, Ag, and Fe). This is done using the concept that a stationary electrode potential is fixed when the rates of competing anodic and cathodic reactions are equal. A sudden strain causes film rupture, and temporary changes of the interface rates occur. The change is in such a direction as to account for the clean metal surface exposed when the film is broken. Metals such as aluminum show transients as high as a volt since, when the highly protective film is removed, the surface of the aluminum, which is very electropositive, reacts to yield aluminum ion. Metals such as iron, however, show much smaller transients, in the range of 100-200 mv. This results since the protective film on iron is sufficiently porous that the straining of the metal causes a relatively small increase in anodic area compared to that obtained by straining aluminum.

According to the same picture metals only slightly electropositive would be expected also to show small transients. The transient of silver is about 50 mv in confirmation of this general picture. The above picture can be written in a quantitative form that approximately describes these voltage transients under various conditions. In particular, an equation has been derived that relates the maximum voltage change, $-\Delta V_m$, to the fractional elongation of the wire electrode. Strain electrometry is another tool that can be used for the elucidation of the complex reactions of corrosion inhibitors. Preliminary results have been obtained in this important field.

The experimental methods used in strain electrometry have been described elsewhere (2, 3). The potentials recorded here are measured and recorded against the saturated calomel electrode.

Strain Transients of Metals

It is convenient to study the potential transients of strain electrometry in relation to Fig. 1. This schematic diagram is similar to one presented in an earlier publication (1), but here it is extended to include an approximate description of several metals.

Each electrode reaction has a reverse reaction acting to charge the electrode in the opposite direction. If only one reaction and its reverse were operative, an equilibrium electrode potential would be realized. These are denoted by the solid lines in Fig. 1. If more than one reaction is operative, the final, steady-state potential will differ from all of the equilibrium potentials. It will, however, lie nearest the equilibrium potential established by the fastest reactions. The steady-state potentials are shown as dotted lines. Potentials shown in Fig. 1 conform to the European sign convention.

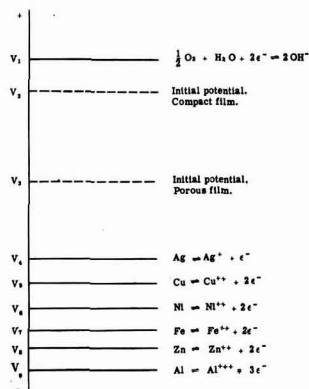


Fig. 1. Schematic diagram of equilibrium potentials and steady-state potentials for electrode reactions.

In most aerated solutions there are two reactions of paramount importance in establishing the steady-state potential. These are the oxygen reaction, tending to establish the potential at V_1 , and the metal, metal-ion reaction tending to establish the potential, in the typical case of Ni, at V_2 . If the metal possesses a highly protective film, the metal, metal-ion reaction is slowed considerably, since it has the equivalent of a small anodic area and the initial (before strain) steady-state potential is near the oxygen equilibrium potential, V_1 . Such metals are Ag, Cu, Ni, and Al with a steady-state potential shown at V_2 . These potentials are not all equal, but schematically they may be considered to be the same.

In the case of metals with a porous film, metal ions can escape easily into solution, and the initial steady-state potential is established nearer the metal, metal-ion pair. Probable examples are Fe and Zn with an initial, steady-state potential, V_2 .

When the metal electrode is suddenly strained, the brittle oxide film is ruptured, thus increasing the anodic area. This greatly facilitates the metal, metal-ion reaction and establishes a new potential nearer the metal, metal-ion pair. This potential is of short duration since various factors, such as re-growth of the oxide film and concentration polarization (caused by corrosion of the metal), tend to re-establish it at the original value.

It is clear from this discussion that the transient potential is dependent on the amount of strain. A larger strain causes the new potential to establish itself nearer the metal, metal-ion pair. Thus the potential difference that is recorded at the point of maximum change, ΔV_m , becomes more negative as strain increases. We return to this point later.

The strain transient recorded for a given metal, ΔV_m , is the difference between the initial steady-state potential and a potential that is close to that particular metal, metal-ion pair. This increases in magnitude (the values of ΔV_m are negative) as (a) the metal becomes more electropositive (higher in the emf series), thus establishing a larger negative potential with strain, and (b) the metal has a more compact film, for which the initial potential is more positive. Silver has the smallest transient, since it is not electropositive. It is likely in this case that hydrogen and metallic impurities in the silver cause the strain transient since, unless Ag^+ is extremely dilute, the Ag, Ag^+ equilibrium is higher than that for oxygen. (The reason, of course, that Fig. 1 is schematic is that every equilibrium potential depends on the concentration of some ionic species. Since these are greatly changed from one metal to another, due to polarization, etc., a completely accurate diagram cannot be made.) The value of $(-\Delta V_m)$ for silver at 7% strain is 39 mv, as shown in Table I.

Beyond silver, the value of $-\Delta V_m$ at 7% strain increases in the order of Cu, Fe, Ni, Zn, and Al; whereas, in order of increasing emf, they are Ag, Cu, Ni, Fe, Zn, and Al. The order of Fe and Ni has been reversed since the emf, by itself, does not account for the magnitude of the transient. This is better illustrated in Fig. 2 where $(-\Delta V_m)$ is plotted against

Table I. Transient potentials in distilled water at 7% strain; temperature, 25°C

Metal	Strain transient (approximate), mv
Aluminum	-800
Zinc	-224
Nickel	-194
Iron	-148
Copper	-95
Silver	-39

emf. A smooth curve is obtained with the exceptions of Fe and Zn. These lie below the curve in accord with the picture that a porous film will reduce the observed magnitude of the transient.

Dependence of Voltage on Relative Strain

It is useful to derive an approximate equation showing the dependence of $(-\Delta V_m)$ on the applied strain on the electrode. An equation derived in an earlier paper (1) reads

$$-\Delta V_m = \frac{kT}{ze} \ln \left(\frac{\epsilon u_{i0} \epsilon v_{i0}'}{\epsilon u_{i0}' \epsilon v_{i0}} \right)$$

where the terms, u_{i0} , u_{i0}' , v_{i0} , v_{i0}' are various reaction velocities ($cm^{-2} sec^{-1}$) of processes that transfer charge across the metal-solution interface: v_{i0} , i th anodic velocity, before strain; v_{i0}' , i th cathodic velocity, before strain; u_{i0} , i th anodic velocity, after strain; u_{i0}' , i th cathodic velocity, after strain. The reaction velocity "after strain" is the reaction velocity where the transient acquires a maximum value. The zero subscript simply means that these reaction velocities are all measured at some standard voltage. This voltage can be arbitrarily picked without changing the ratio of terms in Eq. [1]. The other terms are Boltzmann's constant, k ; the electron charge unit, e ; the temperature, T ; and the average charge, in electron charge units, transferred across the interface in a single process, z .

Approximations made in the derivations of Eq. [1] include, (a) the charge transferred in the i th

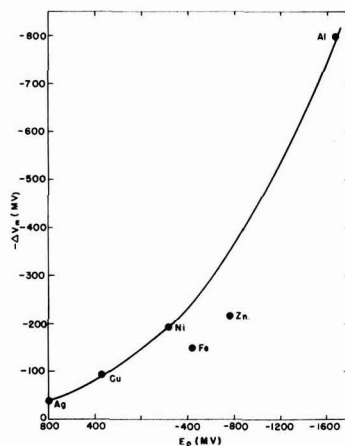


Fig. 2. Strain transients vs. the emf of metal electrodes. Distilled water at 25°C.

process, z , can be replaced by some average charge for all processes, z , and, (b) the potential energy barriers for these charge-transfer processes are symmetrical. In view of these approximations, and those to be introduced, only a rough agreement with experiment is expected.

The simplest assumption that can be made with respect to Eq. [1] is that the cathodic reaction velocity (at the fixed reference potential) is not changed as the electrode is strained.

$$\epsilon v_{i0}^1 = \epsilon u_{i0}^1 \quad [2]$$

The anodic reaction velocities at this potential, however, are increased since deformation of the metal increases the anodic area. We can assume that this increase in the anodic rate is proportional to the relative elongation of the electrode, s .

$$\epsilon u_{i0} = \epsilon v_{i0} + gs \quad [3]$$

where g is the relative anodic rate of a clean metal surface.

As s approaches zero, the anodic velocity after strain, u_{i0} , must approach the anodic velocity before strain, v_{i0} , as in Eq. [3].

When Eqs. [2] and [3] are substituted into Eq. [1], we obtain

$$-\Delta V_m = \frac{kT}{ze} \ln(1 + \alpha s) \quad [4]$$

where $\alpha = g/\epsilon v_{i0}$. This equation follows the approximate form of the experimental data, as shown in Fig. 3 for Cu. Best fit is obtained when $z = 0.92$ and $\alpha = 407$. For most of the metals used, α is considerably larger than unity in the higher range of s . When this assumption can be made, Eq. [4] has only the term (αs) remaining in the logarithm. Although this assumption results in a considerable error, particularly for Ag, Zn, and Fe, it is justified considering the approximate nature of the other assumptions introduced. With this assumption, then, we can write Eq. [4] as

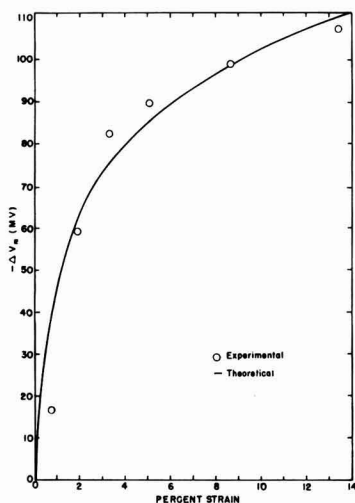


Fig. 3. Strain transient vs. per cent strain of copper

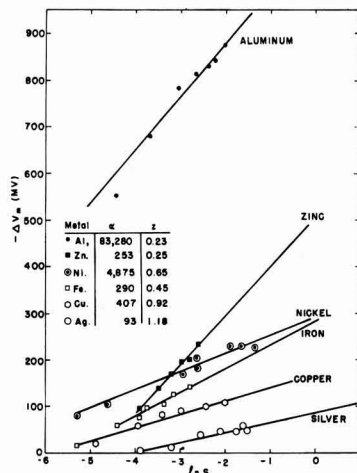


Fig. 4. Strain transients vs. $\ln(s)$. Distilled water at 25°C.

$$-\Delta V_m = \frac{kT}{ze} \ln \alpha + \frac{kT}{ze} \ln s \quad [5]$$

A plot of $-\Delta V_m$ vs. $\ln s$ is shown in Fig. 4. The slope of the line, kT/ze , determines z . The intercept at $\ln s = 0$ is $kT \ln \alpha/ze$. The values of z are of the right order except for Zn and Al. Whether this discrepancy is due to the back reaction of metal ions (thus violating Eq. [2]), or to some other effect, has not been ascertained.

The quantity α , as determined from experimental data, is interesting in its dependence on the nature of the metal and the oxide film. Since $\alpha = g/\epsilon v_{i0}$, it is determined by g , the relative anodic rate of a clean metal surface, and ϵv_{i0} , which is the anodic reaction rate of a metal surrounded by an oxide film. The latter quantity is proportional to the rate of dissolution of the metal ion through the oxide film, or the corrosion rate. The former quantity, g , should be an increasing function of the emf of the metal since the emf is a measure of the anodic rate of the clean metal surface. The values of α increase in the order, Ag, Zn, Fe, Cu, Ni, Al, which is the order in the emf series if Zn and Fe are excluded. Zinc and iron have unusually small values of α since the corrosion rate of these metals, appearing in the term ϵv_{i0} , is large.

Corrosion Inhibitors

The reactions due to corrosion inhibitors and promoters are expected to reflect themselves in the measured strain transients. The nature of the change in these transients depends on the type of reactions occurring. Thus, with most metals, a pH decrease leads to film dissolution, and a resultant decrease in the transient voltage. At the same time corrosion rates have been increased due to decreased film protection. In practice, many other reactions occur simultaneously and complicate the over-all picture, thus a sufficient pH decrease inhibits some corrosion processes (4). It is still valuable, however, to suggest the effects of single contributing reactions. These reactions may be important in the following ways.

Corrosion inhibitors and promoters are responsible for changing the rates of various electrode reactions. The changed reaction rates are reflected both in corrosion measurements and in strain-electrometry measurements. The latter shows promise of providing a rapid and sensitive measurement of reactions involved in corrosion. A good deal of additional knowledge is needed before this method can be employed generally. Preliminary results are reported here.

An acid is a common example of a corrosion promoter. The corrosion rate is greater and the strain-transient is smaller upon the addition of an acid. Both effects are due to the dissolution of the protective film. As indicated earlier, the strain-transient is a measure of the protective nature of the film, and if this is changed by added substances it is indicated immediately in an altered strain transient.

Inhibitors and promoters are involved in a large number of reactions in addition to those that dissolve the protective film. Although these cannot be enumerated fully at present, a number of reasonable postulates can be made. We may assume, for instance, that some added substances alter the structure of the film—something short of dissolution. Depending on the structure change, corrosion may be promoted or inhibited. Another reaction that has been discussed extensively is ion and molecular adsorption; such adsorption is effective in inhibiting the anodic dissolution of the metal (5-8).

It is well known that the corrosion rate of any given metal depends on the potential of the metal with respect to its environment (9). This potential can be altered by electrical means or by chemical reactions. Thus the addition of oxygen to a metal surface leads to a more positive potential in an aqueous environment; this in turn speeds the reaction of metal ions, $M \rightarrow M^{n+} + ne^-$, and thus the corrosion rate is increased. In some cases however, the adsorption of oxygen inhibits corrosion due to its effect on the oxide film. Thus oxygen can work simultaneously in opposite ways in its effect on corrosion rates. Similar effects might be expected for many additives.

One class of corrosion inhibitors are strong oxidizing agents such as $KMnO_4$ and $K_2Cr_2O_7$. These substances usually act in such a way as to make the potential more positive. This effect by itself would promote corrosion, so apparently there are additional effects (6-8, 10). Another effect such as the surface adsorption (7, 8) of MnO_4^- or $Cr_2O_7^{2-}$ must be responsible for the inhibiting effect.

Table II shows the effect of these inhibitors on aluminum, brass, zinc, iron, and copper in different solutions. The value of the potential is given before strain, V_o , and at the maximum of the transient, V_m , the difference, is the maximum value of the strain transient (the potential amplitude) $V_m - V_o = \Delta V_m$.

Several interesting features are shown in Table II. First, it may be seen that the V_o of Al is not shifted in the positive direction by $KMnO_4$. It is expected that in this strongly basic solution other reactions are rapid enough to overshadow the oxidation of the metal by $KMnO_4$. This reaction, of course, would shift the potential in the positive direction. When

Table II. Effect of oxidizing inhibitors on strain transients and electrode potentials. Saturated calomel reference is used, 4% strain.

Electrode and solution	Inhibitors		Without inhibitors, mv	With inhibitors, mv
Copper in HOH	0.2% $K_2Cr_2O_7$	V_o	4	35
		V_m	-81	59
		ΔV_m	-85	24
Copper in $CaCl_2$ (one half saturated)	0.07% Na_2CrO_4	V_o	-350	-250
		V_m	-373	-270
		ΔV_m	-23	-20
Aluminum in 10% NaCl	0.1% K_2CrO_7	V_o	-680	-680
		V_m	-1430	-1430
		ΔV_m	-750	-750
Aluminum in 0.3 N NaOH	0.1% $KMnO_4$	V_o	-1300	-1300
		V_m	-1317	-1274
		ΔV_m	-17	26
Brass in HOH	0.2% $K_2Cr_2O_7$	V_o	-32	142
		V_m	-157	22
		ΔV_m	-125	-120
Brass in $CaCl_2$ (one half saturated)	0.07% Na_2CrO_4	V_o	-400	-215
		V_m	-449	-246
		ΔV_m	-49	-31
Zinc in HOH	0.2% $K_2Cr_2O_7$	V_o	-690	-440
		V_m	-863	-580
		ΔV_m	-173	-140
Iron in HOH	0.2% $K_2Cr_2O_7$	V_o	-250	72
		V_m	-382	-179
		ΔV_m	-132	-107

the electrode is strained, V_m is more positive in the presence than in the absence of inhibitor. It is possible that the reduction of $KMnO_4$ has been catalyzed by some newly exposed surface sites.

Several of the strain transients involve two peaks instead of one. Only the larger peak is shown in Table II. Copper in distilled water with inhibitor shows a negative transient with $\Delta V_m = -15$ mv and a positive transient with $\Delta V_m = +24$ mv. In calcium chloride solution with inhibitor the two amplitudes are -20 mv and +16 mv. The time elapse between the two peaks is approximately 0.25 sec in the first case and 1.5 sec in the second. Only a single peak is observed in the absence of inhibitor. Aluminum shows a similar behavior, but the first peak, a negative one, occurs with an amplitude of only about 1 mv.

In the cases mentioned above, it appears that the reactions occurring in the first 0.01 sec or so after strain are the same as when the inhibitor is not present. After this very rapid negative surge, supposedly due to anodic dissolution of the metal, a cathodic process becomes predominant. Either the effect of cathodic reactions has increased, or anodic reaction rates have decreased. It is possible that new surface sites are exposed with strain, and the anodic reaction proceeds briefly before the inhibitor becomes effective in this newly exposed region. Or it is possible that the inhibitor must diffuse to the new surface, after which it becomes reduced in a cathodic reaction. In either case, this effect is an interesting reflection of inhibitor reactions.

A great number of substances are used to decrease corrosion other than those already discussed. A few examples are shown in Table III. Especially prominent in protecting metals against corrosion are those substances that form a distinct physical coating in addition to any that might exist by virtue of

Table III. Effects of inhibitors and organic coatings on strain transients and electrode potentials. Saturated calomel reference is used; strain, 4%

Electrode and solution	Inhibitors		Without inhibitors, mv	With inhibitors, mv
Nickel in HOH	Black paint	V_o	-170	-250
		V_m	-285	-262
		ΔV_m	-115	-12
Nickel in HOH	Red enamel	V_o	-170	-240
		V_m	-345	-260
		ΔV_m	-175	-20
Iron in HOH	Black paint	V_o	-250	-300
		V_m	-282	-328
		ΔV_m	-132	-28
Iron in HOH	Red enamel	V_o	-250	-334
		V_m	-282	-374
		ΔV_m	-132	-40
Iron in glycerol	0.6% oleic acid	V_o	-125	-180
		V_m	-185	-192
		ΔV_m	-60	-12
Iron in 3% NaCl	20% NaNO ₂	V_o	-520	-200
		V_m	-538	-322
		ΔV_m	-18	-122

the metal oxide on the surface. Films formed by organic substances fall into the general classes (11): paints, varnishes, enamels, lacquers, plastic films, and bitumens. The results of strain-electrometry measurements with a paint and a varnish are reported here as examples of organic coatings. Results were obtained with both Ni and Fe, and are reported in Table III. The initial potentials become negative when the coating is applied (with excessively thick coatings the electrode is insulated to such an extent that the potential cannot be measured). The strain transients are smaller than without the coating. The potential at the maximum of the transient, V_m , is not strongly altered when the coating is used. Apparently the new film is partially ruptured just as

oxide films are. Since V_m is about the same in either case, similar regions of anodic (metallic) surface must be exposed.

These results give an indication of the brittleness and the protective nature of the artificial coatings as well as showing their role in altering the potential in comparison to inhibitors.

Acknowledgment

The authors would like to acknowledge grants from the Atomic Energy Commission, Contract No. At (11-1)-82, Project No. 1, and Army Ordnance Research Contract No. DA-94-495-ORD-959, in support of this work.

Manuscript received May 5, 1958.

Any discussion of this paper will appear in a Discussion Section to be published in the December 1959 JOURNAL.

REFERENCES

1. A. G. Funk, J. C. Giddings, C. J. Christensen, and H. Eyring, *Proc. Nat'l. Acad. Sci.*, **43**, 421 (1957).
2. A. G. Funk, J. C. Giddings, C. J. Christensen, and H. Eyring, *J. Phys. Chem.*, **61**, 1179 (1957).
3. A. G. Funk, D. N. Chakravarty, H. Eyring, and C. J. Christensen, *Z. Physik. Chem.*, **15**, 64 (1958).
4. H. H. Uhlig, "Corrosion Handbook," p. 20, John Wiley & Sons, Inc., New York (1948).
5. G. H. Cartledge, *J. Phys. Chem.*, **60**, 28 (1956).
6. N. Hackerman, and S. J. Stephens, *J. Phys. Chem.*, **58**, 904 (1954); N. Hackerman, and R. A. Powers, *ibid.*, **57**, 139 (1953).
7. H. H. Uhlig and A. Geary, *This Journal*, **101**, 215 (1954); H. H. Uhlig, *Chem. Eng. News*, **29**, 3154 (1946).
8. H. C. Gatos, *Corrosion*, **12**, 39 (1956); H. C. Gatos, *This Journal*, **101**, 433 (1954).
9. O. Gatty and E. C. R. Spooner, "The Electrode-Potential Behavior of Corroding Metals in Aqueous Solutions," Clarendon Press, p. 22, Oxford (1938).
10. U. R. Evans, "Metallic Corrosion Passivity and Protection," Edward Arnold and Co., London (1948).
11. K. G. Compton, *Corrosion*, **4**, 112 (1948).

Oriented Dioxide Films on Uranium

J. T. Waber, J. A. O'Rourke, and R. Kleinberg

University of California, Los Alamos Scientific Laboratory, Los Alamos, New Mexico

ABSTRACT

The growth habit of UO_2 on uranium during the oxidation by water vapor has been analyzed with the aid of detailed x-ray diffraction work and pole figures. The dioxide grows with a (110) planar texture which bears no epitaxial relation to the underlying metal crystallites. Although the polycrystalline alpha uranium has a strong and anisotropic preferred orientation as a result of fabrication, the oxide forms without azimuthal directionality in the plane of contact. The lack of alignment in the plane of contact also was confirmed in an experiment with a single crystal of uranium.

The texture of UO_2 formed during annealing in vacuum also was found to be planar without significant directionality. In such cases, the (100) planes were parallel to the surface of the metal substrate, and large amounts of uranium monoxide always were present in such films. Subsequent oxidation of specimens covered with the (100) texture yielded the characteristic (110) dioxide texture.

In incidental experimental work on the vapor deposition of UO_2 the octahedral or (111) texture was observed on glass and tantalum substrates, and the cubic or (100) texture was developed on several ionic substrates.

In a preliminary investigation, the rate law for the formation of uranium dioxide under conditions which produce such oriented films was found to be logarithmic.

Oriented layers of uranium dioxide form without any evident relationship to the orientation of parent metal during high-temperature exposure to moderate vacuum and water vapor. This occurrence appears to be unusual since it is commonly thought that the first layers of oxide are oriented epitaxially with the parent metal. For example, Gulbransen and Ruka (1), employing electron diffraction, showed that strongly oriented films are obtained on iron in $\text{H}_2 + \text{H}_2\text{O}$ mixtures and that these bear a rational epitaxial relationship to underlying metal. Mehl and McCandless (2) oxidized single crystals of iron in wet hydrogen and obtained the same epitaxial relations by x-ray diffraction on films thick enough to show interference colors.

Mehl, McCandless, and Rhines (3) were probably the first investigators to discuss the orientation of Cu_2O on copper. The results of eleven subsequent studies were reviewed by Lawless and Gwathmey (4). These authors made a very careful investigation of the degree of orientation of Cu_2O as a function of temperature, oxide thickness, and crystal face of the copper crystal. The degree of orientation increased with reaction temperature but decreased with oxide thickness. These studies were all conducted on relatively thick films.

Recently Harris, Ball, and Gwathmey (5) published the results of a very thorough electron microscope and electron diffraction study of the first few Angstroms of Cu_2O formed on copper single crystals. They found that the degree as well as the symmetry of orientation increased with oxide thickness. This confirmed the earlier observation of Pinsker and Tatrino (6). More specifically, Harris, Ball, and Gwathmey observed that the thin films were com-

posed of small oxide crystals having "... particular planes parallel to particular planes of the copper and random orientation about the plane normal. This orientation is designated type II. The oriented oxide of the thicker films was made up of oxide crystals with particular planes parallel to particular planes of the copper but with a common zone axis in the plane. This orientation is designated as type III. The common planes were: (110) Cu_2O /(311) Cu , (111) Cu_2O /(111) Cu , and (111) Cu_2O /(100) Cu . The common zone axis was [110]." That is, in thicker films, the degree of orientation increased so that the [110] direction in the oxide became parallel to [110] direction on the underlying copper. This parallelism was discussed also by Lawless and Gwathmey (4).

Oxide films with only one degree of orientation (type II cited by Harris, *et al.*) generally have not been recognized as they are evidenced only by unusual differences in line intensities on the diffraction pattern. Kerr and Wilman (7), in a recent electron diffraction study, reported that BeO forms on randomly oriented beryllium (either abraded or electropolished) with a (001) planar orientation at temperatures from 400° to 500°C and with a mean (100) orientation above 700°C.

Although unusual differences in line intensities on a diffraction pattern imply preferred orientation of the material under study it is difficult to identify the texture with certainty from these alone. Usually a pole figure technique is the only satisfactory method of studying texture. Very thin films are not readily studied by x-ray diffraction techniques, however, and the more complicated methods entailed in the study of texture by electron diffraction methods must be utilized. As far as the authors are

aware, only Harris, Ball, and Gwathmey have been able to verify in this way the suspected orientation of initially formed films.

Fortunately, for studies of UO_2 films, x-ray diffraction methods are adequate. Films of UO_2 , thin enough to exhibit interference colors (200-300Å), can be studied satisfactorily by x-ray techniques.

It was possible in the present research to form, in a moderate vacuum, one planar orientation of UO_2 without azimuthal alignment in the surface plane and subsequently to convert it to a second planar orientation when the specimens were heated and oxidized in water vapor. To a large extent, the experiments described here deal with oxide films formed on polycrystalline uranium sheet. Both abraded and electropolished samples were studied. An experiment with a single crystal of uranium metal confirmed the conclusion that the growth habit of UO_2 films does not bear a unique relationship to the orientation of the underlying metal.

Pertinent Crystal Structures

An excellent summary of the physical and chemical properties of uranium metal has been published (8). With increasing temperature, at 668°C the orthorhombic alpha phase changes to a complex tetragonal beta phase. Above 774°C, the latter changes to the body-centered cubic phase which is then stable to the melting point at 1132°C.

Uranium dioxide is the principal compound formed during oxidation of uranium. It has the CaF_2 structure, and the stoichiometric compound has a lattice parameter of $a_0 = 5.470\text{\AA}$. Belle and Lustman (9) have reviewed the extensive information on the physical properties and chemical reactivity of UO_2 . An oxide, referred to in this paper as the monoxide, having an x-ray structure compatible with the composition UO (an NaCl type structure with $a_0 = 4.93\text{\AA}$) has been observed by many investigators to form during the vacuum annealing of uranium. There is doubt that it is an equilibrium phase in the U-O system.

Experiment

The texture of the cold-rolled metal was first studied prior to oxidation. The reader is referred to a standard text (11) for details of constructing pole figures and interpreting orientation textures from them. Using a modified Schulz camera mounted on a Norelco wide range goniometer (10), pole figures were prepared from samples of sheet which had received varying amounts of cold reduction, both with and without subsequent annealing. Since only the center 60° of each pole figure could be obtained from the flat sheet as such, longitudinal and transverse sections through the sheet were necessary to complete each pole figure. These were prepared by sectioning the sheet in the appropriate directions, as indicated in Fig. 1, and then rotating the segments 90° about their long axis and bolting them together again. In the following discussions the bolted compacts which had been prepared from longitudinally sectioned segments, i.e., those which had been rotated 90° about the rolling direction RD as axis, are designated by the letter L following the sample number, while those prepared from transverse sections are designated by the letter T.

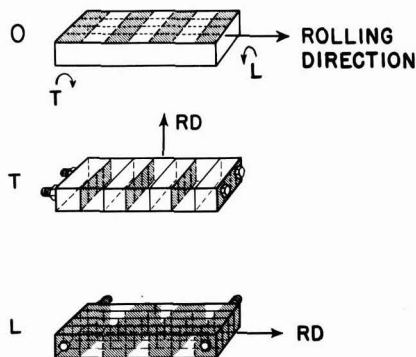


Fig. 1. Surfaces of uranium presented for oxidation by the rolled metal as well as the bolted compacts.

Since the oxide did not deposit epitaxially, details of the various metal textures developed during rolling are omitted here. It is sufficient to show that highly oriented textures were developed. This fact is demonstrated in Fig. 2, which shows the pole figure of an 86% cold-rolled uranium sheet. The same major texture developed here with a spread between $(102)[010]$ to $(203)[010]$ was evidenced by all the unrecrystallized samples used in this work. Different crystallographic planes, then, are predominantly parallel to the surface in the normal, transverse, and longitudinal samples. For example, if the (102) planes are parallel to the surface of the rolled sheet, (010) and (203) planes are parallel to the surface in the transverse and longitudinal sections, respectively.

The pole figure study of the dioxide presented a somewhat different problem. Here the (110) or (100) textures were developed on all of the sections, and were developed independently of the orientation of the underlying metal. Only the inner 60° of the pole figure could be plotted from an examination of the oxidized surfaces as such, and any study of the outer periphery would involve oxidizing the flat segments nearly to completion and then rotating

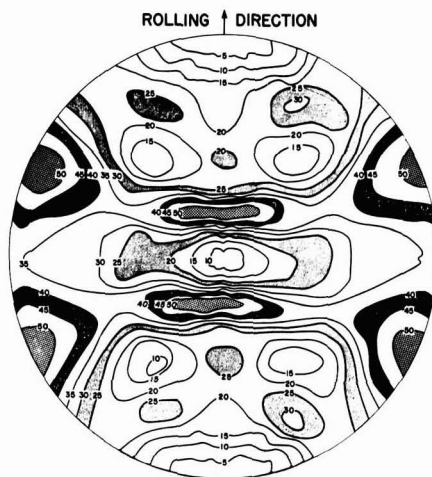


Fig. 2. The (111) pole figure of cold rolled alpha uranium

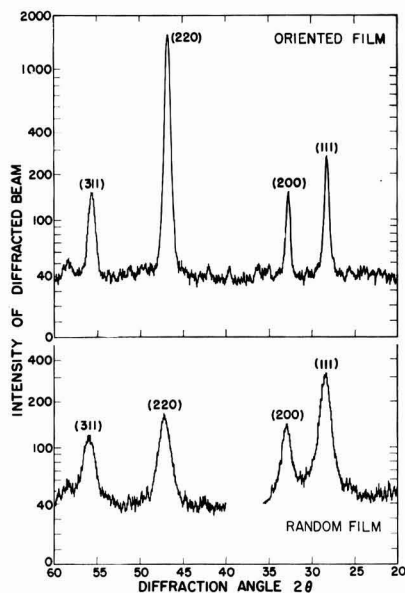


Fig. 3. Powder patterns taken of UO_2 films on uranium. Intensities are plotted on a logarithmic scale. The randomly oriented film occurred on a uranium sample after 10-hr immersion in boiling water. Ratio of the intensity of (220) to (111) is equal to the ideal value of 0.46. The oriented film occurred on the uranium after 40-min exposure to 22 mm water vapor at 400°C . The intensity ratio $I_{(220)}/I_{(111)}$ was 6.6. The triplet of alpha uranium lines which lie near the Debye 2θ angle of 36° has been omitted in the random pattern to simplify the pattern and reduce confusion.

them 90° about the long axis and bolting them together, as illustrated in Fig. 1. The necessity for resorting to this lengthy procedure was overcome by preparing pole traces of several different planes and using known crystallographic relationships for completing the analysis.

Once the nature of the orientation texture has been established, a semiquantitative estimate of the degree of orientation could be obtained from the relative intensities of lines on a diffractometer tracing. The ratios $I_{(220)}/I_{(111)}$ and $I_{(300)}/I_{(111)}$ were utilized in much of the oxidation study to evaluate the development of the (110) and (100) textures. An example of such a tracing is given in Fig. 3, together with a tracing illustrating a nearly random texture. The oriented film pattern is from a sheet sample oxidized in water vapor and exhibiting a fairly strong (110) texture. Here, the ratio of $I_{(220)}/I_{(111)}$ is 6.6, and values as high as 35 were observed in the course of the experiments. The intensity ratios for a random sample using various planes are given in Table I.

Table I. Calculated relative intensities of x-ray diffraction lines for uranium dioxide

Plane (hkl)	$I_{(hkl)}/I_{(111)}$
111	1.00
200	0.38
220	0.46
331	0.51
222	0.11

Table II. Relative intensity of oxide x-ray reflections following oxidation in vacuo

Specimen No.	Test conditions			Relative intensity		UO ₂ intensity ratios	
	$^\circ\text{C}$	hr	mm Hg UO	(111)	UO ₂ (111)	$I_{(200)}/I_{(111)}$	$I_{(220)}/I_{(111)}$
2130	400	1½	10^{-5}	20	25	6.4	1.0
1952	600	½	10^{-6}	170	50	3.0	0.4
1954	600	¼	10^{-6}	70	20	3.75	0.3
1802	1000	19	10^{-5}	210	32	1.56	0.6

Results

Several pole figures were constructed for mechanically polished specimens heated in a vacuum of 10^{-5} mm Hg or better. This metal was oxidized by the residual gas in the vacuum system. Both uranium dioxide and uranium monoxide were present in the film. Analysis of the pole figures for these vacuum treated specimens established that the (100) planes of the dioxide were formed parallel to the metal substrate during vacuum oxidation.

Oxidation experiments were conducted at 400° , 600° , and 1000°C . Results are summarized in Table II. At each of these temperatures, the dioxide is oriented principally with its (100) planes parallel to the specimen surface. Uranium monoxide was formed simultaneously in all such films, and the restraint it imposed on the texture of the dioxide is not known.

The relative amounts of monoxide in the films are indicated somewhat semiquantitatively by the relative intensities of the (111) lines of the UO and UO_2 , since the scattering factor for this plane of the monoxide is approximately 91% of that for the dioxide. More quantitative estimates would require that both oxides have a similar or random orientation.

Oxidation in water vapor appears to favor the formation of the (110) or dodecahedral orientation. Several (110) and (100) pole figures were prepared from samples oxidized in water vapor. One such pole figure is presented in Fig. 4 to illustrate the relatively small spread in the angle of inclination between the pole of plane investigated and the [110] pole of the oxide. The weak directionality indicated by the broken "ring" in Fig. 4 is believed to result from the physical dimensions of the sample (the x-ray beam covered an area slightly larger than the sample in one of its orientations) rather than from any real directionality. A strong (100) texture having little or no directionality was always developed during vacuum annealing.

Starting with the oxidized sheet having the (100) or cubic texture it was possible to oxidize the metal further in water vapor and develop the (110) orientation. Admittedly, the texture was less highly oriented when preformed layers were present. One metal sample was oxidized in vacuum at 600°C and examined by x-ray diffraction to establish the nature of the film. This sample and another mechanically polished piece of the same rolled stock were placed in the furnace and oxidized at 600°C and at a water vapor pressure of 0.3 mm Hg. After x-ray determination, the two samples were replaced in the furnace and oxidized for 1 hr at 6.2 mm pressure. As indicated in Table III a significant increase in the

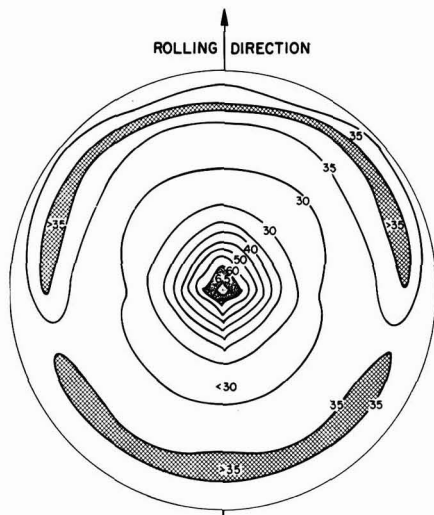


Fig. 4. Typical (110) pole figure of uranium dioxide which was formed on rolled alpha uranium sheet by oxidation in water vapor. Only the inner 60° of the stereographic projection is drawn here. The central peak and the incomplete ring illustrate the lack of significant azimuthal directionality. The intensity ratio $I_{(200)}/I_{(111)}$ was 5.6.

(110) component was observed. Specimen 1954 (Table II) was subsequently oxidized in water vapor at 600°C. Pole figures constructed using the (200) and (220) planes of UO_2 confirmed that the UO_2 was forming with the (110) planes predominantly parallel to the specimen surface.

Bolted metal compacts were oxidized for 40 min at 400°C and at 17–28.4 mm Hg water pressures. Pertinent test data are presented in Table IV. The electropolished specimen, 2130L, was heated in vacuum (10^{-6} mm Hg) at 400°C for 90 min. The predominant orientation appeared to be that of the (100) UO_2 planes parallel to the surface. This sample was oxidized to form sample 2131 which then exhibited a pronounced (110) or dodecahedral texture. The preformed (100) orientation, then, did not deter the (110) formation on subsequent oxidation.

Pole figure studies of samples, oxidized as indicated in Table III and IV, established that the uranium dioxide formed with a planar orientation on

Table III. Comparison of the degree of orientation resulting from the oxidation of preformed films at 600°C

Specimen No.	Treatment given	Orientation ratio*	
		$I_{(200)}/I_{(200)\dagger}$	$I_{(200)}/I_{(111)}$
1952	Vacuum, ½ hr	0.25, 0.09	1.6, 3.8
1952	Vacuum, 1 hr	0.25, 0.20	1.7, 3.3
1952a	Vacuum + 0.3 mm Hg	0.23, 0.30	2.0, 1.5
1952b	Vacuum + 0.3 mm + 6.2 mm	0.45, 0.48	0.79, 0.83
1966	0.3 mm	0.74, 0.89	5.4, 4.0
1966a	0.3 mm + 6.2 mm	1.29, 1.86	4.0, 4.0

* Duplicate values are for observations made, respectively, parallel and transverse to the rolling direction.

† Intensity ratio for random samples is 1.21.

Table IV. Orientation ratios and test conditions

Specimen No.	Preliminary treatment	Water pressure	Ratio of intensities	
			$I_{(200)}/I_{(111)}$	$I_{(200)}/I_{(111)}$
2130L	Electropolished	Vacuum	1.0	6.4
2131L	Vac. anneal	28.4 mm Hg	1.0	0.30
2132L	Electropolished	28.4	1.80	0.59
2133T	Electropolished	17.0	18.2	1.47
2134T	Electropolished	17.0	35.0	2.70
2135L	Front, electropolished	22.1	2.4	0.26
2135L	Back, after mech. polish	22.1	2.7	0.27
2136L	Electropolished	22.1	6.4	0.5

the sheet surface, and that there was definitely no epitaxial relationship between this oxide and the underlying metal. Longitudinal, transverse, and normal samples of the same rolled sheet all exhibited identical textures when oxidized under like conditions.

A second texture develops, during this recrystallization of uranium, with the [140] pole parallel to the original rolling direction and with the poles of the planes parallel to the sheet surface having a small spread about [112]. By using bolted compacts, two other metal planes were examined to ascertain whether they influenced the oxide orientation markedly. Six such compacts were oxidized simultaneously in 20 mm Hg water pressure for 3 hr at 450°C. Data are summarized in Table V.

It is reasonable to conclude that the same dodecahedral texture devoid of azimuthal directionality developed on the recrystallized metal as well.

Single-Crystal Experiment

It was possible to confirm these conclusions with a "single crystal" of uranium obtained from Argonne National Laboratory. It was a cylinder approximately ⅛ in. in diameter and ¾ in. long, and contained five grains. The largest of these grains filled the central cross section of the cylinder and extended along the axis in both directions.

Following oxidation in water vapor at 450°C and a pressure of 15 mm Hg for 17 min, it was examined by Olsen,¹ using a cylindrical x-ray camera. Six photographs were taken at different angles normal to the cylindrical axis; three of these photographs were overlapping oscillation patterns covering an angular range of 44°. Fairly uniform diffraction

¹ C. E. Olsen, Los Alamos Scientific Laboratory, Los Alamos, N. Mex.

Table V. Orientation ratios for the oxidation of rolled and recrystallized uranium sheet

Specimen No.	Ratio of intensities	
	$I_{(200)}/I_{(111)}$	$I_{(200)}/I_{(111)}$
Rolled Sheet		
2918 as rolled	4.82	1.38
2919 longitudinal	2.46	0.34
2920 transverse	3.20	0.38
Recrystallized Sheet		
4123 as rolled	5.21	1.37
4124 longitudinal	1.89	0.43
4125 transverse	1.44	0.57

"rings" were obtained and there was no evidence of preferred alignment between the metal and oxide. The (110) planar orientation was concluded to have formed on the cylindrical metal surface.

Other Observations of Oxide Orientation

Numerous additional examples of the preferred growth habits of UO_2 can be gained from a study of the literature. Uranite and other minerals involving partial replacement of the uranium atoms, such as thorianite, occur mainly as cubes and octahedrons (12). Occasionally, dodecahedrons are found.

The octahedral or (111) growth habit was observed during an electron diffraction (13) study of a vapor deposit of UO_2 formed on a smooth glass substrate. When it was deposited under similar conditions on tantalum, the [111] pole was not perpendicular to the substrate as on glass but was inclined to it, which suggests that the higher thermal conductivity of tantalum reduced the substrate surface temperature and thus reduced the surface mobility.

Wilman and co-workers (7,14-16) have discussed numerous examples of oriented overgrowths. In particular, they evaporated various metals and ionic salts onto substrates in such a way that the line of flight taken by the evaporating substance was oblique to the surface of the substrate. Low melting materials were observed to be arranged with some rational and densely packed plane parallel to the substrate surface. However, with refractory materials, the orientation axis of the deposit was inclined to the surface presented by the substrate, and the direction of preferred growth was approximately parallel to the line of flight. When the substrate has good thermal conductivity the kinetic energy of the depositing material is reduced and the molecules lose a portion of their surface mobility. If the substrate does not conduct heat well, high surface temperatures, high surface mobilities, and thus more perfectly oriented deposits are to be expected.

The cubic or (100) growth habit was observed for heated substrates (17). Uranium dioxide was distilled from a tungsten boat at approximately 2800°C in an evacuated system containing a few millimeters of hydrogen and was deposited onto a polished single crystal of either CaF_2 or KBr which was held at approximately 600°C . The deposit showed preferred orientation with the (200) line being very prominent.

Thus vapor deposition favors the same two growth habits that are found in naturally occurring crystals. The dodecahedral habit, however, is associated with the oxidation of uranium. Mogard (18) reported that, during the corrosion of uranium in molten sodium, uranium dioxide forms by combining with the small amounts of oxygen dissolved and entrained as Na_2O in the molten sodium. The films formed at 475°C exhibited the (110) planar orientation. At higher temperatures, a porous and relatively nonoriented layer occurred on top of the coherent hard oxide layer adjacent to the base metal. During the cathodic vacuum etching of uranium in tank argon, thin UO_2 films form. These films are formed with the (110) planes parallel to the metal substrate.

These observations suggest that the formation of this dodecahedral orientation results from growth of the oxide film in a preferred direction. The interfacial temperature of the uranium is probably high enough during oxidation to permit surface migration and preferred growth of those oxide crystallites which are favorably oriented.

Rate Law Involved

Rate data were obtained in connection with the orientation of the oxide. It is surprising that a logarithmic law is followed. Doubtless this can only occur at such a high temperature because of the low pressure of the oxidant, water.

The change in weight of the specimen was determined from the extension of a fused silica spiral spring. By using three springs, which were each able to support 3-g loads safely, and by arranging them in tandem, a spring constant of 10.84 cm/g was obtained at room temperature. A 1-mg change in weight corresponded to a 0.108-mm extension, which could be read easily with a cathetometer. The spring constant was determined with the furnace in place and with the specimen, bucket, and a portion of the spring at 400°C . For example, it was found that the helix, with the bucket containing a piece of gold, changed in length from 40.950 cm at room temperature to 41.150 cm at 400°C mainly as a result of the change in the spring constant.

The system was evacuated and the specimen brought to temperature and equilibrated for approximately 1 hr. The water was admitted to the system by breaking a sealed ampoule in that portion of the system at room temperature. The initial cathetometer reading was taken approximately $\frac{1}{2}$ min after the reaction commenced.

The high-purity uranium metal used for this test was rolled to approximately 0.002 in. thick sheet and annealed. This annealed sheet was cut and polished through 4/0 metallographic paper. An extension of 0.1 mm corresponded to a weight increase of $30.67 \mu\text{g}/\text{cm}^2$ of the specimen.

Typical weight changes with time are illustrated in Fig. 5 for two separate runs conducted at 400°C

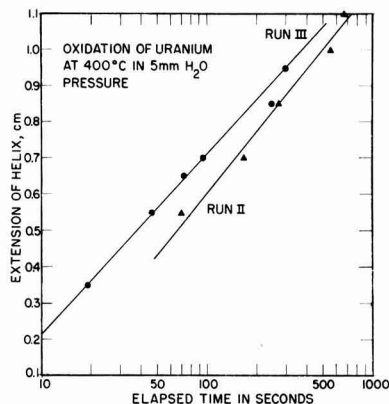


Fig. 5. Semi-logarithmic plot of the length of the silica helical spring vs. the duration of oxidation. Data are for two separate runs at 400°C .

and 5 mm water pressure. A logarithmic growth law was obtained with a fair degree of reproducibility.

The orientation of the oxide was examined after removal of the samples from the furnace. The ratios $I_{(200)}/I_{(111)}$ were found to be 1.1 for Run II and 2.15 for Run III.

Discussion

Several hypotheses could be advanced which would afford an explanation for the formation of the planar texture of the overgrowth. One of the most logical explanations would involve the use of dislocation theory. A thin layer of oxide next to the metal is disorganized and is not aligned epitaxially with the metal. A few oxide grains will contain, or form, one dislocation emerging essentially perpendicular to the specimen surface. Diffusion of ions along this dislocation will be relatively rapid, as has been indicated by the experiments of Turnbull and Hoffman (19, 20) on the self-diffusion of silver along grain boundaries. Inward diffusion of oxygen along such dislocation "pipes" will increase the rate of oxidation. Thus oxide grains with favorably oriented dislocations will penetrate faster. The favored grains need have no azimuthal relation to the substrate. At a later stage, when such a grain has penetrated more deeply than most, the diffusion resistance along this dislocation pipe will increase until it is equal to that along most paths. The tip of the favorably oriented grain will then advance inwardly at almost the same rate as does the bulk of the oxide. However, an alternative path lying partly along the dislocation and partly perpendicular to it has lower resistance. Thus the penetrating grain will spread laterally near the interface and will become roughly pyramidal. The high temperature in the oxide film from the heat of reaction will facilitate the recrystallization of the disorganized oxide thus enlarging the large favorable grains. Experiments to establish the essential features of this explanation are in progress.

Two important studies have been reported recently. Miller and Lawless (22) have obtained electron-photomicrographs of spiral growth terraces such as are associated with screw dislocations on Cu_2O polyhedra formed on copper single crystals. An experiment by Harris, Ball, and Gwathmey (5) strongly indicated that the nucleation and formation of Cu_2O polyhedra was related to dislocations in the copper itself. These polyhedra are oriented with a common [110] zone axis in the interface as cited above for the thick oxide films (4, 5). Webb and Foreng (23) have observed the formation of $\alpha\text{-Al}_2\text{O}_3$ whiskers and platelets during the oxidation of aluminum or of AlTi in wet hydrogen at $1300^\circ\text{--}1500^\circ\text{K}$. Invariably the whiskers were single crystals with the [001] direction parallel to the principal growth direction. Dragsdorf and Webb (24) have shown that these whiskers contain screw dislocations. Terraced growth steps have been observed optically on $\alpha\text{-Al}_2\text{O}_3$ platelets.

The formation of a smooth oxide film of uniform thickness can no longer be envisaged as the proper description. The growth and nucleation of discrete oxide grains are the dominant processes initially. Similar phenomena have been observed for the for-

mation of AgBr on silver by Newman and Pashley (25). More work is needed to elucidate the role of dislocations in the metal substrate and in the compound formed.

Belle and Lustman (9) have reviewed the evidence which leads to the conclusion that ionic migration in UO_2 occurs by the diffusion of anions. The formation of anti-Frenkel defects (interchange between an anion in its sublattice with a vacant interstitial site) contributes to the higher mobility of anions in the fluorite lattice as Ure (21) has shown for doped CaF_2 . Because of this anion diffusion, the dioxide grows inward during the oxidation of uranium leaving superficial markers unaffected on the original surface. Thus external growth patterns are not anticipated in the UO_2 .

Conclusion

It has been shown that uranium dioxide formed by the reaction of uranium with water vapor at moderate temperatures occurs with a distinctive growth habit. The (110) planes of the dioxide lie parallel to the surface of the polycrystalline uranium substrate. No evidence was found for an epitaxial relation between the metal and the oxide. Although preformed dioxide films having a (100) planar texture were developed, subsequent oxidation yielded the (110) texture.

The formation of the dodecahedral texture is uncommon in naturally occurring crystals or in vapor deposition. The planar texture is explained on the basis of recrystallization of the oxide and preferential growth of oxide grains containing favorably oriented dislocations.

Acknowledgment

The authors are deeply indebted to Professor Robert Brick for his interest in the problem and for his valuable suggestions during the course of the work. The single crystal of uranium was generously given by Dr. Frank G. Foote of Argonne National Laboratory. The assistance of many members of the laboratory in connection with the experimental work and the preparation of this report is gratefully acknowledged. Particularly we should like to mention Donald Prys and Marguerite Coleman. Dr. R. B. Roof, Jr., calculated the intensity of the lines in the UO_2 x-ray diffraction pattern. Edward S. Wright, Dawn D. Whyte, and William R. Hickey contributed to the experimental work.

Manuscript received Nov. 26, 1956. A portion of this paper was prepared for delivery before the Cleveland Meeting, Sept. 30-Oct. 4, 1956 and a portion was reported at the Gordon Research Conference on Oxidation Processes, New London, N. H., July 1954. The work was done under the auspices of the Atomic Energy Commission.

Any discussion of this paper will appear in a Discussion Section to be published in the December 1959 JOURNAL.

REFERENCES

1. E. A. Gulbransen and R. Ruka, *This Journal*, **99**, 360 (1952); *Ind. Eng. Chem.*, **43**, 697 (1951).
2. R. F. Mehl and E. L. McCandless, *Trans. Am. Inst. Mining-Met. Eng.*, **125**, 531 (1937); *Nature*, **137**, 702 (1934).
3. R. F. Mehl, E. L. McCandless, and F. N. Rhines, *Nature*, **134**, 1009 (1934).

กรมวิทยาศาสตร์
กระทรวงมหาดไทย

4. K. R. Lawless and A. T. Gwathmey, *Acta Met.*, **4**, 153 (1956).
5. W. W. Harris, F. L. Ball, and A. T. Gwathmey, *ibid.*, **5**, 574 (1957).
6. Z. G. Pinsker and L. I. Tatrinova, "Electron Diffraction," p. 262, Butterworth Scientific Publ., London (1953).
7. J. S. Kerr and H. Wilman, *J. Inst. Met.*, **84**, 383 (1956).
8. J. J. Katz and G. T. Seaborg, "The Chemistry of the Actinide Elements," p. 124 ff, Methuen and Co., London (1957).
9. J. Belle and B. Lustman, "The Properties of UO_2 ," Atomic Energy Commission Document WAPD-184 (Sept. 1957).
10. Anon. "Schulz Integrating Reflection Goniometer," Am. Soc. Test. Mat. Tentative Stand. E49-86T Revised 1954.
11. C. S. Barrett, "Structure of Metals," p. 154 ff, McGraw-Hill Book Co., New York (1943).
12. J. J. Katz and E. Rabinowitch, "The Chemistry of Uranium," p. 77, Nat. Nucl. Ener. Ser. VIII-5, McGraw-Hill Book Co., New York (1952).
13. J. T. Waber, D. D. Whyte, and C. E. Olsen, submitted to *This Journal*.
14. D. M. Evans and H. Wilman, *Proc. Phys. Soc.*, **63A**, 298 (1950).
15. D. M. Evans and H. Wilman, *Acta Cryst.*, **5**, 731 (1952).
16. H. Wilman, *Proc. Phys. Soc.*, **64A**, 329 (1951).
17. E. T. Teatum, Unpublished work.
18. H. Mogard, Int. Conf. Peaceful Uses Atomic Ener., A/CONF./P/787, vol. 9, p. 318.
19. D. Turnbull and R. E. Hoffman, *Acta Met.*, **2**, 419 (1954).
20. R. E. Hoffman, *ibid.*, **4**, 97 (1956).
21. R. W. Ure, Jr., *J. Chem. Phys.*, **26**, 1363 (1957).
22. G. T. Miller and K. R. Lawless, *J. Appl. Phys.*, **29**, 863 (1958).
23. W. W. Webb and W. G. Foreng, *ibid.*, **28**, 1449 (1957).
24. R. D. Dragsdorf and W. W. Webb, *ibid.*, **29**, 817 (1958).
25. R. C. Newman and D. W. Pashley, *Phil. Mag.*, **46**, 927 (1955).

Kinetics of the Uranium-Steam Reaction

B. E. Hopkinson¹

Atomic Energy Research Establishment, Harwell, England

ABSTRACT

Reaction rates of unalloyed uranium with super heated steam at 160°–1400°C and 1 atm pressure have been determined by a thermogravimetric method. Up to 880°C the reaction follows a linear rate law with maximum rates at approximately 300° and 750°C. Above 880°C a parabolic rate law applies for the first 60–120 min, after which corrosion is linear; the oxide formed in the initial period gives protection to the underlying metal, and the subsequent linear rate is as low as that at about 200°C. X-ray diffraction of the reaction product indicated that uranium dioxide was formed over almost the whole temperature range.

Previous quantitative work on this reaction has been confined to temperatures below 600°C. The earliest investigations (1) reported uranium to be attacked rapidly by steam from 150° to 400°C, with a reaction product of uranium dioxide at the lower temperatures; this changed to U_3O_8 on rise of temperature until at 400°C U_3O_8 constituted about 92% of the total oxide produced. Other workers (2) found that steam reacted rapidly with uranium turnings at 250°C to give a mixture of uranium dioxide and uranium hydride, but at 600° and 1000°C only uranium dioxide and hydrogen were formed; no U_3O_8 was reported at any temperature.

Huddle (3) gave some experimental data up to 600°C and also assessed the kinetic possibilities at higher temperatures, concluding that the uranium dioxide formed would be sufficiently protective to give a low reaction rate. The reaction rates obtained here indicate that the uranium oxide does in fact tend to be protective at high temperatures.

Experimental Materials

Uranium.—Two different sizes of uranium specimens were used. The first, of rectangular shape, was

satisfactory at low temperatures but oxidized completely in a few minutes at 750°C. It was therefore replaced by a larger cylindrical sample for experiments above 600°C.

The rectangular specimens weighed about 6.5 g and were approximately 1.3 x 1.9 x 0.15 cm (surface area 5.7 cm²). They were fabricated by rolling as-cast Springfield uranium into a sheet at 450°C and punching out to size. The cylinders weighed 30 g and were approximately 1.26 cm in diameter and 1.27 cm in height. They were cut from a bar of cast uranium and machined to the approximate dimensions. Before the experiment each specimen was polished to 00 emery paper under oil, degreased in acetone, and stood for 12 hr in a desiccator over calcium chloride.

Steam.—Steam was obtained from a main supply, the line pressure being reduced by a valve which maintained the pressure inside the reaction chamber slightly above one atmosphere.

Argon.—Argon was used to provide an inert atmosphere when preheating the specimen to reaction temperature. It was purified from oxygen and nitrogen by passing over calcium turnings at 600°C followed by bubbling through Na/K alloy at room temperature.

¹ Present address: Research Laboratory, The International Nickel Company, Inc., Bayonne, N. J.

Procedure

The reaction rate was followed by continuous weighing of the specimen on a modified thermobalance. The apparatus was as described by Kubaschewski and Hopkins (4) except for the provision of a heater to prevent condensation of steam on the platinum suspension wire where it emerged from the reaction chamber.

A platinum or nichrome wound furnace maintained the specimen temperature, which was measured by a chromel/alumel or platinum/platinum rhodium thermocouple placed adjacent to the specimen in a silica "pocket." The thermocouple measured the temperature of the gas stream, which may be lower than that of the specimen by an amount depending on the degree of self-heating. This self-heating, due to the exothermic nature of the reaction, is unavoidable. At 350°C it can be as large as 150°C (3) but above 880°C, when the protective oxide scale has formed, the heat of reaction is not likely to contribute materially to the specimen temperature when compared with the external heat input. The actual temperature fluctuations recorded were between 10° and 40°C for each experimental run.

When carrying out the experiment, the furnace, argon purifier, and heating tapes were brought up to the appropriate temperature, the specimen placed in the fused silica reaction chamber, and argon flushed through. After elevating the furnace to a position around the specimen and preheating in a flow of

argon to the required temperature for about 30 min, steam was admitted at roughly 2 l/min. Weight increases were recorded at appropriate time intervals. After the required period, the steam flow was stopped and the specimen cooled in argon before removal. In nearly all experiments the specimen showed a small weight increase when being preheated, and this was attributed to impurities still remaining in the argon after purification.

The specimens were always enclosed in a basket of platinum gauze (52 mesh) to retain oxide that fell away from the metal; the basket in turn was suspended from the balance.

Results

The rates of corrosion, i.e., the slope of the curves, are detailed in Table I. Usually several values of the reaction rate were determined at each temperature by independent experiments.

The scatter of rates shown in this table may be due partly to lack of control of temperature because of self-heating and partly to other variations in the experimental conditions, e. g., traces of oxygen in the steam supply.

The behavior of solid uranium in steam from 160° to 880°C is represented by a linear relationship between weight increase and time; an exception is at 230°C. Figures 1(a) and 1(b) show typical curves for this part of the temperature range.

From 880° to 1060°C the curves [Fig. 1(c)] are initially parabolic changing to linear after times ranging from 60 to 120 min. The linear rates are detailed in Table I. The parabolic or near-parabolic nature of the initial part of the curve was shown by the slope of a log-log plot of weight increase per unit area (y) against time (t). This slope should ideally be 0.50. Actual values are reported in Table I, column 3.

Two experiments were carried out with molten uranium. Figure 2 shows that at about 1200° and 1400°C the rate fell initially with time to a steady value of 4-5 mg/cm²/min. Some difference in the form of the two oxidation curves was evident.

Figure 3 shows the linear reaction rate of each specimen plotted against the temperature of the experiment.

Other observations.—The physical nature of the reaction product varied with the temperature of oxidation. Below 500°C the oxide was a voluminous fine powder, but above this temperature larger particles began to appear. Above 880°C the oxide formed a complete shell, which adhered to the uranium and remained intact on cooling the specimen to room temperature. When cold, this shell could be stripped off easily. Figure 4 shows typical changes in the reaction product with temperature. The bulk densities of the oxide produced at higher temperatures were measured by weighing in air and water and are given in Table II.

The reaction products over the temperature range 200°-1400°C were examined by x-ray diffraction. All the samples gave a uranium dioxide type pattern except one at 300°C which appeared to be U₃O₈; this does not imply a stoichiometric composition of UO₂.

Table I. Rates of reaction over the temperature range 160°-1400°C

Average temp, °C	Linear reaction rate as weight gain in mg/cm ² /min	Value of index n in the equation $y = kt^n$ applied to first 60-120 min of reaction
160	0.02	
200	0.1, 0.1, 0.08	
230	0.3, 0.3, 1.6	
250	0.9, 1.6, 1.6	
270	1.7, 1.9, 1.9	
300	2.0, 2.4, 2.7	
330	2.1	
350	1.6	
370	1.9	
380	1.6	
400	1.8	
420	1.2, 1.8, 1.4	
450	1.1, 1.7	
500	0.9, 1.0, 1.3	
520	1.0, 0.6	
550	0.7, 1.0, 0.8, 1.1	
600	1.5, 1.7, 1.3	
650	1.4, 1.5	
700	1.3, 6	
730	6	
780	4	
820	3	
840	3	
880	0.2	0.52
890	0.3	0.46
930	0.3	0.46
970	0.3, 0.2	0.50
1000	0.2, 0.3	0.42
1020	0.2, 0.3	0.50
1060	0.3	0.49
1200	3.8	
1400	4.8	

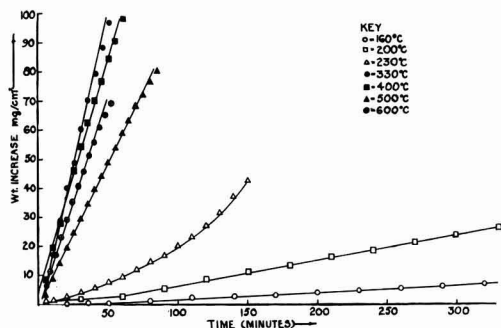


Fig. 1 (a). Uranium in steam 160°-600°C. Plot of weight increase (mg/cm²) V time (min).

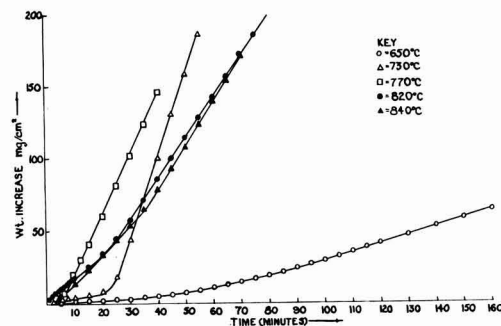


Fig. 1 (b). Uranium in steam 650°-840°C. Plot of weight increase (mg/cm²) V time (min).

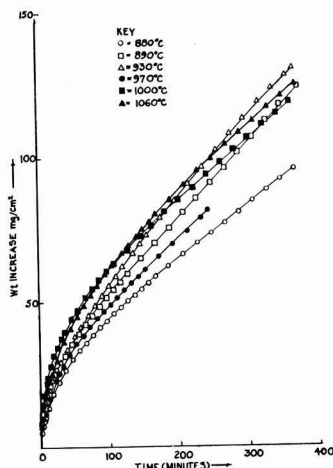


Fig. 1 (c). Uranium in steam 880°-1060°C. Plot of weight increase (mg/cm²) V time (min).

but is typical of compositions between $\text{UO}_{2.0}$ ($\alpha\text{-UO}_2$) and $\text{UO}_{2.24}$ ($\beta\text{-UO}_2$).

Three specimens which had been exposed to steam at 200°, 930°, and 1060°C were examined metallographically. The 930° and 1060°C specimens showed similar characteristics and are considered together. The outer layer of oxide, about 1 mm thick, had flaked off, but an adherent coating approximately 5 μ thick remained. No evidence of preferential grain boundary attack was observed, and inclusions origi-

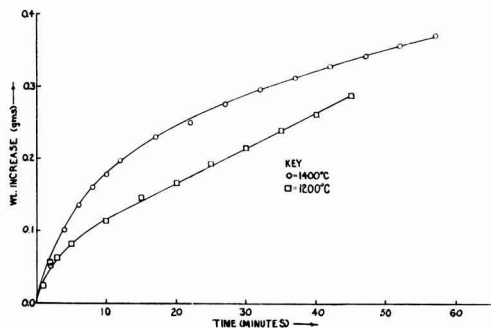


Fig. 2. Molten uranium in steam. Approximate surface area of molten uranium exposed to steam = 0.9 cm².

nally in the uranium appeared unchanged in the oxide. These inclusions were thought to be uranium monocarbide since they etched black in a mixture of equal parts of nitric acid and water. After corrosion, inclusions of a new type were present in addition to the carbide. These consisted of light brown areas (Fig. 5) generally serpent-like in shape at grain boundaries and almost invariably containing a spine of small, dark, fairly equiaxed inclusions. The brown inclusions occupied about 0.25 vol % of the material and were more numerous in the center than the periphery. Mogard and Cabane (5) indicate that this type of inclusion is uranium hydride. The solubility of hydrogen in γ -uranium is 15-17 ppm but is less than 2 ppm in α -uranium (6). Since 0.25 vol % of uranium hydride corresponds to 18 ppm of hydrogen, it appears that during corrosion with steam the uranium becomes saturated with hydrogen which precipitates on cooling.

Examination of the specimen corroded at 200°C showed no such hydride. Except for a few large fissures, attack was fairly uniform, and no trace of preferential attack along the grain boundaries was found. The fissures ran parallel to strings of uranium carbide inclusions, but the carbide content in the region of the fissures did not appear above average. Uranium hydride was found near the tips of the fissures, either along the stringers of carbide inclusions or as needles at an angle to the fissure (Fig. 6).

Discussion

From the results obtained on solid specimens two oxidation maxima are observed at approximately 300° and 750°C, with two minimum at about 550° and from 800°-1050°C.

It is possible to explain the first maximum at 300°C by considering the rate of variation of uranium hydride formation with temperature. Uranium hydride is unstable above 433°C under 1 atm partial pressure of hydrogen, and the rate of reaction be-

Table II. Bulk densities of the oxide scales formed above 880°C

Temperature of formation, °C	Scale thickness, cm	Density g/cc
970	0.07	10.95
1000	0.11	11.00
1020	0.14	10.97

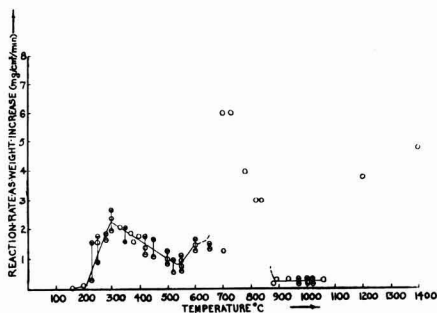


Fig. 3. Plot of reaction rate (mg/cm²/min) V temperature (°C).

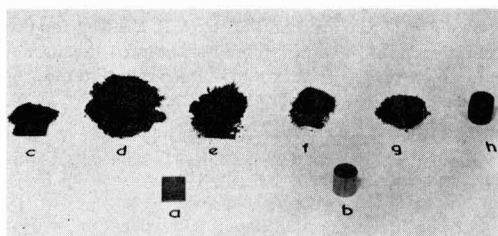
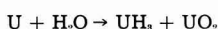


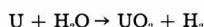
Fig. 4. Photograph of uranium specimens before and after corrosion in steam: (a) rectangular specimen before corrosion; (b) cylindrical specimen before corrosion; (c) specimen after exposure to steam at 200°C for 6¾ hr; (d) specimen after exposure to steam at 300°C for ¾ hr; (e) specimen after exposure to steam at 500°C for 1 hr, 40 min; (f) specimen after exposure to steam at 700°C for 20 min; (g) specimen after exposure to steam at 840°C for 1 hr, 20 min; (h) specimen after exposure to steam at 1000°C for 6 hr.

tween uranium and gaseous hydrogen reaches a maximum at 225°–250°C. It has been reported (7) that below 450°C uranium reacts with steam to give a mixture of hydride and oxide according to the equation



and that the uranium hydride reacts slowly (8) with more steam to give uranium dioxide. Therefore, reaction below 450°C should yield a mixture of uranium hydride and uranium dioxide,² the latter predominating, as confirmed by metallographic examination of a specimen corroded at 200°C. It is probably justified to infer therefore that the maximum oxidation rate of uranium by steam at 300°C is determined by the variation of the rate of uranium hydride formation with temperature.

Above 500°C, hydride formation is improbable and the reaction may be written



the hydrogen being evolved as a gas or dissolving in the metallic uranium. In the temperature region above 500°C the cohesive properties of the oxide become important as a rate-determining factor. Up to 500°C the reaction product is in the form of a fine

² It is not clear whether the U₃O₈ found at 300°C is a definite reaction product (1) or results from air oxidation of uranium dioxide or uranium hydride after removal from the apparatus.

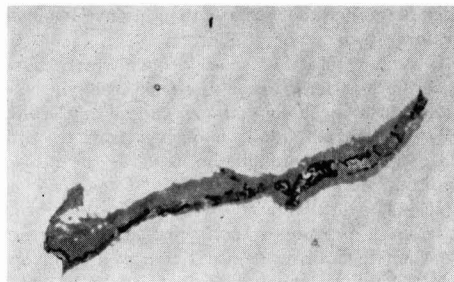


Fig. 5. Hydride precipitate in specimen after exposure to steam at 1060°C and cooled to room temperature. Magnification 1200X.

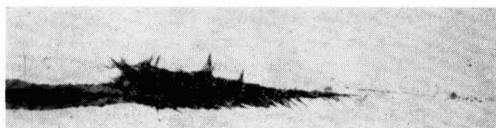


Fig. 6. Tip of fissure in uranium corroded at 200°C. Magnification 312X.

powder, but above 500°C granular particles are formed. Normal sintering of uranium dioxide occurs at about 1300°C (0.6 Tm), but it has been suggested that the presence of steam enhances the sintering characteristics of uranium dioxide (9). Also, an oxide film growing on the metal may behave differently from discrete oxide particles. The high reaction rates observed in part of this temperature range, i.e., 700°–880°C, may result from the increased surface area caused by the specimen splaying out at the top and bottom during oxidation. Why this occurs only between 700° to 880°C is not clear, but it may be that at these temperatures the oxide does not sinter sufficiently to protect the uranium completely, and that the stresses developed as the scale grows prove too much for continued cohesion, resulting in breakdown and high oxidation rate. It was noted that an induction period of up to 20 min occurred in experiments between 650° and 840°C before the reaction rate increased to a high value. This may indicate a change in mechanism but, since the size of the specimen had to be increased to work in this region, this also may have influenced the appearance of an induction period.

It is above 880°C that the most significant change in the rate of the reaction occurs. Above this temperature a hard compact scale forms, the density lying between 10.95 and 11.00 g/cc which compares well with theoretical values from lattice parameters given by Grönvald (10) viz., 10.954 g/cc for UO_{2,00} and 11.297 g/cc for UO_{2,25}.

The results from 880° to 1060°C show large initial weight gains increasing roughly according to a parabolic law. After 60–120 min however, a change occurs and the weight increase becomes linear with time and continues linear for the rest of the experiment.

The rate in the linear range is between 0.2 and 0.3 mg/cm²/min over the temperature range 880°–1060°C. Therefore once an oxide film has been formed, the reaction rate between uranium and

steam is smaller above 880°C than at any lower temperature down to about 200°C.

To explain this, the two rate laws which characterize the reaction may be discussed briefly.

(A) The parabolic rate law can be expressed as $y = kt^{1/2}$ and traditionally is derived from the diffusion of reactants through the oxide as the rate-determining step.

(B) The linear law $y = kt$ can be ascribed to oxidation of metal by the following two mechanisms: (i) when the rate-controlling step is a surface reaction at one of the interfaces; (ii) if the rate is controlled by diffusion through an oxide layer of constant thickness.

The change from parabolic to linear oxidation with time at constant temperature has been reported for a number of reactions (11-16).

To explain the change from a parabolic to linear oxidation rate three mechanisms may be considered. First, the heat of oxidation could result in self-heating of the specimen, thereby increasing the temperature and rate of oxidation. Second, if the surface area changes as oxidation proceeds (i.e., a decrease in roughness) this may cause a change in the oxidation rate. Davies and Birchenall (13) explained the initial parabolic oxidation of titanium in oxygen as being due to a change of surface area as oxidation proceeded, the over-all rate-controlling stage being the interface reaction of oxygen and titanium oxide. Third, there is the idea of a "barrier film" of constant thickness controlling the rate of oxidation. This mechanism has been used to explain the majority of transitions from parabolic to linear-type rate laws.

A mechanism involving control by an oxide layer of constant thickness appears to serve the facts of the uranium-steam reaction above 880°C and is put forward to explain these results.

The actual diffusing species through the oxide layer is probably anionic. The presence of uranium hydride in the metal after corrosion at high temperatures in steam indicates that hydrogen either as molecular hydrogen, protons, or hydroxyl ions is able to penetrate to the uranium in some way. One suggestion (3) is that water vapor is first chemisorbed on the uranium dioxide at the oxide/steam interface. The chemisorbed complex then produces hydroxyl ions, which are further reduced at the metal/oxide interface, the hydrogen dissolving in the metal. The hydrogen is precipitated as hydride in the grain boundaries when the specimen is cooled within the hydride formation range.

Conclusions

The rate of attack of uranium by steam varies with temperature over the range 160°-1060°C, and two maxima are obtained at about 300° and 750°C. Above 880°C however, a protective scale is formed, due to coalescence of the oxide. Once this scale has been produced the rates of oxidation above 880°C are smaller than those found between 200° and 880°C.

From the results given the trend of the reaction has been indicated, but further work will be needed to confirm the true rate-controlling mechanisms over the whole temperature range.

Acknowledgments

Thanks are due to K. A. Peakall for some of the early experimental work, to Dr. D. K. Thomas for the x-ray diffraction studies, and to P. E. Madsen for the metallographic examination. For helpful discussion and constructive criticism the author is indebted to Mr. R. A. U. Huddle, Dr. H. M. Finnieston, Mr. J. N. Wanklyn, and Dr. P. Murray.

Manuscript received Dec. 23, 1957. This paper was prepared for delivery before the Ottawa Meeting, Sept. 28-Oct. 2, 1958.

Any discussion of this paper will appear in a Discussion Section to be published in the December 1959 JOURNAL.

REFERENCES

1. T. Wathen, BR-233. "Corrosion of Uranium Metal in Air and Steam at Various Temperatures," Imperial Chemical Industries, May 1943.
2. J. J. Katz and E. Rabinowitch, "Chemistry of Uranium," N.N.E.S. Vol. VIII, p. 167, McGraw Hill Book Co., New York (1951).
3. R. A. U. Huddle, A.E.R.E., M/R 1281, "The Uranium Steam Reaction," (1953).
4. O. Kubaschewski and B. E. Hopkins, "Oxidation of Metals and Alloys," p. 90 Butterworth's Scientific Publications, London (1953).
5. H. Mogard and B. Cabane, *Rev. Met.*, **51**, 617 (1954).
6. J. J. Katz and E. Rabinowitch, *op. cit.*, p. 183.
7. J. C. Warf, U.S.A.E.C. Report No. MDDC. 1391 (1943).
8. J. J. Katz and E. Rabinowitch, *op. cit.*, p. 202.
9. P. Murray, Private communication.
10. F. J. Gronvold, *Inorganic and Nuclear Chemistry*, **1**, 357 (1955).
11. D. Cubicciotti, *J. Am. Chem. Soc.*, **74**, 1200 (1952).
12. P. Levesque and D. Cubicciotti, *ibid.*, **73**, 2028 (1951).
13. M. H. Davies and C. E. Birchenall, *J. Metals*, **3**, 877 (1951).
14. A. F. Gerds and M. W. Mallet, *This Journal*, **101**, 175 (1954).
15. E. A. Gulbransen and K. F. Andrew, *ibid.*, **97**, 383 (1950).
16. D. Cubicciotti, *J. Am. Chem. Soc.*, **74**, 1079 (1952).

Tarnishing Reactions of Silver in Iodine Atmospheres

Donald M. Smyth and Marjorie Cutler

Sprague Electric Company, North Adams, Massachusetts

ABSTRACT

The tarnishing of silver in halogen vapors, particularly iodine vapor, has been studied as a function of reaction temperature, halogen pressure, silver purity, and concentration of foreign vapors in the halogen atmosphere for reaction times up to several hours. The reaction temperature range studied was 25°–150°C for reactions in iodine and up to 200° in bromine and chlorine. In pure halogen vapor the reactions follow the familiar parabolic rate expression and are proportional to the square root of the halogen pressure. In the presence of small partial pressures of water or carbon tetrachloride vapor, however, the tarnishing rate is suppressed and is independent of the tarnish film thickness.

The tarnishing of silver in halogen atmospheres has been described by several investigators using various techniques (1–4). Since the publishing of Wagner's theory of the mechanism of these reactions (1, 5), however, very little work has been done on the tarnishing of undoped silver in halogen vapor, and, in particular, there has been no evaluation of the role played by foreign gases in the halogen atmosphere. Neither has there been any extensive study of these tarnishing reactions in the temperature range 25°–150°C. This range of reaction temperature has been examined in this laboratory for the silver-iodine system for silver samples of differing purity and for pure iodine atmospheres and iodine atmospheres containing water vapor or carbon tetrachloride vapor. Exploratory experiments have also been made on the effect of water vapor and carbon tetrachloride vapor on the tarnishing rate of silver in bromine and chlorine atmospheres.

Previous publications in this field are in agreement that the high-temperature tarnishing of silver in halogen vapor follows a parabolic rate expression

$$x^2 = kt \quad [1]$$

where x is the tarnish film thickness, t the reaction time, and k the rate constant. The reaction rate has been found to be proportional to the square root of the halogen pressure, $P_{x_2}^{1/2}$, and inversely proportional to the concentration of cation vacancies, $[Ag]$, in the silver halide. The cation vacancy content can be controlled by the addition of polyvalent metallic impurities to the silver (2, 3). Our experiments in the reaction temperature range 25°–200°C indicate that the factors determining the tarnishing rate are essentially the same in the case of tarnishing reactions in pure halogen vapors. In the presence of even small partial pressures of water or carbon tetrachloride vapors, however, the nature of the reaction is altered completely. Reaction rates become independent of tarnish film thickness and follow a linear expression,

$$x = at \quad [2]$$

where a is a new rate constant. Reaction rates are

relatively insensitive to reaction temperature and halogen pressure under these conditions.

Experimental

The reactions were followed by measuring the weight increase of silver foil in a halogen atmosphere by the extension of a quartz fiber spring balance (McBain balance). The silver samples were cut from 0.001-in. foil and had a geometrical surface area of 19.4 cm². The samples were cleaned just prior to use by a dip in concentrated cyanide solution to remove atmospheric tarnish and by a light etch in dilute nitric acid. After being rinsed and air dried, the specimens were weighed and hung in the reaction chamber on the end of the quartz fiber spring. The iodine pressure was determined by thermostating iodine crystals. In order to avoid condensation of iodine, the atmosphere surrounding the experimental system was heated slightly above the temperature of the iodine crystals.

When all parts of the apparatus had reached temperature equilibrium and the system had been evacuated to less than 30 μ pressure, the iodine container was opened to the reaction chamber. As the spring oscillations caused by the flow of iodine vapor into the reaction chamber ceased, an initial spring level reading was taken and the timer started. The spring depression then was measured every 1–5 min for a total time of ½–6 hr depending on the reaction rate. To terminate the reaction, the system was evacuated and flushed with air; then the sample was removed and weighed. The difference between the actual total weight increase and the weight increase which occurred during the measured reaction time as calculated from the total spring depression gave the amount of reaction which occurred before the first reading was taken. This initial amount of reaction was transformed into an equivalent spring depression which was added to each measured spring depression. These corrected values thus correspond to the total weight increase of the sample normalized to the clean, unreacted silver foil. This procedure was necessary because of the possible shift of the equilibrium spring position during the large, initial oscillations. The

square of the corrected spring depression was plotted against the reaction time, and the slope of this line when transformed into appropriate units gives the reaction rate constant k . (Microscopic examination of cross-sectioned samples showed that the bulk density of the silver halides can be used to calculate the film thickness.)

The technique was slightly more involved when the reaction rate was measured in the presence of a foreign vapor. In this case, a second isolated and thermostatted container was added to the apparatus to hold the thoroughly outgassed water or carbon tetrachloride. The two vapor sources generally were held at different temperatures and thus could not be opened to the system at the same time. An initial film of tarnish product was formed on the silver by exposure to halogen and foreign vapor. Then the reaction was halted and this initial film was exposed to the foreign vapor for 15 min after which the reaction rate with iodine was measured. No subsequent readmission of foreign vapor was necessary since additional exposures at the same pressure did not change the reaction rate.

Materials.—The silver¹ was of the following types:

1. Commercial silver, nominally 99.9+ % pure. Spectrographic analysis showed copper to be the major impurity with a concentration of the order of 0.05% with lead, iron, and calcium being present in slightly lesser concentration.²

2. Laboratory refined silver, initially prepared as a powder 99.995+ % pure. Some surface contamination may occur during rolling but this is probably removed by the etch treatment.

3. Cadmium doped silver prepared from laboratory refined silver. This alloy contained 0.046% cadmium according to the suppliers assay. The copper content was 0.003% and no other impurity was present in concentration greater than 0.001%.

Matheson, Coleman, and Bell Reagent iodine crystals (resublimed) were used without further purification. Baker Reagent Grade bromine was dried by several passes through a tube of anhydrous calcium sulfate. Baker and Adamson Reagent carbon tetrachloride was used without further purification. The source of water vapor was demineralized water of greater than 1 megohm cm resistivity.

Several quartz springs were used during this investigation, all having spring constants of about 0.05 g/cm. The spring constants were determined by measuring the extension caused by known loads over the pertinent load range and were found to be constant within $\pm 5\%$ over the entire experimental temperature range. The spring depression could be read to $\pm 5\mu$ through a 10X telescope mounted on a micrometer head.

Results

The experimental results may be summarized as follows: the reaction of silver with pure halogen atmospheres followed parabolic rate expressions, Eq. [1], except for some deviations observed during the first few minutes of reaction; in halogen atmospheres

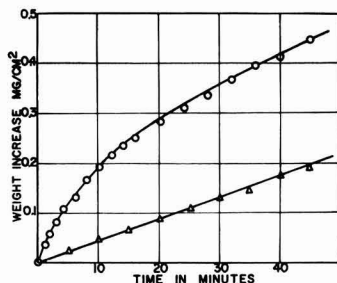


Fig. 1. Tarnishing of silver in 0.2 mm iodine vapor at 39°C. \circ Pure iodine vapor; \triangle iodine vapor plus 0.37 mm H_2O vapor.

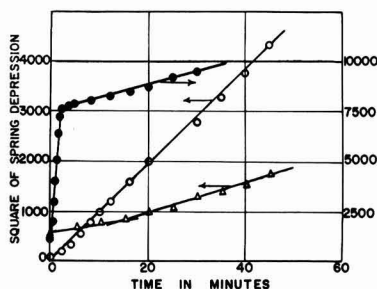


Fig. 2. Tarnishing of laboratory refined silver (99.99+ %) in 0.2 mm pure iodine vapor. Typical experimental data. \circ Parabolic throughput, reaction at 69°C; \triangle slow initial reaction at 68°C; \bullet fast initial reaction at 137°C; the arrows indicate the ordinate scale to be used with each set of data.

containing water or carbon tetrachloride vapor above some minimum pressure the reaction rates were linear with time and followed Eq. [2]. The reaction rates behaved reversibly to changes in halogen pressure and foreign gas pressure but not to changes in reaction temperature since a decrease in reaction temperature does not change the reaction rate to the rate obtained when the reaction is started at the lower temperature. All of these factors will be discussed in detail.

Typical tarnishing data are shown in Fig. 1 for the silver-iodine system. Similar results were obtained for the silver-bromine and silver-chlorine systems. The figure shows data obtained from two reactions performed under identical conditions except for the presence of a small partial pressure of water vapor in one case (laboratory refined silver was used in each experiment). Figure 2 shows the types of initial deviation from parabolic reaction rates observed for the reaction of silver with pure iodine vapor. Almost all of the reactions of fine silver and some of those of laboratory refined silver followed a simple parabolic expression throughout the measured time. A large number of the reactions with laboratory refined silver had an initial, slow reaction rate which changed into a final rate after 2-15 min. For each batch of laboratory refined silver, there was a temperature between 100° and 130°C above which the reaction initially proceeded very rapidly for several minutes before abruptly slowing down to a rate comparable to that observed at lower temperatures. Above 145°

¹ Obtained from Handy and Harman, 82 Fulton St., New York, N. Y.

² Analysis carried out by Lucius Pitkin, Inc., 47 Fulton St., New York, N. Y.

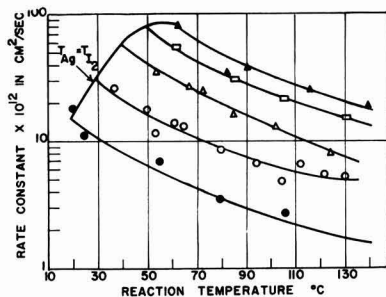


Fig. 3. Tarnishing of "fine" silver (99.9+%) in pure iodine vapor. Iodine pressures: ● 0.20 mm; ○ 0.47 mm; △ 1.0 mm; □ 2.2 mm; ▲ 4.3 mm.

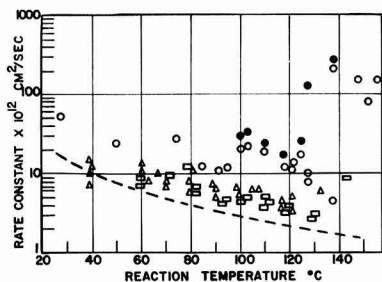


Fig. 4. Tarnishing of laboratory refined silver (99.99+%) in 0.2 mm pure iodine vapor. △, ○ Two different batches of pure silver; ● initial fast reaction for batch designated as O; □ pure silver plus 0.046% cadmium; — — — averaged data for 99.9+ % silver.

(the transition temperature for the phase change $\alpha\text{AgI} \rightarrow \beta\text{AgI}$) the fast reaction rate continued without change. This initial fast reaction also was observed for some lots of fine silver at temperatures just below the transition temperature.

In Fig. 3 and 4 are shown the results of a large number of tarnishing experiments carried out under a variety of conditions. The reaction rates of commercial purity silver (99.9+%) with pure iodine vapor as a function of reaction temperature with iodine pressure as a parameter are shown in Fig. 3. Each point represents an individual tarnishing experiment at constant temperature and iodine pressure, and smooth curves have been drawn through points obtained at the same iodine pressure. The tarnishing rates are expressed in terms of the parabolic tarnishing constant k in Eq. [1] in units of (cm of film thickness)²/sec. The line in Fig. 3 which is labeled $T_{Ag} = T_{i2}$ connects points at which the iodine pressure is in equilibrium with the reaction temperature.

In Fig. 4 are shown the results of a large number of tarnishing experiments on high-purity and cadmium doped high-purity silver. The rate of the brief, initial reaction is not shown in this figure except for the very fast initial reaction observed in the higher temperature range, and this is designated by the symbol ●. The variation in reaction rate for separate lots of silver (represented by different symbols) is apparent in this figure as is the scatter of reaction rates within the same batch. The effect of divalent metallic impurities is shown by the cadmium doped

samples. All of the experiments in Fig. 4 were carried out in 0.2-mm iodine pressure and the dashed line represents the averaged tarnishing data for the commercial grade silver in iodine vapor of this pressure.

The tarnishing rates of the commercial grade silver and of silver heavily doped with cadmium are not reversible with temperature as shown by the following experiment. If a piece of commercial grade silver foil is tarnished at 30° and the reaction temperature is then raised to 100°, the reaction rates correspond to the values for these temperatures shown in Fig. 3. If, however, the reaction temperature is reduced to 30° again, the reaction rate increases only a fraction of the amount required to restore the original rate found at this temperature. The same effect is obtained when a tarnish film is heated a few minutes at the higher temperature without exposure to iodine vapor. A similar but more striking behavior is noted when fine silver containing 0.09% cadmium is tarnished. The initial tarnishing rate is similar to that of undoped silver but, after "annealing" an initial tarnish film, the subsequent reaction rate may be lowered by as much as a factor of 50. Thus, the exposure of a tarnish film to a higher temperature tends to lower the rates of subsequent reactions carried out at lower temperatures, and the effect is more pronounced in less pure silver. These phenomena will be discussed further with respect to the mechanism of these reactions.

Laboratory refined silver was employed for the tarnishing experiments carried out in iodine in the presence of water or carbon tetrachloride vapor. The reaction rates in 0.20 mm of iodine vapor as a function of water vapor pressure at three different reaction temperatures and as a function of carbon tetrachloride vapor pressure at one reaction temperature are shown in Fig. 5. In this case, the reaction rate constant represents the constant, a , in the rate expression of Eq. [2], indicating that the reaction rate is independent of film thickness. For water vapor pressures below 0.1 mm, the reaction follows the same parabolic rate equation found for the anhydrous reaction. There is a narrow, intermediate range of water vapor pressure in which the reaction rate is erratic and is sometimes linear and sometimes parabolic. For higher water vapor pressures, the reaction rate is always linear and gradually decreases with

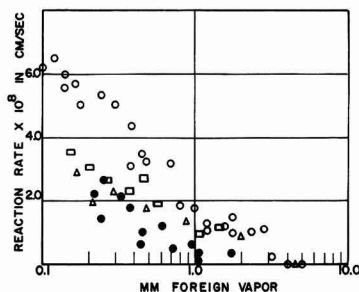


Fig. 5. Tarnishing of laboratory refined silver in 0.2 mm iodine vapor plus H_2O or CCl_4 vapor. □ H_2O vapor, reaction at 40°; ○ H_2O vapor, reaction at 69°; △ H_2O vapor, reaction at 101°; ● CCl_4 vapor, reaction at 33°.

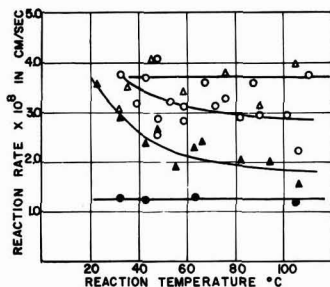


Fig. 6. Tarnishing of laboratory refined silver in iodine vapor plus 0.26 mm water vapor. Iodine pressures: Δ 0.47 mm; \circ 0.20 mm; \blacktriangle 0.11 mm; \bullet 0.04 mm.

increasing water vapor pressure until at a water vapor pressure of 4 mm the reaction becomes too slow to observe. It is not clear whether the reaction actually stops in the presence of larger concentrations of water vapor or whether it decreases steadily but remains finite. The situation is similar for carbon tetrachloride except that this vapor is apparently somewhat more effective in suppressing the tarnishing rate than is water vapor.

Figure 6 shows the reaction rate of silver with moist iodine vapor as a function of reaction temperature with iodine vapor pressure as the parameter. Although the results are scattered, it is clear that the reaction temperature has very little effect on the reaction rate and that the reaction rate increases with iodine vapor pressure.

A few tarnishing experiments were also carried out in bromine atmospheres and the results were similar to those found for iodine. The reaction of silver with anhydrous bromine follows parabolic rate expressions, while the wet bromine atmospheres give linear reaction rates. One major difference from the iodine reactions was that the linear reaction rate did not change with the water vapor pressure. Thus at a reaction temperature of 105° and a bromine pressure of 43 mm, the linear reaction rate constant, a , was $6 \pm 2 \times 10^{-8}$ cm/sec in nine experiments over the water vapor pressure range 0.06–1.5 mm. The reaction temperature was also found to have little effect on the reaction rate since at a water vapor pressure of 1.0 mm and a bromine pressure of 43 mm, the reaction rate less than doubled between 105° and 190°C. Over the same temperature range the anhydrous parabolic rate constant increased by a factor of about 700.

In 600 mm of chlorine vapor and 0.045 mm of water vapor the laboratory refined silver tarnished at a linear rate of 0.5×10^{-8} cm/sec at 172° and 2.0×10^{-8} cm/sec at 194°.

Discussion

Tarnishing in Pure Halogen Vapor

It is assumed that the anhydrous tarnishing reactions proceed according to the theory of Wagner (1, 5). This states that the parabolic reaction rate is determined by the diffusion of an ionic or electronic species across the bulk of the tarnish film and proposes the following equilibrium reaction at the halide-halogen interface

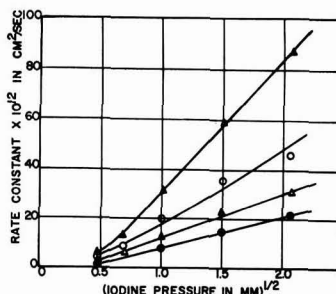
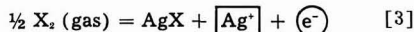


Fig. 7. Tarnishing rate of "fine" silver as a function of $\sqrt{P_{I_2}}$. Reaction temperatures: \bullet 60°C; Δ 80°C; \circ 100°C; \blacktriangle 130°C.



where X is a halogen, $[Ag^{\cdot}]$ is a silver ion vacancy, and (e^{\cdot}) is an electron hole in the electronic structure of the silver halide. If we consider the silver halides as predominantly ionic conductors, the migration of electron holes across the silver halide must be the rate-determining step. Assuming that the ionic disorder of the lattice is large compared with the cation vacancies injected according to Eq. [3], the theory predicts the following dependence of the parabolic rate constant, k , on the halogen pressure, P_{X_2} , the cation vacancy concentration, $[Ag^{\cdot}]$, and the mass action constant, K , for Eq. [3]

$$k \propto \frac{K P_{X_2}^{1/2}}{[Ag^{\cdot}]} \quad [4]$$

The proportionality of the tarnishing rate with $\sqrt{P_{I_2}}$ is shown in Fig. 7 in which reaction rate constants taken from the smooth curves in Fig. 3 are plotted against $\sqrt{P_{I_2}}$ for several different reaction temperatures. This proportionality apparently does not hold for very low iodine pressures. The inverse proportionality to the cation vacancy concentration has been demonstrated by other workers for other silver halides at higher reaction temperatures by adding a sufficient amount of impurity to determine the cation vacancy concentration (2, 3).

All of the rate-determining factors in Eq. [4] should behave reversibly to changes in temperature except perhaps the cation vacancy concentration. The irreversible "annealing" effect observed for reactions of the low-purity silver and the more striking effect observed with cadmium doped silver points to the vacancy content as an important factor in determining the rate. The cation vacancy concentration depends on the purity of the halide since the substitution of a polyvalent cation M^{n+} , for a monovalent silver ion in the lattice requires the formation of $n-1$ cation vacancies to maintain electrical neutrality. Teltow (6) determined the solubility limits of $CdBr_2$, $PbBr_2$, and $ZnBr_2$ in $AgBr$ over a considerable temperature range, and by extrapolation of his results it is clear that the solubilities will be only a small fraction of a per cent at tempera-

tures below 150°. The behavior of the iodides may be assumed to be quite similar. It is not unreasonable to expect that for a silver sample of low purity there will be sufficient polyvalent metal ions to saturate the halide lattice up to an appreciable temperature. Thus as the reaction temperature increases, the concentration of dissolved impurities in the AgI also increases due to the increase in solubility. As a result, the quantity $[Ag]$ increases and from Eq. [4], the reaction rate decreases with increasing temperature. At these low concentrations the concentration of dissolved impurities would probably not decrease reversibly with decreasing temperature but would remain in a state of supersaturation. This would account for the irreversibility of the reaction rate with temperature as observed for the lower purity silver. In addition to this factor, there may be a temperature dependence arising from K , but this should behave reversibly to temperature changes.

If the ionic conductivity of the silver halide is playing any part in controlling the reaction rate, the polycrystalline nature of the tarnish film may be important since there is evidence that ionic conduction takes place very readily along grain boundaries (7). In this case, the annealing effect could be enhanced by a decreased concentration of grain boundaries due to a growth in crystal size in heated tarnish films.

The nature of the temperature coefficient of reaction rate found here supports some of the earlier work on the Ag-I₂ system. Tammann (4) found no change in reaction rate in the temperature range 15°-100°C. Dubrisay (8) observed a slight decrease in tarnishing rate as the reaction temperature was raised from 24° to 60°. Balarew (9) found a very slight increase in reaction rate between 50° and 70°, followed by a slight decrease again at 100° and a sharp dip in reaction rate at 120°. This pronounced minimum in tarnishing rate has not been reported elsewhere. All of these works employed the interference color technique to measure the tarnish film thickness and thus deal with thinner films than discussed in this paper. It is of interest to note that the behavior is similar over such a wide range of film thickness. Evans and Bannister (10) made an extensive study of the rate of reaction of silver with organic solutions of iodine and found that the reaction rate at 35° is about twice that at 0° for carbon tetrachloride solutions of iodine. The use of organic solvents may invalidate a direct comparison to reactions in pure iodine vapor however.

The brief, rapid reaction rates noted for pure silver reacting with iodine vapor at reaction temperatures just below the α - β phase transition temperature of AgI (145°C) are of the same magnitude as the continuous reaction rates observed above the transition temperature. Thus it appears that the initial film may have the α phase structure for 1-3 min after which it abruptly changes back to the phase in equilibrium at the reaction temperature. It was considered that the samples might be heating themselves above the transition temperature by their own heat of reaction. This possibility was investigated numerically by Miss Alma Marcus of these labora-

tories, who computed the temperature rise of a sample considering the heat evolved by the reaction and the heat loss through radiation and conduction. It was found that for typical reaction conditions the rise in sample temperature would reach a maximum of 1.4°C after 1.7 sec and this is insufficient to explain the experimental results. It is possible that the crystalline structure of the silver substrate may influence that of the initial silver iodide film and that close to the transition temperature the high temperature structure is favored. This would conflict with the observation of Tammann and Köster (11) that the phase transition takes place at 145°C even for layers of silver iodide on silver which show optical interference colors.

The initial, slow reaction rate observed in some reactions of high-purity silver at temperatures below 100° does not fit in with the general behavior outlined above and is not understood at present.

Tarnishing in the Presence of Foreign Vapors

The linear rate expression, Eq. [2], followed by the tarnishing reactions carried out in the presence of foreign vapors implies that the rate-determining factor is an interface phenomenon and hence independent of the tarnish film thickness. This factor has not been identified experimentally but it is suspected that adsorption of the impurity gas on the halide surface results in modification in the space charge layer at the AgI surface adjacent to the iodine atmosphere. Speculations along this line will be the subject of a future publication from this laboratory. The diffusion rate of the halogen through the adsorbed film of foreign vapor may also be of importance.

The experimental results from the Ag-I₂ system (see Fig. 4 and 5) indicate that the amount of foreign vapor is the main rate-determining factor since the reaction temperature has no significant effect and the influence of iodine pressure is small. The two gaseous atmospheres extensively investigated in this work, iodine with water vapor and iodine with carbon tetrachloride vapor, show that the effect is not dependent on the polarity of the foreign molecule since the nonpolar carbon tetrachloride is even slightly more effective in suppressing the reaction rate than is water. This fact implies that a wide variety of vapors would act similarly to the two investigated here. The results also show that a foreign vapor is not consumed by the tarnishing reaction. Once the tarnish film has been exposed thoroughly to the foreign vapor, the reaction rate continues unchanged for hours without further addition of water or CCl₄ vapor, and neither do subsequent additions at the same vapor pressure alter the reaction rate. The effect is perfectly reversible and the tarnishing rate can be changed immediately in either direction by suitable adjustment of the pressure of the foreign vapor.

Since the character of the tarnish film does not seem to be altered by the presence of the foreign vapor, the reaction rate for any particular experiment will be parabolic or linear depending on whether the bulk diffusion process or the interface process is the slower. Thus for very low foreign vapor pressures,

the interface process will not be slower than hole diffusion and the reaction will be parabolic. The rate of diffusion will decrease as the tarnish film thickens and it will eventually become the rate-determining step regardless of the experimental conditions unless the foreign vapor completely stops the reaction. The ideal situation can be described by the following simplified considerations. The reaction rate will follow the linear rate equation (Eq. [2]) unless the diffusion process is rate determining, in which case the reaction follows the parabolic rate expression (Eq. [1]). A change from the linear to the parabolic reaction will occur at the film thickness, x_1 , at which the reaction rate dx/dt is the same for both equations

$$x_1 = \frac{k}{2a} \quad [5]$$

This thickness will be reached after a reaction time t_1 ,

$$t_1 = \frac{k}{2a^2} \quad [6]$$

Subsequent to the time t_1 the reaction will follow the expression

$$x^2 = k \left(t - \frac{k}{4a^2} \right) \text{ for } x > x_1 \quad [7]$$

where $k/4a^2$ is the difference in times that the parabolic and linear reactions would require to build up a tarnish film x_1 cm thick starting from bare silver. This behavior is illustrated in Fig. 8 which compares the tarnishing rate in dry iodine with two reactions carried out in the presence of water vapor. In the presence of 0.94 mm of water vapor the reaction follows a linear rate throughout (Eq. [6] indicates that the transition to a parabola should occur after 295 min of reaction). The data shown for reaction in the presence of 0.26 mm of water vapor have been found to follow Eq. [2] and [7] with $a = 3.3 \times 10^{-8}$ cm/sec, $k = 8.7 \times 10^{-12}$ cm²/sec, and a transition time of 52 min. (The fact that the initial linear reaction does not extrapolate to the origin of coordinates has been taken into account.) These rate values are in satisfactory agreement with the average anhydrous tarnishing rate, $k = 9.5 \times 10^{-12}$ cm²/sec, and moist tarnishing rate, $a = 3 \times 10^{-8}$ cm/sec, observed under similar conditions for the same batch of silver foil.

The effect of moisture on the tarnishing rate explains some of the previously published results of

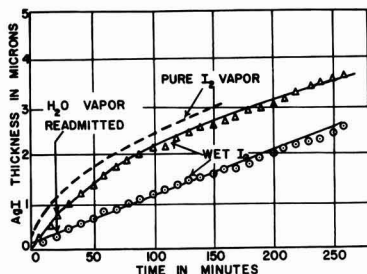


Fig. 8. Influence of moisture content of atmosphere on tarnishing rate of laboratory refined silver at 35°C in 0.2 mm iodine vapor. — — — Averaged data from reactions in pure iodine vapor; Δ 0.26 mm H₂O vapor; \circ 0.94 mm H₂O vapor.

tarnishing reactions of silver with halogens. In many instances the reactions did not follow a parabolic rate expression and this can almost invariably be explained by the presence of moisture in the halogen vapor. For example, Hartung measured the tarnishing rate of silver with iodine and bromine at 25° (12, 13). The iodine atmosphere was obtained from an aqueous KI-I₂ solution and thus was saturated with water vapor. The tarnishing rates followed linear rate equations for the range of iodine concentrations studied. Hartung does not describe any purification or drying of his bromine and it was undoubtedly moist since the reaction rates were found to be linear after an initial fast reaction lasting about 100 sec.

Kohlschütter and Krähenbühl investigated the reaction of silver with iodine and found some variation in reaction rate depending on the dryness of the halogen atmosphere (14). Their results do not follow either parabolic or linear rate expressions but some intermediate rate equation. It is possible that their data follow the linear expression for the initial reaction period and then transform into a parabolic reaction rate as described above, but since the authors give no quantitative data, it is not possible to investigate this possibility thoroughly. Using Cl₂ and Br₂, Kohlschütter and Krähenbühl found faster reactions with silver in the presence of moisture than in the dry halogen. The use of streams of N₂ or CO₂ to carry the halogen over the silver may have had some influence on the reaction rate.

Several publications report observations which conflict with those described here (15-19). In general, these papers contain very little quantitative data and are therefore difficult to evaluate.

Other tarnishing reaction systems have been observed to be affected by the presence of water vapor. Solovjev (20) has found that there is apparently an optimum water vapor pressure for maximum reaction rate of copper with iodine. He also noted a decrease in reaction rate of iron with iodine with decreasing water vapor pressure. Bircumshaw and Everdell found a linear reaction rate for copper reacting with aqueous solutions of KI and I₂ (21) whereas the reaction rate depended on the tarnish film thickness in organic iodine solutions (22). The authors attribute this behavior to a wetting and penetration of the tarnish film by the aqueous solutions while the organic solutions do not wet the film and the reaction can proceed only by bulk diffusion through the iodide. Campbell and Thomas (23) investigated the oxidation of copper in dry and moist oxygen. In dry oxygen the reaction was parabolic while in moist oxygen the results had a smaller dependence on the film thickness. In general, these experiments show the care necessary in controlling all of the experimental conditions in order to obtain meaningful results. Even the presence of what might be usually considered "inert" gases may drastically alter the nature of the reaction.

Acknowledgments

The work reported herein was carried out under United States Army Signal Laboratories Contracts DA-26-039-sc-63151 and DA-36-039-sc-72349. The

authors wish to express their appreciation to Dr. Kurt Lehovc of these laboratories for much stimulating discussion and advice.

Manuscript received March 12, 1958.

Any discussion of this paper will appear in a Discussion Section to be published in the December 1959 JOURNAL.

REFERENCES

1. C. Wagner, *Z. physik. Chem.*, **32B**, 447 (1936).
2. C. Gensch and K. Hauße, *ibid.*, **195**, 386 (1950).
3. K. Hauße and C. Gensch, *ibid.*, **195**, 116 (1950).
4. G. Tammann, *Z. anorg. Chem.*, **3**, 78 (1920).
5. C. Wagner, *Z. physik. Chem.*, **21B**, 25 (1933).
6. J. Teltow, *Ann. Phys.*, **6**, 63 (1949).
7. I. Pfeiffer, K. Hauße, and W. Jaenicke, *Z. Elektrochem.*, **56**, 728 (1952).
8. R. Dubrisay, *Compt. rend.*, **229**, 829 (1949).
9. D. Balarew, *Koll. Z.*, **101**, 47 (1942).
10. U. R. Evans and L. C. Bannister, *Proc. Roy. Soc., London*, **125A**, 370 (1929).
11. G. Tammann and W. Köster, *Z. anorg. u. allgem. Chem.*, **123**, 196 (1922).
12. E. J. Hartung, *J. Chem. Soc.*, **1926**, 1349.
13. E. J. Hartung, *ibid.*, **1924**, 2198.
14. V. Kohlschütter and E. Krähenbühl, *Z. Elektrochem.*, **29**, 570 (1923).
15. H. B. Linford and M. J. Ford, *J. (and Trans.) Electrochem. Soc.*, **93**, 16 (1948).
16. M. H. Brown, W. B. DeLong, and J. R. Auld, *Ind. Eng. Chem.*, **39**, 839 (1947).
17. R. Weiner, *Arch. Metallk.*, **1**, 281 (1947).
18. S. Shimadzu, *Mem. Coll. Sci. Kyoto Imp. Univ. Ser.*, **A19**, 229 (1936); *Chem. Zentr.*, (1937) II, 3575.
19. E. Raub, *Degussa-Metallberichte*, **1**, 39 (1941).
20. A. V. Solovjev, *Compt. rend. USSR*, **4**, 185 (1935).
21. L. L. Bircumshaw and M. H. Everdell, *J. Chem. Soc.*, **1942**, 598.
22. L. L. Bircumshaw and M. H. Everdell, *ibid.*, **1947**, 1119.
23. W. E. Campbell and U. B. Thomas, *Trans. Electrochem. Soc.*, **91**, 623 (1947).

Potential Studies on Passivity to Corrosion Induced by Pretreatment Processes for Metals

I. Aluminum

K. S. Rajagopalan

Central Electrochemical Research Institute, Karaikudi, India

ABSTRACT

Potential and polarization characteristics of aluminum which has been subjected to various chemical oxidation processes are reported. It is shown that a more negative initial electrode potential is recorded by the treated metal as compared to the untreated metal. The cathodic polarization curve of the treated metal is also much steeper. These results are satisfactorily explained by the application of the Glasstone, Laidler, and Eyring theory of electrode processes to the potential of a corroding metal.

Electrode potential measurements have been widely used in studying corrosion and corrosion inhibition (1-6). Such measurements have thrown valuable light on the intrinsic corrodibility of metals and alloys, the manner in which corrosion-inhibitive constituents added to the corrosive medium affect the corrosion process, and have also helped in understanding the role played by various types of pigments. Similarly, anodic and cathodic polarization curves of corroding metals have given valuable information on the mechanism of inhibition by corrosion inhibitors (7, 8). Numerous chemical processes have been developed in recent years which improve the resistance of metals to corrosion in different corrosive environments by the formation of thin, protective oxide, chromate, or phosphate films (9-14). The resistance to corrosion conferred by these treatments have been studied mainly by means of accelerated corrosion and field tests. Potential and polarization studies with the object of obtaining an insight into the mechanism by which chemical surface treatments confer passivity to the metal surface have, however, not yet been carried out. This paper is the first of a series describing such studies and concerns aluminum for which a number of simple processes involving only a dip treatment are known.

Experimental

Metal.—Indal 2 S to B.S. 1470 (commercially pure aluminum of 99% purity) from Indian Aluminum Co., Belur, Calcutta, cut into 1 x 1 in. specimens was used.

Scratch-free material was cut into the size required and given a high degree of polish with cloth buff soaked with wet pumice (15). This was followed by solvent cleaning in hot benzene and acetone, cleaning with alkaline cleaner (16), rinsing with cold water, and treatment in one of the following processes:

1. **MBV process (17):** 5-min treatment at 90°-100°C in solution containing 5% sodium carbonate and 1.5% sodium chromate.
2. **E.W. process (18):** 10-min treatment at 90°-100°C in MBV solution to which 0.1% sodium silicate has also been added.
3. **Pylumin process (19):** 5-min treatment at 95°-100°C in solution containing 6% sodium carbonate, 2% sodium chromate, and 0.2% disodium phosphate.
4. **Alrok process (20):** 20-min treatment at boiling point in solution containing 2% sodium chromate and 0.5% potassium dichromate.

5. *Chrome pickle* (21): Dipping for 2 min at 60°–70°C in solution containing 17.5% (w/v) chromic acid and 3.5% (w/v) H_2SO_4 .

6. *Phosphoric acid pre-treatment* (22): 5-min treatment in cold solution containing 10% (v/v) of orthophosphoric acid (85%), 70% (v/v) butyl alcohol, and 20% water.

7. *Acid cleaning* (23): 5-min immersion in cold solution of 5.6% of phosphoric acid (v/v) and 1.7% chromic acid.

8. *Chemical polishing* (24): 5-min treatment at 90°C in solution 80% (v/v) of phosphoric acid (85%), 3.5% (v/v) nitric acid, and 16% water. After treatment, the specimens were given a thorough rinse in cold water and dried with a hot air blower.

Procedure

The procedure followed was similar to that described by Brasher (25) with the difference that the sealing of the junction between metal and the external lead and glass tube was done in three stages using different mixtures of beeswax-rosin, beeswax-ceresin, and ceresin. This seal remained unaffected up to 60 days. The corroding medium, 3% NaCl in water, was contained in a 600 ml beaker and the specimen was fitted by means of rubber cork to the perspex cover of the beaker and lowered into the solution to a depth of 1 in. below the solution level. The test solution was aerated for 15 min before test to saturate it with oxygen.

Potentials were measured against a saturated calomel electrode using a Beckman pH meter as the null instrument. Only 10^{-11} amp passed on off balance. Polarization studies were carried out by external application of current with a duplicate specimen as the auxiliary electrode and the potentials measured as before. All measurements were made at $35^\circ \pm 0.1^\circ\text{C}$.

Results

Potentials given by a replicate number of untreated specimens and specimens treated by the MBV

Table I. Reproducibility of initial electrode potential vs. saturated calomel electrode at 35°C

No.	Untreated metal	Metal treated by MBV process
1	−0.761	−1.028
2	−0.745	−1.128
3	−0.753	−1.081
4	−0.740	−1.052

Table II. Change in potential in the first few hours

No.	Time	Potential of untreated metal	Potential of treated metal
1	0 min	−0.745	−1.081
2	5 min	−0.745	−1.021
3	10 min	−0.748	−0.991
4	15 min	−0.748	−0.954
5	30 min	−0.748	−0.825
6	1 hr	−0.748	−0.740
7	2 hr	−0.748	−0.745
8	3 hr	−0.748	−0.753
9	4 hr	−0.753	−0.787
10	1 day	−0.835	−0.857
11	2 days	−0.837	−0.868

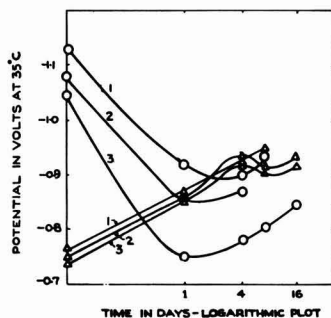


Fig. 1. Reproducibility of potential-time curves of untreated aluminum and aluminum treated by MBV process. Δ , untreated Al, \circ , Al treated by MBV process. Potentials were measured against saturated calomel electrode.

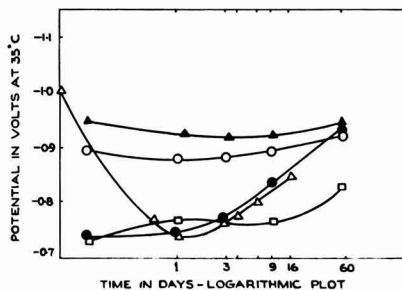


Fig. 2. Potential-time curves of aluminum treated by different pretreatment processes. \bullet , untreated Al, \square , EW process, Δ , Alro process, \circ , Pylumin process, \diamond , MBV process. Potentials were measured against saturated calomel electrode.

process immediately after immersion in sodium chromate solution are given in Table I. The instantaneous potentials of untreated aluminum are found to be reproducible with ± 10 mv while more variation is observed in the case of the treated specimens.

Potentials of treated and untreated metal were recorded frequently up to a period of 4 hr and then at the end of 1 and 2 days. Results are given in Table II.

The potential of untreated aluminum is found to be fairly steady for several hours at -0.745 v and then falls to more negative values, indicating failure of the protective oxide film in the corroding medium containing chloride ion in solution. The potential of the treated metal, which is highly negative to start with, rises quickly to the potential of untreated aluminum and falls again.

Reproducibility of potential-time curves with untreated and treated metal.—Potential-time curves given by replicate specimens of treated and untreated metal up to a period of 60 days are plotted in Fig. 1. It is seen from the figure that the potential-time curves of the untreated metal are generally characterized by a gradual drift in the course of 4 days to a constant potential which is 200 mv more negative; that of treated metal is, on the other hand, characterized by a rapid rise in the course of a day to the initial potential of untreated aluminum followed by a much slower fall. The extent of drift with

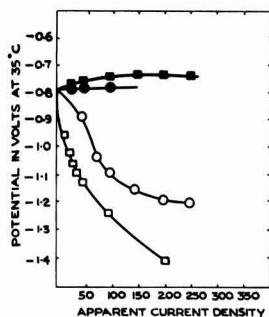


Fig. 3. Polarization curves of treated and untreated aluminum. Untreated Al, O cathodic, • anodic; MBV treated Al, □ cathodic, ■ anodic. Potentials were measured against saturated calomel electrode. Current density is in $\mu\text{A}/\text{in.}^2$.

time of immersion is, however, not so reproducible in the case of treated metal.

Potential-time curves of aluminum treated by different pretreatment processes.—Potential-time curves of aluminum treated by three more processes are given in Fig. 2 along with those of untreated metal and metal treated by MBV process.

It is seen from Fig. 1 and 2 that the rise in potential of untreated metal is not significant beyond 7 days. The initial potential of metal treated by the EW process is the same as that of untreated metal, and this potential falls at a much slower rate than that of untreated metal. The metal treated by the Alrok process gives a highly negative initial potential to start with, and there is not much change in this potential with time. Metal treated by the Pylumin process behaves similarly.

Initial potentials and changes in potential of aluminum treated by etching and polishing solutions.—An understanding of the data obtained with various passivating solutions may be facilitated if the effects of chemical treatments which involve etching, cleaning, or polishing of the surface on the potential are known. Therefore, the metal was treated by four solutions, one of which just etched the surface, the other cleaned it free of oxide film, the third one primed the surface for painting, and the last one gave a chemical polish. Results obtained are given in Table III.

It is seen from Table III that the behavior of the metal treated by any of the above methods is generally similar to that of untreated metal. The initial potential is the same as that of untreated metal, and this potential increases fairly rapidly to a more negative potential similar to untreated metal.

Polarization curves of untreated aluminum and aluminum treated by MBV process.—It is known that increased cathodic polarization of aluminum

takes place when dc currents of the order of $100 \mu\text{A}$ are passed from an external source through the metal as cathode, and hardly any polarization is observed with the metal as the anode (26-28). The effect of MBV treatment on the anodic and cathodic polarization curves of aluminum is, therefore, of interest. Anodic and cathodic polarization curves of treated and untreated aluminum are compared in Fig. 3.

It is seen that the cathodic polarization curve is made much steeper by treatment, and comparatively little change is observed at the anode.

Discussion

The fall in potential of untreated aluminum with time in the chloride medium is readily understood in terms of classical ideas on the meaning of electrode potential. It is associated with the breakdown of the protective oxide film and the final potential of -0.9 v signifies the equilibrium state between the breakdown of the oxide film by the corrosive action of chloride ions and repair of this film by oxygen present in the liquid. It is more difficult to understand the highly negative initial potential observed with metal treated by MBV, Pylumin, and Alrok processes. Passivation of a metal surface is usually accompanied by the potential becoming ennobled. Here, however, there are a number of systems where this is not the case. Mears (29) has shown, however, that, if the over-all electrode potential of a corroding metal is given by the convergence point of the polarization curve of the local anodes and cathodes (30), then instances can occur where passivity of the metal surface is accompanied by shifting of the electrode potential in the negative direction.

The greater corrosion resistance of more electro-negative aluminum as compared to steel in salt solutions is believed to arise from such a mechanism. This shift of potential in the negative direction, according to Mears, arises from increased polarization of the local cathodes. When the MBV treated metal is polarized cathodically by the application of external emf (see Fig. 3), the treated metal is polarized to a much greater extent than the untreated metal at equal current densities. The extent to which the two metals are polarized anodically does not differ to a significant extent. The more negative initial potential of MBV-treated aluminum and the polarization data are, therefore, explained satisfactorily in terms of this mechanism. But, as Mears pointed out, this approach has substantial limitations. First, it may not be correct to assume that anodic and cathodic polarization curves obtained by the application of an external current reproduce the polarization behavior of the local anodes and cathodes in the absence of an applied emf. Second, the indirect methods (7, 31) that have been suggested for measuring the polarization curves of the local anodes and cathodes stipulate a number of conditions which cannot be met in the case of the present systems. Further, the changes in potential with time, e.g., rapid rise in potential of MBV treated metal to that of untreated aluminum, do not lend themselves easily to explanation on the basis of the above mechanism.

Table III. Effects of chemical treatments not involving passivation

No.	Time	Chrome pickle	Phosphoric acid wash	Acid cleaning	Chemical polishing
1	0 hr	-0.737	-0.727	-0.760	-0.767
2	1 day	-0.813	-0.769	-0.796	-0.752
3	45 days	-0.922	-0.933	-0.939	-0.887

It was considered worth while, therefore, to see if the Glasstone, Laidler, and Eyring theory of rate processes (32) threw more light on the significance of such potential changes. According to this theory, the rate of the forward and reverse processes taking place at an electrode and the magnitudes of the currents flowing in the two directions as a result can be expressed in the form of an equation involving the concentration terms controlling each reaction, the specific velocity of the reaction, energy transfer coefficient, number of electrons involved in the electrode reaction, and the potential of the electrode, each of which can be measured under well-defined circumstances. The reactions taking place at each of the two electrodes constituting any one of the innumerable local cells present on a corroding metal also can be expressed in terms of such an equation. At each electrode, there is a forward and reverse reaction and there is a net flow of current. The local cells of a corroding metal are, however, short circuited through the metal and the total net current at all the local anodes equals the total net current at all the local cathodes. The two currents can, therefore, be balanced as follows:¹

Net cathodic current from all the local cells:

$$i_1 = Z \cdot f \cdot A_c \left\{ \prod_1^{p_1} (a_i \cdot \nu_i) \cdot K_1 \cdot e^{-\alpha'' Z f \cdot v / RT} - \underbrace{\prod_1^{p_1} (a_i \cdot \nu_i) \cdot K_1 \cdot e^{(1-\alpha'') Z f \cdot v / RT}}_{\text{negligible}} \right\} \quad [1]$$

where A_c = total cathodic area in cm^2 , $\prod_1^{p_1} (a_i \cdot \nu_i)$ = product of concentration terms controlling the cathodic reaction, K_1 = specific velocity of the reduction reaction in cathodic areas, α' = symmetry factor or energy transfer coefficient, Z = No. of electrons involved in the electrode reaction $f = 96,500$ (coulombs/mole, v = potential, R = gas constant, and T = temp $^\circ\text{K}$

Net anodic current from all the local cells:

$$i_2 = A_a \cdot Z f \left\{ \underbrace{\left(\prod_1^{p_2} (a_i \cdot \nu_i) \cdot K_2 \right)}_{\text{negligible}} - \prod_1^{p_1} (a_i \cdot \nu_i) \cdot K_2 \cdot e^{(1-\alpha'') Z f \cdot v / RT} \right\} \quad [2]$$

where A_a = total anode area in cm^2 , K_2 is the specific velocity of the oxidation reaction in anodic areas and α'' is the symmetry factor.

In the present case, potentials of the treated and untreated metal in 3% NaCl solution are all in the range of -0.7 to -1.2 v in which the anodic reaction terms of Eq. [1] and the cathodic reaction term of Eq. [2] would be negligible. Therefore, $i_1 = i_2$, where positive value denotes a cathodic current and negative value denotes anodic current, and

$$e^{-\alpha'' Z f \cdot v / (1-\alpha'') RT} = \frac{A_a \prod_1^{p_2} (a_i \cdot \nu_i) \cdot K_2}{A_c \prod_1^{p_1} (a_i \cdot \nu_i) \cdot K_1} \quad [3]$$

¹ After this paper was completed, the author came across an interesting paper by M. Takahashi (J. Electrochem. Soc. Japan, 25, (4) E 36 1957) giving the derivation of the equations for the potential of the corroding metal on the basis of the Glasstone, Laidler, and Eyring theory of rate processes as well as the experimental verification of the same.

and

$$-v = \frac{RT}{Z \cdot f \cdot (\alpha' + 1 - \alpha'')} \cdot \ln \frac{A_a \prod_1^{p_2} (a_i \cdot \nu_i) \cdot K_2}{A_c \prod_1^{p_1} (a_i \cdot \nu_i) \cdot K_1} \quad [4]$$

$$-v = \frac{RT}{Z \cdot f \cdot (\alpha' + 1 - \alpha'')} \cdot \ln \frac{A_a \cdot X_2}{A_c \cdot X_1} \quad [5]$$

where

$$X_2 = \prod_1^{p_2} (a_i \cdot \nu_i) \cdot K_2 \text{ and } X_1 = \prod_1^{p_1} (a_i \cdot \nu_i) \cdot K_1$$

Application of Eq. [5] to the behavior of untreated and treated aluminum in chloride solutions is of interest. From the tendency of aluminum to suffer localized corrosion or pitting, it may be concluded that A_a must be small compared to A_c . From the fact that the corroding metal registers a high negative potential, it also may be concluded with the help of the above equation that $A_a \cdot X_2$ must be greater than $A_c \cdot X_1$ and X_2 must be much greater than X_1 . The observed steep polarization of the metal when it is made cathodic by an external emf is in agreement with the idea of $A_c \cdot X_1$ being small. Similarly, the sluggishness with which the metal polarizes, when it is made the anode, is in agreement with the idea of $A_c \cdot X_2$ being large. The steeper cathodic polarization curve for the treated metal means that $A_c \cdot X_1$ is smaller than it was before treatment. This change is more likely to have taken place in respect to the effective area of the cathode A_c rather than in respect to the velocity factor. The effective cathodic area must, therefore, be considered to have diminished as a result of treatment. It also is seen from the above equation that when $A_c \cdot X_1$ becomes smaller the potential of the metal also falls. This is exactly what is observed in the case of the passivation treatments under study.

According to this interpretation the shift of potential of treated aluminum in the negative direction after immersion in the corroding solution arises from an increase in the anodic area, which is in conformity with the idea of breakdown of the film. The rise in potential of treated metal immediately after immersion should, according to this view, indicate an increase in the effective cathodic area, and this apparently comes to a stop when the solution has permeated all the pores of the treated metal. This approach also explains why treatments such as the EW process, which form extremely thin films similar to the naturally formed oxide films and which are practically free from pores, do not show such a tendency. In this case, the fall in potential with time is slower than that of untreated aluminum, thereby indicating that the production of anodic points is much less favored by the film formed under the conditions of this process than in the case of the natural oxide film. Observations made with specimens treated in solutions which have essentially a cleaning or smoothing effect on the metal surface are also explained. The initial potentials as well as the main trend of the potential time-curves of these specimens are parallel to the untreated metal. This shows that no film formation or conversion of the surface has taken place which is different from that which

happened to the untreated metal during exposure to air. The final potentials of untreated aluminum and aluminum treated by the different passivation processes do not differ considerably. This nearness of these electrode potentials despite the fact that the corrosion rate of treated aluminum is much lower than that of untreated aluminum can only be understood if the factor dominating the observed potential is the ratio between the anodic and cathodic areas. As long as this ratio remains the same, the potential will not differ considerably, but the corrosion rate may be markedly minimized if both anodic and cathodic areas are diminished. This leads to the important conclusion that the factor responsible for passivation by these treatments is the diminution in the cathodic area. The tendency of aluminum to be subjected to localized corrosion or pitting may, therefore, be expected to be minimized by the chemical oxidation processes investigated, unlike anodic inhibitors, e.g., chromates and phosphates.

Acknowledgment

Thanks of the author are due to Dr. K. S. G. Doss, Director of the Central Electrochemical Research Institute, for his valuable suggestions in regard to the discussions in this paper.

Manuscript received Nov. 12, 1957.

Any discussion of this paper will appear in a Discussion Section to be published in the December 1959 JOURNAL.

REFERENCES

1. O. Gatty and E. C. R. Spooner, "The Electrode Potential Behaviour of Corroding Metals in Aqueous Solutions," Clarendon Press, Oxford (1938).
2. U. R. Evans, "Metallic Corrosion, Passivity and Protection," Edward Arnold and Co., London (1946).
3. H. H. Uhlig, Editor, "Corrosion Handbook," John Wiley & Sons, Inc., New York (1948).
4. Internationales Kolloquium Über Die Passivität Der Metalle, Heiligenberg, 1957.
5. M. Cohen, *Corrosion*, **9**, 372 (1953).
6. M. J. Pryor, *This Journal*, **101**, 141 (1954).
7. T. P. May and F. L. LaQue, *Corrosion*, **10**, 91 (1954).
8. H. C. Gatos, *ibid.*, **12**, 23 (1956).
9. S. Wernick and R. Pinner, "Surface Treatment and Finishing of Aluminium and Its Alloys," Robert Draper Ltd., England (1956).
10. W. E. Pocock, *Metal Finishing*, **52**, 49 (Dec. 1954).
11. H. A. Holden, *Sheet Metal Ind.*, **23**, 1539 (1946).
12. R. P. Drysdale, *Trans. Inst. Metal Finishing*, **31**, 23 (1954).
13. R. Kerr, *J. Soc. Chem. Ind.*, **65**, 101 (1946).
14. S. C. Britton and R. M. Angles, *J. Appl. Chem.*, **4**, 351 (1954).
15. A.S.T.M. Standards, 1944, B 117-44T, (1), 1843.
16. Aluminium Development Association Information Bulletin No. 13 "Surface Finishing of Aluminium."
17. G. Eckert, *Hauszeit V.A.W. Erftwerk A.G. Aluminium*, **3**, 349 (1931).
18. W. Helling and H. Neunzig, *Aluminium*, **20**, 536 (1938).
19. Pyrene Co., Ltd., British Pat. 441,088 (1936).
20. S. Wernick and R. Pinner, *op. cit.*, p. 189.
21. H. Bengston, *Trans. Electrochem. Soc.*, **88**, 307 (1945).
22. U.S. Army Specn. 98-20007.
23. Reynolds Metal Co., "Finishes for Aluminium" Sec. 1 (1946).
24. Aluminium Co., of America, British Pat. 659,747 (1951).
25. D. M. Brasher, *Electroplating and Metal Finishing*, **9**, 280 (1956).
26. R. H. Brown and R. B. Mears, *J. (and Trans.) Electrochem. Soc.*, **94**, 495 (1948).
27. R. Ergang, H. Masing, and M. S. Mohling, *Z. Elektrochem.*, **56** (1952).
28. M. J. Pryor and D. S. Keir, *This Journal*, **102**, 605 (1955).
29. R. B. Mears and R. H. Brown, *ibid.*, **97**, 75 (1950).
30. U. R. Evans, *J. Franklin Inst.*, **208**, 52 (1929).
31. W. J. Schwerdtfeger and O. N. McDorman, *This Journal*, **99**, 407 (1952).
32. S. Glasstone, K. J. Laidler, and H. Eyring, "Theory of Rate Processes," McGraw Hill Book Co., New York (1941).

Mechanism of Electrodeposition of Nickel from Liquid Ammonia Solutions of Spin-Free Nickel(II) Complexes

George W. Watt and David A. Hazlehurst

Department of Chemistry, The University of Texas, Austin, Texas

ABSTRACT

Data on cathode current efficiencies for the electrolysis of solutions of $[\text{Ni}(\text{NH}_3)_6]^{2+}$, $[\text{Ni}(\text{en})_3]^{2+}$, and $[\text{Ni}(\text{dn})_2]^{2+}$ in the presence of Br^- , I^- , and SCN^- are interpreted on the basis of an $\text{S}_{\text{N}}2$ mechanism in which the rate-controlling step is most probably dependent on the translabilizing effect of the entering ligand that is involved in the formation of an initial transition state complex.

Continued interest in the electrodeposition of metals from nonaqueous media (1-5) from both theoretical and practical viewpoints has prompted us to re-examine certain data that were obtained several years ago. It was observed that deposition from ammonia solutions of hexamminenickel(II) bromide, trisethylenediaminenickel(II) bromide, and bisdi-

ethylenetriaminenickel(II) bromide occurred at negligibly low rates; upon addition of the potassium salts of Br^- , I^- , and SCN^- , however, deposition occurred at markedly increased rates that were dependent on the identity of the added anionic ligands. It is of interest to consider these data in the light of generalizations and mechanisms proposed by Lyons

(6-8) with reference to deposition from aqueous solutions, and to propose an alternative mechanism for the genesis of a transition state complex.

Experimental

Materials.—Hexamminenickel(II) bromide (calculated: Br^- , 49.9; found: Br^- , 50.0) was prepared as described elsewhere (9). Trisethylenediaminenickel(II) bromide 1-hydrate was prepared as described by Werner and Megerle (10); the anhydrous salt (calculated: Br^- , 39.9; found: Br^- , 40.1) resulted upon heating the 1-hydrate for several hours at 100°–105°. Similarly, bisdiethylenetriaminenickel(II) bromide (calculated: Br^- , 37.6; found: Br^- , 37.6) was formed from the corresponding 1-hydrate (11).

Equipment and procedures.—The equipment employed was essentially the same as that described by Booth and Merlub-Sobel (12) except that the design of the electrode holders was such that the electrodes could be removed readily for direct weighing before and after electrolysis. Nickel anodes (Ni, 99.5) and bright platinum cathodes were used in all of the experiments reported here. The electrical circuit included a silver coulometer and otherwise was conventional in all respects.

The electrolysis cell was predried, thoroughly, and strictly anhydrous conditions were maintained in all experiments. The solvent ammonia was dried over sodium amide and, just prior to use, was bubbled through a solution of potassium in ammonia. The ammonia was condensed at –45°, after which the temperature was raised to and maintained at a temperature just slightly below the normal boiling point of the solvent (–33.5°). Following electrolysis, the ammonia solution was siphoned from the cell and the electrodes were washed, dried, and weighed. After evaporation of the solvent from the combined electrolytic solution and washings, Ni^{2+} could be determined gravimetrically by the dimethylglyoxime method.

Experimental data.—In a series of experiments involving the cationic nickel(II) complexes indicated above, the total solution volume was 75 ml, the concentration of the nickel(II) salt was 0.02M, the concentration of the added potassium salts was 0.1M, and the current density was 0.54 ± 0.05 ma/cm². Other pertinent data are included in Table I.

Table I. Electrolysis of liquid ammonia solutions of nickel(II) salts

Added salt	Potential, v	Time, hr	Cathode current efficiency, %
[Ni(NH ₃) ₆]Br ₂	KBr	2.85	3.0
	KI	1.57	3.0
	KSCN	1.50	3.0
[Ni(en) ₃]Br ₂	KBr	3.00	2.0
	KI	1.72	2.1
	KSCN	1.48	3.0
[Ni(dn) ₂]Br ₂	KBr	2.80	1.0
	KI	1.88	1.5
	KSCN	1.55	3.0

Although bright adherent deposits of nickel were obtained in the electrolysis of ammonia solutions of tetramminenickel(II) thiocyanate (13), the deposits in the experiments reported here were less satisfactory but nevertheless sufficiently adherent not to introduce appreciable errors in determining the total nickel deposited by direct weighing of the cathodes. Neither microscopic examination nor electron photomicrographs served to reveal any consistent characteristics of the deposits as a function of the ligands employed.

Discussion

With reference to the electrodeposition of metals from cationic complexes, Vlcek (14) has proposed that the essential step involves the formation of a zerovalent species, after which metal-ligand bond breaking leaves the free metal as a deposit on the cathode. If such a mechanism were operative, it is not immediately apparent in the present case why cathode current efficiencies should be influenced so profoundly by specific anionic ligands.

Lyons (7) suggested a primary heterolytic dissociation, or $\text{S}_{\text{N}}1$ mechanism¹ in which metal-ligand bond breaking provides an available bonding orbital for the establishment of a partially metallic bond with the cathode lattice.

We wish to propose, largely on the basis of the results reported above, that there is an alternative and more probable mechanism. The nickel(II) complexes used in the present studies are all of the octahedral sp^3d^2 or spin-free type. If the observed trends in cathode current efficiencies may be assumed to have even qualitative kinetic significance, it seems reasonable to assume that the primary reaction involves an initial nucleophilic attack by the added anions, e.g., Br^- , I^- , and SCN^- . Thus, it is assumed that an $\text{S}_{\text{N}}2$ mechanism is operative, that the coordination number of nickel in the transition state complex is seven, and that rupture of one of the original metal-ligand bonds occurs trans to the incoming anionic ligand. Accordingly, a bonding orbital is made available and the subsequent events may well occur as pictured by Lyons (7). Irrespective of the stereochemical configuration of the transition state complex and regardless of whether cis or trans attack is involved, the proposed $\text{S}_{\text{N}}2$ mechanism suggests two possible rate-limiting steps both of which must take into account the fact that the neutral solvent molecules as incoming ligands are potentially competitive with the added anionic ligands. In view of the data in Table I, however, it seems apparent that the solvent molecule is not thus competitive.

First, the formation of a transition state complex may be rate limiting and dependent on the relative nucleophilic character of the incoming ligands. From Table I it may be seen that the increasing order of cathode current efficiencies for the three added anionic ligands is $\text{Br}^- < \text{I}^- < \text{SCN}^-$. Although still of questionable status (15) and in any event probably not quantitatively applicable to ammonia solutions, the order of nucleophilic constants (16, 17) for these

¹ The nomenclature employed herein is that recommended by Basolo and Pearson (15).

ions is $\text{Br}^- < \text{SCN}^- < \text{I}^-$. A second and more attractive alternative would assume that bond breaking is the rate-limiting step; in this case the observed rates should correspond to the relative translabelizing effects of the entering ligands. If we may assume the same order for octahedral as for square planar complexes (18), i.e., $\text{NH}_3 < \text{Br}^- < \text{I}^- < \text{SCN}^-$ (where only the relative position of the latter is in doubt, but nevertheless reasonable) then the correlation with the data of Table I is self-evident.

It is our intention to provide further experimental data bearing on this question.

Acknowledgments

This work was supported in part by the U. S. Atomic Energy Commission, Contract AT-(40-1)-1639. The nickel anodes used in these studies were supplied by the International Nickel Co.

Manuscript received Sept. 3, 1958.

Any discussion of this paper will appear in a Discussion Section to be published in the December 1959 JOURNAL.

REFERENCES

1. A. Brenner, *This Journal*, **103**, 652 (1956).
2. J. H. Connor and A. Brenner, *ibid.*, **103**, 657 (1956).

3. W. E. Reid, Jr., J. M. Bish, and A. Brenner, *ibid.*, **104**, 21 (1957).
4. G. B. Wood and A. Brenner, *ibid.*, **104**, 29 (1957).
5. J. H. Connor, W. E. Reid, Jr., and G. B. Wood, *ibid.*, **104**, 38 (1957).
6. E. H. Lyons, Jr., *ibid.*, **101**, 363 (1954).
7. E. H. Lyons, Jr., *ibid.*, **101**, 376 (1954).
8. E. H. Lyons, Jr., J. C. Bailar, Jr., and H. A. Laitinen, *ibid.*, **101**, 410 (1954).
9. G. W. Watt, "Inorganic Syntheses," Vol. 3, p. 194, McGraw-Hill Book Company, Inc., New York (1950).
10. A. Werner and W. Megerle, *Z. anorg. Chem.*, **21**, 213 (1899).
11. J. G. Breckenridge, *Can. J. Research*, **26B**, 11 (1948).
12. H. S. Booth and M. Merlub-Sobel, *J. Phys. Chem.*, **35**, 3303 (1931).
13. G. W. Watt and D. A. Hazlehurst, Unpublished work.
14. A. A. Vlcek, *Nature*, **177**, 1043 (1956); *Z. Elektrochem.*, **61**, 1014 (1957).
15. F. Basolo and R. G. Pearson, "Mechanisms of Inorganic Reactions," John Wiley & Sons, Inc., New York (1958).
16. C. G. Swain and C. B. Scott, *J. Am. Chem. Soc.*, **75**, 141 (1953).
17. J. O. Edwards, *ibid.*, **76**, 1540 (1954).
18. J. Chatt, L. A. Duncanson, and L. M. Venanzi, *J. Chem. Soc.*, **1955**, 4456.

Electrodeposition of Molybdenum

T. T. Campbell

U. S. Bureau of Mines, Albany, Oregon

ABSTRACT

Electrodeposition studies performed at the Northwest Electrodevelopment Laboratory of the U. S. Bureau of Mines, Albany, Oregon, are described. Research was directed toward the electrodeposition of molybdenum from non-aqueous media such as liquid ammonia, formamide, acetamide, hydrazine, and other organic solvents and the preparation of pure anhydrous molybdenum halides. While thin plates of molybdenum were obtained, the growth of massive deposits was not realized.

The requirements of modern technology for materials possessing high temperature strength and corrosion resistance properties has, in recent years, stimulated an intensified interest in molybdenum.

Molybdenum is produced commercially by hydrogen reduction of molybdenum oxides. The metal powder resulting from this treatment is not of uniform quality and purity although it can be converted into usable forms by powder metallurgy techniques.

While the literature reports many claims for the successful electrodeposition of Mo (1), thorough analyses of and attempts by later investigators to duplicate these claims lead to the conclusion that the only practicable method of electrodepositing molybdenum is from the fused salt bath recently developed by Brenner and Senderoff of the U. S. Bureau of Standards (2). The prevailing opinion is that electrodeposition of pure Mo from aqueous solutions is unlikely. On the other hand, the use of organic solvents, fused salt baths, and other nonaqueous solvents such as hydrazine or liquid ammonia as media for the electrodeposition of Mo has had only

limited attention. Efforts to electrodeposit Mo at the Albany station of the U. S. Bureau of Mines were restricted mainly to studies in nonaqueous solvents since a preliminary period spent in duplicating other published methods proved fruitless.

Discussion

It is doubtful whether simple ions as such are present in solutions containing Mo compounds, either because of reactions occurring between the solutes and solvents or because of the tendency of Mo ions to form polyions by polymerisation and condensation reactions. In addition, Mo compounds may disproportionate to give complex compounds in which the metal ion may exist in any of its oxidation states. It is probable that only complex systems result during efforts to electrodeposit Mo, regardless of the media used.

Studies of electrode potentials in fused salt baths carried out by Brenner and Senderoff (2) indicate that the reduction of Mo to trivalent oxides proceeds at a more noble potential than does reduction to

metal. The same situation apparently holds true either in aqueous or organic solutions, and on this basis it would seem that oxygen or oxygen containing compounds must be absent from the electrolytic system in order to obtain the metal. Reduction of Mo ions *in situ* by hydrogen, postulated as a mechanism in chromium deposition, does not occur; this fact, and the low hydrogen overvoltage of Mo (3) are major factors preventing deposition of Mo from aqueous systems.

While the metal can be deposited from the fused salt baths developed by Brenner and Senderoff, the utility of their techniques from an economic standpoint does not appear promising. The procedures outlined offer formidable difficulties such as operation of corrosive fused salt baths at temperatures ranging from 600° to 900°C with the necessity of complete exclusion of air or moisture from the cell. While these baths presumably could be useful for specialized electroplating or electroforming operations, it is doubtful if they could be adapted to widespread general usage.

On the basis of the foregoing discussion, it appears obvious that a practicable solution to the problem of Mo deposition is needed. The application of nonaqueous solvents other than fused salt baths to the problem of Mo deposition offers many interesting possibilities: (a) studies can be made on systems from which oxygen or oxygen containing compounds can be completely excluded; (b) exploration in a comparatively new and untried field of research is possible; and (c) if successful, research of this type may provide a new approach for the electrodeposition of other rare and refractory metals.

Experimental Procedures and Apparatus

For reasons previously expressed, it was considered desirable to conduct tests in systems which completely excluded oxygen either in the solutes or the solvents. This program necessitated careful examination of methods for preparing Mo compounds. Much of the work was restricted to molybdenum chlorides and bromides since these compounds proved reasonably soluble in many of the solvents studied. Most of the solvents had relatively high dielectric constants although solvents were not excluded from study even when the dielectric constant was of a rather low order.

Since the majority of the work carried out in this study was exploratory in nature, the equipment and procedures utilized were varied in nature. In general, Pyrex beakers of 250-500 ml capacity were used as cells, although small rectangular glass cells (800 ml capacity), U tube cells, and 3-necked Pyrex flasks were utilized during various phases of the investigation. Those tests carried out under an inert atmosphere usually were carried out in 3-necked flasks or in Pyrex tubes sealed with rubber stoppers. Argon or helium atmospheres were maintained above those systems which were sensitive to carbon dioxide, oxygen, or moisture. The liquid ammonia study was carried out in equipment similar to that described by Merlub-Sobel (4). Liquid ammonia cells were operated at either low temperatures (below -33°C) and atmospheric pressure, or at room

temperature when a high pressure (above 145 psig) cell was used. After initial study in the field of aqueous electrolysis proved unsuccessful, the solubility of various Mo compounds in organic and other nonaqueous solvents was determined. Quantitative solubility tests were carried out in a temperature controlled ($\pm 1^\circ\text{C}$) water bath in the 25°-100°C range and in an ondina oil bath (a USP grade mineral oil) for temperatures up to 200°C. The Mo compounds were added in 100-mg quantities to 50 ml of the solvent until insoluble material remained for at least 1 hr. The temperature was increased by 20°C increments with periodic additions of solute until the highest practicable operating temperature for the particular solvent was reached. The maximum solubility of the solutes over a wide temperature range was obtained by this procedure. Qualitative data on solubilities were also obtained on many of the systems studied. Since solubility data of Mo compounds in nonaqueous solvents are not generally available in the literature, the results of this work are presented in Table I.

Conductivity tests were made on all of the solvents in which Mo compounds were reasonably soluble. Column 5 of Table I indicates those solvents which were conducting or nonconducting, along with other pertinent remarks. Anodes and cathodes of graphite, copper, iron, platinum, molybdenum, stainless steel, lead, etc., were used, the particular electrode material used depending on the type of solvent employed. A Beckman (Model H-2) pH meter was used to determine pH values during the course of the study. A 50 amp-24 v capacity selenium rectifier was used as a source of d-c current.

Electrolytic tests generally covered a wide range of current densities and temperatures over varying periods of time. The course of electrolyses was followed by observation of current, voltage, and pH readings. The effectiveness of any particular system for Mo deposition was determined by visual inspection of the cathode. Whenever metallic deposits were obtained they were subjected to x-ray diffraction study and to spectrographic analyses. While no massive deposits of Mo were obtained from any of the systems studied, thin deposits of Mo and alloys of Mo with Fe, Pb, or Pt were readily obtained. The usual cathode products were lower oxides, hydroxides, or other reduced compounds of Mo.

Because of the great number of systems covered during this study and the negative character of some of the results, it is impracticable to show all the data obtained. For this reason, Table II shows only the data for those experiments which either gave thin deposits of pure Mo or alloys of Mo with other metals.

Preparation and Handling of Mo Halides

Since much of the work described utilized either the chlorides or bromides of Mo as solutes, the preparation of these compounds required detailed attention. The preparation of the dichloride and dibromide of Mo posed no particular problem as disproportionation of molybdenum tribromide in a 2-in. Vycor tube was found to proceed smoothly at 600°C to give molybdenum dibromide and disproportiona-

Table I. Solubility of Mo Compounds in water and non aqueous solvents

Compound	Solvent	Temp, °C	Solubility g/l	Remarks
MoS ₂	Alkaline polysulfide	—	51.5	Low solubility
MoS ₂	Formamide	180	Insol.	
MoS ₂	Acetamide	200	Insol.	
MoS ₂	Triethanolamine	215	50	
MoS ₂	Pyridine hydrochloride	70	v.s.l.s.	
MoS ₃	Alkaline polysulfide	—	>50	Low solubility
MoBr ₂	Water	To 100	Insol.	
MoBr ₂	Carbon tetrachloride	Room	Insol.	
MoBr ₂	Hydrazine hydrochloride (65%)			
	Water (35%)	Room	>1.0	
MoBr ₂	Water (75%)			
	Hydrazine (25%)	Room		Violent reaction
MoBr ₂	Ethylene diamine	Room	Sol.	Visible reaction
MoBr ₂	Cyclohexanol	Room	Insol.	Suspension formed
MoBr ₂	Aniline	Room		
MoBr ₃	Hydrazine (95%)	25-30	—	Violent reaction
MoBr ₃	Cyclohexanol	Room	51.5	Suspension formed
MoBr ₃	Water (50%)			
	Tartaric acid (50%)	Room	51.5	Conducting
MoBr ₃	Dextrose (50%)			
	Water (50%)	Room	51.5	Conducting
MoBr ₃	Tartaric acid	170	51.5	Conducting
MoBr ₃	Liquid ammonia	—35	—	Reaction to give solid ppt.
MoBr ₃	Liquid ammonia	20	10	Nonconducting
	Ammonium nitrate eutectic			
MoCl ₃	Pyridine hydrochloride	70	~570	Soluble with reaction to give clear amber solution that solidifies at 35°-40°C conducting
MoCl ₃	Liquid ammonia	—35	Insol.	
	Diethyl amine			
MoCl ₃	Liquid ammonia	—35	15-20	Some reaction to give solid ppt.
MoCl ₃	Ethyl chloride (10 ml)	Room	10	
	Benzene (20 ml)			
MoCl ₃	Liquid ammonia			
	Ammonium nitrate eutectic	20	10	Nonconducting
MoCl ₃	Aniline (10 ml)			
	Ethyl bromide (5 ml)	Room	10	Conducting
MoCl ₃	Carbon tetrachloride	Room	51.5	Conducting
MoCl ₃	Pyridine hydrochloride	70	~400	Soluble with reaction to give clear brown solution
MoCl ₃	Methyl alcohol	Room	v.s.	Soluble with reaction to give conducting solution
MoCl ₃	Ethyl alcohol	Room	v.s.	Soluble with reaction to give conducting solution
MoCl ₃	Liquid ammonia	—35	—	Reaction to give solid ppt.
MoCl ₃	Aniline	Room	<5	Nonconducting
MoCl ₃	Ethyl bromide	Room	16	Nonconducting
MoCl ₃	Benzene	Room	<5	Nonconducting
MoCl ₃	Ethylene diamine	Room	—	Reaction
MoCl ₃	Hydrazine (95%)	Room	—	Violent reaction
MoCl ₃	Acetone	Room	Sol.	Reaction to give green solution, conducting
MoCl ₃	Acetic anhydride (10 ml)	Room	300	Conducting
	Formamide (15 ml)			
MoCl ₃	Aniline (10 ml)	Room	50	Low conductivity
	Ethyl bromide (5 ml)			
MoCl ₃	Liquid ammonia	20	40	Nonconducting
	Ammonium nitrate Eutectic			
MoCl ₃	Phenyl ethyl bromide	150-200	180-200	Conducting
MoCl ₃	Pyridine hydrobromide	40	~60	Soluble with reaction to give red solution
MoCl ₃	Pyridine (10 ml)	50	~100	Soluble with reaction to give green solution
	Phenol (10 ml)			
MoCl ₃	Ethyl chloride (10 ml)	Room	10	Low conductivity
	Benzene (20 ml)			
MoCl ₃	Ethyl bromide (10 ml)	Room	~60	Low conductivity
	Benzene (20 ml)			
Na ₂ MoO ₄	Formamide	150	200	Solidification-conducting
Na ₂ MoO ₄	Acetamide	203	Insol.	Conducting
Na ₂ MoO ₄	Triethanolamine	215	>50	Low conductivity
Na ₂ MoO ₄	Pyridine hydrochloride	70	~38	
(NH ₄) ₂ MoO ₄	Formamide	180	~200	Solidification-conducting
(NH ₄) ₂ MoO ₄	Acetamide	170	~100	Conducting
(NH ₄) ₂ MoO ₄	Triethanolamine	170	~250	Conducting
(NH ₄) ₂ MoO ₄	Pyridine hydrochloride	70-100	~95	Soluble with reaction, pyridine decomp. at 100°C, conducting

Key: v.s., very soluble, in excess of 50 g/l; s., soluble, 10-50 g/l; s.l.s., slightly soluble, 1-10 g/l; insol., <1 g/l.

Table II. Electrolytic test data on the electrodeposition of Mo

Solvent	Vol, ml	Solute	Weight, g	E, v	I, amp	Cathode current density, amp/ft ²	Temp, °C	Anode	Cathode	Remarks
Acetic acid	108	MoO ₃	1	Max 15	2.9-29	47-470	18-80	Graphite	Copper	Slight deposit at low CD. At higher CD's thin deposits of metal, then oxides. pH = 5.8-6.4
Ammonium hydroxide (concentrate)	100									
Acetamide	100	MoCl ₅	1	—	—	465	120-130	Platinum	Copper	Metallic appearing deposit
Acetamide	100	MoCl ₅	2	—	—	93	105-150	Platinum	Copper	Dark metal deposit. Heating indicates Mo present
Acetamide	200	MoCl ₅	7	—	—	74.3-557	80-130	Platinum	Copper	Metallic deposit covered with oxide
Acetamide	100	MoCl ₅	7	—	—	56	80-115	Molybdenum	Copper	Black oxides with faint blush of metal. Slight attack on anode
Acetamide	500	MoCl ₅	25	7.5	0.75	0.35	80	Graphite	Copper	Metallic blush
Acetamide	200	MoCl ₅	1-7	—	—	74.5-567	80-155	Iron	Copper	Thin metallic deposits
Acetamide	116	MoCl ₅	1	—	—	46.5-111.5	100	Platinum	Copper	Pt-Mo deposit
Acetamide	258	MoCl ₅	23.6	4.0	1.11	20	80-90	Graphite	Copper	Metal blush at 4 hr, nonadherent deposit on cathode
Hydrazine	10									
Ethylene diamine	200									
Acetamide	195.6	MoCl ₅	20	3.8	0.5	1.03	90	Graphite	Copper	Metal blush on back of cathode
Hydrazine	10									
Ethylene diamine	100									
Acetamide	300	MoCl ₅	23.6	4.0	1.1	2.0	80-90	Graphite	Copper	Metal blush after 4 hr
Hydrazine	10									
Ethylene diamine	200									
Acetamide	86.3	MoCl ₅	5	5.0-7.0	0.5	102	75-80	Graphite	Copper	Metallic blush formed. Was displaced by dense black film
Pyridine	10									
Acetamide	432	MoCl ₅	25	0.75	7.5	9.39	80	Graphite	Copper	Metallic blush on one side
Pyridine	300									
Acetamide	100	MoCl ₅	5	5-7	0.5	173	75-80	Graphite	Copper	Metal blush replaced by black film
Pyridine	10									
Formamide	100	MoCl ₅	2.4	—	—	140-460	80-120	Graphite	Copper	Blushes on metal and oxides. Higher CD produces dull deposit
Formamide	100	Na ₂ MoO ₄	10	—	—	74-148	40-140	Platinum	Copper	Metallic blush. Pt-Mo alloy
Formamide	100	MoO ₃	10	—	—	18.5-371	25-110	Platinum	Copper	Metal blush on edges of cathode
Formamide	100	(NH ₄) ₂ MoO ₄	10	—	—	186-372	23-90	Platinum	Copper	Thin deposit covering cathode
Formamide	50	MoCl ₅	1	—	—	37-613	30-89	Graphite	Copper	Few oxides. Faint blush of metal
Water	5									
Formamide	400	MoCl ₅	15	0.1	1.5	1.6	35	Graphite	Stainless steel	Metallic blush covered by spongy black deposit
Pyridine	100									
Hydrazine	5									
Formamide	100	Na ₂ MoO ₄	5	10	1	46.5	—	Graphite	Copper	Thin bright metallic-like deposit
Versene	10									
Formamide	100	Na ₂ MoO ₄	5	7.5-8.5	0.5	23.2	25-35	Graphite	Copper	Light metallic deposit on edges of cathode
Versene	10									
Formamide	100	Na ₂ MoO ₄	5	9-18	1.5	69.6	25-65	Graphite	Copper	Thin metallic plate on face of cathode
Formamide	100	Na ₂ MoO ₄	5	11	1	46.4	25-55	Graphite	Copper	Same as above run
Versene	10									
Formamide	100	Na ₂ MoO ₄	5	9-18	2	92.9	35-95	Graphite	Copper	Metal blush
Versene	10									
Formamide	100	MoO ₃	5	5	1	46.5	25-60	Graphite	Copper	Bluish cast. Metallic deposit covered with oxides
Versene reg.	100	MoO ₃	5	5	2	92.9	25-85	Graphite	Copper	Deposit similar as previous run
Formamide	10	85%								
Versene reg.	100	MoO ₃	5	7-15	3	139.5	25-105	Graphite	Copper	No metal deposit. Temp. probably too high
Versene reg.	10	85%								
Glycol	500	Na ₂ MoO ₄ ·2H ₂ O	17.5	20	—	3.6	20	Iron	Copper	Thin gray metallic deposit
Glycol	500	Na ₂ MoO ₄ ·2H ₂ O	17.5	3.5	—	19	80-112	Iron	Copper	Gray deposit mostly iron. Some Mo
Hydrazine	25	MoCl ₅	5	2.4	0.7	100	22	Stainless steel	Copper	Metal blush on Cu cathode
Ammonium hydroxide (concentrate)	25									
Hydrazine	25	MoCl ₅	5	2.4	0.7	101	22	Graphite	Copper	Metal blush
Ammonium hydroxide (concentrate)	25									
Water	170	H ₂ MoO ₄	320	—	—	185-465	22-55	Lead	Copper	Thin Pb-Mo alloy deposit
Sulfuric acid (concentrate)	1665	85% N ₂ H ₄ ·2HCl	20	2.1-3.0	0.5-3.3	18-108	20-50	Copper	Stainless steel	Thin metallic deposit on cathode
Water	200	MoO ₃	8							
		NH ₄ Cl	20							
Water	100	N ₂ H ₄ ·2HCl	10	2.0	2.4	—	22	Copper	Stainless steel	Metal blush on cathode
		MoO ₃	8							
Water	100	NH ₄ Cl	20	2.4	2.0	—	22	Copper	Stainless steel	Metal blush
		MoO ₃	8							
		NH ₄ Cl	20							
Water	500	N ₂ H ₄ ·2HCl	10	3.5	—	20	45-50	Graphite	Copper	Metal blush on cathode
		KOH	50							
Water	500	Na ₂ MoO ₄ ·2H ₂ O	100							
		Na ₂ C ₂ H ₃ O ₇ ·2H ₂ O	44	4	—	93	26-44	Iron	Copper	Fe-Mo alloy
		Na ₂ MoO ₄ ·2H ₂ O	36.5							
Water	500	Na ₂ SO ₄	14							
		Na ₂ C ₂ H ₃ O ₇ ·2H ₂ O	44	7	—	1.85	30-66	Iron	Copper	Fe-Mo alloy
		Na ₂ MoO ₄ ·2H ₂ O	36.5							
Water	500	Na ₂ SO ₄	14							
		Na ₂ C ₂ H ₃ O ₇ ·2H ₂ O	44	4	—	93	26-40	Graphite	Copper	Bluish black metallic deposit
		Na ₂ MoO ₄ ·2H ₂ O	36.5							
Water	500	Na ₂ SO ₄	14							
		Na ₂ C ₂ H ₃ O ₇ ·2H ₂ O	44	20	—	93	28-52	Graphite	Copper	Bluish black metallic deposit
		Na ₂ MoO ₄ ·2H ₂ O	36.5							
Water	500	NaOH	120	2.0	—	90	50-55	Iron	Copper	Thin gray metallic deposit
		Na ₂ MoO ₄ ·2H ₂ O	50							
Water	500	NaOH	120	3.25	—	180	20-40	Iron	Copper	Thin gray metallic deposit
		Na ₂ MoO ₄ ·2H ₂ O	50							
Water	500	NaOH	120	5.0	—	360	20-65	Iron	Copper	Thin gray metallic deposit
		Na ₂ MoO ₄ ·2H ₂ O	50							
Water	50	MoO ₃	5	6.2-14	8.2-16.3	70-300	28-85	Graphite	Copper	No massive deposits. Only thin plates. pH = 5.5-7.0
Acetic acid	10	KC ₂ H ₃ O ₂	50							
		NH ₄ C ₂ H ₃ O ₂	50							
Water	130	KC ₂ H ₃ O ₂	100	—	—	90-180	22-72	Graphite	Copper	Metal blushes obtained at low CD's. Oxides only at higher CD. pH = 5.5-6.75
Acetic acid	50	MoO ₃	5							
Water	50	Na ₂ C ₂ H ₃ O ₂	20	—	—	18-300	20-75	Lead	Copper	No deposit at low CD
Acetic acid	36	MoO ₃	5							
Water	200	NH ₄ Cl	20	2.1-3.0	0.5-3.3	18-108	22-50	Graphite	Stainless steel	Lead deposits at higher CD along with Mo. pH = 4-5
Hydrazine hydrochloride	20	MoO ₃	8							
Water	100	MoO ₃	8	1.7-2.4	2.0-2.4	—	22-70	Stainless steel	Copper	Metal blush
Hydrazine hydrochloride	10	NH ₄ Cl	20							
Water	100	MoO ₃	1	2.4	0.5	—	22	Stainless steel	Graphite	Very thin metal blush
Hydrazine hydrochloride	20									

tion of molybdenum trichloride at 600°-650°C gave good yields of molybdenum dichloride.

Direct chlorination of Mo powder at 350°-400°C was found to give a product whose major constituent was the pentachloride. The product almost always contained some unreacted metal powder and small amounts of lower valent chlorides. Direct chlorination of molybdenum disulfide in a Ni-lined vertical shaft type chlorinator at 500°C was attempted. Pure molybdenum pentachloride could not be isolated by this method. The product was contaminated with molybdenum compounds that contained sulfur (Mo_2S_3) which tended either to sublime along with the molybdenum pentachloride or were carried over by entrainment. Efforts to free the molybdenum pentachloride of sulfur compounds by sublimation at 280°C were unsuccessful.

Molybdenum trichloride was prepared by the reaction of molybdenum pentachloride with powdered molybdenum at 350°C as shown in the equation below:



Direct bromination of Mo powder at 300°-350°C produced a mixture of molybdenum tribromide and molybdenum tetrabromide; however, analyses indicated the product to be primarily tribromide.

With the exception of the dibromides, tribromides, and the dichlorides, the halides of molybdenum are all hygroscopic, sensitive to oxygen and moisture in the air, and form oxycompounds readily.

The preparation of definite compounds was not successful except in the case of the divalent halides; in all other cases the products were contaminated to some extent with unreacted metal powder or were a mixture of tri, tetra, and pentavalent halides.

In order to prevent the formation of oxy compounds, it was necessary to exercise extreme precautions while transferring the halides from the reaction tubes to storage vessels and finally to the electrolytic cells. Large rubber transfer tubes, filled with argon gas, were used at all times to prevent air contamination of the halides. The prepared halides were stored in bottles under an argon atmosphere and sealed with polyethylene tape which was in turn paraffin covered. Avoidance of these procedures inevitably led to rapid contamination of the halides and the formation of oxy compounds.

Conclusions

The inability to obtain pure massive Mo deposits from either aqueous or nonaqueous systems containing oxygen compounds probably is caused in part by the low overvoltage of hydrogen on Mo and by the fact that deposition of oxides occurs at a more noble potential than does reduction to metal. While many thin plates of Mo were obtained during this study, once the cathode was covered with a thin film of Mo, the following situations developed: (a) passivation set in, (b) hydrogen, nitrogen, or ammonia evolved at the cathode, (c) lower oxides, hydroxides, or other reduced compounds continued to deposit at the cathode.

In several instances, alloys of Mo with Fe, Pt, or Pb were obtained; the source of the alloying agent in most instances originated from the anode.

Reduction of molybdenum ions to metal *in situ* by hydrogen, postulated as a possible mechanism for Cr deposition, does not seem to occur. Recovery and examination of the Mo salts, after evaporation of the solvents, indicated that Mo halides readily form a wide variety of complex compounds with nonaqueous solvents. It is doubtful if simple molybdenum ions were present in any of the systems studied.

Both qualitative and quantitative solubility data for a number of Mo compounds in a variety of organic solvents are shown.

While massive deposits of Mo were not obtained, the results obtained in this study are encouraging. The application of much higher current densities than those reported in this study, coupled with more stringent atmosphere control, may well provide a means toward the electrodeposition of massive Mo.

The use of nonaqueous solvents in conjunction with anhydrous Mo compounds, while faced with serious difficulties, offers an interesting and challenging approach to a very difficult problem.

Manuscript received April 13, 1956. This paper was prepared for delivery before the San Francisco Meeting, April 29-May 3, 1956.

Any discussion of this paper will appear in a Discussion Section to be published in the December 1959 JOURNAL.

REFERENCES

1. T. T. Campbell and A. Jones, Information Circular 7723, U. S. Dept. of Interior, July 1955.
2. A. Brenner and S. Sanderoff, *This Journal*, **101**, 16, 33 (1954).
3. J. O. Bockris, *Trans. Faraday Soc.*, **43**, 417 (1947).
4. H. S. Booth and M. Merlub-Sobel, *J. Phys. Chem.*, **35**, 3303 (1931).

Microfurnace for Thermal Microscopy and Studies at High Temperatures

W. A. Lambertson and G. Lewis

Research and Development Division, The Carborundum Company, Niagara Falls, New York

ABSTRACT

A small laboratory furnace is described for use in high-temperature microscopy and for determining chemical compatibility, wetting, sintering, and temperatures of apparent melting up to 3000°C (5433°F). The furnace shell is a water-cooled, 5-in. copper tee and is of such construction as to afford a controlled atmosphere. Water-cooled electrodes are designed to hold refractory metal strip heaters (either plain or with a wedge for better black body conditions) or special-machined graphite heaters. Stepless power input is provided by variac-controlled, saturable core reactor.

Furnace Description

Figure 1 shows the furnace diagram. The furnace shell was fabricated from 12.7 cm (5 in.) ID copper tubing which was cut and welded to form a "T". Cooling was provided by 6.25 mm ($\frac{1}{4}$ in.) copper tubing tracing welded to the outside of the shell. The ends of the furnace through which pass the terminal connections were isolated electrically from the furnace shell by Teflon rings, and an atmospheric seal is provided by "O" ring seals. Water-cooled terminal connections, fabricated from 1.9 cm ($\frac{3}{4}$ in.) diameter copper rod, were led into the furnace through rubber gasketed CGB cable connector seals in the end plates. The seals provide both an electrical and atmospheric seal, and, when loosened, permit the terminals to be rotated easily or moved in and out. Each terminal had interchangeable threaded end pieces which served as adapters so that several types of heater configurations may be used.

The furnace is loaded through an "O" ring sealed cover, about 5 in. in diameter, on the center leg of the "T." This cover has a 1-in. diameter sight port for visual observation and temperature determination of the sample. There are two additional sight ports, one directly opposite the sight port in the cover and one displaced 30° from the center line passing through the two former ones. Three ports are needed for high-temperature microscopy work,

one for the microscope, one for an arc light which provides additional illumination when necessary, and one for an optical pyrometer.

Heaters.—Three types of resistors have been used. The furnace was originally designed to use two refractory metal strip heaters 7.6 x 1.27 x 0.00127 cm (3 x 0.5 x 0.005 in.) (top Fig. 2) for wetting angle studies. The metal strips are clamped in copper holders; the sample rests on the lower heater while the upper strip functions as a radiation guard heater. For oxidizing atmospheres, a platinum-40% rhodium metal strip (mp 1900°C) is used. With inert atmospheres, a tantalum, tungsten, or molybdenum strip is used for still higher temperatures.

Reaction of some samples with metal heaters is sometimes a problem, and crucibles of boron nitride or thoria are placed on the lower heater to hold the sample. Boron nitride is satisfactory as a crucible up to 2000°C, but at higher temperatures it reacts with the heater. A guard ring of tungsten is placed around the crucible to reduce radiation loss from the side and to make the temperature more uniform.

In melting point studies it was found that reactions between the materials under study and the heater strip were sometimes severe, so a heater was constructed from a graphite block 7.6 cm (3 in.) long by 1.9 cm ($\frac{3}{4}$ in.) square at the terminals. The central section was made considerably smaller in area and contains a thin-walled cylindrical furnace chamber (Fig. 2). This cylinder provides a hot zone with a 6.25 mm ($\frac{1}{4}$ in.) inner diameter by 1.59 cm ($\frac{5}{16}$ in.) high. The sample is generally formed into 3.2 mm ($\frac{1}{8}$ in.) diameter rod about 2.54 cm (1 in.) long and is supported on a graphite pedestal. Several refractory metal shields are placed around the heater to reduce radiation losses.

At temperatures above 2500°C, even with a flowing argon atmosphere, there is sufficient vaporization of graphite to cause problems of contamination of the sample. A small amount of work has been done on the possibility of using heaters made from the high melting tantalum carbide-zirconium carbide solid solution. These heaters are difficult to fabricate and very susceptible to thermal shock. A few have

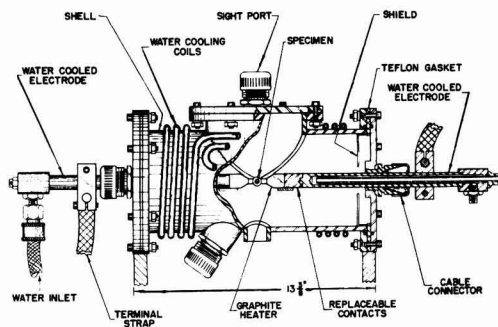


Fig. 1. High-temperature microscopy furnace

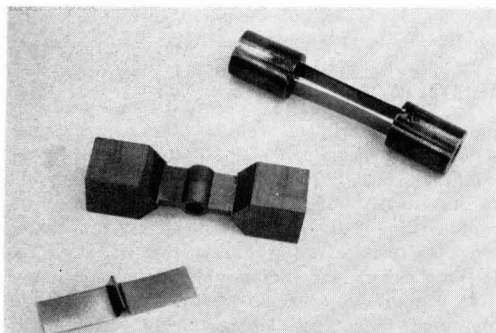


Fig. 2. Furnace heaters, double wedge, graphite block, and "V" types.

been used satisfactorily, but further development work is needed to reduce thermal shock problems. A second technique which has proved helpful is to line the inside of the graphite heater with tantalum or tungsten foil.

Power supply.—The saturable core reactor d-c bias is controlled by a manually operated powerstat on a 110-v line, through a small transformer which reduces the voltage, and then through a rectifier to provide d-c control. This manual control is entirely satisfactory for most applications of the furnace, because the firing times are usually short. Four 5 kva step-down transformers are used with the primaries in parallel and the secondaries in series. Figure 3 shows the power consumption for various types of heaters. Maximum secondary current drawn is slightly in excess of 500 amp.

Temperature measurement.—In addition there are two other sources of uncertainty in knowing the temperature of the sample.

The optical pyrometer is accurate to $\pm 13.9^\circ\text{C}$ and this was checked regularly by comparison with a standard. Temperature is read through a Vycor sight glass which adsorbs a certain, though small, amount of energy at the wave length used for measurement, 0.65μ . The sight glass was calibrated using an optical standardization apparatus, and the correction factor corresponded with the simplified Wein equation, $1/T_i - 1/T_a = C$, where T_i is equal to the true absolute temperature, T_a is the apparent ab-

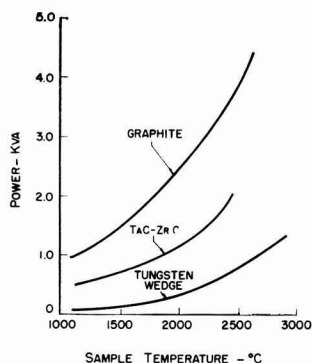


Fig. 3. Micro furnace-power-temperature relationship.

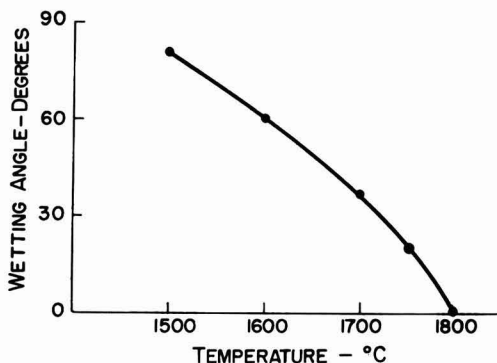


Fig. 4. Wetting of SiC by FeSi₂.

solute temperature, and C is the calibration constant. The value of this constant was found to be -6.7×10^{-6} and resulted in the addition of 35°C at 2040°C , the melting point of aluminum oxide.

The variation from black body conditions in the furnace constitutes a source of error. Because the sample can be seen when it is melted in this furnace, true black body conditions are not obtained. The effective emissivity falls between one and the true emissivity of the material under test. Using a material of high purity for which the melting point is well established, it is possible to calculate the apparent emissivity if the correction constants are known for the optical pyrometer and the sight glass. The apparent melting temperature of aluminum oxide and the literature value for aluminum oxide, 2040°C was used to calculate the emissivity as 0.9594. Assuming that the apparent emissivity does not change at higher temperatures, and for other oxides the emissivity correction for the zirconia melting point, 2656°C , is 16°C , and for the urania melting point 2740°C , 17°C .

Experimental Results with Furnace

Melting Points

Table I shows some of the melting points which have been obtained compared with values from the literature. Aluminum oxide is readily available in high-purity form and its melting point is well established. This material was used as a standard for checking the sight glass calibration and for calculating the effect of emissivity on the experimental conditions. High-purity zirconia is available in quantity, and represents an excellent high-temperature standard material. Zirconia with 2% hafnia was chosen as a standard because of some previous work (3). High-purity urania is available, but may not be a good standard because of the possible variations in the uranium to oxygen ratios.

The reason the melting point of alumina checked satisfactorily and those for zirconia and urania by two different methods did not is not understood. Lambertson and Mueller (3) used a tungsten crucible $\frac{1}{4}$ in. in diameter by 2 in. long heated in a tungsten heater $\frac{3}{4}$ in. in diameter by 6 in. long. They obtained black body conditions. Melting was determined by observing the sample before and after

Table I. Oxide melting points

Material	Number of tests	Melting point, °C \pm 20°C	Value from literature
Al ₂ O ₃	5	2030 (A) *	2040 \pm 5°C (2)
		2040 (B) †	2040 \pm 20°C (3)
ZrO ₂ (2% HfO ₂)	3	2656 (A)	2710 \pm 20°C (3)
		2672 (B)	2677 (4)
ZrO ₂ (HfO ₂ free)	4	2690 (A)	
HfO ₂ (5% ZrO ₂)	4	2770 (A)	2777 (4)
UO ₂	3	2740 (A)	2750 \pm 40°C (2)
		2757 (B)	2878 \pm 22°C (3)
			2860 \pm 45°C (5)

* (A) Corrected for sight glass absorption.

† (B) Corrected for sight glass absorption and a calculated emissivity of 0.9594.

Table II. Sources and compositions of melting point materials

1. Al ₂ O ₃	—99.99+ Linde Air Products, Type A —5175, Lot #P—196
2. ZrO ₂	—99.87% (ZrO ₂ + 2% HfO ₂)—Titanium Alloy Manufacturing Division, National Lead Co.—Specially purified
3. ZrO ₂ —Hf free	—99.5% ZrO ₂ —The Carborundum Metals Co., Akron, Ohio
4. HfO ₂	—95+ %—The Carborundum Metals Co., Akron, Ohio.
5. UO ₂	—99.9+ %—The Mallinckrodt Chemical Co., Source Grade

heating. The crucible bottom may have been at a lower temperature than that indicated through radiant heat loss. In the present work only the part

that melts is seen but deviation from black body conditions presents a source of error.

Wetting Angles

Wetting angles of FeSi₂ on SiC vs. temperature are plotted in Fig. 4. In this work the sample is placed on a pin or in a crucible on strips and heated to the test temperature. It is then held for a few seconds, the furnace turned off, and the sample quenched by the rapid cooling of the furnace. The sample is removed from the furnace and ground so that the angle between the melt and the crystal can be seen easily. This is then projected on a screen and the angle measured.

Acknowledgments

The authors would like to express their appreciation to Mr. Henry N. Baumann for his suggestions, to Dr. F. K. Davey for his work on the power supply and the development of the graphite heater, and to many others of the Carborundum Company who contributed their ideas, suggestions, and help in obtaining the data presented in this report.

REFERENCES

1. H. N. Baumann, Jr., *Bull. Am. Ceram. Soc.*, **27** (7), 267 (1948).
2. L. G. Wisnyi and S. W. Pijanowski, *Ceramic Information Meeting held at Oak Ridge National Laboratory*, Oct. 1-3, 1956, TID-7530 (Pt. 1) p. 46, April 1957.
3. W. A. Lambertson and M. H. Mueller, *J. Am. Ceramic Soc.*, **36**, (10) 329, (11) 365, (12) 397 (1953).
4. F. von Henning, *Naturwissenschaften*, **13**, 661 (1925).
5. T. C. Ehlert and J. L. Margrave, *J. Am. Ceram. Soc.*, **41**, [8], 330 (1958).

Zirconium Coating of Uranium by the Iodide Process

W. L. Robb¹

Knolls Atomic Power Laboratory

(Operated for Atomic Energy Commission by General Electric Company), Schenectady, N. Y.

ABSTRACT

A method for coating uranium metal with a bonded layer of crystalline zirconium metal has been developed. It consists of thermally decomposing zirconium iodide vapors on the surface of uranium metal heated to about 1100°C in vacuum. Prior to coating, the uranium metal surface is cleaned by iodizing it and then vaporizing the uranium iodide. Greatly increased diffusion between the uranium and deposited zirconium can be obtained if the uranium is alloyed previously with as little as 0.5% zirconium. This increased diffusion improves the corrosion resistance of the coatings.

The desirability of coating uranium or uranium alloy fuel elements with zirconium arises from the excellent corrosion resistance of zirconium, plus its low thermal neutron cross section. Of particular interest are 1-10 mil thick zirconium "sweater" coatings, for use as secondary corrosion resistant barriers. This paper describes one of the more successful methods for achieving such a coating.

The coating process examined in this study was based on the van-Arkel-de-Boer (1) process for producing pure zirconium metal. It consisted of first

forming volatile zirconium iodides, and second, decomposing or disproportionating these iodides on the hot surface of a uranium specimen (2). The process is carried out most successfully in an evacuated system, although coatings of less desirable nature can be obtained in the presence of an inert gas or a reducing gas such as H₂.

Experimental

The apparatus used to coat 1 x ¾ in. uranium disks is shown in Fig. 1. The uranium disk was heated inductively by a 5 kw Ajax converter, the disk's temperature being measured by an optical

¹ Present address: Research Laboratory, General Electric Company, Schenectady, N. Y.

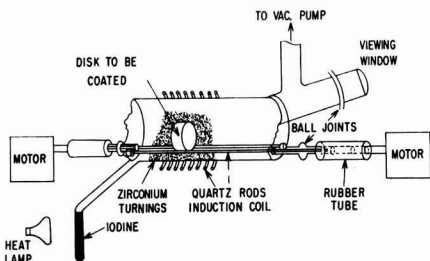


Fig. 1. Cut-away viewing of vapor coating apparatus with disk rotator.

pyrometer through a glass window. Uranium temperatures of 1050°–1100°C could be maintained to $\pm 5^\circ\text{C}$. The zirconium was in the form of 10-mil turnings twisted into cigar shaped bundles which were then placed in the tube around the uranium. It was necessary that the ends of the bundles did not complete a circle within the induction field. Thus the zirconium was heated mainly by radiation from the uranium disk. This was sufficient to heat the zirconium to 200°–400°C. The iodine pressure was controlled by regulating the temperature of the iodine supply tube generally between 20°–50°C.

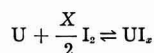
The coating cell was evacuated continuously, using a fore pump and diffusion pump, although once a thin coating of zirconium had been deposited and the uranium and zirconium had been completely degassed, the coating cell could be operated without continuous evacuation.

A somewhat thicker coating was obtained near the edge of the sample as compared to the middle due to (a) the nearness to the zirconium supply, and (b) the higher temperature of the edge of the disk as compared to the middle.

In order to coat a disk completely in one operation, the uranium disk was supported on rods which could be rotated continuously. Quartz rods were found suitable for the rollers as long as the rate of rotation was sufficiently rapid and the weight of the disk not too high. Otherwise the uranium was oxidized by the quartz, and nonbonded coatings resulted. Required rates of rotation for the rods were 1–3 rpm. The rod diameters for 1-in. diameter uranium disks were about 3/16 in. Thin metal foils of tantalum and molybdenum were tried as covers for the quartz rods but were not useful since the foil stuck to the hot uranium.

Prior to coating a specimen, the uranium was cleaned by an acid dip or by electrocleaning. The simplest method of cleaning consisted of dipping the uranium sample in concentrated nitric acid, followed by a water rinse and an acetone rinse. The sample was placed in the coating cell, which then was evacuated as quickly as possible. After the cell had been evacuated to better than $0.01\mu\text{ Hg}$ (with leak rates of less than $8\mu\text{ ft}^3/\text{hr}$) the liquid nitrogen was removed from the iodine supply and the induction furnace turned on. As the uranium disk became hot it was iodized, forming UI , which vaporized from the surface as the disk reached red heat. This served to clean the surface just prior to coating and was a

most important step in obtaining bonded coatings. As the temperature of the uranium approached 1080°C the equilibrium of the reaction:



shifted more and more to the left. Thus, at coating temperature, the iodization rate of U could be reduced greatly by maintaining the iodine pressure below $60\mu\text{ Hg}$ (3).

By the time the uranium had reached 1050°C (2–4 min), ZrI_4 was already being formed and could be seen condensed on the cold outlet of the deposition cell. Coating of the uranium had to begin immediately in order to prevent the formation of a diffusion blocking layer of uranium oxide. Coating times of 1/2–6 hr were tried, with rates as high as 2–3 mils/hr being obtained. Runs usually were 2–3 hr long, at 1 to 2 mils/hr coating rate.

Coated samples were removed from the apparatus under a purge of N_2 , A, or He gas to prevent oxidation of the condensed ZrI_4 . This eliminated the need to clean the apparatus after every coating test.

Results and Discussion

By means of the equipment and procedures described above, zirconium coatings have been applied on uranium disks and cylinders of various shapes and sizes. A photograph of a typical coating, shown in Fig. 2, illustrates the very crystalline nature of the deposited zirconium. The nature of the diffusion bond of the zirconium to the uranium can be seen in Fig. 3. The diffusion was considerably less than expected from measured diffusion rates of uranium and zirconium (4). Furthermore, the annealing of coated uranium disks did not increase the diffusion layer thickness noticeably.

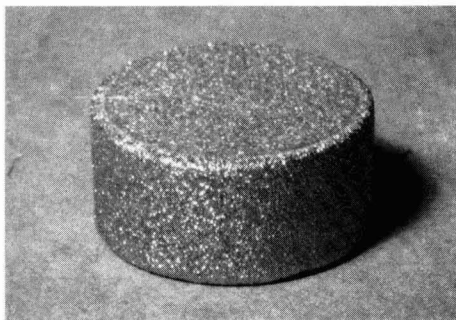


Fig. 2. Zirconium coated uranium disk, actual size

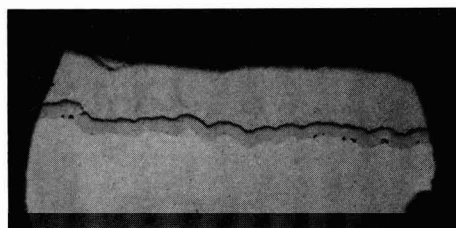


Fig. 3. Zirconium coating on uranium. Magnification 250X B.F.

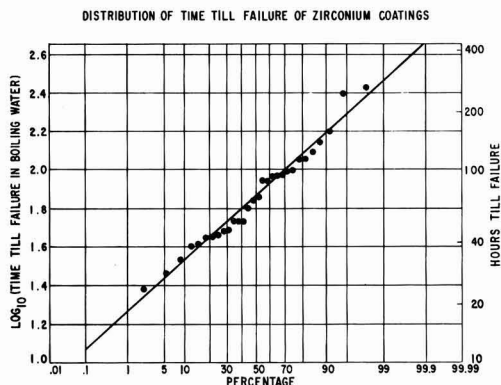


Fig. 4. Distribution of time until failure of zirconium coatings.

The corrosion resistance of these coatings was determined by noting the time required for their rupture or penetration in boiling water. More specifically, failure was indicated by UO_2 powder in the water, by a blister on the surface of the coated specimen, or by the enlarging of a pore hole on the surface. The times required until failure of coatings on pure uranium are shown on a probability graph, Fig. 4, and it is seen that the log mean time till failure for 30 samples was 73 hr.

Except for the cases where failure of the coatings was due to a poor diffusion bond (caused by poor cleaning or by uranium oxidation on heating), the most common cause of failure was porosity of the crystalline coatings. As a result, several methods for reducing this porosity were tried. These methods and their results are listed in Table I.

As is seen from the table, no major improvement in corrosion resistance was observed for any of the additional treatments. It was observed, however, that coatings on the sides of disks which were rolled on the quartz rods while the zirconium was being deposited were not nearly as porous, nor as brightly crystalline, as were the unpressed faces of the disks. If a practical way could be found to deform or to press the zirconium deposit continually over the entire disk while the deposit was being laid down, less porous coatings could be obtained.

Table I. Corrosion times in boiling water of zirconium coatings on pure uranium disks

	Hours until failure in boiling water
Coatings deposited in 1-2 hr	115, 115, 161, 87, 44, 49, 29
Coatings deposited in 2-3 hr	94, 73, 126, 54, 88, 72, 54, 54, 94, 91, 64, 41, 98, 45, 48
Coatings deposited in 3-5 hr	250, 24, 100, 34, 46, 40
Coatings deposited in 5-6 hr	142, 271
Coatings vacuum annealed after coating	69, 47, 112, 164, 48, 78
Coatings ball milled	51, 121, 21
Coatings shot blasted	74, 74
Coatings hot pressed	116, 114, 73, 71
Coatings with Ni and Zr co- deposited	49, 88, 21, 38, 24, 117, 134, 157, 67, 67, 116, 70, 41, 17, 72, 73, 22, 77
Coatings deposited in reverse plating runs	190, 60

The codeposition of Ni from $\text{Ni}(\text{CO})_4$ and Zr from ZrI_4 results in a lower melting Ni-Zr and Ni-U alloy being formed. This causes increased diffusion between the U and Zr, and when carefully controlled could result in improved coatings. Figure 5 shows this increased diffusion. The presence of Ni in the coating was verified by x-ray fluorescence measurements, but the occlusions in the Zr coating were not identified and could be either nickel, zirconium oxide, or zirconium carbide. The scattered appearance of these occlusions is due to the intermittent introduction of nickel-carbonyl into the coating chamber.

Depositing the zirconium coating on a uranium alloy disk previously alloyed with a small amount of zirconium resulted in markedly improved corrosion resistance of the zirconium coatings. This had been noticed by Campbell and Powell (5) on a cementation process for depositing zirconium on uranium. Figures 6 and 7 show zirconium deposited on a 99% U-1% Zr alloy and illustrate the type of diffusion obtained when zirconium is deposited on the uranium alloy. As would be expected from previously measured diffusion rates of U in Zr (4), the uranium is completely diffused through the zirconium coating and 1 mil layers machined off the outer surface of coatings have analyzed as high as 43% uranium. X-ray diffraction measurements on successive 1 mil layers indicate a concentration profile going from alpha zirconium through epsilon phase uranium-zirconium alloy to alpha uranium. Uranium metal alloys containing from 0.5 to 4% zirconium were coated and over this range the results were very similar. Figure 8 shows several coated alloy disks. The

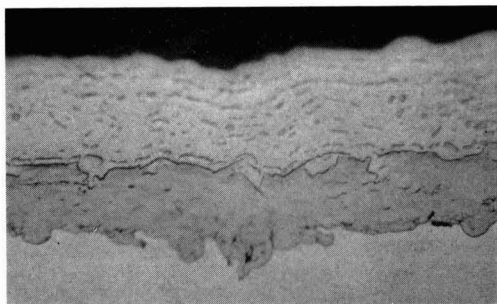


Fig. 5. Codeposited coating of Ni and Zr on U. Magnification 500X B.F.

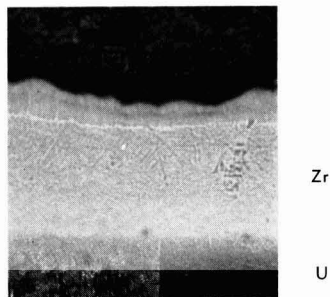


Fig. 6. Zirconium coating deposited on 99.5% U-0.5% Zr alloy. Magnification 250X B.F.

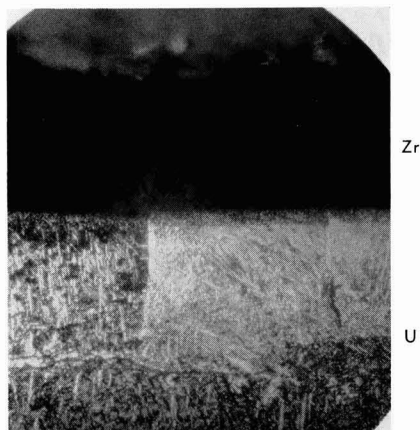


Fig. 7. Zirconium coating deposited on 99.5% U—0.5% Zr alloy. Magnification 250X Pol.

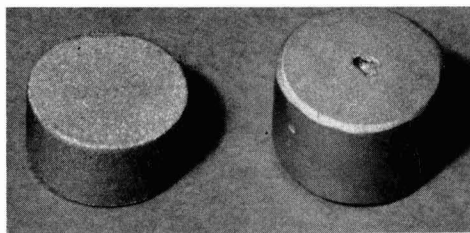


Fig. 8. Photographs of Zr deposited on U-Zr alloy. Magnification 1X.

coatings on these alloy disks are very smooth compared to the macro crystalline coating deposited on uranium and shown in Fig. 2. Corrosion tests on the coated alloy samples showed greatly increased protection (Table II). For example, a coating deposited in 1 hr and annealed for 1 hr lasted 447 hr and was still intact at the end of the test. Some failures occurred in less than 100 hr but they could be accounted for largely by pits or holes in the uranium alloy metal used. Although the inside of the holes were coated to some extent, the holes still presented weak spots in the coatings.

The zirconium apparently fixes the carbon usually found in uranium, thus preventing its migration to the uranium-zirconium coating interface. Since ZrC is more stable than UC, it would be expected that the carbon in the uranium would diffuse to the zirconium, and in this way cause a ZrC diffusion blocking layer to be formed at the U-Zr interface. This explains why the expected amount of codiffusion between U and Zr was not observed in the initial coating experiments.

Conclusions

It is possible, but difficult, to obtain pore-free zirconium coatings on present grade uranium metal. Under carefully controlled conditions the coatings probably can be made to resist boiling water consistently for over 100 hr. On low zirconium alloy specimens (or possibly on uranium containing very little carbon) pore free coatings can be obtained easily, and coatings to resist 100°C boiling water for over

Table II. Corrosion times of zirconium coatings on uranium-zirconium alloy disks

Run No.	% Zr alloyed with U	Time of run	Annealing		Time to failure in water at °C
			Time	Temp	
248	0.5	3			232+
274	0.5	2			47
277	0.5	2			37
259	1.0	2			168
278	1.0	2			177
260	1.0	1	1	1100	447+
261	1.0	0.5	0.5	1100	141
263	1.0	1.5	1.5	1100	214
265	1.0	2	1	1100*	242
253	2.5	3			85
255	2.5	2.5			309+
280	2.5	2			
254	4.0	2.5			264
279	0.5	2	65	800	80
266	1.0	1.5			12
267	1.0	1			18
268	1.0	1	48	800	72
255	2.5	2.5			24
262	4.0	3	0.5	1100	24

* Quenched from the beta phase for grain refinement.

200 hr or 170°C water for 80 hr should be produced easily.

So far only coatings on uranium or uranium-zirconium alloys have been described. However, the method also has been used at KAPL to coat thorium and graphite. Other reactor materials including beryllium metal, beryllium carbide, beryllium oxide, boron, and boron carbide, may also be coated in the same manner.

Although this method of coating is limited in use by the high temperature required for the decomposition of zirconium tetraiodide, it does represent a possible method for producing coatings of zirconium metal. The cost for this type of coating probably will be higher than that for electroplated coatings. But, for specialized cases where diffusion bonded and corrosion resistant coatings of low neutron cross section are required, it alone affords a method of producing thin bonded zirconium coatings.

Acknowledgment

The author wishes to thank F. J. Shipko, F. J. Clark, R. L. Myers, and A. C. Schafer for their technical assistance during this project.

Manuscript received June 27, 1958. This paper was prepared for delivery before the New York Meeting, April 27-May 1, 1958.

Any discussion of this paper will appear in a Discussion Section to be published in the December 1959 JOURNAL.

REFERENCES

1. A. E. van Arkel and J. H. de Boer, *Z. anorg. u. allgem. Chem.*, **148**, 345 (1925).
2. I. E. Campbell, C. F. Powell, D. H. Nowicki, and B. W. Gonser, *J. (and Trans.) Electrochem. Soc.*, **96**, 318 (1949).
3. C. H. Prescott, Jr., F. L. Reynolds, and H. A. Holmes, "The Preparation of Uranium Metal by Thermal Dissociation of the Iodide," MDDC-437, April 18, 1946.
4. Y. Adda, J. Philibert, and C. Mairy, *Compt. rend.*, **243**, 1115 (1956).
5. I. E. Campbell and C. F. Powell, Private communication.

Transport Numbers and Ionic Mobilities in the System Potassium Chloride-Lead Chloride

Frederick R. Duke and Richard A. Fleming

Institute for Atomic Research and Department of Chemistry, Iowa State College, Ames, Iowa

ABSTRACT

Values of ionic transport numbers and ionic mobilities were determined for the fused system potassium chloride-lead chloride. Cation transport numbers were found: 0.24 for PbCl_2 at 525°C , 0.62 for KCl at 850°C . In each mixture, t_- deviated positively and t_+ and t_{++} deviated negatively from linearity when plotted against equivalent fraction. The initial, very rapid depression of total equivalent conductance from that of pure KCl , caused by addition of small amounts of PbCl_2 , was found to be due to the depression of the ionic conductance of K^+ rather than complexing between Pb^{++} and Cl^- as had been supposed previously. The relative mobilities of K^+ and Pb^{++} were compared with those of Li^+ and Pb^{++} in the system LiCl-PbCl_2 , calculated from available literature data.

The transport numbers and mobilities of the ions in a mixture of AgNO_3 and NaNO_3 have been determined (1). This system proved to be ideal in the sense that the ionic mobilities were independent of composition. The system $\text{PbCl}_2\text{-KCl}$ is of interest because of the possibility of complex ion formation involving Pb^{++} and Cl^- ; furthermore, it might be expected that a mixture of a biunivalent salt with a uniunivalent one would show a different behavior from the $\text{AgNO}_3\text{-NaNO}_3$ system.

Complex ions of Pb^{++} and Cl^- in the molten system $\text{PbCl}_2\text{-KCl}$ have been reported on the basis of phase diagram (2), electrical conductance (3), surface tension (4), and molar volume measurements (5). In addition, previous studies on transport numbers in this system have indicated that complex ions might play a large role in the mobility of the ions. Lorenz and Ruckstuhl (6) observed that the lead ions are apparently anionic (PbCl_3^- or PbCl_4^{2-}) in mixtures containing more than about 25 mole % KCl . Wirths (7), using radioactive Pb^{++} as tracer, obtained some evidence that lead ion migrated toward the anode in mixtures of PbCl_2 and KCl . These transport studies were lacking in precision, however. With more precise experimental techniques available, the present work on the $\text{PbCl}_2\text{-KCl}$ system was done.

Experimental

Two experimental quantities must be determined in order to calculate the transport numbers of the three ions. One of these, designated ϕ by Aziz and Wetmore (8) (where $\phi = 1 - t_{++} - E_1 t_-$), is related to experimental values by $\phi = (E_2 N_1 - E_1 N_2)/Z$, where t_{++} , t_+ , and t_- are the transport numbers of Pb^{++} , K^+ , and Cl^- ions, respectively, E_1 and E_2 are the original equivalent fractions of PbCl_2 and KCl , respectively, N_1 and N_2 are the total number of equivalents of PbCl_2 and KCl in the anode compartment after electrolysis between Pb electrodes, and Z is the charge transferred in faradays. The other experimental quantity is t_- measured directly by radio tracer methods.

Apparatus.—The cell used in the determination of ϕ and t_- is shown in Fig. 1. The low temperature runs were done in Pyrex with the membrane consisting of an ultrafine Pyrex disk. For high temperature, the cell was made of quartz; the membrane was specially prepared for each cell from commercial fine porosity quartz disks. To reduce the porosity of the fine quartz disks, ethyl silicate and concentrated HCl were allowed to react in the disk, with a heating period (850°C) after each treatment, until sufficiently fine porosity was obtained. The porosity was calibrated by measuring the time required for 1 ml of water to pass through the disk under 1 atm pressure. Disks having "water times" above 600 sec were found to be satisfactory. Contact to the electrodes was made through loosely fitting caps, with tungsten wires passing through the center tube in the cap.

The furnace used was a Marshall tube furnace with external compensating taps on the heating coil. The temperature was controlled by a chromel-alumel thermocouple which operated a Brown indicating controller. In addition, the furnace contained an indicating chromel-alumel thermocouple connected to a L&N No. 8662 potentiometer with reference junction compensator. The center zone of the furnace

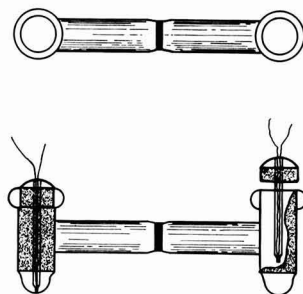


Fig. 1. Transport cell

had a temperature gradient of less than 5° and could be controlled to $\pm 1^\circ\text{C}$ of any desired temperature at a given point. Direct current up to 300 ma was available through a bank of selenium rectifiers in a smoothing capacitance-inductance circuit. A Model 100 Berkeley Decimal Scalar was used in making all radioactivity counts.

Determination of ϕ .—The cell shown in Fig. 1 was loaded with an intimate mixture of reagent grade solid KCl and PbCl_2 . Pure lead metal was used for the electrodes. In general, the amount of molten salt filled the horizontal tube of the cell only partially, allowing a large surface area and minimizing differences in head across the membrane as the experiment proceeded. After a suitable quantity of electricity had been passed, the cell was broken at the membrane and the catholyte and anolyte collected separately and analyzed as follows. The weighed samples were pulverized, heated in boiling water, cooled, and filtered. This procedure was repeated three times, thus removing all of the KCl and part of the PbCl_2 . The remaining PbCl_2 was dried and weighed. The filtrate was titrated with the sodium salt of cyclohexanediaminetetraacetic acid (9) to determine the dissolved lead, and K^+ was precipitated and weighed as the tetraphenylborate (10).

Determination of t_- .—Radioactive Cl^{36} with a half-life of 3.08×10^6 years, was used as tracer. If all the radioactive chloride is placed initially in the cathode compartment of the cell shown in Fig. 1, it can be shown that

$$t_- = K_a C_a E_c / K_c C_c Z \quad [1]$$

where C_a is the counting rate of the anolyte, corrected for diffusion, after passage of Z faradays, C_c is the counting rate of the catholyte before the run, and E_c is the total number of equivalents of Cl^- in the catholyte initially. K_a and K_c take into account the aliquation and the geometry of the counted sample so that, for example, $K_a C_a$ gives the amount of Cl^* in the anode compartment. For K_a to equal K_c , the counting efficiencies and the aliquation and other similar variables must be the same when counting catholyte and anolyte.

After the current was run, the cell was broken at the membrane and the anolyte and catholyte samples were collected carefully and weighed. For analysis, a $\text{NaCl}^*-\text{PbCl}_2^*$ sample was homogenized by completely dissolving it in boiling water. This was followed by concentrating portions of the solution by evaporation and then cooling to precipitate PbCl_2^* , the form in which Cl^{36} was counted. The original portion size and the extent of concentration by evaporation were adjusted so that a final PbCl_2^* weight

of about 0.1 g was obtained, after water and acetone rinses to remove KCl^* . From the observed counting rates of five or six samples, the counting rate of a 0.1000-g sample of PbCl_2 was determined. This weight represents 0.000719 equivalents of Cl^- . By knowing the total number of equivalents of Cl^- in the sample, the radioactive Cl^- aliquot of 0.1000 g PbCl_2 was determined, and the total counting rate of the sample was found by multiplication.

The final weight of the anolyte sample was known. The final concentration of the anolyte was calculated from the results of ϕ runs made on samples of the same composition. Thus, total Cl^- and then the anolyte's uncorrected counting rate were calculated. To determine C_a , one need only correct the observed counting rate for leakage and diffusion of Cl^* into the anolyte.

Values of C_c were obtained in two ways. Proceeding exactly as in the case of the anolyte sample, one can determine an observed final counting rate for the catholyte. Then one need only add the uncorrected anolyte counting rate to this term to determine the initial counting rate of the catholyte. Alternatively, one may proceed so that in every run exactly the same number of equivalents of Cl^- are present initially in the catholyte. Also, one may introduce Cl^* from an active KCl^* (or PbCl_2^*) stock and use the same weight of stock for each run. Then C_c will be the same for each run and, if the same number of faradays are passed in each run, Eq. [1] simplifies to

$$t_- = AC_a \quad [2]$$

This method demands care in weighing out a homogeneous radiochlorine source, but it is time saving. The value of A is known once $K_c C_c$ has been determined, and each catholyte need not be collected individually and counted.

Diffusion leakage corrections were made by reference to a calibration plot of "water times" vs. diffusion leakage determined on a number of membranes. The calibration plot is a straight line, and corrections amounted to 5% or less of the total radioactivity transferred across the membrane in all experiments.

Results

Experimental results are summarized in Table I. The equivalent and mole fractions of KCl in the $\text{KCl}-\text{PbCl}_2$ mixtures are listed in the first two columns, for seven compositions studied (a to g) at the temperatures listed in the third column. The experimentally determined values of ϕ and t_- are listed in the fourth and fifth columns, respectively. The definition $\phi = 1 - t_+$, $-E_c t_-$ involves the equivalent

Table I. Values of the parameter ϕ , of the ionic transport numbers, and of the equivalent conductance λ in the $\text{KCl}-\text{PbCl}_2$ system

E (KCl)	X (KCl)	Temp, $^\circ\text{C}$	ϕ	t_-	t_+	t_{++}	λ
0.000	0.000 (g)	525	0	0.76 ± 0.01	0.00 ± 0.016	0.24 ± 0.01	45.28
0.087	0.160 (f)	525	0.115 ± 0.011	0.74 ± 0.02	0.05 ± 0.023	0.17 ± 0.023	42.64
0.185	0.312 (e)	525	0.257 ± 0.015	0.71 ± 0.02	0.12 ± 0.023	0.17 ± 0.024	39.65
0.297	0.458 (d)	525	0.389 ± 0.012	0.68 ± 0.03	0.19 ± 0.024	0.13 ± 0.025	36.23
0.461	0.631 (c)	525	0.599 ± 0.012	0.60 ± 0.03	0.32 ± 0.032	0.08 ± 0.023	35.14
0.461	0.631 (c)	850	0.604 ± 0.012	0.58 ± 0.03	0.32 ± 0.035	0.10 ± 0.023	72.99
0.681	0.810 (b)	850	0.789 ± 0.012	0.50 ± 0.04	0.46 ± 0.037	0.04 ± 0.023	79.97
1.000	1.000 (a)	850	1.000	0.38 ± 0.04	0.62 ± 0.04	0.00	118.75

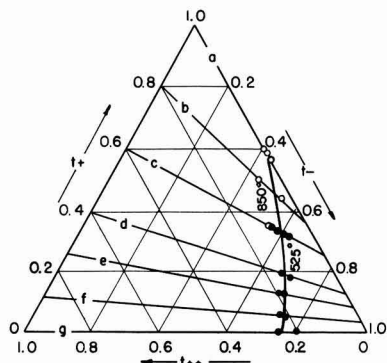


Fig. 2. Triangular diagram of the three transport numbers t_- , t_+ , and t_{++} in fused KCl-PbCl₂ systems at several compositions: (a) pure KCl; (b) 19.0 mole % PbCl₂; (c) 36.9 mole % PbCl₂; (d) 54.2 mole % PbCl₂; (e) 68.8 mole % PbCl₂; (f) 84.0 mole % PbCl₂; (g) pure PbCl₂; and at 525° (●) and 850° (○). The straight lines (a to g) correspond to the experimental values of the parameter ϕ (Table I). Experimental points correspond to the measured values to t_- (Table I), plotted for each composition (a to g) on the appropriate ϕ line. The smooth curve drawn through the points defines the transport numbers t_- , t_+ , and t_{++} as a function of composition (a to g).

fraction E_1 of PbCl₂, which is simply equal to $1 - E_2 = 1 - E(\text{KCl})$. The corresponding mole fractions are $X_1 = E_1/(2 - E_1)$ and $X_2 = 2E_2/(1 + E_2)$ for PbCl₂ and KCl, respectively.

Since t_- was determined independently by the use of a radiochlorine tracer, as described, the definition of ϕ above and the relation $1 = t_- + t_+ + t_{++}$, provide a system of two equations which can be solved for the two unknowns t_+ and t_{++} , once the value of ϕ has been determined experimentally, as described.

Since the three transport numbers add up to unity, the equilateral triangular diagram (Fig. 2) lends itself particularly well to this solution for two unknowns. The defining equation for the parameter ϕ corresponds to a straight line in this diagram, whose intercept on the $t_- = 0$ axis (left side of Fig. 2) is $t_{++} = 1 - \phi$, and whose intercept on the $t_{++} = 0$ axis (right side of Fig. 2) is $t_- = (1 - \phi)/E_1$.

Seven straight lines (marked a to g) have been drawn in Fig. 2, corresponding to the seven composi-

tions studied and to their experimentally determined values of ϕ (Table I). For line c, the values of ϕ at 525° and 850°C coincided within experimental error. Once the ϕ lines were drawn in Fig. 2, the experimentally determined t_- points (Table I) could be plotted, each set of points being plotted on the ϕ line corresponding to the same composition. The locus of these t_- points defines the three transport numbers for each one of the seven compositions studied. The smooth curve drawn through the points shows how the transport numbers t_- , t_+ , and t_{++} vary as the composition goes from line a (KCl) to g (PbCl₂). The lack of a break in the curve in line c suggests that the transport numbers are insensitive to temperature changes between 525° and 850°C. The values of t_+ and t_{++} given in the sixth and seventh columns of Table I were read off the intersections of the smooth curve with the ϕ lines in Fig. 2.

Equivalent conductance data for the PbCl₂-KCl system are available from density data of Boardman, Dorman, and Heymann (11) and specific conductance data of Bloom and Heymann (3). The conductance data of Yaffe and Van Artsdalen (12) were used for pure KCl. The total equivalent conductances λ of the mixtures are given in the last column of Table I. The ionic equivalent conductances λ_i may be calculated from the equation $\lambda_i = t_i \lambda / E_i$, where t_i is the transport number and E_i the equivalent fraction of the i^{th} ion. The ionic mobilities, $u_i = \lambda_i / F$, are shown in Fig. 3, as a function of composition. It is noteworthy that the transport numbers for pure PbCl₂ determined here with radiotracers agree very well with those determined using the bubble cell (13, 14).

Discussion

The most striking observation provided by the data is the rapid decrease in mobility of K⁺ ion upon addition of PbCl₂ to KCl. This observation is understandable if Pb²⁺ ion is present in PbCl₂ and if Pb²⁺ ion combines with negative holes, the holes into which K⁺ ion would normally move. The lowering of the K⁺ ion mobility cannot be due to the formation of complex ions; the chemical nature of K⁺ ion is not that of complex former. On the other hand, the fairly high mobility of Pb²⁺ ion is greater than one would expect on the assumption that Pb²⁺ ion moves into doubly charged negative holes; such doubly charged holes should be difficult to create energetically and, in the presence of the singly charged Cl⁻ anion, should split readily into two singly charged holes. To accommodate both facts, the mobility of Pb²⁺ ions and the combining of Pb²⁺ ion with negative holes, it is necessary to postulate an equilibrium between Pb²⁺ and PbCl⁺, the latter accounting for the mobility of the Pb²⁺ ions. The general change in mobility of Cl⁻ and Pb²⁺ ions with composition change is gradual enough to be accommodated by general changes in the properties of the medium in which the ions move.

The disagreement between the present data and those of Lorenz and Ruckstuhl (6) is explained easily on the basis of leakage of salt through the membrane of the cell. Values of ϕ are very insensitive to such leakage. As mentioned previously, there is no effect on ϕ if the composition of the melt flow-

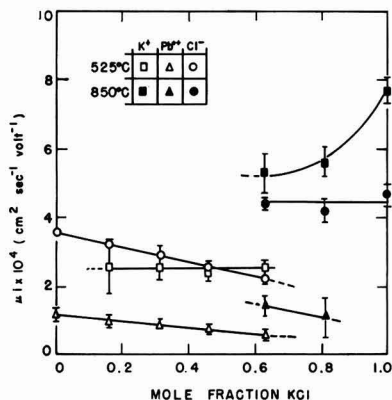


Fig. 3. Mobility of the ions vs. mole fraction in the fused KCl-PbCl₂ system.

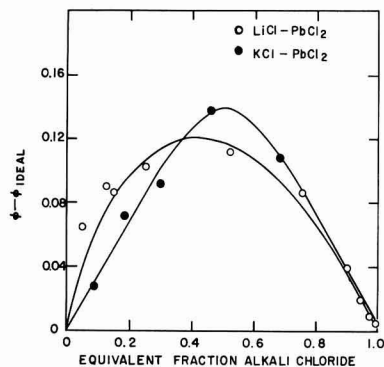


Fig. 4. Comparison of the ϕ parameter for fused LiCl-PbCl₂ systems at 650°C [O, cf. Ref. (15)] and for fused KCl-PbCl₂ systems at 525° and 850°C (●, cf. Table I); ϕ_{ideal} is here taken equal to the equivalent fraction of alkali chloride in both mixtures (see text).

ing through the disk is that of the original sample. Values of t_i determined by a change of weight method, such as that used by Lorenz and Ruckstuhl, are extremely sensitive to leakage, while values of t_i determined radiochemically in an experiment such as is outlined here are much less sensitive. This is because of the immediate dilution of Cl³⁶ by the anolyte. The effect of temperature on the transport number is small. In changing from 525° to 850°C, the transport numbers for all of the ions remain constant within experimental error. The temperature change here is sufficiently large that if there were significant differences in the activation energies for mobility of the ions, there would be a sensible change in the transport numbers. Note that the mobilities of the ions change very appreciably in this temperature interval.

An interesting experiment was performed recently by Klemm and Monse (15). With an ingeniously devised moving boundary, they determined relative mobilities of cations in the system LiCl-PbCl₂. In essence, they determined ϕ for this system. It can be shown that $\phi = b_{12}E_1 / (b_{12}E_1 + b_{23}E_2)$, where b_{12} and b_{23} are Klemm and Monse's notation for the mobility of 1(Li⁺) and 2(Pb²⁺) with respect to 3(Cl⁻), and E_1 and E_2 are (here only) the equivalent fractions of uni- and divalent salts. The similarities and dissimilarities of the two alkali chloride-lead chloride systems are such as to make their data of obvious

interest. Values of ϕ in this system were computed together with values of $\phi - \phi_{ideal}$; ϕ_{ideal} becomes numerically equal to the equivalent fraction of the alkali chloride, if the simplifying assumption can be made that uni- and divalent cations have the same mobility.

With this simplifying assumption, ϕ_{ideal} is the same for corresponding equivalent concentrations in the two systems; values of ϕ are compared most easily by looking at the sensitive function, $\phi - \phi_{ideal}$. These values are presented in Fig. 4. It is interesting to note the close similarity in the behavior of the two systems. Nothing can be said regarding absolute values of t_i and λ_i in the LiCl-PbCl₂ system, however, until an independent set of determinations relating them to measurable quantities is available.

Manuscript received Dec. 27, 1957. Contribution No. 581. Work was performed in the Ames Laboratory of the U.S.A.E.C.

Any discussion of this paper will appear in a Discussion Section to be published in the December 1959 JOURNAL.

REFERENCES

1. F. R. Duke, R. Laity, and B. Owens, *This Journal*, **104**, 299 (1957).
2. R. Lorenz and W. Ruckstuhl, *Z. anorg. Chem.*, **51**, 70 (1906).
3. H. Bloom and E. Heymann, *Proc. Roy. Soc. (London)*, **A188**, 392 (1946).
4. J. L. Dahl, "Surface Tensions of Some Binary Fused Salt Systems," unpublished Ph. D. Thesis, Iowa State College Library, Ames, Iowa (1957).
5. N. K. Boardman, F. H. Dorman, and E. Heymann, *J. Phys. and Colloid Chem.*, **53**, 375 (1949).
6. R. Lorenz and W. Ruckstuhl, *Z. anorg. Chem.*, **52**, 41 (1907).
7. G. Wirths, *Z. Elektrochem.*, **43**, 486 (1937).
8. P. M. Aziz and F. E. W. Wetmore, *Can. J. Chem.*, **30**, 779 (1952).
9. T. C. Loomis, "Metal Chelates of Cyclohexanediaminetetraacetic Acid," Thesis, Iowa State College Library, Ames, Iowa.
10. H. J. Cluley, *Analyst*, **80**, 354 (1955).
11. N. K. Boardman, F. H. Dorman, and E. Heymann, *J. Phys. and Colloid Chem.*, **53**, 375 (1949).
12. I. S. Yaffe and E. R. Van Artsdalen, *J. Phys. Chem.*, **60**, 1125 (1956).
13. F. R. Duke and R. W. Laity, *J. Phys. Chem.*, **59**, 549 (1955).
14. M. R. Lorenz and George J. Janz, "Transference Numbers in Molten Salts," Armed Services Technical Information Agency Technical Note 57-240. ASTIA Document Service Center, Dayton 2, Ohio. 1957. (Mimeographed).
15. V. A. Klemm and E. H. Monse, *Z. Naturforsch.*, **12a**, 319 (1957).

Galvanic Behavior in Fused Electrolytes

I. The Nominal System Mg/LiCl-KCl/Ni

Sidney M. Selis,¹ Guy R. B. Elliott,² and Laurence P. McGinnis

Diamond Ordnance Fuze Laboratories, Washington, D. C.

ABSTRACT

The galvanic function of cells containing hygroscopic molten electrolytes involves hydroxide ion as an active material if no stronger oxidizing agent is present. For the system without additional components two sets of reactions are postulated; the operative set would depend on the temperature range. At lower temperatures (390°–440°C), hydroxide ion is cathodically reduced to hydrogen gas plus oxide ion; at higher temperatures (445°–535°C), nickel (II) oxide, formed by the action of hydroxide ion on nickel metal, is the cathodically reduced species. In both temperature ranges magnesium oxide is formed at the anode. At higher temperatures, the magnesium and nickel electrodes obey Nernst's law with respect to the additions of magnesium, nickel, and oxide ions in the concentration range of interest. The electrodes are reversible and of the second kind.

The galvanic system of interest here nominally includes a magnesium anode, an electrolyte which is a molten mixture of potassium chloride and lithium chloride, and a nickel cathode. In the course of the work, the effects of additional components were noted but only to assist in the postulation of electrode reactions. The system is related to some which have been discussed before (1), but it contains no strong oxidant and therefore is not capable of supplying appreciable currents.

On the basis of the present work, half-cell reactions are postulated and, at least under certain conditions, electrode reversibility is demonstrated.

Experimental

Materials.—The nickel (II) oxide, potassium chloride, lithium chloride, lithium carbonate, nickel (II) chloride hexahydrate, and silver chloride were of the usual reagent grade and were not purified further. The nickel content in the nickel (II) chloride hexahydrate was determined gravimetrically by the dimethylglyoxime method. Reagent grade magnesium chloride hexahydrate was dehydrated by a method similar to that of Kelley and Moore (2). All solid chemicals were handled, as far as possible, in a "dry room" (relative humidity 6% under usual room temperature and pressure).

The hydrogen and helium gases were dried by bubbling through concentrated sulfuric acid followed by passage over potassium hydroxide pellets.

The sheet magnesium, generally 0.13 mm thick, was of the commercial electrolytic grade (over 99.5% pure). The impurities included small amounts of silver, aluminum, copper, and calcium as determined by spectrographic analysis. Just prior to use, the dark film on the metal was removed by immersion in 1% hydrochloric acid solution followed

by thorough rinsing in distilled water. The metal was wiped dry with a soft lint-free paper.

The sheet nickel was also 0.13 mm thick and was of a good commercial grade (over 99.5% pure). A spectrographic analysis revealed small amounts of zinc, iron, and cobalt. It was found that, other than a thorough washing with a mild soap and water, no treatment of the metal surface was needed.

Another type of electrode material was sintered nickel plate. The preparation and properties of this material have been described by Fleischer (3). This porous material was thoroughly rubbed with nickel (II) oxide to provide a nickel, nickel oxide electrode. (The original sintered plate was not impregnated with nickel hydroxide as described by Fleischer.)

Procedure.—The electrodes were prepared from 3.8-mm strips of the magnesium and nickel. One end of each strip was joined to tungsten wire leads by spot welding. These strips were inserted into lengths of 7-mm Pyrex tubing which were sealed at one end to the tungsten so that copper wire could be joined to the latter. At the other end of the glass tubes, 10 mm of electrode strip protruded. The total length of the electrode assemblies was about 25 cm, of which 3–4 cm was to be submerged in the electrolyte.

Except for minor differences, the cell arrangement was similar to that pictured by Jennings (4). A magnesium and a nickel electrode assembly, a Pyrex thermocouple protection tube, and a Pyrex gas inlet tube were inserted through a cap and sealed in place. The faces of the electrodes were oriented directly opposite to each other and the thermocouple occupied a central position. The electrode tubes were placed approximately 3 cm apart.

For individual electrode polarization measurements, a large cylindrical working electrode of sheet nickel was used. The reference electrodes were contained in 7-mm Pyrex tubing closed at one end. The

¹ Present address: Catalyst Research Corporation, Baltimore, Md.
² Present address: University of California, Los Alamos Scientific Laboratory, Los Alamos, N. Mex.

reference system was either Ag(c), AgCl (1, unit mole fraction), or Ni(c), KCl-LiCl-NiCl (1, mole fraction 1.00×10^{-3}) in glass. The silver or nickel electrode leads were 2-3 mm in diameter.

To start a run, a 38 x 200 mm Pyrex test tube was charged with the initial electrolyte salts. This was then placed in a noninductively wound electric furnace, and the cell temperature was adjusted to approximately 320°C by the use of a variable autotransformer. This temperature was maintained until most of the adsorbed water was removed. The temperature then was increased and when the electrolyte was molten, the electrodes, thermocouple tube, and gas inlet tube were positioned.

When a hydrogen or helium atmosphere was used, the gas was slowly bubbled through the melt for 30-60 min. (The loose fit between cap and test tube permitted the escape of gas.) The gas flow was stopped some minutes before emf readings were made.

Electromotive forces of cells and of chromel-p-alumel thermocouples were measured with a null-balancing potentiometer (cell emf's to the nearest centivolt). Temperature values are correct to about $\pm 1^\circ\text{C}$. The current through the polarized electrodes was measured with a d-c milliammeter. The current source was a storage battery with a voltage divider.

The x-ray analysis of the matter insoluble in the molten electrolyte, which was observed on the electrodes and at the bottom of the cell, was accomplished with powder samples mounted in a Debye-Scherrer camera. A copper target was used in providing the 30 kv x-radiation. Sixteen-hour exposures were made, and d/n values as determined were checked against known tabulated values.

Results

Electrolyte composition.—Nominally the electrolyte composition was the eutectic mixture of potassium and lithium chlorides and the stated amounts of added components. This eutectic composition is 58 mole % of lithium chloride and 42 mole % of potassium chloride. The eutectic temperature as 354°C [cf. Solomons, *et al.* (5)]. Actually, water and hydroxide ion were also included as demonstrated by Laitinen, *et al.* in terms of polarographic residual current measurements and cold trap collection of water (6). The presence of these species also was shown clearly by the present authors. Quantities of water were collected in a cold trap on evacuation of tubes containing electrolyte; pieces of calcium reacted with the electrolyte to release hydrogen gas. Of course, the presence of hydroxide ion at elevated temperatures implies the additional presence of oxide ion.

Measurements of hydrogen-ion concentration were made on water solutions of frozen electrolyte containing only the eutectic chloride mixture. The pH values were such as to indicate concentrations of hydroxide and oxide ions in the electrolyte ($[\text{OH}^-] + 2[\text{O}^{2-}]$) to be of the order of 10^{-8} moles/liter.

Behavior at lower temperatures (390°-440°C).—To assist in the postulation of reactions, the effects of internal atmosphere were determined for cells Mg/KCl-LiCl/Ni at 420°C. Unit pressures of air,

hydrogen, and helium were used; cells under reduced pressure were measured also. Steady cell potentials were reproducible to within ± 0.01 v.

The results of measurements with different atmospheres at 420°C can be summarized as follows: (a) with ordinary air atmosphere, the emf was 1.67 v; (b) with dry hydrogen atmosphere, 1.58 v; (c) with dry helium atmosphere, 1.67 v; and (d) under reduced pressure (10μ Hg), 1.61 v.

It is apparent that, while the use of dry hydrogen gave a lower potential than that of an air-atmosphere cell, the use of dry helium had no such measurable effect. Moreover, evacuation of a cell also depressed the potential, but not as much as the hydrogen atmosphere did.

When an external resistive load was placed across the electrodes, such that electrode current densities were about 10 ma/cm², gas was evolved from the nickel cathode. This evolution ceased when the load was removed.

In order to obtain some qualitative information as to the reversibility of the magnesium and nickel electrodes at 420°C, anodic and cathodic polarization measurements were made on both electrodes. For current densities of 3 ma/cm², there were no overpotentials within experimental error (± 0.01 v). Apparently because of the low ohmic resistance of the electrolyte and the small amounts of current used, measured polarizations were independent of the placement of the reference electrodes.

Starting with a temperature of about 390°C, cells of the type Mg/KCl-LiCl/Ni were heated slowly to 440°C, and the emf was studied as a function of temperature. The portion of the curve in Fig. 1, which has a steep slope, is fairly well established. The points were derived from three separate cells. For a given temperature in this region, the potential remains stable for at least 1 hr. On reversing the direction of temperature change, the emf eventually stabilizes at the value associated with a given temperature.

From the observed dE/dT in the 390°-440°C region, a cell reaction entropy of 55 cal/°C/mole was calculated for a two-electron transfer.

X-ray examinations of the scrapings from electrodes used in the lower temperature range revealed magnesium oxide. No oxide of nickel was detected.

Behavior at higher temperatures (445°-535°C).—

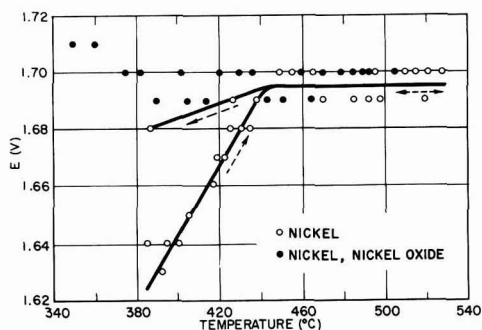


Fig. 1. Electromotive force vs. temperature for the nominal system Mg/KCl-LiCl/Ni.

Upon increasing the temperature of the system Mg/KCl-LiCl/Ni to 445°C , a leveling-off occurs, and on lowering the temperature, a higher potential persists as shown in Fig. 1. The higher potential of 1.70 v also was observed at all temperatures, on heating and cooling, by using a sintered nickel positive electrode into which had been rubbed nickel(II) oxide (NiO).

Examination of cells in the higher temperature region with magnesium and bright nickel electrodes (NiO not deliberately added) revealed the presence of insoluble matter on the electrodes and at the bottom of the cell. X-ray analysis of this material indicated MgO and NiO .

The potentials of magnesium and nickel electrodes at 480°C were studied as a function of concentrations of magnesium (Fig. 2), nickel (Fig. 3), and oxide (Fig. 4) ions in the electrolyte. The ions were introduced by adding to the electrolyte magnesium chloride, nickel chloride hexahydrate, and lithium carbonate, respectively. Often as much as 2 hr was required for stabilization of the potential. However, a stable potential would usually remain so for several hours, and emf values could be confirmed by repetitive measurements with duplicate cells.

Values given in Fig. 2-4 are electrode potentials with respect to the $\text{Ag, AgCl (1), glass}$ electrode. At the beginning of a run, the composition of the electrolyte would nominally include both magnesium and nickel chlorides at mole fractions of 3.16×10^{-4} ($\log N = -3.50$). In any one run, only one type of ion was added.

It will be noted that the addition of magnesium or nickel ions causes the electrode potentials of both magnesium and nickel electrodes to rise (become more noble) linearly with the logarithm of the mole fraction of the added ion (Fig. 2 and 3); on the other hand, the addition of oxide ion causes the potentials of both electrodes to fall (become less noble, Fig. 4).

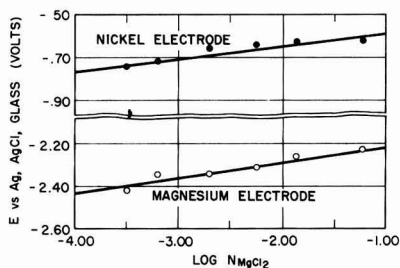


Fig. 2. Reversibility with respect to Mg^{2+} at 480°C

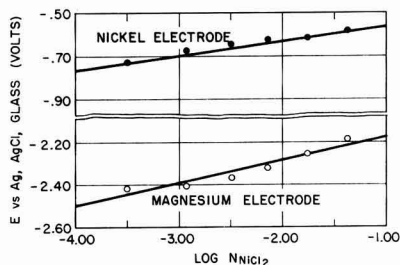


Fig. 3. Reversibility with respect to Ni^{2+} at 480°C

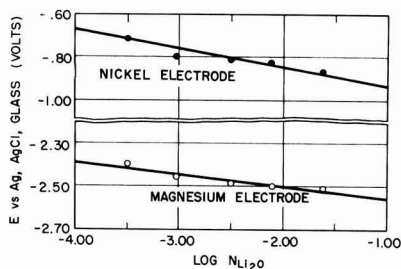


Fig. 4. Reversibility with respect to O^{2-} at 480°C

The slopes of the potential-log N curves are given in Table I. The theoretical slopes of ± 0.075 are equal to $2.303 RT/2F$.

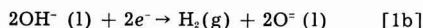
Discussion

Cells at Lower Temperatures

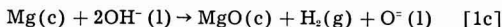
On the basis of experimental observations reviewed above, the authors suggest reactions [1a, b, and c] below for the system at $390^\circ\text{--}440^\circ\text{C}$. At the anode,



At the cathode,



Net reaction,



Supporting evidence may be summarized as follows: (a) The emf was responsive to changes in the internal atmosphere. As compared with an air atmosphere, the use of hydrogen resulted in a depressed emf; vacuum partially restored the cell potential; a helium atmosphere had no particular effect. (b) There is definite evidence for the presence of hydroxide ion and/or water. (c) With fairly low current densities, gassing at the cathode was observed upon application of load. Attendant cell polarization was not excessive. (d) The cell reaction has a high apparent entropy, which is consistent with the formation of gas. (e) X-ray analysis of the anode surface revealed magnesium oxide. A study of the cathode showed no oxide of nickel for cells used in the lower temperature range.

Cells at Higher Temperatures

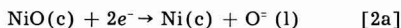
On heating above 445°C , the emf was relatively unresponsive to temperature change. The observed (and reproducible) discontinuity in the emf-temperature curve suggests a change in mechanism, and indeed, nickel(II) oxide is to be found on the cathode surface if the latter is heated above 450°C in the electrolyte. The negligible entropy of reaction at the

Table I. Slopes of electrode potential vs. log N curves at 480°C

Added Ion	Electrodes			
	Observed Mg v	Ni v	Theoretical Mg v	Ni v
Mg^{2+}	+0.070	+0.060	+0.075	+0.075
Ni^{2+}	+0.110	+0.070	+0.075	+0.075
O^{2-}	-0.057	-0.090	-0.075	-0.075

higher temperatures indicates disappearance of the gas phase reaction.

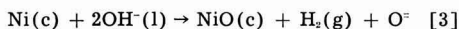
Reactions postulated for the system at higher temperatures are as follows. At the anode, [1a] as above, and at the cathode,



Net reaction,

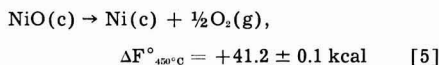
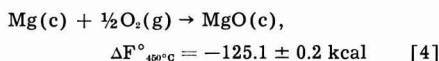


It is suggested that the nickel oxide is formed by reaction [3]



This reaction becomes thermodynamically possible in the temperature region of interest. The presence of water and hydroxide ion, which react with both magnesium and nickel to form metal, metal oxide electrodes, has been discussed above.

Lack of information on the free energy of oxide ion in solution does not permit calculation of emf's in the lower temperature region. However, reaction [2b] is amenable to an approximate calculation of potential. Coughlin (7) gives the following standard free energies at 450°C



The sum of reactions [4] and [5] gives, for reaction [2b] $\Delta F^\circ_{450^\circ\text{C}} - 83.9 \pm 0.3 \text{ kcal}$. This is equivalent to a standard emf of $1.82 \pm 0.01 \text{ v}$. The observed value is $1.70 \pm 0.01 \text{ v}$.

The difference between the calculated E° and the observed emf is about a tenth of a volt. However, it should not be inferred that the nickel oxide in the actual cell is at unit activity. Verwey (8) and Tichenor (9) discuss the presence of lithium ion in the nickel oxide lattice. The former induces the presence of nickel(III) oxide which can combine with Li_2O (10). Nickel(II) oxide itself forms a solid solution with lithium oxide, at least on the surface (11).

In any case, the half-reactions [1a] and [2a] are electrodes of the second kind as evidenced by the data in Fig. 2, 3, and 4. That is to say, the magnesium and nickel electrodes are constituted by a metal, a partially soluble metal oxide, and oxide ion in solution. As metal ion is added, it reacts with oxide ion in the electrolyte, and since the oxides are only partially soluble, relationships [A] and [B] will hold:³

$$[\text{Mg}^{++}][\text{O}^-] = K'_1 \quad [\text{A}]$$

$$[\text{Ni}^{++}][\text{O}^-] = K'_2 \quad [\text{B}]$$

The Nernst equations for the electrode potentials of the magnesium and nickel electrodes are given by the relationships,

$$E(\text{Mg, Mg}^{++}) = E^\circ(\text{Mg, Mg}^{++}) + (RT/2F) \ln [\text{Mg}^{++}] = E^\circ(\text{Mg, Mg}^{++}) + (RT/2F) \ln K'_1/[\text{O}^-], \quad [\text{C}]$$

$$E(\text{Ni, Ni}^{++}) = E^\circ(\text{Ni, Ni}^{++}) + (RT/2F) \ln [\text{Ni}^{++}] = E^\circ(\text{Ni, Ni}^{++}) + (RT/2F) \ln K'_2/[\text{O}^-] \quad [\text{D}]$$

The slopes of E vs. $\log N_{\text{MgCl}_2}$ or $\log N_{\text{NiCl}_2}$ curves are calculated to be $+0.075 \text{ v}$; the slope of the E vs. $\log N_{\text{Li}_2\text{O}}$ curve is calculated to be -0.075 v . These are to be compared with the experimental values in Table I. The authors consider the agreement to be good considering the various experimental difficulties.

Relationships [C] and [D] may be combined to give relationship [E] which expresses the emf of the nominal system:

$$E(\text{system}) = E^\circ(\text{Ni, Ni}^{++}) - E^\circ(\text{Mg, Mg}^{++}) + (RT/2F) \ln K'_2/K'_1 \quad [\text{E}]$$

It can be seen that this latter emf should be independent of the concentrations of magnesium, nickel, or oxide ions for a given temperature.

Manuscript received June 14, 1954. This paper was prepared for delivery at the Cincinnati Meeting, May 1-5, 1955.

Any discussion of this paper will appear in a Discussion Section to be published in the December 1959 JOURNAL.

REFERENCES

1. R. B. Goodrich and R. C. Evans, *This Journal*, **99**, 207C (1952).
2. K. K. Kelley and G. E. Moore, *J. Am. Chem. Soc.*, **65**, 1264 (1943).
3. A. Fleischer, *Trans. Electrochem. Soc.*, **94**, 289 (1948).
4. C. W. Jennings, *This Journal*, **103**, 531 (1956).
5. C. Solomons, J. Goodkin, H. J. Gardner, and G. J. Janz, *J. Phys. Chem.*, **62**, 248 (1958).
6. H. A. Laitinen, W. S. Ferguson, and R. A. Osteryoung, *This Journal*, **104**, 516 (1957).
7. J. P. Coughlin, *Bur. of Mines Bull.* 542, Washington (1954).
8. E. J. W. Verwey, *Bull. soc. chim. France*, Mises au point D122 (1949).
9. R. L. Tichenor, *Ind. Eng. Chem.*, **44**, 973 (1952).
10. L. D. Dyer, D. S. Borie, and G. P. Smith, *J. Am. Chem. Soc.*, **76**, 1499 (1954).
11. P. J. Fensham, *J. Am. Chem. Soc.*, **76**, 969 (1954).

³ E° and K' imply the use of concentrations instead of activities. Activity coefficients are not known but it is assumed that they are constant throughout the concentration ranges of interest.

Enhanced Surface Reactions

III. Adsorption of Gases on Prepared Ruthenium Surfaces

Manfred J. D. Low and H. Austin Taylor

Nichols Laboratory, New York University, New York, New York

ABSTRACT

Rates of adsorption of H_2 , CO , and O_2 on $Ru \cdot Al_2O_3$ catalyst surfaces prepared by pre-adsorption of gases were studied. Pre-adsorption of CO increases the rate and extent of H_2 adsorption. Adsorption of CO and of O_2 irreversibly poisons the surface. The Elovich equation is applicable to the data. The results are discussed in terms of a site-creation mechanism. It is found that the pre-adsorption of a gas may influence both the initial and the ambient rates of adsorption to various and at times opposite extents, resulting in several types of "poisoning."

In the study of chemisorption, catalysis, and similar surface processes it is of interest to examine the effects of one gas on the reaction of another with a solid surface. Whereas numerous examples of the "poisoning" of chemisorption and heterogeneous, catalytic processes exist, relatively few data on the opposite effect are to be found in the literature. A study of the effects of one pre-adsorbed gas on the adsorption kinetics of another has been undertaken, and is presented here.

Experimental

A commercial catalyst of 0.5% Ru on alumina was used as adsorbent. A 28-g sample of the solid was placed in a Vycor tube which was subsequently sealed to a conventional constant volume adsorption system. The adsorbent was heated to $500^\circ C$ and evacuated for about 10 hr to a pressure of 10^{-6} mm Hg or less. Appreciable amounts of gas and water were evolved during the first hour of pumping. The catalyst retained its original black color.

Palladium-filtered H_2 was admitted to the catalyst at $500^\circ C$ and 1 atm pressure. After a few minutes the catalyst turned gray and retained that color until exposure to oxygen occurred. Subsequent reduction with hydrogen restored the gray color. After being in contact with H_2 for 10 min the system was pumped on for 2 hr at 500° to 10^{-6} mm Hg or less. Experiments on H_2 adsorption were then made. All experiments were done with the adsorbent at $100^\circ C$ and were numbered consecutively in the order of execution. Volumes are reported in ml. N.T.P. At the completion of each experiment the system was evacuated, the adsorbent heated to $500^\circ C$ and pumped on at that temperature for 10 hr, with the exception of several "pretreatments" described later. All H_2 was purified by passage through Pd. Carbon monoxide was prepared by dehydration of formic acid with H_2SO_4 . Oxygen was purified by passage through a train of ascarite and drierite traps.

Surface preparation.—To prepare the catalyst by pre-adsorption, the following general procedure was adopted. After the 10-hr pumping period, the catalyst was isolated from the system, cooled, and then ther-

mostatted to $100^\circ \pm 0.1^\circ C$ in a steam bath. A predetermined amount of pre-adsorbate was placed in the system of known volume, and the pressure was measured. The stopcock isolating the adsorbent was then opened, admitting the gas to the catalyst chamber. Within 1 min or less the pressure in the system, measured on a manometer containing dibutyl phthalate (DBP), fell to less than 0.1 mm. After about 30 min the adsorbent was isolated and the system evacuated. Gas to be adsorbed "on top of" the first gas was placed in the system at a predetermined pressure. This gas was then admitted to the prepared adsorbent, and the rate of gas-uptake was measured.

Results

Adsorption of hydrogen.—The rate of adsorption of H_2 was measured on the catalyst immediately after the initial H_2 treatment described above. The kinetics of H_2 adsorption on this adsorbent have been studied previously (1). It was found then, as now (Table I), that the kinetics obeyed the Elovich equation (2)

$$\frac{dq}{dt} = a e^{-\alpha q}$$

q being the amount of gas adsorbed at time t , a and α constants depending on temperature and initial gas pressure (1-3, 7). The data were internally con-

Table I. Adsorption of H_2 on Ru surfaces pretreated with CO

Run No.	P_i , cm DBP	q_{CO} , ml NTP	α_1 , ml $^{-1}$	α_2 , ml $^{-1}$	$\ln a_{\alpha_1}$	$\ln a_{\alpha_2}$
1	69.9	—	3.5	4.6	6.44	8.80
2	69.5	—	3.65	4.8	6.68	10.98
3	70.6	0.30	2.7	3.8	4.88	7.41
4	70.2	—	3.4	4.7	6.15	8.99
6	70.2	1.01	1.33	2.6	1.95	4.98
7	70.0	3.18	0.98	1.4	1.34	2.53
8	69.9	6.50	0.65	0.74	0.73	1.01
9	70.0	1.01	1.76	3.3	2.72	6.39
10	69.9	1.33	1.58	3.1	2.42	6.28
11	70.2	0.27	2.4	4.3	3.87	7.92
12	69.8	1.64	1.46	2.4	2.16	4.58
13	69.9	—	3.3	4.8	5.22	8.10
30	70.8	—	2.5	4.3	4.03	7.75

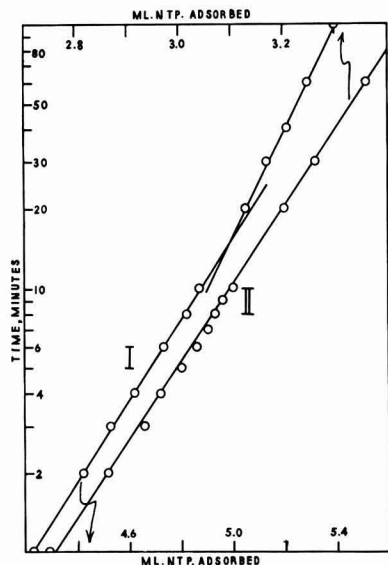


Fig. 1. Adsorption of H_2 on untreated Ru surfaces: I, Run No. 1, 100°C; P_i : 73.8 cm DBP; II, 100°C; P_i : 65 cm DBP.

sistent and well represented by the integrated Elovich equation,

$$q = \frac{2.3}{\alpha} \log_{10} (1 + a\alpha t)$$

Because $a\alpha t > 1$, this is tantamount to representation of data by $q - \log_{10} t$ plots. Whereas in the previous study linear $q - \log_{10} t$, or Elovich, plots were obtained, isothermal anomalies (2) were found in plots of the data of present experiments. Figure 1 shows a plot of the data of Run No. 1 and also that of a comparable run of the previous investigation.

At the end of the previous investigation (1) the catalyst was removed. Fresh adsorbent from the same batch of catalyst used previously was added to the sample to bring its weight to 28 g. It seems plausible, in view of the results to be discussed later, that the break in plot I of Fig. 1 and in other Elovich plots was caused by contamination, possibly

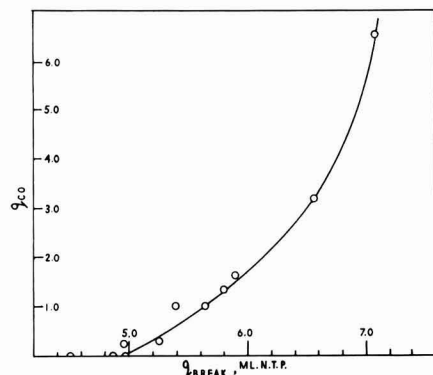


Fig. 2. Adsorption of H_2 on top of CO. The variation of the q -coordinate of the isothermal anomaly, q_{break} , with variation in q_{00} .

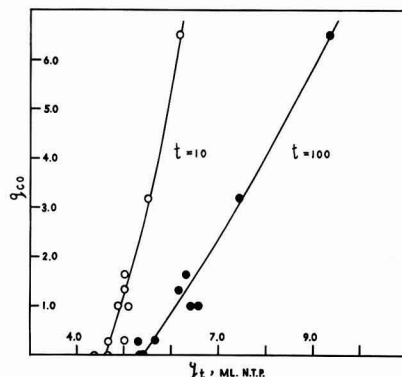


Fig. 3. Adsorption of H_2 on top of CO. The variations of the amount of H_2 adsorbed at time t , qt , with variation in q_{00} .

by atmospheric oxygen not removed by the initial H_2 treatment of the present investigation.

Adsorption of hydrogen on surfaces containing CO.—Data for eight such experiments are given in Table I. The rate of H_2 adsorption on surfaces containing varying amounts of CO was measured. In each case, the $q - \log_{10} t$ plot of the data resulted in a straight line which, after a certain time, abruptly changed in slope in a fashion similar to that of plot I, Fig. 1. The constants a and α for the initial and final part of each plot were designated by subscripts 1 and 2, respectively. All runs were made at approximately the same initial hydrogen pressure. Inspection of the data reveals some scatter of parameter values, but nevertheless interesting results.

Figure 2 to 4 show the type of relation obtained on plotting several parameters against the amount of pre-adsorbed CO, q_{00} . In general, it appears that the ambient rates and extents of H_2 adsorption are enhanced, but that the initial rates are decreased, by the pre-adsorption of CO.

Adsorption of CO.—At the end of run 13 the system was evacuated and the temperature of the adsorbent raised to 500° in 20 min. The hot adsorbent was exposed to CO at 80 cm DBP for 2 min, and then pumped on at 500° for 5 min. This CO pretreat-

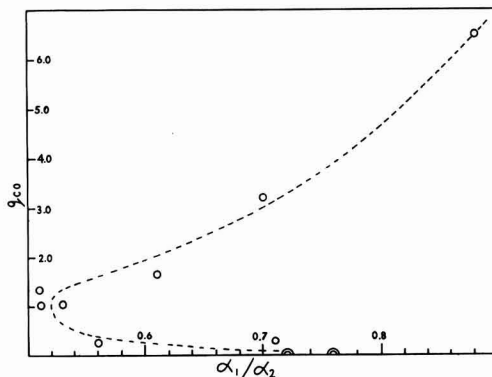


Fig. 4. Adsorption of H_2 on top of CO. The variation of the ratio α_1/α_2 , the ratio of ambient rates, with q_{00} .

ment was repeated twice. The adsorbent was then pumped down to 10^{-4} mm Hg or less for about 12 hr at 500° . Various runs using CO were then made, the parameters of four being given in Table II.

It was found that the experiments were not reproducible and that extreme scatter of parameter values was obtained: there was no gradual change in parameter values with change in the amount of pre-adsorbed H_2 . Also, the total amounts of CO adsorbed at 100 min show a steady decrease, dropping from 16.28 ml (run 16) to 13.70 ml (run 29), suggesting that progressive poisoning of the surface occurred.

It is interesting to note that in the first runs using CO on the unprepared surface, Elovich plots without breaks were obtained, whereas the data of experiments on surfaces prepared with H_2 (with the exception of the terminal run 29 with 0.08 ml pre-adsorbed H_2) gave discontinuous Elovich plots.

Repetition of hydrogen adsorption.—In order to determine whether the adsorbent had been damaged by the CO pre-adsorption experiments, the H_2 adsorption on an unprepared surface was repeated. After the usual pump-off at the end of run 29, H_2 was admitted to the catalyst at 500° for 5 min at 42 cm DBP. The catalyst was then pumped on for 5 min at that temperature. This treatment was repeated three times, after which the catalyst was pumped on overnight at 500° . Run 30 was then made. The magnitude of the parameters of that run, in comparison to those of runs, 1, 2, and 4, suggests that the surface had been permanently damaged. In view of this it seems possible and perhaps probable that CO poisoning was responsible for the failure of H_2 on O_2 and of O_2 on H_2 experiments, since all may be on top of CO.

Adsorption of oxygen.—An attempt was made to determine the influence of pre-adsorbed H_2 on the adsorption of O_2 , and the influence of pre-adsorbed O_2 on the adsorption of H_2 . The experiments were not reproducible. It seems probable that, as in the case of CO, an accumulation of irremovable gas occurred on the surface.

Some qualitative information was obtained from ten experiments. (A) Each experiment showed internal consistency in obedience of the Elovich equation. (B) Pre-adsorption of O_2 enhances the rate and extent of adsorption of H_2 (Fig. 5).

Discussion

The adsorption of H_2 on top of CO is faster and more extensive than that on untreated surfaces. An explanation, in classical terms, comes readily to mind. After 100 min, 5.40 ml of H_2 (run 1) but 16.28 ml CO (run 16) are adsorbed on untreated surfaces. Pretreatment of a surface with CO might therefore cause a part of the surface, originally inert, to take up H_2 , or H_2 may form surface H-CO complexes, or H_2 may literally be adsorbing on top of adsorbed CO molecules.

Such effects and mechanisms have been found previously, mainly in equilibrium studies such as the following. The work of Griffin (4) on the effect of pre-adsorbed CO on the adsorption of H_2 , and that of White and Benton (5) on the effect of H_2 on Ni

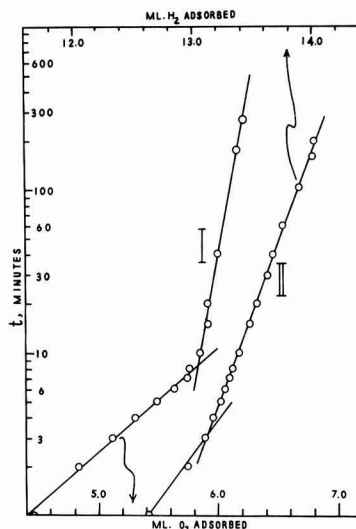


Fig. 5. Adsorption of O_2 and of H_2 : I. Adsorption of O_2 on unprepared Ru, Run 33; II, H_2 on top of 0.78 ml O_2 , Run 35.

“poisoned” with CO are examples. A more recent work is that of Sastri and Wiswanathan (6). The adsorption of CO and H_2 was studied on a Fischer-Tropsch Co- ThO_2 -kieselguhr catalyst on which H_2 and CO, respectively, had been pre-adsorbed. It was found that at any temperature the H_2 adsorption was enhanced the higher the amount of pre-adsorbed CO, that for a particular amount of CO the enhancement was larger the higher the temperature, and that the enhancement caused was relatively larger the smaller the volume of gas pre-adsorbed. These effects were explained in terms of surface complexes, since the amounts of pre-adsorbed gas were too small to account for the enhancement by a mechanism whereby one gas became adsorbed on top of the other. A similar postulate was made by White and Benton who, finding that CO enhanced H_2 adsorption, argued that “. . . either the CO can increase the activity of the already active areas, or it can stimulate those areas which do not function until higher pressures, or it can create entirely new areas . . .” (5). Because only small amounts of CO gave the effect, it was suggested that increased adsorption was due to an enlargement of active areas, which are produced by having very small amounts of CO adsorbed on them.

Examination of the present data and reference to “poisoning” effects discussed previously (2, 7, 8) suggest that a more generally applicable approach is desirable. A more general mechanism may be deduced from the theories of Taylor and Thon. It has been shown (2, 7-10) that surface site creation can occur by a branching chain mechanism initiated by the reaction of an active particle, G, with a surface atom, S, causing a “dissociation” of the atom into two adsorption sites, V. The over-all reaction for the branched chain may be written,



Table II. Adsorption of CO, O₂, H₂

Run No.	P _i , cm DBP	α_1 ml ⁻¹	α_2 ml ⁻¹	$\ln \alpha_1 \alpha_2$	$\ln \alpha_2 \alpha_2$	
16	73.8	1.90	—	11.45	—	(a)
17	74.2	2.00	—	11.88	—	(a)
24	73.7	0.98	2.4	5.00	13.08	(b)
28	74.2	0.65	2.4	3.2	12.01	(c)
33	60.2	1.48	15.3	2.83	2.89	(d)
35	75.6	2.3	4.5	12.61	25.17	(e)

(a) CO on untreated surface.

(b) CO on top of 2.58 ml pre-adsorbed H₂.(c) CO on top of 0.65 ml pre-adsorbed H₂.(d) O₂ on untreated surface.(e) H₂ on top of 0.78 ml pre-adsorbed O₂.

The excess (2n-1) sites can be active for adsorption or, alternatively, may suffer bimolecular decay. Enhancement or retardation of chemisorption rates or of the extent of chemisorption by pre-adsorbed gases may be explained in terms of that general mechanism. The effect of an impurity may be expected to be either one, or a combination of, two general effects: (A) the initial site creation process may be affected, i.e., the parameter n (chain length) may be greater or smaller than usual; (B) the bimolecular decay process may be affected, poisons permitting easier recombination of sites, promoters hindering the decay and thus permitting a longer "site-life." Several combinations of A and B are thus possible.

In the present case of H₂ adsorbed on top of CO, the initial rate, a_1 , is seen to decrease with increasing q_{CO} (Table I), a_1 falling from about 10⁶ on the pure surface to about 10¹ on a surface having 6.5 ml of pre-adsorbed CO. Simultaneously, the total amounts adsorbed at $t = 100$ min increase (Fig. 3) and the parameters α_i , reflecting the reciprocal ambient rates, decrease. It appears that the initial site creation process was hindered, and that fewer sites were available initially for the adsorption of H₂. Thus the increase in the adsorption process seems to be wholly due to a reduced site decay rate.

Conversely, the parameters of run 35 (Table II) suggest that the site creation process was affected mainly. In this case, on adsorbing H₂ on top of 0.78 ml O₂, a_1 was changed from 10⁶ to 10¹², while α_1 declined slightly: it appears that many more sites were created initially than in the case of H₂ adsorption on the untreated surface. The over-all effect is thus one of "promotion."

Further over-all effects may be predicted. An outright "poisoning" may occur, where both the initial and ambient rates of adsorption are decreased. The lack of reproducibility of CO adsorption rates and the diminution in the extent of adsorption of that gas, noted above, may be ascribed to such an effect: the rate of site recombination is greatly increased and the initial site creation process hindered, resulting in outright, true poisoning. Such true poisoning is also shown by Iijima's data (11, 12): the pre-adsorption of mercury or of CN by a Ni catalyst decreases both the initial and ambient rates of adsorption of H₂.

Also, a "pseudo-poisoning" may occur, in which case the ambient rate is decreased, but the initial

rate is increased. The pre-adsorption of a gas thus may cause increased total adsorption, but at greatly reduced rates, the bulk of the gas adsorbing in a very short time.

It appears that the reverse of the last example may exist: there may be decreased total adsorption, but at a higher rate. Agliardi and Morelli (13) thus found that when cobalt catalyst is poisoned with CO, less H₂ is adsorbed, but also that the rate of adsorption is greater, than by cobalt not poisoned by CO. This case may be ascribed to the dual action of a decreased initial site creation and a hindered rate of site decay. A further example of pseudo-poisoning is given by Iijima's data (12) on the adsorption of H₂ on top of CO on a Ni catalyst. The total adsorption after 19 hr decreases, the parameters α_i increase, and the initial rates a_i increase, with increasing amount of pre-adsorbed CO.

These considerations suggest that the determination of rates of adsorption may be more fruitful in pre-adsorption studies than the usual static isotherm or isobar measurements.

It has been postulated previously (2) that the isothermal anomalies sometimes found are due to a change-over of the adsorption process from one type of adsorption site to another. Recently this postulate has been supported by Meller (14), who derived the Elovich equation by assuming the chemisorption process to consist of two independent but simultaneous processes.

Such a mechanism also is implied to be operative at the present time. Thus the appearance of a break in the Elovich plots of data of CO adsorption on H₂-treated surfaces, while no such breaks were found to occur with CO adsorptions on untreated surfaces, may be said to be due to the influence of H₂ on the site creation of decay mechanism. Similarly, the displacement of amount adsorbed, q_{BREAK} , at the discontinuity in Elovich plots with increasing amounts of pre-adsorbed gas—a behavior also apparent in the data of Iijima—may be bound up with such a mechanism (Fig. 2).

Not enough data exist at present for a quantitative treatment of these effects, but qualitatively the above mechanism may be applied to the various relations shown by Fig. 2-4. However, because the presence or absence of isothermal anomalies seems to depend on the past history of the surface, there may be no real significance, from a general quantitative point of view, between the relations of parameters vs. q_{poison} for several different poisons. Further work is in progress.

Acknowledgment

The authors wish to thank Dr. T. Freund for performing several experiments.

Manuscript received Jan. 24, 1958.

Any discussion of this paper will appear in a Discussion Section to be published in the December 1959 JOURNAL.

REFERENCES

1. M. J. D. Low and H. A. Taylor, to be published.
2. H. A. Taylor and N. Thon, *J. Am. Chem. Soc.*, **74**, 4169 (1952).
3. L. Leibowitz, M. J. D. Low, and H. A. Taylor, *J. Phys. Chem.*, **62**, 471 (1958).

4. C. W. Griffin, *J. Am. Chem. Soc.*, **49**, 2136 (1927); **56**, 845 (1934); **57**, 1206 (1935).
5. T. A. White and F. Benton, *J. Phys. Chem.*, **35**, 1784 (1931).
6. M. V. C. Sastri and T. S. Viswanathan, *J. Am. Chem. Soc.*, **77**, 3967 (1955).
7. H. A. Taylor, *Ann. N. Y. Acad. Sci.*, **58**, 798 (1954).
8. H. A. Taylor, Peter C. Reilly Lectures in Chemistry, Vol. XII, Univ. of Notre Dame Press (1956).
9. M. J. D. Low and H. A. Taylor, *This Journal*, **104**, 439 (1957).
10. M. J. D. Low, *ibid.*, **105**, 104 (1958).
11. S. Iijima, *Rev. Phys. Chem. Japan*, **12**, 148 (1938).
12. S. Iijima, *ibid.*, **13**, 1 (1938).
13. N. Agliardi and S. Morelli, *Gazz. chim. ital.*, **78**, 707 (1948).
14. A. Meller, *Monatsh.*, **87**, 491 (1956).

Technical Notes



Electrolytic Preparation of Titanium from Fused Salts

II. Design of Laboratory Cells

Marshall B. Alpert, James A. Hamilton, Frank J. Schultz, and William F. Sullivan

Titanium Division, Research Department, National Lead Company, Sayreville, New Jersey

Previously a process was described for the preparation of Ti metal by the electrolysis of an alkali or an alkaline earth metal chloride melt containing the reduced chlorides of Ti (1). The reduced chlorides were prepared *in situ* by electrolytically reducing TiCl_3 introduced through a hollow cathode. Variables important in obtaining a good yield of coarsely crystallized, ductile Ti metal adhering to the cathode included careful sealing of the cell, maintenance of the soluble Ti largely in the divalent state, and avoidance of melt agitation during metal deposition. Provision of an adequate diaphragm and gas barrier arrangement to avoid oxidation of soluble reduced Ti at the anode was also considered.

The relation between design and function of externally heated laboratory cells is an important factor. Modifications were made in the single diaphragm cell leading, on the one hand, to diaphragm cells operating continuously rather than on a charge-strip basis and, on the other hand, to alternative deposition procedures. These include both one-step diaphragmless and electrorefining procedures.

Single Diaphragmed Cell

The usual laboratory single diaphragm cell used, of approximately 10-liter capacity and externally heated by a Globar furnace, is similar to the cell illustrated in Fig. 1, except that no diaphragm surrounded the introduction cathode. The porous, fused alumina diaphragm rests on a pedestal, since it has been found that, as long as the diaphragm is not under tension by support from above, no difficulty is experienced with breakage in the fused salt system. The gas barrier is fitted inside the diaphragm so that the Cl_2 atmosphere does not contact the catholyte containing reduced Ti; spacing is sufficiently close to insure that practically no rising Cl_2 bubbles slip between the diaphragm and the gas barrier. Current efficiencies for Cl_2 gas were about 90% with this

arrangement. The cell may be pressure tested for air leakage even while hot by use of an attached manometer. It is essential that the cell be sealed carefully from atmospheric contamination. Laboratory equipment of this type has been operated for periods of over three months without breakdown.

Certain limitations are inherent in this cell. The current for extended periods of operation is limited to about 60-100 amp to avoid obstructing the relatively small cross section (7.5 cm diameter) of the diaphragm and gas barrier with salt spray. The relatively small size of the anode and cathodes resulted in a rather high cell resistance, for example, 0.06 ohm with $\text{SrCl}_2\text{-NaCl}$ supporting electrolyte at 700°C . This situation was improved by a concentric design with the graphite anode as a ring external to the diaphragm. Such a cell with a resistance of only 0.01 ohm was studied. The small amount of catholyte (2.8 l) resulted in an inconveniently short charging

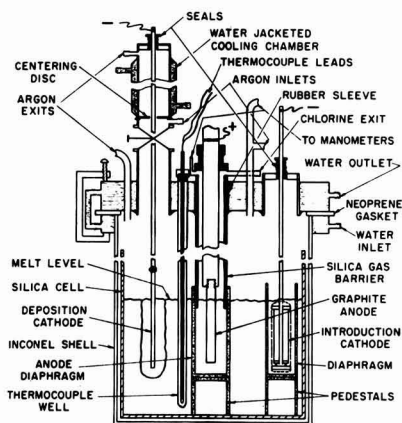


Fig. 1. Schematic drawing of double diaphragm cell

and stripping cycle, and the placing of the necessary accessory parts was difficult because of the small space available.

A major disadvantage of the single diaphragm cell is that the TiCl_4 must first be charged to the cell and then the reduced titanium chlorides electrolyzed to yield Ti metal in cyclic rather than continuous operation. Two factors imposed this requirement. Operation of the hollow cathode caused agitation of the melt in the vicinity of the deposition cathode and thereby reduced the crystal size and quality of the metal produced. In the second place, polarization of the hollow cathode at current densities above about 0.1 amp cm^{-2} resulted in the deposition of significant amounts of Ti metal at this electrode. Therefore, introduction of TiCl_4 at a rate of one mole per two faradays gave less than optimum degree of reduction for the melt, unless low hollow cathode current densities were employed or the melt was further reduced at low current densities prior to the metal deposition stage.

Some of the difficulties with cyclic operation may be eliminated by avoiding the use of a diaphragm entirely. If the current through the introduction cathode is increased to a value of approximately $4/f$ faradays per mole of TiCl_4 , where f is the current efficiency of the cell, the reduced titanium chlorides formed exist only transiently and do not escape in significant amounts from the vicinity of the introduction cathode. The melt therefore is substantially free of reduced Ti salts and no diaphragm is required (6,7).

Double Diaphragm Cell

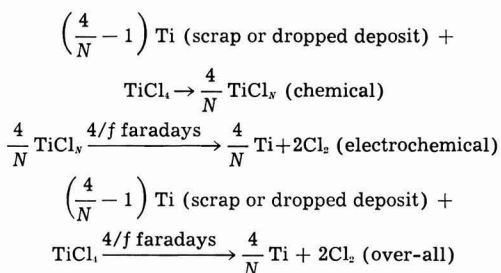
Figure 1 shows a cell in which the introduction cathode is also surrounded with a porous fused alumina diaphragm similar to the anode diaphragm (2). This cell permitted continuous reduction of TiCl_4 to Ti metal. When a high soluble Ti concentration was built up within the introduction diaphragm, the amount of Ti introduced as TiCl_4 and the amount leaving the introduction catholyte for the deposition catholyte were balanced by hydrostatic flow. The hydrostatic head resulting in this flow stems from the weight of TiCl_4 being added and from ionic migration effects (1). The deposition of coarsely crystallized, ductile metal was obtained while TiCl_4 was continuously introduced, since agitation of the melt about the hollow cathode no longer disturbed the electrolyte about the deposition cathode. In addition, polarization of the hollow cathode did not prevent maintenance of the degree of reduction of the melt desired, a level of at least 70% Ti^{++} . In this case polarization of the hollow cathode occurred at a higher current density because of the higher concentration of total Ti and hence of Ti^{+++} in the introduction catholyte melt. Also, metal produced by polarization was ultimately dissolved in the introduction catholyte by reaction with either TiCl_4 or TiCl_3 .

During continuous operation of the cell illustrated in Fig. 1 approximately 50 amp was passed through the introduction cathode while 45 amp was the deposition current. Typically, using the $\text{SrCl}_2\text{-NaCl}$ eutectic melt as supporting electrolyte, the concen-

tration of reduced titanium chloride was about 6M in the introduction catholyte and about 0.6M in the deposition catholyte; approximately 80% was Ti^{++} . Current efficiencies averaged 90% and recoveries were about 80% ductile Ti metal. The anode gas was 98.6% Cl_2 and 1.4% TiCl_4 .

Titanium Bed Introduction Cell

An alternative cell design which also allows continuity of operation and, in addition, can be used to produce secondary as well as primary metal, is shown in Fig. 2. In this design, TiCl_4 was reacted with a bed of Ti metal to produce the reduced titanium chlorides required for the deposition of Ti metal. The bed of Ti metal may be replenished either by adding a portion of the deposited metal or by adding Ti metal scrap. In the cell illustrated in Fig. 2 alternate deposits were dropped to the bed. The net reactions are given by the equations



where N is the apparent valence of the Ti dissolved in the melt and f is the current efficiency of the cell. Note that when scrap Ti is employed instead of dropped deposits and the Ti dissolved in the melt is maintained largely in the divalent state, each $4/f$ faradays produced 1 mole of primary metal and also almost 1 mole of secondary metal. In a simple primary cell the same amount of current would produce only 1 mole of Ti metal. In the cell illustrated the electrolyte selected was a mixture of 8% SrCl_2 and 92% NaCl , requiring an operating temperature of about 830°C . The current was 65 amp with the TiCl_4 feed rate at 1.6 g/min. The concentration of reduced titanium chloride, approximately 80% divalent Ti, was maintained about 0.25M in the catholyte.

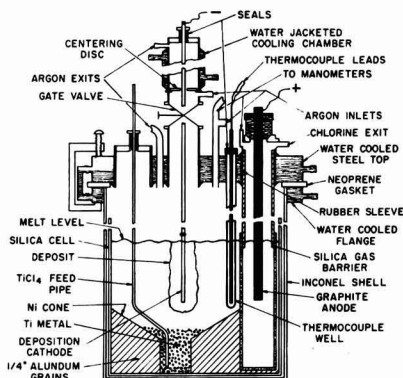


Fig. 2. Schematic drawing of titanium bed cell

Recovery averaged about 83% of ductile Ti metal. A further improvement in design which completely avoids any disturbance of the catholyte during TiCl_4 introduction may be realized in the case of scrap metal by using a design similar to the double diaphragm cell. The scrap metal is added to the introduction catholyte.

Refining of scrap Ti metal may also be accomplished separately by using a cell with a scrap Ti anode. Such cells are particularly simple to construct, since neither a gas barrier nor a diaphragm is used, and no protection against corrosive Cl_2 is required. At low current densities the anode dissolves to yield reduced titanium chlorides substantially at concentrations set by the equilibrium



and, since Ti is deposited from the same melt at close to reversible conditions, the cell emf is small, less than 0.1 v at 700°C, SrCl_2 -NaCl melt, anode current density 0.25 amp cm^{-2} . At higher anode current densities increasing amounts of Ti^{3+} are produced because of anodic polarization and the cell emf is increased. Most contaminating metals are left effectively at the anode and oxygen remains as a reduced titanium oxide anode sludge (3-5).

Process for Electrolytic Extraction of Titanium Metal from Titanium Carbide Anodes

Guy Ervin, Jr., Herbert F. G. Ueltz, and Malcolm E. Washburn

Research and Development Department, Norton Company, Worcester, Massachusetts

Extractive metallurgy of titanium has been discussed in several review articles (1-8). Increasing interest has been shown in molten salt electrolysis using soluble anodes, but confined chiefly to electrorefining, in which high-purity metal is recovered from scrap or other sources of impure metal. However, one article (9) and several patents (10-14) deal with production of Ti by electrolysis of soluble anodes containing TiC.

The key to the process is the fact that, although TiC is a metal carbide with a limiting composition of 1:1, it behaves during electrolysis as though it were metal with high carbon content. Since the other refractory carbides probably have the same property, the method is potentially applicable to production of Zr and other refractory metals.

The work reported here was started in this laboratory several years ago. It shows that better than 90% of the Ti in TiC can be extracted electrolytically in fused halide baths and deposited as dendritic Ti metal. The dendritic deposit contains entrapped electrolyte which must be removed by leaching with dilute acid. Current efficiency and product quality are variable and depend on several factors including electrode configuration, physical and chemical characteristics of the TiC anode, chemical composi-

Acknowledgments

The technical assistance of Thomas M. Buck, Daniel Kaufman, Bryce H. McMullen, and Lawrence S. White is gratefully acknowledged.

Manuscript received July 2, 1958. This paper was prepared for delivery before the Ottawa Meeting, Sept. 28-Oct. 2, 1958.

Any discussion of this paper will appear in a Discussion Section to be published in the December 1959 JOURNAL.

REFERENCES

1. M. B. Alpert, F. J. Schultz, and W. F. Sullivan, *This Journal*, **104**, 555 (1957).
2. M. B. Alpert and J. A. Hamilton (To National Lead Co.), U. S. Pat. 2,760,930, Aug. 28, 1956.
3. J. R. Nettle, D. H. Baker, Jr., and F. S. Wartman, "Electrorefining Titanium Metal," U. S. Bur. Mines, Rept. Invest. 5315 (1957).
4. R. S. Dean, W. W. Gullett, F. X. McCawley, and I. Hornstein, *Industrial Laboratories*, **8** (4), 4 (April 1957).
5. F. J. Schultz and T. M. Buck, (To National Lead Co.), U. S. Pat. 2,734,856, Feb. 14, 1956.
6. M. B. Alpert, W. R. Opie, F. J. Schultz, and K. Svanstrom (To Titan Company, Inc.), Argentine Pat. 88,505, March 17, 1953.
7. W. R. Opie and K. A. Svanstrom, "Electrodeposition of Titanium from Fused Chloride Baths Using TiCl_4 as a Feed Material," to be published in *Trans. A.I.M.E.*

tion of the electrolyte, and to a lesser extent on current densities and temperature of the bath.

Experimental

The cell used for most of the experiments consisted of a graphite crucible lined with carbon-bonded TiC and containing the molten electrolyte, with a metal cathode mounted centrally in the bath, and with an external container of nickel or steel, closures being made with rubber O-rings clamped between water-cooled flanges. Operation was in a purified argon atmosphere, and precautions were taken to remove traces of air and moisture from all raw materials and cell parts. Several sizes of cell were used, varying in metal product capacity from 20 g to 12 lb.

Carbon-bonding of TiC in the anode was achieved either by sintering at about 2300°C or more commonly by forming a mixture of the carbide with pitch, molding to shape, and baking at 1000°-1200°C in inert atmosphere to drive off pitch volatiles. Anodes formed in this way from pitch were strong and porous, with good electrical conductivity, and their use permitted rather complete electrolytic extraction of the Ti in the TiC.

Some typical results are shown in the following Tables I and II.

Table I. Electrolytic titanium from titanium carbide

Anode composition,† %			Electrolyte composition*	Cathode C.D., amp/cm ²	Voltage	Current efficiency Ti ⁺ basis	Metal Composition, %			Hardness‡ BHN
Ti	C	Fe					Fe	C	O**	
69	24	0.15	LiCl-KCl	2	3.8	45%	0.2	0.4	0.3	310
66	31	0.15	NaCl-TiCl ₃	2	3.6	65	0.5	0.5	0.5	380
70	27	0.6	NaCl-K ₂ TiF ₆	2	4.5	49	0.6	0.02	0.14	174
67	31	0.1	NaCl-K ₂ TiF ₆	2	4.5	47	0.1	0.3	0.3	250
79	20	0.03	NaCl-K ₂ TiF ₆	2.5	4.1	51	0.1	0.05	0.12	157

Table II. Electrolytic refining of titanium

99.4	0.15	0.1	NaCl-TiCl ₃	1.5	0.7	130	0.03	0.02	0.12	120
99.1	0.02	0.7	NaCl-K ₂ TiF ₆	1	0.5	105	0.01	0.00	0.11	104

* When TiCl₃ or TiCl₂ was present the concentration was 5% Ti, K₂TiF₆ in the bath corresponded to 3% Ti. Temperature approximated 850°C in all cases.

** Oxygen was calculated from hardness plus Fe and C analyses.

† Measured as Rockwell C or B and converted to BHN.

‡ Exclusive of the carbon bond. Note that in all cases but one, substantial quantities of free carbon were present, above the stoichiometric value of 20%.

Metal could be produced with electrolytes containing no Ti initially, or with TiCl₃ present, but coarser crystals were produced with electrolytes containing K₂TiF₆. Figure 1 shows metal dendrites typical of the cathode deposits described in the last row of Table I, made from relatively pure TiC.

Table II shows data on electrorefining of primary metal made electrolytically from TiC. This produced much coarser crystals, of the type shown in Fig. 2, and purity was improved.

Discussion

Dissolved Ti in the bath is trivalent, when the anode is TiC. If a bath containing TiCl₃ is used, it rapidly converts to TiCl₂, contrary to the behavior with Ti metal anodes. The theoretical basis for this is that the electrode potential at the anode due to decomposition of TiC is lower for formation of Ti³⁺ (0.59 v) than for Ti²⁺ (0.89 v). Furthermore this potential probably exceeds that for oxidation of Ti²⁺ to Ti³⁺ so that, before any Ti ion is produced anodically from the TiC, all of the TiCl₃ in the vicinity of the anode is oxidized to TiCl₂. This makes it impossible to use iron cells and iron anodes as has been done elsewhere (15) because TiCl₃ attacks iron. For

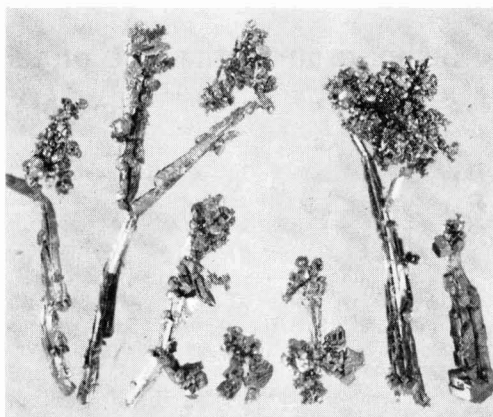


Fig. 2. Titanium crystals 99.8% Ti, BHN 110, made by two-stage electrolysis from TiC. Magnification X8.

the same reason little refining with respect to iron can be expected when the anode is TiC.

Important impurities other than iron to be considered are carbon and oxygen. Carbon contamination was caused by loosening of particles from the anode, but could be kept below about 0.05% C by proper bonding of the anode. Oxygen contamination kept decreasing during the course of the project as techniques were improved. There was no evidence of any transfer of oxygen from the carbide anode to the product, and it seems probable that metal of suitably low oxygen content could be produced in larger equipment. However, direct oxygen analyses of TiC and the metal produced from it were not made so that direct evidence for refinement with respect to oxygen is lacking. Estimating oxygen by difference indicated that metal with 0.1 to 0.2% oxygen was produced from arc-furnace TiC containing 0.5% or more oxygen.

Conclusion

Titanium metal powder can be produced in fused salt electrolyte from titanium carbide anodes. Purity of the metal is adequate for many uses including

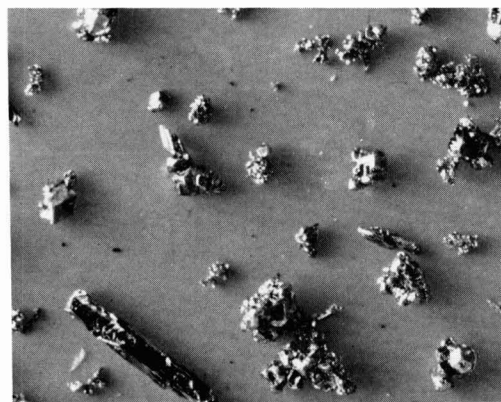


Fig. 1. Titanium metal dendrites 99.6% Ti, BHN 157, made from TiC anode. Magnification, X25.

powder metallurgy and for feed material to an electrorefining process making maximum purity metal. There is a reasonable expectation that commercial development would lead to higher product purity direct from TiC.

One of the cheapest ways to get metal from its oxide is to reduce the oxide with carbon, if possible. Reduction of titanium oxide with carbon does not yield metal but does yield metal-like carbide from which metal can be produced electrolytically. Viewed in these simple terms the method has strong commercial potential for titanium metal production.

Manuscript received May 8, 1958.

Any discussion of this paper will appear in a Discussion Section to be published in the December 1959 JOURNAL.

REFERENCES

1. N. S. Spence, *Can. Mining Met. Bull.*, **1951**, 21.
2. M. Cook, *J. Inst. Metals*, **82**, 93 (1953).
3. W. J. Kroll, *Metall.*, **9**, 1, 366 (1955).
4. *Chemical Week*, **76**, No. 8, pp. 35-54, Feb. 19, 1955.
5. P. Herasymenko, New York Univ.-Amer. Soc. for Metals Titanium Course, Sept. 12-16, 1955.
6. M. E. Sibert and M. A. Steinberg, *J. Metals*, **8**, 1160 (1956).
7. L. M. Pidgeon, *Metal Prog.*, Vol. 70, Aug. '56 p. 81; Oct. '56 p. 79; Nov. '56 p. 75.
8. *Chemical Week*, **79**, No. 23, pp. 55-64, December 8, 1956.
9. B. S. Hickman and G. M. Willis, *Proc. Australasian Inst. Mining & Met.*, **178**, 29 (1956).
10. S. C. Pyk, Swedish Pat. 137,626, July 24, 1952.
11. E. Wainer (to Horizons Titanium Corp.) U. S. Pat. 2,722,509, Nov. 1, 1955.
12. G. Ervin, Jr. and H. F. G. Ueltz (to Norton Co.) Brit. Pat. 744,396, Oct. 5, 1956; U. S. Pat. 2,837,478, June 3, 1958.
13. B. C. Raynes, M. E. Sibert, and J. T. Burwell, Jr. (to Horizons Titanium Corp.) U. S. Pat. 2,813,069, Nov. 12, 1957.
14. M. E. Washburn (to Norton Co.) U. S. Pat. 2,838,454, June 10, 1958.
15. D. H. Baker, Jr. and J. R. Nettle, Paper presented at New York Meeting AIME, February 1956.

Comparison of the Life of Linings in Rotating and Stationary Phosphorus Furnaces

M. M. Striplin, Jr., J. M. Potts, and E. C. Marks

Tennessee Valley Authority, Wilson Dam, Alabama

The first commercial-size rotating phosphorus furnace, a TVA development (2), was placed in operation in October 1950. The furnace is similar to the rotating alloy and carbide furnaces described by Ellefsen (1). It is of about 10,000-kw capacity and has been operated with conventional stationary furnaces as an integral part of the TVA plant. Except for information on the life of the furnace lining, which is a factor of major importance, fairly complete operating results on the rotating furnace have been published (3). Now, further information is presented which compares the life of the lining in this furnace with those of the TVA stationary furnaces.

TVA operates five rectangular stationary furnaces of conventional design and one round rotating furnace. Unless hot spots show up to indicate the need for repairs, the furnaces are normally operated at least 2 years between lining inspections. At the time of inspection, superficial damage to the lining is repaired by ramming in hot carbon paste, although such repairs to the surface of the hearth are of doubtful value. Major repairs involve replacement of a substantial number of carbon blocks used in the lining, or the entire lining.

Data on the performance of the linings in the TVA furnaces during the 8 years since the rotating furnace was started show a big advantage in favor of the rotating furnace (see Table I). For the stationary furnaces, the record shows that during the 8-year period, there were 12 times when holes developed in the furnaces unexpectedly spilling the molten contents (tapouts). Only minor repairs that could be made from the outside of the furnaces were suffi-

cient in some cases, while others involved major repairs. Hot spots developed frequently, causing a need for decreased power input and special precautions to avoid further damage. Operation on low power usually was continued until such time as the hot spots disappeared or it was decided to shut down for major repairs to the lining. Twelve major repairs were made to the stationary furnaces during this period; this averaged a major repair to each furnace once every 3 years.

In comparison, during the same period, the rotating furnace had no hot spots, no tapouts, and no major repairs. The only patching has been after each of the four inspections, when carbon paste was used to cover eroded surfaces caused by normal wear and by the tools used to dig out the charge. The last inspection showed the original floor of this furnace to be in excellent condition. Erosion of the carbon amounted to about 2.54 cm/year (the thickness of the carbon floor is 104 cm).

Even at the slag line, there has been little or no wear of the carbon blocks in the rotating furnace. In the stationary furnaces, this is an area of high normal wear. This contrast was experienced even though the outer surfaces of the electrodes in the rotating furnace are 27% closer to the side walls than in any of the other furnaces. Maintenance costs have been considerably less on the rotating furnace than on the stationary furnaces.

For the same hearth area, the rotating furnace has a higher kilowatt capacity than the stationary furnaces. As an example, this factor expressed as kilowatts per square meter of hearth area (power density) shows the rotating furnace to have been oper-

Table I. Comparison of TVA rotating and stationary phosphorus furnaces

	Stationary furnace No.					Avg	Rotating furnace No.
	2	3	4	5	6		1
Nominal rating, kw	9500	8700	7500	16,000	16,000	—	10,000
Area of hearth, sq m	26.8	28.1	23.6	37.6	40.1	—	19.9
Hearth power density, kw/sq m	354	310	318	426	399	361	503
Distance from outer surface of electrode to side wall, m	1.52	1.55	1.37	1.77	1.77	—	1.12
Maximum voltage (transformer taps), v	375	300	260	500	500	—	375
Age of lining as of October 1950, yr and mo	6-2	2-2	1-10	2-0	1-10	2-10	0
Calendar time in operation,* %	78.4	75.3	66.0†	79.3	86.9	77.1	79.9
Number of major repairs to lining* ‡	2	2	2	4	2	2.4	0

* Since October 1950.

† Retired from service in 1957.

‡ Substantial replacement of carbon blocks required, as distinguished from minor repairs with carbon paste.

ated at a value of 503 as compared with 310 to 426 for the other furnaces. Localized overheating or overexposure of the lining to corrosive conditions occurs in stationary furnaces because the furnace lining remains in the same relative position with respect to the tips of the electrodes, which are the focal points of energy input to the furnaces. In the rotating furnace no area of the lining remains near the tips of the electrodes very long. Localized overexposure is thereby avoided and more energy can be concentrated into the same space. Also, whatever normal wear is encountered is more uniformly distributed.

One of the few features of the original design of the rotating furnace that failed to give completely satisfactory service was the molten lead seal, which was provided at the juncture between the stationary roof and rotating crucible to prevent the escape of gas. This seal required considerable attention and maintenance. After 5½ years of operation, the seal was replaced with a 51-cm water seal. Fresh water is fed continuously to the seal and is allowed to overflow down the furnace shell as supplemental cooling water. The new seal has required no maintenance and has given good service.

The TVA rotating furnace, although relatively small in comparison with the furnaces constructed recently by industry, has demonstrated adequately that rotating furnaces have important advantages

over stationary furnaces. The feasibility of rotating larger phosphorus and other types of furnaces has been demonstrated by industry.

The trend in the phosphorus industry seems to be away from furnaces with the electrodes arranged in line and toward furnaces with a triangular arrangement of the electrodes. The electrical load is more equally distributed to each electrode in these furnaces than in furnaces with the electrodes arranged in line. Even distribution of the electrical load may contribute to longer life of the furnace lining and is beneficial in other respects. Inasmuch as it is possible to operate a round furnace at a slightly higher power input when the furnace is rotated, the cost of a rotating furnace per unit of capacity is essentially the same as that of a stationary round furnace. Additional rotating phosphorus furnaces may be expected as soon as the benefits to be derived from this type furnace are fully appreciated.

Manuscript received June 16, 1958.

Any discussion of this paper will appear in a Discussion Section to be published in the December 1959 JOURNAL.

REFERENCES

1. J. Ellefsen, *Trans. Electrochem. Soc.*, **89**, 307 (1946).
2. M. M. Striplin, Jr., S. A. Hardin, and W. H. Bundy, U. S. Pat. 2,744,944, May 8, 1956.
3. M. M. Striplin, Jr., G. H. Megar, and J. M. Potts, *Chem. Eng.*, **60**, 201 (September 1953).

June 1959 Discussion Section

A Discussion Section, covering papers published in the July-December 1958 JOURNALS, is scheduled for publication in the June 1959 issue. Any discussion which did not reach the Editor in time for inclusion in the December 1958 Discussion Section will be included in the June 1959 issue.

Those who plan to contribute remarks for this Discussion Section should submit their comments or questions in triplicate to the Managing Editor of the JOURNAL, 1860 Broadway, New York 23, N. Y., not later than March 2, 1959. All discussion will be forwarded to the author, or authors, for reply before being printed in the JOURNAL.



Electrolysis of Organic Solvents with Reference to the Electrodeposition of Metals¹

Abner Brenner

National Bureau of Standards, Washington, D. C.

This lecture was instituted to honor the memory of one of the founders of our society, J. W. Richards. Since it is now many years since he died, and since few of us had a personal acquaintance with him, it is fitting that I say a few words about him. He was not only one of the organizers of the Society, but also its first president, holding office in 1903. He served as Secretary-Treasurer for 17 years until his death in 1921. He was very active in both the administrative and scientific affairs of the Society and commented on most of the papers that were presented at the annual meetings. He was known the world over as an eminent metallurgist and served on numerous technical committees. He made one of his greatest contributions to science in his capacity as Professor of Metallurgy at Lehigh University where he taught until the time of his death. He was the author of two textbooks on metallurgical subjects.

In appraising the list of previous Richards Lectures, I note that 12 lectures have been given previously at an average interval of 2.5 years. Since there is an interval of five years between this lecture and the previous one, I assume that the Society intentionally passed the thirteenth, and that this one should be considered as the fourteenth. Can it be that the directors of the Society are superstitious?

I have also noted with interest that the previous lectures have covered such subjects as history, metallurgy, and electronics. Only one lecture, the last one, dealt with an electrochemical subject—over-voltage. I believe that the lecture that I am giving this afternoon is also an innovation, because it is the first one concerned with electrodeposition. No doubt some members of the audience are glad to see that electrochemistry is finally winning public recognition.

The subject of this lecture is the "Electrolysis of Organic Solvents with Reference to the Electrodeposition of Metals." Since this is a rather specialized subject and since electrodeposition is not usually presented at the Spring Meeting, I was pleased to see so many members assembling for the lecture. I mentioned this to Dr. Steinberg just before starting,

and he replied that, inasmuch as it was raining outside, the members had no where else to go.

Research on the electrolysis of organic solutions has been sadly neglected in favor of a slavish devotion to aqueous systems. I did not understand this attitude until I happened to see a cartoon pinned on a laboratory bulletin board that made clear the reason for this. It depicted a students' laboratory. A voluptuous young woman was working at the bench blissfully unaware that she was the cynosure of two pairs of male eyes, focused from across the room. One male student was saying to the other, "and just think, she is over 90% water!" The great practical importance of water in our daily living has induced scientists to study aqueous systems far beyond their scientific importance. There are many more new phenomena to be discovered in the study of nonaqueous² systems.

The subject matter of this lecture is divided into two parts. Beginning with the more complex subject, attempts to electrodeposit metals from nonaqueous media are discussed and next, the more fundamental subject, the electrolysis of nonaqueous solvents themselves.

Deposition from Nonaqueous Media

The first interest in electrodeposition of metals from nonaqueous media developed in connection with the measurement of the conductivity of solutions. It was natural that the investigator should seek to determine whether conducting solutions would yield electrodeposits as do aqueous solutions. The first record is the work of Laszczynski (1) in 1895, who was measuring the conductivity of solutions of salts in acetone. He electrolyzed several of the solutions and observed that the deposits on the cathode gassed or sparked if placed in water. He concluded that lithium and potassium had been deposited. He also deposited silver. Within the next five years both he (2) and Kahlenberg (3) electrodeposited several metals from pyridine solutions. Kahlenberg showed that, under the best conditions, the theoretical quantity of metal deposited.

During the next 25 years the deposition of metals from a small number of solvents was studied in a qualitative fashion. This early work has been re-

¹ This paper was presented as the J. W. Richards Memorial Lecture, April 28, 1958, at the New York Meeting.

² In this paper nonaqueous systems do not include fused salts.

viewed by Audieth (4). Among the solvents used were acetone, pyridine, ethylenediamine, ammonia, formamide, and acetamide. Apparently nitrogen-containing solvents commanded the most attention. Grignard reagents were electrolyzed and yielded mossy deposits of magnesium (5).

The amount of early work was rather small and attracted little interest. Within the last decade there has been a revived interest in the study of non-aqueous media because of the possibility of depositing some of the less common metals which cannot be deposited from aqueous solution.

About 30 metals can be deposited from aqueous solution. These metals will be referred to as the aqueous group and the other metals as the non-aqueous group. The early studies of nonaqueous solvents dealt mainly with the aqueous group of metals. Since these metals can be deposited more readily and in a purer condition from water solution, these studies were of little practical interest. Few of the nonaqueous group of metals were deposited. Lithium and some other alkali metals were purported to have been deposited. However, the purity was not substantiated by analysis and certainly many of the deposits were far from pure, as Pospekhov (6) has shown. Furthermore, since the metals could be obtained more readily by deposition from fused electrolytes, there was no incentive to further study.

The nonaqueous group of metals which has been of more recent interest contains the light metals, beryllium, aluminum, and magnesium; the semiconductor, germanium; and the refractory metals, titanium, zirconium, tungsten, and molybdenum. Of these by far the most attention has been given to the deposition of aluminum. Furthermore, aluminum is the only nonaqueous metal that can be considered to have been successfully deposited. By this is meant that the metal can be obtained at high cathode current efficiency in high purity and with good physical properties.

Studies at the National Bureau of Standards

This lecture is largely, although not exclusively, concerned with the work done by the Electrodeposition Section of the National Bureau of Standards. Our work in this field started rather suddenly. About 1950 we became interested in the electrodeposition of aluminum and were repeating some of the recently published work. About this time lithium aluminum hydride became commercially available and we studied the electrolysis of ether solutions of this compound. These experiments led to the development of a new type of nonaqueous plating bath (7). The Navy Bureau of Aeronautics sponsored further investigations of the process because of the possibility of electroforming aluminum wave guides. This interest seemed to have kindled a spark. Other Government agencies became interested in depositing some one of the less common metals for various purposes. The AEC sponsored a project on the deposition of beryllium (8); the Wright Air Development Center, on the deposition of titanium and zirconium (9); and Springfield Armory, on the deposition of molybdenum. An investigation of the deposition of magnesium (10) was also carried out.

Although some interesting developments resulted, they were not the practical objectives desired by the sponsors, and after a period of three or four years the program ceased about as suddenly as it had started.

I wish to mention briefly some of the equipment used in our work with nonaqueous solvents. Since many of the experiments involved the preparation and use of compounds, such as metal alkyls and borohydrides, which were sensitive to air or moisture or even spontaneously inflammable, the techniques and equipment used were somewhat different from those used in ordinary plating experiments. Indispensable to our work were inert atmosphere chambers (11) of which two were constructed. A dry atmosphere of helium was circulated continuously through the chambers and deoxygenated. For running electrolytic experiments in the laboratory some special cells were designed (12) which excluded the air and yet allowed the cathodes to be removed and examined, and fresh ones put in if necessary.

Since aluminum is the nonaqueous metal which has received most study and also is the one most successfully deposited, it is discussed in some detail as a typical example. Space does not permit the mention of all of the early attempts to deposit this metal from organic solvents. A partially successful deposition was done by Blue and Mathers (13) from organic solutions similar to the Friedel-Craft reagents and from aluminum alkyl halide solutions. The deposits were not of good quality. The first successful deposition of aluminum from a nonaqueous solution at room temperature was accomplished by Hurley and Wier (14) using a solution of aluminum chloride in ethyl pyridinium bromide. This bath had more the characteristics of a molten salt bath than a typical bath made from an organic solvent. Menzel (15) deposited aluminum from solutions of aluminum ethyl or aluminum phenyl and aluminum chloride in toluene.

At the National Bureau of Standards a hydride plating bath was developed which yielded a pure, ductile deposit of aluminum (7). The bath consisted of aluminum chloride dissolved in ether with the addition of lithium aluminum hydride. Evans and Kennedy (16) by conductometric studies have shown that the ionizing complex in this type of solution is probably $Al_2Cl_6 \cdot AlH_4^-$. Deposits several hundredths of an inch thick were readily obtained from the bath. To prevent formation of nodules, methyl borate was used as an addition agent.

The bath had some interesting characteristics. It had a limited life and could tolerate the presence of oxygen but not moisture. Baths were used up to periods of a year or more by occasionally rejuvenating them with lithium aluminum hydride. Decomposition of the bath occurred mainly during electrolysis, not as a result of atmospheric attack. During operation hydrogen was given off at both the cathode and anode, but the quantity was greater at the anode than at the cathode. Apparently the decomposition of the bath occurred anodically, although aluminum went into solution with 100% anode current efficiency. Another peculiarity of the

bath was that the amount of aluminum deposited from it was about equivalent to the amount of aluminum that had been added to the bath as aluminum chloride. The aluminum that went into solution anodically did not appear to enter into the same kind of chemical combination as the aluminum initially introduced, and apparently metal did not deposit readily from this anodically dissolved aluminum. Thus, additional aluminum chloride had to be added to the bath at intervals. Eventually, the bath became so viscous that it could not be used any longer. Up to this point about 250 g Al had been deposited from about 1 l of bath.

Some experiments were made to determine whether the hydrogen that was liberated at the anode in the electrolysis of the aluminum plating bath would cause embrittlement of steel. We used steel rings to test this and found that the rings were embrittled more severely than in a water solution. The decrease in breaking load was 30-50%. Cathodic discharge of hydrogen from several other organic solvents did not cause appreciable hydrogen embrittlement.

More recently another bath for depositing aluminum has been developed by Ziegler (17) in Germany, the man of polyethylene fame. This bath is unique because it involves the formation of a complex between triethyl or methyl aluminum and sodium fluoride. The aluminum alkyl by itself does not conduct the current, but the complex does and yields very pure aluminum on electrolysis. We have prepared the bath and confirmed that it does operate satisfactorily. Also the complex can be prepared in ether solution and then is much less inflammable.

Most recently, Murphy and Dumas (18) reported the deposition of aluminum from aluminum chloride dissolved in an ethereal solution of butyl amine. We have not had much success with this bath. A private communication to me indicates that the deposit may be an aluminum compound.

I shall briefly touch on our work with some of the other elements (8-10) of the nonaqueous group and then attempt to summarize the state of our knowledge. I believe that the work will be easier to follow if it is organized with respect to the type of compound involved rather than to take each metal separately.

The success of the hydride bath for depositing aluminum led us to attempt the deposition of other metals from similar types of baths, but the hydride bath appears to be specific for aluminum. Soluble hydrides of titanium and zirconium could not be prepared as lithium aluminum hydride precipitated the elements or a compound from ether solution. Ethereal solutions containing beryllium aluminum hydride and magnesium aluminum hydride were prepared and yielded alloys containing aluminum and the other metal, but the quality of the deposits was rather poor.

The metal alkyls were investigated as electrolytes because Grignard reagents had yielded magnesium on electrolysis. Our experience with the magnesium deposits was unsatisfactory as they were not dense and coherent. Beryllium was deposited from an

ethereal solution of beryllium dimethyl, the best results being obtained from a solution that contained both beryllium dimethyl and beryllium chloride. The beryllium was about 95% pure under the best conditions. We made a number of attempts to prepare alkyl derivatives of titanium and zirconium but all of these ended in failure, although a number of interesting compounds were encountered which we did not have time to investigate. Solutions of the cyclopentadienyl derivatives of titanium and zirconium conducted poorly and did not yield metal on electrolysis.

The most interesting phase of the work was the preparation and electrolysis of metallic borohydrides. The metallic borohydrides had only recently been prepared when we started our work. The pure borohydrides of aluminum and zirconium are liquids but they do not conduct. In ether solution, the borohydrides of aluminum, magnesium, and beryllium conduct, and alloys are obtained containing the metal and boron. The most interesting deposit was one containing about 30% boron, the remainder beryllium. The ether solutions of titanium and zirconium borohydrides did not yield the metals on electrolysis. However, by mixing the aluminum hydride plating bath with borohydride solutions of titanium or zirconium, deposits were obtained which contained aluminum, boron, and titanium or zirconium. The refractory metals were not present in large percentages. The titanium content was about 7% and zirconium between 15 and 40%.

We also attempted to prepare a molybdenum borohydride, by the dry reaction of molybdenum pentachloride, or molybdenum hexafluoride, with LiBH_4 , but after the apparatus blew up twice we gave up. However, a molybdenum compound containing borohydride radical and chloride was obtained by a reaction in solution. In the course of our program on nonaqueous plating we made a considerable number of attempts to deposit molybdenum, but all these were negative and it is not likely that we shall publish the results of that investigation.

To complete the picture of the deposition of the less common metals from organic solutions, germanium was deposited from a solution of germanium tetrachloride in propylene glycol by Szekely (19). Because the cathode current efficiency was less than 1%, the process is not practicable. The claim of Müller and associates (20) to having deposited some of the alkaline earth metals from pyridine solution is open to question since they did not actually isolate the metals but only examined the current density potential relations during the electrolysis. Several investigators have made unsuccessful attempts to deposit the rare earths from basic solvents (21). Jonassen (22) has been unsuccessful in depositing tungsten or molybdenum from a wide variety of compounds and complexes dissolved in various organic and inorganic solvents.

Discussion of Nonaqueous Plating

Now I wish to evaluate the work that has been done in the field of nonaqueous deposition with respect to its practicability, its achievements, and its theoretical interest. Certainly there is no practical

interest in the deposition from nonaqueous media of those metals which can be deposited from water solution. The success which has attended the efforts to obtain the nonaqueous group of metals has not been very great. As already mentioned, aluminum is the only nonaqueous metal that can be deposited conveniently in a satisfactory physical condition and with a good cathode current efficiency. Some commercial interest has been manifested in the deposition of aluminum, but no actual uses have developed. At one time there was some interest in depositing aluminum on copper wire. The aluminum was to be anodized and thus form a high temperature insulation for the wire, but it is not known whether this process was actually tried. The deposition of other nonaqueous metals has not been sufficiently successful even to consider practical applications.

In general the metals which separate from nonaqueous media are less pure than those obtained from water solution. This may be caused partly by incomplete reduction and partly by adsorption of the organic material on the nascent surface of the metal. Adsorption also occurs to some extent in deposition of metals from aqueous solutions, but since the solvent molecules are much smaller the adsorption is much less. As examples of the contamination of metals deposited from nonaqueous solution, Pospekhov (6) showed that the alkali metals deposited from nitrobenzene solution in some instances contained only 25% of the metal. In our own work we were unsuccessful in obtaining satisfactory nickel or cobalt deposits from organic solvents. They were stressed and exfoliated. The nickel deposits were only 85% metallic. Some of the beryllium deposits obtained from the alkyl baths contained so many inclusions that if scratched they spontaneously ignited.

The last topic to be considered concerns the generalizations that are helpful in investigating nonaqueous deposition. Before taking these up, it is necessary to dispose of some ideas that have been suggested but which are not applicable. The magnitude of the dielectric constant of a solvent has been considered an index of its ability to form conducting solutions and, by inference, good plating baths. However, this criterion is not valid because ether is a good nonaqueous solvent for depositing several metals and yet its dielectric constant is only about 4.5. On the other hand, anhydrous HCN, which has a high dielectric constant, is not a particularly good electrolytic solvent. Incidentally, even if one could predict solutions that would be conductive, it would be of little help to nonaqueous plating, because the difficulty is not in finding conductive solutions but in finding conductive solutions that yield metals on electrolysis.

Water and a number of other polar solvents such as acetone, alcohol, and dimethylformamide, which readily form conducting solutions, have themselves in the pure state an appreciable electrical conductivity of about 10^{-7} ohm $^{-1}$ cm $^{-1}$. This conductivity might seem to be an index of a good electrolytic solvent. However, this generalization is vitiated by the fact that ether has a conductivity of about 4×10^{-13} ohm $^{-1}$ cm $^{-1}$. Toluene has a conductivity of 10^{-14}

ohm $^{-1}$ cm $^{-1}$, and yet aluminum can be deposited from certain toluene solutions.

The crystal structure of a compound is regarded as an index of its ability to ionize and form a conducting solution when dissolved. This idea is expressed tacitly when a salt is said to have an ionic structure. However, the solute is not the only factor, inasmuch as the solvent plays an equally important role. An "ionic" compound which forms a conducting solution in water does not necessarily form a conducting solution in nonaqueous solvents.

In considering those few generalizations which are helpful in nonaqueous plating, it is necessary to discuss the aqueous and nonaqueous groups of metals separately. The aqueous group can be deposited readily from polar solvents using common salts in many instances. This subject is not of interest in the present discussion and need not be considered further.

The nonaqueous group of metals may be divided into two subgroups: (A) active metals like the alkali and alkaline earth metals, which are too active to be deposited from aqueous solution, and (B) less active metals such as tungsten, germanium, etc., which are thermodynamically capable of depositing from aqueous solution (12, 23) but do not because of the non-reactivity of their ions. The alkali metals, as already mentioned, have been deposited from a few organic solvents. Presumably this is possible because in these solvents the hydrogen is more strongly bound than in water and the deposition potential of these metals can be attained.

However, little success has attended the deposition of the (B) subgroup of nonaqueous metals. The non-reactivity of their ions seems to be as much of a stumbling block in nonaqueous as in aqueous media. In fact, alloys of tungsten and molybdenum are more readily deposited from aqueous than from nonaqueous solutions. The fact that lithium and sodium can be deposited from the very solution containing one of the subgroup (B) metals further confirms the fact that the difficulty is not one of thermodynamics.

The metals magnesium, aluminum, titanium, zirconium, and beryllium, because of the difficulty of depositing them, seem to belong more to subgroup (B) than (A). The following generalizations apply to them. The best plating solutions appear to be made from solvents and solutes that can coordinate mutually. The solvents and solutes are probably similar to the classes of compounds that have been designated as Lewis bases and acids. The only useful solvents are those containing a weak coordinating center, for example, the oxygen atom of an ether or the double bond of an aromatic hydrocarbon. Other solvents with a more unsaturated coordinating center, for example, nitrogen or carbonyl groups, form too stable a complex. On the other hand, solvents which have virtually no coordinating ability, such as aliphatic hydrocarbons, do not even form conducting solutions.

The solutes found useful for depositing metals are very specific: certain halides, metal alkyls, hydrides, and borohydrides. The conventional solutes—ordinary salts—which are useful for aqueous solutions are of no value in nonaqueous plating. In no case

has the salt of an oxyacid been useful for depositing the metals considered here.

To summarize, the electrodeposition of the nonaqueous group of metals is intensely interesting from an academic and theoretical point of view, but it does not have a bright future for practical purposes. It is unlikely that baths for depositing the subgroup (B) metals can be developed by systematically and empirically trying all available compounds of the elements in all available solvents. The further developments will probably depend on the general development of the chemistry of complexes; that is, new types of complexes will have to be produced. It is likely that the type of complex that will solve the problem of depositing some of the nonaqueous metals has not yet been prepared.

Electrolysis of Organic Solvents

Background and Literature

Our attempts to electrodeposit some of the metals of the nonaqueous group, although lacking in practical success, have made us cognizant of the vast, unexplored field of nonaqueous electrochemistry. In our researches many nonaqueous conducting solutions were prepared and electrolyzed without obtaining a metal at the cathode, indeed, in many instances without any visible signs of reaction. Thus we became interested in the nature of the electrode reactions, not only as a matter of curiosity, but also because basic information might eventually lead to a better approach to the electrodeposition of metals.

After some deliberation and exploratory work we decided on a research dealing with the electrolysis of pure nonaqueous solvents, mainly organic solvents, as being the most basic study in electrolysis that could be undertaken. We were interested in the mechanism of the electrode reactions, the products formed, and the dynamic potentials involved. The electrolyses to be studied were analogous to the electrolytic decomposition of water. Electrolyses in which a compound was added to the solvent to impart conductivity were not excluded from the investigation, but it would be necessary to show, eventually, that the electrolytic decomposition of the solvent, as in the case of water, was independent of the nature of the conducting additive.

In the introduction to the previous section, the statement was made that the electrochemistry of nonaqueous systems has been largely neglected. To this can be added the observation that, in the study of the electrochemistry of the nonaqueous systems, dynamic electrode processes have been slighted in favor of the measurement of static potentials and conductivities. Measurements of potentials without an identification of the electrode reactions do not possess much meaning. The lack of interest in electrolyses of nonaqueous systems becomes evident from a perusal of several monographs. The books by Jander (24) and Audrieth (25) which deal with nonaqueous solvents contain little information on electrolyses. Brockman's book (26) deals almost exclusively with the electrolysis of organic compounds in aqueous solutions. The "Elektrochemie Nichtwässriger Lösungen" of Walden (27) is mainly concerned with the conductivity of solutions. Measure-

ments of conductivity have little direct relation to electrolysis. This is evident, since conductivities can be measured by methods that do not involve electrolysis, for example, by the use of induced currents.

Studies of the electrolysis of inorganic solvents other than water are few. In most instances the interest centered on the electrolysis of a dissolved substance rather than of the solvent. Cady and Taft (28, 29) attempted to study electrolytic oxidation and reduction in liquid sulfur dioxide and in phosphorus oxychloride but were not very successful. The electrolysis of sulfur dioxide and of solutions of salts in sulfur dioxide was studied by several investigators (30), but the results were inconclusive. Stefan and Nagel (31) noted that electrolysis of solutions of various organic compounds in ammonia yielded only nitrogen and hydrogen on electrolysis, and the organic compound was frequently recovered unchanged.

Although a number of investigations have involved the electrolysis of organic solutions, in most of these the interest also was centered on the electrolytic decomposition of a substance dissolved in the solvent, the latter playing a minor role. The attempts to deposit metals from organic solutions form the largest group of investigations and these already have been discussed adequately. The remainder of the literature deals with organic solutions that undergo complicated reactions on electrolysis. The electrolysis of ether solutions of Grignard reagents (5) has been studied thoroughly. The electrolysis of organic solvents containing dissolved hydrogen fluoride (32) has become of commercial importance. Another 15 or 20 references (33) cover most of the subject of electrolysis of organic solutions, but as already noted these dealt with the dissolved substances rather than with the solvent.

Work at the National Bureau of Standards

The study of the electrolysis of nonaqueous solvents at the NBS is at an early stage. Preliminary investigation showed that various difficulties attended the electrolysis of some organic solvents, for example, the formation of tarry materials. One class of compounds that seemed amenable to study was the amides. Thus far we have electrolytically decomposed several simple amides. Most of the work has been done with formamide and dimethylformamide in a simple cell having both electrodes in the same compartment. The main products of the electrolysis of formamide are hydrogen and cyanuric acid. This had previously been shown by Schaum and Schneider (33c). The products formed in the electrolysis of dimethylformamide have not yet been identified.

Since eventually the anode and cathode reactions must be studied separately, a divided cell must be used. Conventional equipment, such as U-tubes or H-tubes of the types used for transference experiments, is not suitable, because a considerable electrical migration of material occurs when an appreciable fraction of a faraday is passed during electrolysis to provide sufficient reaction products for examination. The use of a porous diaphragm between the cathode and anode compartment, which is a common practice, is not successful in dealing with

nonaqueous solvents because electro-osmosis is considerable. To prevent it the diaphragm must be very porous.

Several different types of divided cells have been constructed. The most promising type consists of three compartments, one each for the anode and cathode and a chamber between these two. By allowing fresh solvent continually to flow through the middle compartment to a discard, products from either the anolyte or catholyte that migrate into the center chamber are removed before they can migrate into the opposite electrode chamber. Some further modifications of the flowing junction type of cell are contemplated.

The performance of a given electrolytic cell in keeping the anolyte and catholyte from mixing was determined qualitatively by electrolyzing boron trifluoride etherate with copper electrodes. Copper which dissolved at the anode was precipitated as metal by reaction products that formed in the catholyte. Thus the presence of copper on the walls of the vessel was evidence that mixing or electrical transport of the contents of the compartments had occurred. The apparatus with the flowing junction had only a slight deposit of copper.

Future Program

The study of the variables involved in electrolysis will be directed toward answering the following questions:

1. Are the products of electrolysis of the pure solvent the same as those obtained in the presence of a conducting additive or obtained in the electrolysis of an aqueous solution of the solvent?

2. Do the solvents have a definite decomposition potential?

3. Can the solvents be arranged in a series, either on the basis of the decomposition potential or of the enthalpy change of the electrolysis, such that in a mixture the solvent lower in the series is preferentially decomposed electrolytically?

More specifically, by electrolyzing various substituted amides we hope to arrive at an understanding of the mechanism of the electrolysis.

In conclusion, a systematic study of the electrolysis of nonaqueous media will greatly advance the science of electrochemistry and contribute to the chemistry of nonaqueous solvents. The electrolysis of nonaqueous media is probably the most neglected field of inquiry in both electrochemistry and the chemistry of nonaqueous solutions. At the present time most of the knowledge of electrolysis has been obtained from aqueous solutions, and many of the phenomena observed for water may be specific for that solvent. The study of the electrolysis of a large number of other solvents will lead to generalizations that cannot be obtained from a study of a single solvent.

Manuscript received Sept. 8, 1958. This paper is the Richards Memorial Lecture presented at the New York Meeting, April 27-May 1, 1958.

Any discussion of this paper will appear in a Discussion Section to be published in the December 1959 JOURNAL.

REFERENCES

1. St. v. Lacszyński, *Z. Elektrochem.*, **2**, 55 (1895).
2. St. v. Lacszyński and St. v. Gorski, *ibid.*, **4**, 290 (1897).
3. L. Kahlenberg, *J. Phys. Chem.*, **3**, 602 (1899); *ibid.*, **4**, 349 (1900).
4. L. F. Audrieth and H. W. Nelson, *Chem. Rev.*, **8**, 335 (1931).
5. Jolibois, *Compt. rend.*, **155**, 353 (1912); *ibid.*, **156**, 712 (1913).
Rodebush and Peterson, *J. Am. Chem. Soc.*, **51**, 638 (1929).
Kondyrew and Manojew, *Ber.*, **58**, 469 (1925).
J. Kondyrew, *J. Russ. Phys. Chem. Soc.*, **60**, 545 (1928).
J. M. Nelson and W. V. Evans, *J. Am. Chem. Soc.*, **39**, 82 (1917).
L. W. Gaddum and H. E. French, *ibid.*, **49**, 1295 (1927).
H. E. French and M. Drane, *ibid.*, **52**, 4904 (1930).
W. V. Evans and F. H. Lee, *ibid.*, **55**, 1474 (1933).
W. V. Evans and F. H. Lee, *ibid.*, **56**, 654 (1934); *ibid.*, **57**, 489 (1935).
W. V. Evans and E. Field, *ibid.*, **58**, 720 (1936).
W. V. Evans and E. Field, *ibid.*, **58**, 2284 (1936).
W. V. Evans and D. Braithwaite, *ibid.*, **61**, 898 (1939).
W. V. Evans, D. Braithwaite, and E. Field, *ibid.*, **62**, 534 (1940).
W. V. Evans and Fang-Hsun Lee, *Nanking J.*, **6**, 29 (1936).
6. D. A. Pospekhov, *J. Appl. Chem. USSR*, **27**, 552 (1954).
7. D. E. Couch and A. Brenner, *This Journal*, **99**, 234 (1952).
J. H. Connor and A. Brenner, *ibid.*, **103**, 657 (1956).
8. G. B. Wood and A. Brenner, *ibid.*, **104**, 29 (1957).
9. W. E. Reid, Jr., J. M. Bish, and A. Brenner, *ibid.*, **104**, 21 (1957).
10. J. H. Connor, W. E. Reid, Jr., and G. B. Wood, *ibid.*, **104**, 38 (1957).
11. J. M. Sherfey, *Ind. Eng. Chem.*, **46**, 435 (1954).
12. A. Brenner, *This Journal*, **103**, 652 (1956).
13. R. D. Blue and F. C. Mathers, *Trans. Electrochem. Soc.*, **63**, 231 (1933); **65**, 339 (1934); **69**, 519 (1936).
14. F. H. Hurley and T. P. Wier, Jr., *This Journal*, **98**, 203 (1951); *ibid.*, 207.
15. W. Menzel, *Z. anorg. u. allgem. Chem.*, **269**, 52 (1952).
16. G. G. Evans, J. K. Kennedy, Jr., and F. P. Del Greco, *J. Inorg. & Nuclear Chem.*, **4**, 40 (1957).
17. K. Ziegler and H. Lehmkuhl, *Z. anorg. u. allgem. Chem.*, **283**, 414 (1956).
18. A. C. Doumas, Virginia Polytechnic Inst. (1955).
N. F. Murphy and A. C. Doumas, *Proc. Am. Electroplaters' Soc.*, 162 (1956).
19. G. Szekely, *This Journal*, **98**, 318 (1951).
20. R. Muller, F. Holz, W. Knaus, F. Planisberg, and K. Pretz, *Monatsh.*, **44**, 219 (1923).
21. P. A. Zimmerman, Doctoral dissertation, Univ. of Illinois (1951).
V. D. Aftandilian, *ibid.*, (1954).
G. W. Cullen, *ibid.*, (1956).
T. Moeller and P. A. Zimmerman, *Science*, **120**, 539 (1954).
G. W. Cullen, *Dissertation Abst.*, **17**, 234 (1957).
T. Moeller and T. M. Yappan, *J. Inorg. & Nuclear Chem.*, **4**, 216 (1957).
22. H. B. Jonassen, Tulane Univ. (Last report, March 12, 1957).
23. A. Brenner, *Rec. Chem. Progress*, **16**, 241 (1955).
24. G. Jander, "Die Chemie In Wasserähnlichen Lösungsmitteln," Springer-Verlag, Berlin (1949).
25. L. F. Audrieth and J. Kleinberg, "Non-aqueous Solvents as Media for Chemical Reactions," John Wiley & Sons, Inc., New York (1953).
26. C. J. Brockman, "Electro-organic Chemistry," John Wiley & Sons, Inc., New York (1926).

27. P. Walden, "Electrochemie Nichtwässriger Lösungen," Johann Ambrosius, Leipzig (1924).
28. H. P. Cady and R. Taft, *J. Phys. Chem.*, **29**, 1075 (1925).
29. H. P. Cady and R. Taft, *ibid.*, 1057 (1925).
30. B. D. Steele, *Chem. News*, **96**, 224 (1908).
L. S. Bagster and B. D. Steele, *Chem. News* **105**, 157 (1912); *Trans. Faraday Soc.*, **8**, 51 (1913).
- M. Centnerszwer and J. Drucker, *Z. Elektrochem.*, **29**, 210 (1923).
31. S. Goldschmidt and F. Nagel, *Ber.*, **64B**, 1744 (1931).
32. J. H. Simons and Co-workers, *J. (and Trans.) Electrochem. Soc.*, **95**, 47 (1949).
- 33a. K. Hopfgartner, Electrolysis of Salts of Aliphatic Acids in Solutions of their Respective Anhydrous Parent Acids, *Monatsh.*, **32**, 523 (1911).
- b. C. Schall, Electrolysis in Nonaqueous Solvents, *Z. Elektrochem.*, **19**, 830 (1914).
- c. K. Schaum and H. Schneider, Über die Darstellung von Cyanursäure und Allophansäure-Estern aus Formamide auf Elektrochemischem Wege, *Ber.*, **56**, 2460 (1923).
- d. F. Fichter and R. E. Meyer, Electrolysis of Acetates in Absolute Methanol, *Helv. Chem. Acta*, **16**, 1408 (1933).
- e. F. Fichter and R. E. Meyer, Electrolysis of Benzoic and 2,6 Dimethyl -4 -tert-butyl-benzoic Acids mixed with their Salts in Absolute Methanol, *Helv. Chim. Acta*, **17**, 535 (1934).
- f. G. Giacomello and A. Mayer, The Electrolysis of Some Organic Substances in Nonaqueous Media I, *Gazz. chim. ital.*, **65**, 546 (1935).
- g. G. Giacomello and M. Lentine, The Electrolysis of Some Organic Substances in Nonaqueous Medium II, *Gazz. chim. ital.*, **66**, 350 (1936).
- h. M. Centnerszwer and J. Szper, Electrolysis of Salts in Anhydrous Glycerol, *Bull. intern. acad. polon. sci., (Classe sci. math. nat.)*, **A**, 378 (1936).
- i. A. Hickling and J. V. Westwood, Electrolytic Oxidation, XI. The Electrolysis of Acid Ester Salts in Nonaqueous Solutions and the Mechanism of the Crum Brown-Walker Synthesis, *J. Chem. Soc.*, **1939**, 1109.
- j. J. J. Lingane, C. G. Swain, and M. Fields, Polarographically Controlled Synthesis, with Particular Reference to Organic Chemistry, *J. Am. Chem. Soc.*, **65**, 1348 (1943).
- k. E. D. Fultz and J. H. Wood, Electrolysis Studies in Organic Solvents. Rensselaer Polytechnic Inst. ASTIA 103081 Aug. 1956.
- l. H. C. Mandell, Jr. (Univ. of Pa., Philadelphia) Univ. Microfilms (Ann Arbor, Mich.) Publ. No. 7801, 196 pp.; *Dissertation Abstr.*, **14**, 769 (1954); Chemical and Electrochemical Studies of Nonaqueous Solutions of Boron Tribromide.
- m. S. Wawzonek, E. W. Blaha, R. Berkey, and M. E. Runner, Polarographic Studies in Acetonitrile and Dimethylformamide II. Behavior of Aromatic Olefins and Hydrocarbons, *This Journal*, **102**, 235 (1955).
- n. G. Jander and H. Knauer, Ionic Reactions in Absolute Diethyl Ether as a Solvent. III. The application of high-voltage electrolysis to the investigation of the dissociation of several metal halides in ether solution and their transposition with alkali alcoholates, *Z. anorg. Chem.*, **287**, 138 (1956).
- o. H. Breederveld and E. C. Kooyman, The electrolysis of some 3-arylpropionic acids; isomerization of free radicals, *Rec. trav. chim.*, **76**, 297 (1957).
- p. A. P. Stuart, Hydrazine Manufacture U. S. Pat. 2,813,067, Nov. 12, 1957.

Brief Communication



Composition and Properties of Saturated Solutions of ZnO in KOH

Thedford P. Dirkse

Calvin College, Grand Rapids, Michigan

In many alkaline batteries a soluble zinc anode is used. This produces, on discharge, a solution of ZnO or zincate in the electrolyte. To deal with such solutions theoretically, it is often necessary to know the values for certain physical properties of such solutions. For that reason saturated solutions of ZnO in KOH were prepared and studied at different temperatures.

All KOH solutions were made by addition of water to a saturated stock solution. C.P. ZnO was added to these KOH solutions. Because of the possibility of phase changes, the solutions were allowed to stand at least several months before analysis. Pyrex glass and polyethylene containers were used. Several different series of solutions were prepared at 25°C and run independently of each other. Some of the solutions were saturated at a higher temperature before being cooled and allowed to equilibrate at the desired temperature; some solutions were saturated at the temperature indicated; some were saturated by allowing water to evaporate at a consider-

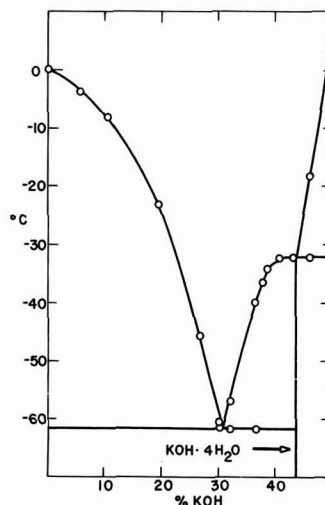


Fig. 1. Phase diagram of aqueous KOH solutions

ably reduced pressure; and some were prepared by dilution of more concentrated solutions.

Each solution was analyzed for potassium and zinc. All the potassium analyses were made spectrophotometrically (1, 2). Zinc was determined most often by titration with standardized potassium ferrocyanide solution, but also spectrophotometrically using dithizone (3). All solutions were filtered through glass filtering crucibles before analysis. Precautions were taken to avoid contact with CO₂. The melting points of aqueous KOH solutions were determined from cooling and warming curves. Duplicates and checks were run constantly and the results agreed to within 0.1°C.

Results are given in the accompanying Tables I and II and Fig. 1. The solid phases were ZnO and various hydrates of KOH. In operating batteries the zinc content, and hence density and viscosity, may rise temporarily considerably above the values given here (4).

Table I. Composition and properties of saturated solutions of ZnO in aqueous KOH at 25°C

% K	% Zn	Density, g/cm ³	Relative viscosity	Sp. cond. ohm ⁻¹ cm ⁻¹
3.66	0.28			
4.93	0.48			
8.18	0.55	1.1076	1.302	0.370
15.0	1.83	1.2258	1.865	0.521
21.3	3.61	1.3616	3.120	0.500
21.9	3.71	1.3637	3.123	0.492
28.9	6.34	1.5356	7.624	0.317
30.9	8.41			
35.3	10.20			
36.0	11.05			
36.1	10.53			
36.3	7.91			
36.4	6.02			
37.7	2.28			

Table II. Composition of saturated solutions of ZnO in aqueous KOH

44.6°C		3°C	
% K	% Zn	% K	% Zn
10.05	0.80	7.90	0.55
17.62	2.30	14.01	1.74
22.1	4.33	20.01	3.82
31.8	7.48	21.29	3.97
34.4	9.29	26.9	5.36
34.7	11.05	32.2	7.89
38.6	0.81	32.6	4.31
38.8	2.03		
38.3	3.49		
39.1	2.78		
40.1	2.29		
-20°C		-30°C	
17.4	2.38	17.1	2.43
18.8	2.96	19.4	3.04
15.4	2.38	17.4	2.46
17.3	2.28	21.9	3.85
21.4	3.80	24	4.89
24.3	5.28	29.9	0.52
28.0	0.95	30.8	0.32
28.6	0.25		

REFERENCES

1. E. Amdur, *Ind. Eng. Chem., Anal. Ed.*, **12**, 731 (1940).
2. R. Faber, T. P. Dirkse, *Anal. Chem.*, **25**, 808 (1953).
3. H. Cowling, E. J. Miller, *Ind. Eng. Chem., Anal. Ed.*, **13**, 145 (1941).
4. T. P. Dirkse, *This Journal*, **102**, 497 (1955).

Manuscript received Oct. 13, 1958. Work on this paper was performed under Contract N7 onr-496, T.O. 1 with the Office of Naval Research. Reproduction in whole or in part is permitted for any purpose of the United States Government.

Any discussion of this paper will appear in a Discussion Section to be published in the December 1959 JOURNAL.

FUTURE MEETINGS OF The Electrochemical Society



Philadelphia, Pa., May 3, 4, 5, 6, and 7, 1959

Headquarters at the Sheraton Hotel

Sessions will be scheduled on

Electric Insulation, Electronics (Including

Luminescence, Semiconductors, Thermionics, and Devices), Electrothermics and Metallurgy,

Industrial Electrolytics, and Theoretical Electrochemistry

★ ★ ★

Columbus, Ohio, October 18, 19, 20, 21, and 22, 1959

Headquarters at the Deshler-Hilton Hotel

Sessions probably will be scheduled on

Batteries, Corrosion (including a joint Corrosion—Electronics—Semiconductors session),

Electrodeposition (including symposia on "Electrodeposition from Organic Solvents"

and "Electro- and Chemical-Polishing"),

Electronics (Semiconductors), Electro-Organics,

and Electrothermics and Metallurgy

★ ★ ★

Chicago, Ill., May 1, 2, 3, 4, and 5, 1960

Headquarters at the Lasalle Hotel

★ ★ ★

Houston, Texas, October 9, 10, 11, 12, and 13, 1960

Headquarters at the Shamrock Hotel

★ ★ ★

Papers are now being solicited for the meeting to be held in Columbus, Ohio, October 18-22, 1959. Triplicate copies of each abstract (*not exceeding 75 words in length*) are due at Society Headquarters, 1860 Broadway, New York 23, N. Y., *not later than June 1, 1959* in order to be included in the program. *Please indicate on abstract for which Division's symposium the paper is to be scheduled, and underline the name of the author who will present the paper.* Complete manuscripts should be sent in triplicate to the Managing Editor of the JOURNAL at 1860 Broadway, New York 23, N. Y.



The Language of Electrochemistry

First William Blum Lecture¹

William Blum²

Popular writers and speakers often ridicule scientists for using a "jargon" that the average person cannot understand, an accusation that should not be too lightly dismissed by scientist. But even more serious from the standpoint of scientific progress is the use by scientists of terms with uncertain or confused meanings, and the disregard of accepted practices in the use of terms, symbols, and units. While it is usually sufficient for a general author to so express himself that the intended meaning can be understood, it is necessary for the scientist to write in such a way that the meaning cannot be misunderstood. There is no place in scientific publications for technical terms with dual or contradictory meanings.

In the following discussion of definitions, conventions, and units, it is not my purpose to urge the adoption of any specific usages, though some of these may be employed as illustrations. My aim is to point out the need for (a) the adoption of national or international standards of scientific expression, and (b) the acceptance and use of such standards in textbooks and scientific publications. With the present warranted emphasis on more and better education in science, we cannot afford to waste the time of teachers, students, authors, and readers in efforts to understand vague statements, or to reconcile conflicting usages.

In everyday language it is recognized that no two so-called "synonyms" have identical meanings, and that the exact shade of meaning may vary with the context or locality. Similarly, a given word may have two or more distinct meanings, depending again on the context. While these fluctuations in meaning may add to the beauty of our literature, they are out of place in articles or books written by scientists for scientists.

Ideally, in scientific writing, no term should be used, at least in a given field, with two distinct meanings, and no two terms should be employed with identical meanings. But, as will be shown by examples of electrochemical terms, such usages are all too frequent and confusing. There is no simple, short-time solution for this dilemma. What I propose is that an appropriate representative organization be set up, or, if already in existence, be supported, whose duty it is to approve and adopt definitions and conventions, after they have been submitted to all interested groups of scientists for comment and criticism. Such standards should then be adopted and employed in all publications of these societies, and be subject to formal revision at reasonable intervals such as every ten years.

At once the objection will be raised that such enforced conformance represents "dictatorship" or "regi-

mentation." But the very existence and progress of science depend upon the adoption and use of certain terms and abbreviations, for example the names and symbols of the elements. However, there are still disagreements on certain of these terms, for example the use of "Columbium" or "Niobium," or of "Tungsten" or "Wolfram." Dissenters to a standard usage should be permitted to employ other terms or meanings, provided that in each such case they call attention to their divergence from the accepted standards. A society that does not accept the recommended standards should request their reconsideration, and not merely ignore or reject the proposals.

In a broad sense, all definitions and usages may be considered as "conventions," mutually agreed upon to facilitate understanding and progress. By definition, conventions are arbitrary, and are not in themselves "right" or "wrong," except insofar as they have been agreed upon and adopted. The convention that most directly affects the safety and indeed the lives of all of us is the side of the road upon which to drive. Just because, in England and several other countries, cars are driven on the left side of the road does not make these drivers "wrong." But in this or any country, after a rule for driving is adopted, failure to observe it involves a physical hazard and a moral and legal wrong. I do not propose that violators of scientific conventions be prosecuted! I do urge that if, after full and adequate consideration, such standards are adopted, nationally or internationally, the societies concerned should "police" their usage by their control over their publications.

In a certain sense, the title of this talk might well have been "The Language of Science," since modern developments have largely eliminated the boundaries between, for example, physics and chemistry, and between physical chemistry and electrochemistry. Obviously, scientists in all fields should be able to understand each other. But then the questions become more complicated. For example, there are several distinct and only distantly related meanings of the term "polarization" in electricity and optics. Hence, I have confined my subject and illustrations principally to electrochemistry.

A glaring example of the use of a word with two distinct and sometimes contradictory meanings is furnished by the term "electrolyte." Most physical chemists define this term as the solute, for example, "a substance which when dissolved in a specified solvent produces a conducting medium." On the other hand, electrochemists and engineers generally use this term to designate the resultant solution, for example, the liquid present in a battery or in an electrolytic cell. Discussions of what

¹ Delivered at an award dinner held November 20, 1958 (see p. 11C, Jan. 1959 JOURNAL).

² National Bureau of Standards, Washington, D. C. (Retired).

Michael Faraday meant when he first used this term are futile and not necessarily pertinent.

In such a case, the obvious remedy would be to coin a new word to express one of the dual meanings. Not so obvious is the possibility of getting scientists to accept or adopt the new term. I may cite a personal experience. About 1925, I pondered over this dilemma and finally with my meager knowledge of Greek "coined" the word "ionogen," i.e., ion former, to refer to the solute, then and still called by many the electrolyte. I published a short note on this subject in *Science*. A few months later, one of my colleagues at the National Bureau of Standards remarked to me that he felt sure that he had seen this word ionogen used previously with the same meaning. A search revealed that about 20 years previously Dr. Alexander Smith had coined this word and used it in his "General Chemistry," a textbook very widely employed in our colleges during the first two decades of this century. And yet, so far as I know, few if any authors have employed the term ionogen in textbooks or articles, and the dilemma is as real today as it was 50 years ago!

Another example of the apparent lack of interest of scientists in precise definitions of scientific terms is supplied by the common failure to employ the "American Standard Definitions of Electrical Terms" sponsored by the American Institute of Electrical Engineers and approved in 1941 by the American Standard Association. A revised edition was published in 1957.

Of particular interest to us are the definitions in Group 60 on "Electrochemistry and Electrometallurgy," prepared by a committee with representatives of all fields. Dr. George W. Vinal was the committee chairman, and I can testify from close association with him that a vast amount of time and effort was spent in attempting to make these definitions represent the consensus of all persons concerned. It might be assumed that once the definitions were adopted and published they would be widely known and used. Actually, for reasons not fully understood, these definitions in electrochemistry are scarcely known to, used by, or referred to by authors in these fields. Numerous inquiries and observations showed that many persons or committees directly concerned with definitions made no reference to or direct use of these standards. For example, the "Corrosion Handbook," an exhaustive text edited for The Electrochemical Society by Dr. H. H. Uhlig and published in 1948, includes a "Glossary of Terms used in Corrosion," prepared by the Editorial Advisory Board and Subcommittee V of the American Coordinating Committee on Corrosion. No reference is made in this Glossary to the American Standards definitions, even though many of the same terms appear. It is not suggested that the authors of the Glossary should have adopted "blindly" the American Standards definitions, but they might well have referred to the latter and have adopted literally those with which they agreed. The meaning is more important than the exact wording, but repetition of the latter may help toward retention and use. It is not advisable to have several sets of definitions in a given field, even though they may be similar.

About ten years ago, a subcommittee of the ASTM Committee B-8 on Electrodeposited Coatings started to prepare a list of definitions without reference to, or perhaps knowledge of, the ASA definitions. I am glad to report that the present subcommittee has adopted many of the latter definitions.

One obstacle to the greater use of the ASA definitions has been their limited distribution. If, e.g., the Section on Electrochemistry had been originally printed as a

separate edition and sufficient copies sent at nominal cost to all organizations directly interested, these could have been mailed out free to all members of these societies, and frequent references made to them in society publications. This procedure might have required distribution, including the American Chemical Society, of about 100,000 copies. The added cost would have been a very small fraction of the cost of the thousands of hours spent in drafting the Standards. The societies represented in the American Standard Association should have been asked to adopt these definitions and to require their use in their publications, unless specifically excepted.

With the apparent difficulty of obtaining actual use in the U.S.A. of ASA Standard Definitions, it may appear hopeless to seek international agreement. Yet that goal is highly desirable, especially with the increased emphasis on international cooperation in science, e.g., in the Geophysical Year. One serious obstacle is the language difference, which makes it difficult to agree on equivalent words in different languages that will carry the same shade of meaning. Nevertheless, international agreement on the meaning of scientific terms and the use of conventions is essential to cooperation of scientists for the welfare of the world. The efforts in recent years of certain scientists, including Pierre Van Rysselbergh, Marcel Pourbaix, and Erich Lange to develop a set of international definitions and conventions in electrochemistry deserve the support and cooperation of scientific groups in all countries. The purpose of the following discussion is to point out some reasons for the apparent lack of interest in and acceptance of these proposals, and some ways in which this situation may be remedied.

In an article by Erich Lange and Pierre Van Rysselbergh in the July 1958 *JOURNAL of The Electrochemical Society*, some of the proposed definitions and conventions are explained and illustrated. These proposals are largely based on reports of the "International Committee of Electrochemical Thermodynamics and Kinetics," (CITCE), which is now affiliated with the "International Union of Pure and Applied Chemistry" (IUPAC).

The items of greatest interest to electrochemists are (a) the definitions of such terms as polarization and overvoltage (or their proposed substitutes), and (b) the signs to be assigned to electrode potentials. Among the suggestions, not yet officially recommended, is the use of the term "tension" for potential or voltage, e.g., "overtension," "electric tension," "chemical tension," etc. There is still some confusion between polarization and overvoltage, and indeed as to whether the latter term should ever be used, since it is not subject to precise measurement.

The confusion regarding the sign of potentials arises in part from the different uses to be made of these data. Physical chemists are usually concerned with reaction potentials, while electrochemists often wish to measure the static potential of an electrode with respect to a reference electrode, and its change in potential when it is made anodic or cathodic, i.e., the polarization. The sign to be attached to a reaction potential, as in the "electrochemical series," depends upon the direction in which the reaction is written. The potential of a metal electrode with respect to a reference electrode is a directly measurable quantity, the sign of which depends solely upon the definitions of positive and negative charges. The present dilemma stems in part from the unconscious effort to describe two different concepts by the same term. One remedy might be some new term to cover one of these meanings.

The principal reason that the international recommendations have not been accepted or used by American organizations such as The Electrochemical Society is that their existence, much less their content, has been known to so few chemists in this country. The reports of CITCE have rarely been referred to in American journals, and the reports of the IUPAC are not widely distributed in the U.S.A.

Part of this lack of knowledge or interest of Americans in these recommendations comes from the absence of formal representation of, e.g., The Electrochemical Society in the IUPAC, the delegates to which represent primarily their countries, and not the specific scientific organizations of which they may be members. It is now possible for a society to appoint a nonvoting "associate" to any commission in which it is interested. Without changing the organization of the IUPAC, it should be possible to develop a simple workable system, whereby the delegates from each country would be expected (or instructed) to submit, as far as possible in advance, the agenda for forthcoming meetings of the IUPAC Commissions to each of the societies in their country likely to be interested. Each society in turn should have one or more standing committees whose duty it is to ascertain the consensus of its members on important decisions, and to transmit these views to their national representatives. Such action should not constitute "instruction" to a delegate, but it would insure that the commissions would take these views into account in their deliberations. All such decisions involve some compromises. These are more likely to be accepted, adopted, and used by the pertinent societies if they feel that their views were considered in advance, than if they learn, perhaps accidentally, that certain conventions have been internationally adopted. Any delays resulting from such advance discussions will be more than compensated for by the earlier acceptance of the international recommendations. Unless and until the conclusions are adopted and used by societies, authors, teachers, and students, the time and effort spent by such bodies as the IUPAC largely are wasted.

Such efforts should lead ultimately to a self-contained list of definitions and conventions, expressed in clear simple terms (whatever the language) that can be fully understood by all concerned. The reasons and arguments for a particular choice must enter into the decisions, but they are not essential to the adoption and use of the standards. When a person is arrested

for driving on the wrong side of the road, it is immaterial whether he knows the reasons for the adoption of that rule!

One problem that warrants more attention from American scientists is the use of the metric system in researches and publications. Practically every scientist will, on occasion, discuss glibly the advantages of the metric system. Then, all too often, he cuts his specimens to be 4 by 6 in., hangs them in a solution containing 16 oz/gal of copper sulfate, plates copper on them at 10 amp/ft², and finally determines the weight of the deposit in milligrams per square inch, or the thickness in thousandths of an inch. The metric system is one convention which scientists of all nations understand and use. If our publications are to be read and understood in other lands, we should express all values in the metric system. When appropriate, equivalent English units may also be included. There is no place for "hybrid units." I once remarked that "the obstinacy with which some scientists cling to hybrid units reminds one of the best known but least admired of the hybrids."

We can all agree with the conclusion of Lange and Van Rysselbergh that, "In view of the rapid development of electrochemistry in recent times, only a rational system of concepts, definitions, symbols, etc., can provide a firm basis for further research and teaching"; even though as individuals we may not agree with all of their recommendations, or indeed fully understand them. The problems confronting us involve practical means for (a) agreement on acceptable conventions, and (b) adoption and use of these by all pertinent societies in their publications. I can cite numerous instances in which a society or institution adopted a certain convention, such as the sign of standard potentials, but soon completely ignored this practice in their publications.

In 1935 when Mrs. Blum and I first visited Europe, an intimate American friend gave us an envelope containing four flags, of the United States, England, France, and Germany, together with a card reading "Be internationally minded," advice which we have since tried to follow. In these troubled days, we as scientists may not be able to read or speak fluently French, German, or Russian, but at least we can work toward the more general use of one international language of scientific definitions and conventions. Failure to do so may well lead to a "scientific tower of Babel."

Manuscripts and Abstracts for Fall 1959 Meeting

Papers are now being solicited for the Fall Meeting of the Society, to be held at the Deshler-Hilton Hotel in Columbus, Ohio, October 18, 19, 20, 21, and 22, 1959. Technical sessions probably will be scheduled on Batteries, Corrosion (including a joint Corrosion—Electronics-Semiconductors session), Electrodeposition (including symposia on "Electrodeposition from Organic Solvents" and "Electro- and Chemical-Polishing"), Electronics (Semiconductors), Electro-Organics, and Electrothermics and Metallurgy.

To be considered for this meeting, triplicate copies of abstracts (*not exceeding 75 words in length*) must be received at Society Headquarters, 1860 Broadway, New York 23, N. Y., *not later than June 1, 1959. Please indicate on abstract for which Division's symposium the paper is to be scheduled, and underline the name of the author who will present the paper.* Complete manuscripts should be sent in triplicate to the Managing Editor of the JOURNAL at the same address.

* * *

The Spring 1960 Meeting will be held in Chicago, Ill., May 1, 2, 3, 4, and 5, 1960, at the Lasalle Hotel. Sessions will be announced in a later issue.



R. A. Schaefer Appointed Director of New Research Department at Bunting Brass

The Bunting Brass and Bronze Co., Toledo, Ohio, recently announced the creation of a research and development department and named Dr. Ralph A. Schaefer to be its director. Dr. Schaefer formerly was technical advisor to the president of the Cleveland Graphite Bronze Division of the Clevite Corp.

William M. Hankins, Jr., Bunting president, said that the creation of an adequate research and development department under the direction of a national authority in the field had been on the agenda since early in 1958.

Dr. Schaefer is well known for his research and development in the sleeve bearing field. He holds numerous patents, is the author of many published works, and has explored developments in many phases of the bimetal and trimetal field, as well as in powdered metals.

During the Second World War Dr. Schaefer was active in the field of powdered metallurgy on clutch plates and friction elements for the aircraft industry. He also played a



R. A. Schaefer

major role in developing the electroplating processes for sleeve bearings, first in heavy silver deposits, and later in thin precision Babbitt type overlays in the bearing field.

His entire professional career has been with the Cleveland Graphite

Bronze Co. and its allied enterprises. On graduation from Western Reserve University, where he received his A.B., M.S., and Ph.D. degrees, he joined this company as a research chemist and was director of research from 1946 to 1952. In 1952 the Clevite Corp. was formed by a merger of Graphite Bronze and other enterprises. After the consolidation the corporation created a centralized research and development division with Dr. Schaefer as vice-president. He was promoted to technical advisor to the president of the corporation in 1955.

Dr. Schaefer is a Vice-President of The Electrochemical Society, past president of the American Electroplaters' Society, a member of the Society of Testing Materials, Society of Metals, Sigma Xi, American Institute of Mining and Metallurgical Engineers, American Ordnance Association, and many other professional organizations. He has headed the Cleveland Sections in both The Electrochemical Society and the Electroplaters' Society.

Edward Goodrich Acheson Hall of Chemistry

Rapidly growing University of Buffalo has named its new chemistry building, now under construction, the "Edward Goodrich Acheson Hall of Chemistry" as a memorial to one of America's most distinguished inventor-scientists whose major industrial activities for many years centered at Niagara Falls.

Acheson's discoveries and researches in electrochemistry and electrometallurgy ranged over a wide field. His invention in 1891 of the diamond-like abrasive for which he coined the trade name "Carborundum" made modern mass industrial production possible. Without "Carborundum" silicon carbide and the other man-made abrasives that followed it, the manufacture of precision ground, interchangeable parts essential to economical large-scale

production would have been impossible; and The Carborundum Co., which Acheson formed in 1891 to manufacture and market silicon carbide, has grown to be one of the giant industries of the country.

Another Acheson invention that has played a major part in modern industry is chemically pure, man-made graphite. To exploit that invention Acheson organized the International Acheson Graphite Co. at Niagara Falls in 1899, and its graphite products, particularly its world-famous "Acheson electrodes," found a broad market in the rapidly developing electrochemical, and now also in the electronics, industries.

Acheson received many honors in recognition of his great contributions to science, and particularly to electrochemistry. These included the

John Scott Medals in 1894 for his discovery of "Carborundum" silicon carbide, and in 1901 for the discovery of artificial graphite; the Gold Medal Award of the Trans-Mississippi and International Exposition in 1898; the Grand Prix at the Paris Exposition in 1900; the Gold Medal at the Pan-American Exposition in Buffalo in 1901; the Grand Prize at the Louisiana Purchase Exposition at St. Louis in 1904; the Count Rumford Medal of the American Academy of Arts and Science in 1908; the honorary degree of Doctor of Science from the University of Pittsburgh in 1909; the Perkin Medal of the Society of Chemical Industry in 1910; appointment as an officer of the Royal Order of the Polar Star by the King of Sweden in 1914; and the Acheson Medal, named for him, of

The Electrochemical Society in 1929.

Dr. Acheson was a Charter Member and a Past President (1908) of The Electrochemical Society.

When on July 6, 1931 Acheson died, Thomas Edison said of him, "As a former associate I know the world loses a great genius," and the

press generally acclaimed him "one of the inventive geniuses of his time."

The Acheson Hall of Chemistry will be a permanent memorial to Dr. Acheson on the Niagara Frontier where he achieved his most important successes as an inventor and industrialist.

Pittsburgh's Bicentennial

Thanksgiving Day, 1958, was the start of the bicentennial celebration of the City of Pittsburgh, marking 200 years since a British army under the command of General Forbes drove the French and their Indian allies permanently from this strategic site located at the junction of three navigable streams, the Allegheny, the Monongahela, and the Ohio Rivers.

The basic reasons for the formation of an industrial complex around Pittsburgh are adequate water resources, good transportation facilities, and great fuel resources. The rivers are a never-failing source of water. The Allegheny River, for example, is 310 miles long and drains an area of 11,400 square miles. With regard to transportation, Pittsburgh is served by six Class I railroads and has an extensive water transport system. Both the Allegheny and the Monongahela Rivers are navigable upstream from Pittsburgh. The Ohio River is navigable over its entire length (967 miles) and connects with the Mississippi river system. In the early 1800's, sailing vessels were constructed at Pittsburgh and cleared from the Port of Pittsburgh for Europe. The construction of ocean vessels was resumed during the Second World War, when many landing craft were built in Pittsburgh and by transit via the Ohio and Mississippi Rivers reached the ocean. Pittsburgh is the largest inland river port in the United States. The combined water and rail freight tonnage is greater than that of any other industrial area in the world. The major portion of the water tonnage is fuel (coal and coke) which accounts for about 75% of the total tonnage. Other large tonnage items are sand, gravel, iron and steel, and petroleum products.

Pittsburgh is located, roughly, in the center of the Appalachian Field, from which are obtained petroleum, natural gas, and coal. The commercial production of petroleum started at Titusville, north of Pittsburgh, in 1859. Natural gas was first used as a fuel in the steel industry in 1874. Although petroleum and natural gas

are still being produced, the Pittsburgh Metropolitan area is an importer of such fuels. Coal was discovered early in Pittsburgh; a visitor to Pittsburgh in 1760 described a coal mine located opposite to Fort Pitt on the south bank of the Monongahela River. The famous Pittsburgh Seam covers an area of over 200 square miles and is, without doubt, the most valuable mineral deposit ever discovered. The mines of Western Pennsylvania produced 45,000,000 tons of bituminous coal in 1955. The coal mines of Pennsylvania have produced about 3,000,000,000 tons of bituminous coal to date. After 200 years of mining, the Pittsburgh District still has ample resources.

The Pittsburgh Metropolitan area is primarily an area of steel, iron, and coal production. In this area is about 20% of the steel-making capacity of the United States, and in this area about 25% of the nation's iron ore is smelted. In 1955, the Pittsburgh-Youngstown District produced about 41,000,000 tons of steel.

According to the U. S. Census figures for 1954, the largest users of electricity in terms of kilowatt hours per worker per year were: chemicals with 83,000; primary metal, 62,700; and paper, 44,400. Among the primary metal industries, the top user is aluminum reduction with 1,274,000 kwhr per worker per year, followed by electrometallurgical products with 521,800, primary zinc with 161,000, and iron and steel production with 48,300. The production of electricity in the Metropolitan area is about 2,000,000,000 kwhr. Although Pittsburgh is the home of the Aluminum Co. of America, no electrolytic reduction of alumina is carried out in the district. Recently, a new aluminum reduction plant located on the Ohio River, but outside the Metropolitan district, was placed in operation and similar plants are being planned.

Although electrometallurgical operations are common in the Pittsburgh district, the largest industrial application of electrochemistry is to be found in the production of plated

steel sheet. The Aluminum Co. of America in its fabrication plants uses a number of electrochemical treatments to provide decorative and protective finishes to aluminum products. Pittsburgh is the home city of many large corporations such as United States Steel, Westinghouse, Jones & Laughlin, Westinghouse Air Brake, Crucible, Koppers, Gulf, Alcoa, H. J. Heinz, Pittsburgh Plate Glass, Allegheny Ludlum, Mine Safety Appliances, and Consolidation Coal Co. The central research laboratories of most of these companies are located in the Metropolitan area and many different types of electrochemical research are carried out in these laboratories.

Section News

Indianapolis Section

The Indianapolis Section of the Society held its first meeting of the season on December 5, 1958, at the Atherton Center (Student Union Bldg.) of Butler University in Indianapolis. The speaker was Dr. Daniel S. Eppelsheimer from the Missouri School of Mines and Metallurgy, Rolla, Mo., whose subject was "Metallurgy and Engineering in Russia Today."

Dr. Eppelsheimer visited Russia in July 1958, along with visits to metallurgical laboratories in France, Sweden, Luxembourg, Belgium, and England. This trip was made at the request of the president of his university, as a representative of the Resources and Development Commission of the State of Missouri. Dr. Eppelsheimer's presentation was extremely interesting and informative. It was illustrated with color slides taken during his visit to Russia, and was accompanied by many interesting anecdotes relating to his experiences there.

At the conclusion of the talk, a number of questions were asked by the audience concerning further amplification of certain points relative to technical, social, and economic conditions as observed during the visit.

T. C. O'Nan, Sec.-Treas.

Pittsburgh Section

The Section's annual fall meeting was held at the Westinghouse Research Labs. on November 14, 1958. Approximately 70 members and guests attended the day-long symposium on "Surface Phenomena," which consisted of six very interesting papers. Professor H. S. Frank of the University of Pittsburgh was chairman of the morning session on

oxidation and adsorption. Papers on oxidation were given by Dr. P. Kofstad, University of Pittsburgh; Dr. P. E. Blackburn, Westinghouse Research Labs.; and Professor W. W. Smeltzer, Carnegie Institute of Technology. Dr. D. S. MacIver, Gulf Research, presented a paper on adsorption.

Professor R. Smoluchowski of Carnegie Institute of Technology was chairman of the session on surface structure. A paper on the measurement of surface areas was presented by Dr. J. E. Lewis, Aluminum Co. Research Labs. The keynote address was given by Professor E. W. Müller of Penn State. Professor Müller presented a fascinating and informative paper on his recent investigations with the field emission microscope and with the ion emission microscope. Emission patterns were used to show grain boundaries, structural faults, adsorption, and structural changes brought about by the high fields.

A short business meeting was held after the luncheon. The members voted favorably on the following prizes being presented by the Pittsburgh Section of The Electrochemical Society:

(A) For the best exhibit, on any subject covered by The Electrochemical Society, at the Buhl Planetarium Science Fair (for high school students). Prize, \$25.

(B) For the best thesis, on any subject covered by The Electrochemical Society, written at a Pittsburgh University (for graduate students). Prize, \$50.

A report was given on plans for the spring meeting. To help celebrate the Pittsburgh Bicentennial, the subject of this meeting will be Pittsburgh's contribution to electrochemistry. The spring meeting will be preceded by a round-table discussion on this subject to be carried by WQED, the local educational TV station.

J. W. Faust, Jr., Sec.-Treas.

Battery Division Extended Abstracts

Battery Division Extended Abstracts from the Ottawa 2, 1958, may be ordered from the Secretary-Treasurer, Chas. Meeting, September 28-October H. Clark, 34 Pleasant Place, Deal, N. J.

Their price is \$2.00 per copy, postpaid, and payment must accompany all orders (by action of the Battery Division Executive Committee).

ECS Membership Statistics

The following three tables give breakdown of membership as of Jan. 1, 1959. The Secretary's Office feels that a regular accounting of membership will be very stimulating to membership committee activities. In Table I it should be noted that the totals appearing in the right-

hand column are *not* the sums of the figures in that line since members belong to more than one Division and, also, because Sustaining Members are not assigned to Divisions. But the totals listed are the total membership in each Section. In Table I, Sustaining Members have been credited to the various Sections.

Table I. ECS Membership by Sections and Divisions

Section	Division										Total as of 1/1/59	Total as of 1/1/58	Net Change
	Battery	Corrosion	Electric Insulation	Electrodeposition	Electronics	Electro-Organic	Electrothermics & Met.	Industrial Electrolytic	Theoretical Electrochem.	No Division			
Boston	17	26	7	38	65	7	25	13	26	6	151	131	+20
Chicago	17	35	4	46	28	10	14	12	23	13	132	111	+21
Cleveland	57	34	2	50	38	10	29	30	36	14	198	203	-5
Columbus, Ohio	4	11	0	14	5	2	24	3	8	4	49	45	+4
Detroit	9	20	5	50	11	7	8	6	21	19	91	84	+7
India	7	6	3	18	8	6	9	13	14	3	53	36	+17
Indianapolis	11	7	3	10	10	4	5	2	6	2	39	40	-1
Midland	9	15	0	5	2	2	7	15	11	2	43	45	-2
Mohawk-Hudson	4	13	14	7	13	3	8	2	11	4	54	51	+3
New York	87	107	25	142	141	33	75	67	102	43	517	482	+35
Niagara Falls	13	26	1	23	9	5	83	67	31	20	183	175	+8
Ontario-Quebec	11	25	1	17	7	3	36	26	9	13	82	75	+7
Pacific	5	10	0	8	3	1	10	10	10	10	44	47	-3
Northwest	28	32	4	36	66	11	23	19	50	30	185	174	+11
Philadelphia	4	47	3	26	28	5	41	18	35	9	133	130	+3
Pittsburgh	6	14	2	20	19	4	16	22	18	4	71	64	+7
San Francisco	16	22	2	27	30	4	16	16	24	10	105	95	+10
S. Calif.-Nevada	34	36	7	39	24	3	12	9	31	6	129	128	+1
Washington	60	91	14	85	80	42	68	76	115	30	408	395	+13
Baltimore	42	61	6	62	34	30	40	60	75	87	262	224	+38
U. S. Non-Section													
Foreign Non-Section													

Total as of Jan. 1, 1959	441	638	103	723	621	190	549	486	656	329	2911		
Total as of Jan. 1, 1958	409	638	100	705	518	193	479	485	620	313		2735	
Net Change	+32	—	+3	+18	+103	-3	+70	+1	+36	+16			

Table II. ECS Membership by Grade

	Total as of 1/1/59	Total as of 1/1/58	Net Change
Active	2538	2448	+90
Faraday (Active)	30	0	+30
Deutsche Bunsen Gesellschaft (Active)	15	0	+15
Delinquent	70	61	+9
Active Representative Patron Members	10	8	+2
Active Representative Sustaining Members	99	70	+29
Total Active Members	2762	2587	+175
Life	17	16	+1
Emeritus	49	54	-5
Associate	31	31	0
Student	46	42	+4
Honorary	6	5	+1
Total	2911	2735	+176

The figures pertaining to Patron and Sustaining Member Representatives, and Faraday and Deutsche Bunsen Gesellschaft members subscribing to the JOURNAL, have been added to reflect reclassifications and changes in membership status.

Table III. ECS Patron and Sustaining Membership

	Total as of 1/1/59	Total as of 1/1/58	Net Change
Patron Member Companies	5	4	+1
Sustaining Member Companies	148	127	+21

Personals

Marvin R. Paullus has been elected president and chief executive officer of Leonard Construction Co., Chicago, Ill. One of the company's functions is the design and construction of electrochemical process plants. Dr. Paullus previously was associated with Monsanto Chemical Co., St. Louis, Mo., in various engineering and sales capacities.

David R. Stern has been promoted to manager of research at the Los Angeles plant of American Potash & Chemical Corp. He had been assistant manager of the corporation's research laboratory at Whittier, Calif.

William von Fischer has been elected vice-president, research, of The Glidden Co., Cleveland, Ohio. Dr. von Fischer, formerly coordinator of research and development, joined the firm in that capacity in 1956.

Milton J. Allen, director of the physical research laboratories of CIBA Pharmaceutical Products Inc., Summit, N. J., left on December 18, 1958 for Karaikudi, India, to present the opening address at the "Sym-

Notice to Members

According to the Constitution of the Society, Article III, Section 9, "Any member delinquent in dues after April 1 of each year shall no longer receive the Society's publications . . ." Such delinquents will not receive the May issue of the JOURNAL. A reminder notice will be mailed to delinquents about the middle of February and a final notice about the middle of March.

posia on Electrolytic Cells," held in that city from December 30 to January 7 at the Central Electrochemical Research Institute. The first stop for Dr. Allen was England, where he delivered a lecture on electrochemistry at Imperial College, London. Following this speaking engagement, he flew to Karaikudi for the "Symposia" and five additional lectures; then on to Tokyo, Japan, to address the Japanese Electrochemical Society and to give a series of lectures at Tokyo and Kyoto Universities. Dr. Allen returned to Summit the end of January.

Dept., Monsanto Chemical Co., Lindbergh & Olive St. Rd., St. Louis 24, Mo.

Pittsburgh Technical Conference on Stress-Corrosion Fracture, April 1959

A Technical Conference on "Physical Metallurgy of Stress-Corrosion Fracture" will be held at the Mellon Institute, Pittsburgh, Pa., April 2 and 3, 1959.

Sponsor of the Conference will be the Corrosion-Resistant Metals Committee of the Institute of Metals Division, The Metallurgical Society, American Institute of Mining, Metallurgical, and Petroleum Engineers, in cooperation with The Electrochemical Society, the National Association of Corrosion Engineers, and the American Society for Testing Materials. The Pittsburgh Section of AIME will be host.

The program has been designed to provide a broad base for presentation and discussion of recent fundamental advances in stress-corrosion cracking. Meetings will be of the discussion type. Speakers will give summaries of their papers, emphasizing what they regard as new and significant. Papers will be preprinted

and circulated prior to the Conference. Thus, much of the Conference will be given over to discussion and exchange of scientific information.

The program, as developed by December 1958, is as follows.

April 2—morning

Introduction and Theoretical Aspects of Stress, Corrosion, and Fracture with G. M. Pound presiding

Introductory remarks by Thor N. Rhodin

"New Perspectives in the Stress Corrosion Problem" by H. H. Uhlig

"Characteristics of Stress-Corrosion Cracking" by A. W. Dana

"Relationships of Microstructure to Fracture" by J. J. Gilman

"Relationships between Stress and Chemical Potentials" by Ling Yang, C. T. Horne, and G. M. Pound

"Effects of Solid Structure on Surface Behavior" by David Turnbull and G. Ehrlich

April 2—afternoon

Experimental Aspects of Stress, Corrosion, and Fracture with H. H. Uhlig presiding

"Crack Propagation in Ductile Crystals and Its Bearing on Stress Corrosion" by A. J. Forty

"Role of Corrosion Products" by N. A. Nielson

"Effect of Stress and Environment on the Microtopology of the Corrosion Product" by E. A. Gulbransen and Thomas Capon

April 3—morning

Physical Metallurgical Aspects of Stress Corrosion with E. J. Kreh presiding

"Effect of Composition on Stress-Corrosion Cracking of Some Alloys Containing Nickel" by H. R. Copson

"Propagation of Stress-Corrosion Cracks" by C. Edeleanu

"Dependence of Stress-Corrosion Cracking Susceptibility on Age-Hardening in a Copper-Nickel-Silicon Alloy" by W. D. Robertson, I. G. Grenier, W. Davenport, and V. Molle

Summary and comments on the Conference by L. R. Sharfstein

Professor William R. Bitler, Dept. of Metallurgy, Carnegie Institute of Technology, Pittsburgh, is chairman of the Arrangements Committee. Facilities will limit participants to 400.

Appalachian Underground Corrosion Short Course for 1959 Planned

Forty members of The Appalachian Underground Corrosion Short Course General Committee met in Pittsburgh, Pa. on December 4, 1958.

News Items

New Sustaining Member

Erie Resistor Corp., Erie, Pa., recently became a Sustaining Member of The Electrochemical Society.

1958 Annual Index

The Annual Index for Vol. 105 (1958) of the JOURNAL appears in this issue (pp. i-viii). Reprints of the Index can be obtained about the middle of March by writing to The Electrochemical Society, 1860 Broadway, New York 23, N. Y.

Nominations for ECS Honorary Membership

Harold M. Scholberg, Chairman of the Honors and Awards Committee of The Electrochemical Society, would like to receive suggestions for candidates for two Honorary Memberships in the Society, to be awarded in May 1959.

Nominations should carry a résumé of the candidate's career and of his contributions to the Society and the Science.

Nominations should be submitted as soon as possible to H. M. Scholberg, Inorganic Division, Research

Third Printing of "Vacuum Metallurgy"

Now Available

The third printing of "Vacuum Metallurgy," edited by J. M. Blocher, Jr., of Battelle Memorial Institute, is now available from Society Headquarters, 1860 Broadway, New York 23, N. Y., at the price of \$5.00, less a 20% discount to ECS members.

The 216-page book, in hard paper binding, contains papers presented at the Vacuum Metallurgy Symposium held in Boston, Mass., October 6 and 7, 1954.

Sponsored by the Electrothermics and Metallurgy Division of The Electrochemical Society, this symposium

brought together, for the first time, those interested in the relation of vacuum to metallurgy.

In the keynote address, J. D. Nisbet, director of research of the Universal-Cyclops Steel Corp., outlines the rapid progress in this field, together with a consideration of what the future may hold. Eighteen papers follow on vacuum melting, vacuum heat treating, vacuum distillation of metals, and on new apparatus. A valuable review of the present status of theory and techniques for the determination of the vapor pressures of metals and alloys is included.

The dates June 2, 3, and 4, 1959 were selected for the School which is held annually at the University of West Virginia, School of Mines, Morgantown, W. Va.

This will be the fourth annual corrosion short course to be held. Registration for the 1958 course was 500, representing personnel from 27 States and Canada.

The course covers both technical and nontechnical presentations of the practical and theoretical aspects of corrosion and has received the acceptance of The American Gas Association and endorsement of the National Association of Corrosion Engineers.

As of December 1958, 38 firms had been authorized to exhibit at the meeting. George G. Campbell, University of West Virginia, is Exhibits Chairman.

R. C. Elderfield Appointed Chairman-Designate of NRC Division of Chemistry

Dr. Detlev W. Bronk, president of the National Academy of Sciences-National Research Council, has appointed Professor Robert C. Elderfield as chairman-designate of the Academy-Research Council's Division of Chemistry and Chemical Technology. Professor Elderfield will assume his duties as chairman on July 1, 1960. The present chairman is Dr. Ernest H. Volwiler.

The Academy-Research Council, a nongovernmental organization of distinguished scientists, is dedicated to the furtherance of science and its uses for the general welfare. It is also called upon by its Congressional charter to advise, upon request, the Federal Government in all matters of scientific and technical interest.

Each of the eight divisions of the

Academy-Research Council, embracing all the natural sciences, works to stimulate scientific research in its area and includes representatives of major scientific and technical societies, individual members-at-large, and liaison representatives of pertinent Government agencies. Participating in the activities of the Division of Chemistry and Chemical Technology are the American Chemical Society, American Ceramic Society, American Institute of Chemical Engineers, American Oil Chemists' Society, American Society of Biological Chemists, The Electrochemical Society, and the Geochemical Society. The Division participates in the activities of the International Union of Pure and Applied Chemistry (IUPAC) and the International Union of Biochemistry (IUB) through the U. S. National Committee for each Union.

Dr. Elderfield has been professor of chemistry at the University of Michigan since 1952.

He is chairman of the Chemistry Panel and has been consultant to the Cancer Chemotherapy National Service Center since 1955; member (since 1951) and chairman (since 1955) of the Scientific Advisory Committee of the Academy-Research Council's Prevention of Deterioration Center; member (since 1958) of the U. S. National Committee for the International Union of Pure and Applied Chemistry; and member (since 1953) and chairman (1956-1958) of the Committee on Nominations and Elections of the American Chemical Society.

In 1948, Dr. Elderfield received the Presidential Certificate of Merit; in 1952, Williams College bestowed upon him the honorary degree of Doctor of Sciences; and, in 1958, he

was selected National Lecturer for Sigma Xi.

He has carried on extensive research in the fields of natural products, specifically, cardiac drugs and alkaloids, on sugars, and on heterocyclic compounds. He was the discoverer of the antimalarial drug, primaquine. He is editor of the set of books entitled "Heterocyclic Compounds."

Olin Mathieson Metallurgical Research Center

A metallurgical research center for Olin Mathieson Chemical Corp. that combines laboratories and an integrated pilot production plant will be completed in New Haven, Conn., by mid-1959. The facility will cost approximately \$4,000,000.

The New Haven Metallurgical Labs. was created to provide research, development, and integrated pilot plant production facilities and services for the corporation's metals and nuclear fuel activities.

It will include a Metals Research Labs. to service the corporation's Metals Division, which produces Olin Aluminum and Western Brass. A Nuclear Fuel Research Labs. will service that area of the corporation's Energy Division, and do contract work for private industry and Government agencies.

Glidden Lecture Program

Continuation of a lecture program in chemistry at top universities in the United States and Canada was announced recently by Dr. William von Fischer, coordinator of research and development for The Glidden Co., Cleveland, Ohio.

Established in 1957 to stimulate a greater interest in chemistry and chemical engineering, the program, known as "The Glidden Company Lectures in Chemistry," has been so enthusiastically received that Glidden will continue this activity during the present academic year. Lectures will be sponsored at Johns Hopkins University, University of Illinois, University of Michigan, University of Minnesota, University of Florida, Case Institute of Technology, and the University of Toronto.

Scientific Translations Now Available at a Substantial Saving

The Custom Translations Club, a unique profit-sharing plan designed to furnish scientists in all fields with translations of pertinent material from Russian, Czechoslovakian, and Polish, has just been inaugurated by Consultants Custom Translations, Inc., 227 W. 17 St., New York 11, N. Y.

Full details about club participation are available upon request from Steven H. Smith, Manager.

Club members are entitled to a 10% royalty on resales of translations they order, and may also purchase other translations at a 50% reduction in price. Membership entails no obligation—there are no dues or fees, and a specified number of orders is not required.

Book Reviews

Modern Materials, Advances in Development and Applications, Vol. 1. Edited by Henry H. Hausner. Published by Academic Press, Inc., New York City and London, 1958. 402 pages; \$12.50.

This is the first of a series which eventually will cover recent developments in most of the important engineering materials. This volume discusses new developments and applications in the fields of eight materials, each of which is covered by a separate chapter written by an outstanding expert in the particular field: 1. Some New Developments in Wood, by Carl de Zeeuw; 2. Synthetic Rubbers for Special Service Conditions, by F. A. Bovey; 3. Fiber Materials, by T. D. Callinan; 4. High Voltage Insulation Papers, by Wm. A. Del Mar; 5. Special Glasses for Nuclear Engineering Applications, by N. J. Kreidl and J. R. Hensler; 6. Characteristic Properties of Modern Ceramics, by John H. Koenig and Edward J. Smoke; 7. Germanium and Silicon, by Gustav Szekely; 8. Zirconium, by G. L. Miller.

The volume is not a textbook. Its purpose is to present the latest authoritative information about the materials mentioned above, and it has been written primarily for the engineer with broad interests and for those who actually are engaged in industries using the subject materials. Each chapter contains an excellent, extensive bibliography of great value for those wishing to investigate the subject further.

The chapter on Wood is very detailed and would be of most value to those who have a fair knowledge of high polymer science.

The Synthetic Rubber chapter is excellently written and very complete. It does not require that the reader be mathematically trained, but treats the subject from the practical engineering viewpoint.

The Fiber Materials chapter devotes only five pages to all the organic fibers but takes thirty-

seven pages to discuss inorganic fibers including fibers of glass, ceramics, asbestos, silica, and metals. This information is very well presented.

The rather specialized chapters on High Voltage Insulation Papers and on Germanium and Silicon would be of particular interest mainly to workers in the electrical industry.

The chapters on Special Glasses and Zirconium would be of greatest value to those working in the nuclear energy field.

The chapter on Modern Ceramics is well balanced and should be of interest to technical and executive people in most engineering fields. The recent developments described cover new refractories, abrasives, cermets, dielectrics, ferroelectrics, piezoelectrics, semiconductors, thermistors, varistors, and ceramics for nuclear applications.

The price of the book appears high considering its physical size, but people in many different fields of interest will find it useful and a sound investment.

Henry S. Myers

Reports of the Fourth Soviet Conference on Electrochemistry. Published by Consultant's Bureau, Inc., New York City, 1958. 82 pages; \$12.00.

In 1956, Soviet scientists held their Fourth Conference on Electrochemistry. The published abstracts of their papers, released and translated by the Consultant's Bureau, give a fascinating and tantalizing glimpse into what is being done in Russia.

There are 121 abstracts organized into sections: 22 papers on "Electrochemical Kinetics and the Reaction Mechanism of Electrochemical Reduction"; 11 on "Mechanisms of Electrode Processes in Melts"; 8 on "Diffusion Kinetics"; 8 on "Mechanism of Oxidation Reactions"; 10 on "Passivity of Metals and Chemisorbed Layers"; 30 on "Electrodeposition of Metals"; 14 on "Chemical Sources of Current"; 9 on "Electrolysis in Chemical Industry"; and 9 on "Electrochemical Processes of Nonferrous Metallurgy"; an approximately equal division of basic and applied research. All papers apparently were based on experimental studies, rather than reviews or surveys.

These abstracts, unfortunately, give no details of the actual work, usually merely stating subject matter and some general conclusions, but it is obvious that the

articles themselves when released and translated will be of immense value. However, considerable information can be obtained by going through the abstracts and inferring certain details left unmentioned. The price of the abstracts is not high considering the limited market.

The publishers are making every effort to persuade the Soviet authorities to release the original papers. Meanwhile, a list of the various abstracts available will be furnished on request.

H. W. Salzberg

Announcements from Publishers

"Process Dynamics," Dynamic Behavior of the Production Process, by Donald P. Campbell. Published by John Wiley & Sons, Inc., New York City, 1958. XIX + 316 pages; \$10.50

This book translates process dynamic performance into mathematical form, showing its influence on process control system design. It is not intended for beginners. Knowledge of differential equations and principles of feedback is assumed.

"The Encyclopedia of Chemistry, Supplement," by George L. Clark and Gessner G. Hawley. Published by Reinhold Publishing Corp., New York City, 1958. 330 pages; \$10.00.

This consists of about 200 additions to the "Encyclopedia of Chemistry," published in 1957. The articles are condensed summaries of basic topics for those who are not chemists. Biographies of great chemists are included. No further supplements are to be issued.

"Modern Materials: Advances in Development and Applications," first volume of a new series. Edited by Henry H. Hausner, assisted by an Advisory Board. Published by Academic Press Inc., New York City, 1958. 402 pages; \$12.50.

"Modern Materials" is designed for use by the engineer, executive, research and development specialist, student, and all those who are concerned with the production, properties, and uses of natural and synthetic materials. Vol. 1 discusses a variety of materials and the recent developments in connection with them: zirconium and the semiconductors germanium and silicon; ceramic engineering materials and their increasingly wider applica-



Lepel
HIGH FREQUENCY
INDUCTION
HEATING
UNITS

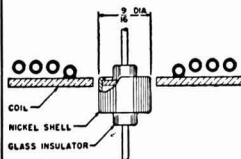
BRAZING
BOMBARDING
SOLDERING
MELTING
HARDENING
ANNEALING

The Lepel line of induction heating equipment represents the most advanced thought in the field of electronics as well as the most practical and efficient source of heat yet developed for industrial heating.

If you are interested in induction heating you are invited to send samples of the work with specifications. Our engineers will process and return the completed job with full data and recommendations without any cost or obligations.

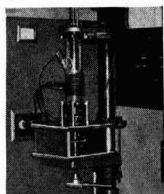
TYPICAL INDUCTION HEATING APPLICATIONS IN THE MANUFACTURE OF TRANSISTORS

SOLDERING TRANSISTOR ASSEMBLIES BY INDUCTION HEATING



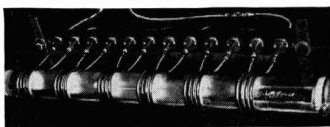
Concentrator-type coil creates high intensity, restricted heating at joint of nickel shell and tinned glass, thus causing solder to flow for permanent seal.

SINGLE CRYSTAL PULLER



General arrangement for pulling single crystals. Induction heating coil is shown surrounding quartz tube containing crucible with molten germanium in suitable atmosphere.

MULTIPLE ZONE REFINING



Induction heating apparatus used in zone refining. The six coils shown provide simultaneous molten zones in the ingot as it passes through the tube containing the protective atmosphere.

Electronic Tube Generators from 1 kw to 100 kw.
Spark Gap Converters from 2 kw to 30 kw.

WRITE FOR THE NEW LEPER CATALOG . . . 36 illustrated pages
packed with valuable information.



All Lepel equipment is certified to comply with the requirements of the Federal Communications Commission.

LEPEL HIGH FREQUENCY LABORATORIES, INC.

55th STREET and 37th AVENUE, WOODSIDE 77, NEW YORK CITY, N. Y.

tions; insulating papers for high voltages; glasses required to withstand strong irradiation in nuclear engineering; synthetic rubbers for special purposes; new uses of wood as a structural material; organic and inorganic fiber materials.

"Study, Standardization of Specifications for Insulated Cable," R. E. Barbieri, P. M. Costanzi, and B. J. Compton, RCA Service Co., Inc., for Wright Air Development Center, U. S. Air Force, Dec. 1957. Report PB 131805,* 244 pages; \$3.50.

"Rapid Determination of Polyacrylonitrile in Coatings by Infrared Absorption Spectrometry," M. L. Adams, Aberdeen Proving Ground, U. S. Army, Oct. 1957. Report PB 131539,* 16 pages; 50 cents.

"Rapid Detection of Phthalic Acid Isomers and Benzoic Acid in Alkyd Resins by Infrared Absorption Spectrometry," M. L. Adams, Aberdeen Proving Ground, U. S. Army, Oct. 1957. Report PB 131540,* 19 pages; 75 cents.

"Development of an Improved Corrosion Inhibitor for Water-Alcohol Solutions," D. B. Conklin, B. G. Peacock, and J. E. Cole, Wyandotte Chemicals Corp., for Wright Air Development Center, U. S. Air Force, July 1956. Report PB 131781,* 82 pages; \$2.25.

"P-M Junction Theory and the Junction Transistor," AEC Report SCR-21,* June 1958. 20 pages; 75 cents.

"Pressure Induced Metallic Transitions in Insulators," AEC Report UCRL-5210,* Nov. 1957. 7 pages; 50 cents.

"The Extraction of Protactinium from Solid Thorium Fluoride," AEC Report BNL-482,* Nov. 1954. 24 pages; \$1.00.

"Diffusion of Cerium and Zirconium in Molten Uranium," AEC Report NAA-SR-2628,* July 1958. 26 pages; 75 cents.

"Determination of Thorium in Uranium Ores and Feeds by Solvent Extraction Employing Thenoyltrifluoroacetone," AEC Report NLCO-742,* May 1958. 27 pages; \$1.00.

"A Review and Evaluation of Maintenance Concepts for Liquid Metal Fuel Reactors," AEC Report BAW-1047,* March 1958. 115 pages; \$3.00.

* Order from Office of Technical Services, U. S. Dept. of Commerce, Washington 25, D. C.

"Scientific Activities in Six State Governments." Available from Superintendent of Documents, U. S. Government Printing Office, Washington 25, D. C., at 40 cents a copy.

This summary report, recently released by the National Science Foundation, is based on studies of scientific activities in California, Connecticut, New Mexico, New York, North Carolina, and Wisconsin, selected as representative of major geographical regions, and of varying resources, physical size, and economic characteristics. The project was conducted by the Institute for Research in Social Science of the University of North Carolina, and this report analyzes expenditures of the states for the conduct of research and development as well as other related scientific activities for the fiscal year 1954.

International Powder Metallurgy Glossary

To assist the development of powder metallurgy in various countries of the world, the journal "Metal Powder Report" will include, as a special supplement to forthcoming issues, a glossary or list of definitions of all important terms used in powder metallurgy.

This glossary will be published in all the principal European, Asian, and African languages. It is being prepared, in each language, by a distinguished scientist or technologist in the country concerned.

"Metal Powder Report" is published monthly by Powder Metallurgy, Ltd., Berk House, Portman Square, London, W. 1, England. Vol. XIII commences with September 1958. The annual subscription is \$20.00.

"Soviet Research in Fused Salts—1956"

Complete English translations of 42 papers reporting on research in fused salts, which originally appeared in 1956 issues of various Soviet chemical journals, have been published as a convenient collection by Consultants Bureau, Inc., 227 W. 17th St., New York 11, N. Y. The price is \$40.00.

Part I of "Soviet Research in Fused Salts—1956" includes 23 phase diagram studies of binary, ternary, and quaternary reciprocal systems. This section may be purchased separately at \$30.00.

Part II contains 19 reports on the electrochemistry of aluminum and magnesium, corrosion, and theoretical aspects of fused salts re-

search, as well as 5 reports on thermodynamics and slags. It may be purchased separately at \$20.00.

Tables of contents listing the 42 reports are available without charge from the publisher, as are the tables of contents to the 125 reports included in "Soviet Research in Fused Salts (1949-1955)," which was released in 1956 and priced at \$150.00.

Catalogs List Reports of Titanium Research

Three "Catalogs of Technical Reports" for the field of titanium have been published by the Office of Technical Services, U. S. Dept. of Commerce, Washington 25, D. C., and are available at 10 cents each.

The CTR's list all reports of research into the metal, its alloys, carbides, and compounds, and barium titanate, available to the public from the OTS collection.

The catalogs are: CTR 349, "Titanium—Part 1: Titanium and Alloys," 1930-1958; CTR 350, "Titanium—Part 2: Titanium Carbides and Compounds," 1920-1958; and CTR 351, "Titanium—Part 3: Barium Titanate," 1946-1958.

Price List of AEC Reports

A new free list of Atomic Energy Commission unclassified research reports for sale by the Office of Technical Services, U. S. Dept. of Commerce, Washington 25, D. C., is available from OTS on request.

This cumulative listing of the more than 4000 AEC reports in the OTS collection includes new documents acquired since January 1958. To obtain the new list, request AEC Research Reports Price List No. 30.

Literature from Industry

Anodes, Plating Chemicals. A new 8-page, 2-color bulletin describing a complete line of anodes and plating chemicals is offered by Hanson-Van Winkle-Munning Co. Illustrated by photographs and line drawings are a wide variety of anodes, anode hooks, and anode bags. Details are set forth as to composition, shapes, and specific application. Specifications are given for round, flat, elliptical, and specially shaped anodes, including nickel, cadmium, brass and bronze, copper, zinc, and lead. Also described are the new Lo-Sludge Nickel Anodes recently developed in H-VW-M's electrochemical laboratory.

For copies, write Bulletin No. AC-111, Hanson-Van Winkle-Munning Co., Matawan, N. J.

Propionaldehyde. Applications of propionaldehyde in almost every segment of the chemical industry are discussed in a newly revised 12-page Technical Information sheet available from Union Carbide Chemicals Co., Div. of Union Carbide Corp., 30 E. 42 St., New York 17, N. Y.

Propionaldehyde is used in the resin, pharmaceutical, rubber chemical, perfume and flavor, and photographic chemicals industry as an intermediate. It also finds application as an additive in the electrolytic purification of zinc. These uses and other typical reactions are described and documented by 22 selected references to patents and periodical literature. The new bulletin also includes storage, handling, and shipping information, as well as physiological and physical properties of propionaldehyde. Vapor pressure and water solubility data are presented in graphical form.

Foamsil®. A 4-page folder describing its new insulating and refractory material, Foamsil, is available from the Pittsburgh Corning Corp. The folder contains background information on the unique new foamed silica material which is 99% pure fused silica and has a practical operating range of -450° to 2200°F. The material is unaffected by practically all commonly used acids and is unaffected by thermal shock. A list outlining the physical characteristics of the material, along with recommendations for its possible uses, is contained in the folder. Sizes and shapes available are also illustrated.

Copies can be obtained by requesting Booklet FS-1, Pittsburgh Corning Corp., One Gateway Center, Pittsburgh 22, Pa.

Cobalt. The Cobalt Information Center has available a data sheet on the metal cobalt. This new 5-page publication includes general information on the element, data on electrical and magnetic properties, mechanical properties, high-temperature properties, transformations, diffusion, solubilities of oxygen in cobalt, and hot hardness. Also included are data on 99.6% pure cobalt—ultimate tensile strength, elongation, reduction of area, elastic modulus vs. temperature, etc.

Requests for the new data sheet or for a complete listing of CIC

publications should be addressed on company letterhead to the Cobalt Information Center, c/o Battelle Memorial Institute, 505 King Ave., Columbus 1, Ohio. Those outside the Americas should write to the main office, Centre d'Information du Cobalt, 35, rue des Colonies, Brussels, Belgium.

"Hastelloy" Alloy B. An alloy that combines the advantages of excellent resistance to corrosion with good strength at high temperatures is the subject of a new 12-page booklet. Latest information on "Hastelloy" alloy B, one of a group of nickel-base alloys bearing this trade mark, has been consolidated in the recently published technical literature. The alloy was developed primarily to offer chemical processors excellent resistance to hydrochloric acid over a wide range of concentrations and temperatures. In addition, alloy B has become a valuable high-temperature material because it retains over two-thirds of its room temperature yield strength at 1600°F.

"Hastelloy" alloy B is a product of Haynes Stellite Co., Div. of Union Carbide Corp., Kokomo, Ind., from which copies of the booklet can be obtained.

"Hastelloy" Alloy D. Physical, chemical, and mechanical properties of "Hastelloy" alloy D, a cast nickel-base alloy that offers outstanding resistance to corrosion from sulfuric acid at all concentrations and temperatures, are presented in a new folder. Included is a chart on penetration rates in sulfuric acid.

"Hastelloy" alloy D is a product of Haynes Stellite Co., Div. of Union Carbide Corp., Kokomo, Ind., from which copies of the booklet can be obtained.

Mercury Arc Rectifier Transformers. Bulletin GEA-6845, 6 pages, provides detailed information on the construction features and function of mercury arc rectifier transformers used in electrochemical, transportation, and industrial applications. It includes photos, circuit diagrams, rating tables, and a listing of standard features and accessories. Available from General Electric Co., Schenectady 5, N. Y.

Anode Switchgear, Type AG-6. Bulletin GEA-6841, 6 pages, gives information on the function and application of General Electric's Anode Switchgear, Type AG-6—a protective component of mercury arc rectifier equipment when continuity of service for large and/or essential

d-c loads is necessary. It also includes construction features, circuit diagram, and photographs. Available from General Electric Co., Schenectady 5, N. Y.

New Products

Zone Refiner Purifies Organic Salts Automatically. Fisher Scientific Co. has designed an automatic, lab-bench zone refiner that chemists can use to literally "freeze out" high-purity reagents from run-of-the-bottle chemicals. The new Fisher Zone Refiner will be of greatest use for purifying the vast number of organic compounds that are difficult to refine by conventional methods. It will purify any material that melts between 50° and 300°C.

For information, ask for Bulletin FS-276, Fisher Scientific Co., 717 Forbes St., Pittsburgh 19, Pa.

Expanded Titanium Sheet for Use in Plating and Chemical Industries. Mallory-Sharon Metals Corp. recently announced the development of expanded titanium sheet for use in the plating and chemical industries. The expanded sheet will be available in gauges from 0.050 in. to 0.125 in. into ½ in. to 1½ in. diamonds, in standard 48 in. by 96 in. sheets. Expanded sheet will be available in unflattened or flattened mesh, with the flattened mesh being primarily for decorative purposes.

Mallory-Sharon technicians believe the new material will have wide applications in acid plating, in protection shields for immersion heating electrodes, and in acid dipping baskets. Chief advantages of the material are its extreme resistance to corrosion, and the fact that in plating operations the titanium itself does not draw any current.

Further information can be obtained by writing Mallory-Sharon Metals Corp., Niles, Ohio.

Nerofil. A family of specially processed carbon-based filteraids for basic caustic producers has been developed by Great Lakes Carbon Corp. for 'difficult' filtrations involving strongly alkaline or fluorated solutions.

The filtration of brine over and above ordinary clarification increases the efficiency of mercury cell operations such as the DeNora. Due to its low vanadium content, Nerofil has become the preferred filteraid for brine preparation.

Advertiser's Index

Enthone, Incorporated	Cover 4
Grace Electronic Chemicals, Inc.	22C
Great Lakes Carbon Corp., Electrode Division	Cover 2
Nerofil Division	25C
Lepel High Frequency Laboratories, Inc.	36C
Rowe Products Inc.	23C
E. H. Sargent & Company	ix
Stackpole Carbon Company	26C

Employment Situations

Please address replies to box shown, c/o The Electrochemical Society, Inc., 1860 Broadway, New York 23, N. Y.

Positions Wanted

Physical Chemist, Ph.D. 1958, desires research position in electrochemistry and/or solid state. Strong instrumentation background; research experience; publications; honor societies. Will consider position in New York City or Metropolitan New Jersey area only. *Reply to Box 365.*

Battery Chemist, 11 years' experience with manufacturers of automotive, stationary, and industrial lead-acid batteries. Thoroughly experienced in grid design and casting, oxide production, paste formulation, assembly, fast formation, and dry charging; development, quality control, and cost reduction. B.Sc. degree. Age 32. *Reply to Box 366.*

Position Available

Electrochemist for Basic Studies in Corrosion, position open in small laboratory in Virginia. Opportunity for solid-state physics approach or conventional electrochemical approach to aqueous corrosion. Position is such that either a strong individualist or a team man could be happy. Reply to Virginia Institute for Scientific Research, 2820 Grove Ave., Richmond, Va.

JOURNAL ELECTROCHEMICAL SOCIETY

Wanted to Buy.

Back sets, volumes, and issues of this JOURNAL and TRANSACTIONS.

Especially volumes 1, 3 and from volume 60 to date.

We pay good prices.

Buy also Technical and Scientific Periodicals.

E. O. ASHLEY, 27 E. 21 St., New York 10, N. Y.

THE SARGENT



Designed and Manufactured by
E. H. SARGENT & CO.

LABORATORY RECORDER

(Patents Pending)

An automatic, self-balancing potentiometric recorder which measures voltages or current and graphically records these variables as a function of time.

- **MULTI-RANGE—40 ranges.**
- **MULTI-SPEED—9 standard chart speeds with provision for optional 1-5 range multiplication or 5-1 range reduction.**
- **VOLTAGE OR CURRENT RECORDING—for measurement of voltage or current or any other variable which can be translated to voltage or current signals.**
- **FLEXIBILITY OF APPLICATION**
- **DESIGNED FOR BENCH OPERATION**

Style: Vertical strip chart recorder, designed for laboratory bench operation. Assembly of three individual, separable, and self contained units; viz., control panel assembly, amplifier and power supply chassis, and chart and pen drive chassis unit.

Automatic null balancing potentiometric system with standard cell standardization by panel control, conventional chopper-amplifier method with special Sargent high gain amplifier and high stability Sargent bridge power supply using combined or alternate dry cells and mercury cells. Use of the latter obviates need for standardization over very long periods.

Ranges: Multiple full scale ranges selected by panel range switch as follows: 1.25, 2.5, 5, 12.5, 25, 50, 125, 250, 500, 1250, 2500. All ranges are made direct reading as full scale deflection in millivolts, milliamperes, or microamperes by use of an associated units selector switch. All 33 scales provide true potentiometric measurement. An additional series of the same eleven ranges in terms of volts is provided by an additional selector switch position, this series using a divider input with an impedance of one megohm.

True potentiometric measurements are thus provided to a maximum of 2.5 volts, higher voltages only being measured through a divider.

Accuracy: 0.1% or 20 microvolts, whichever is greater.

Chart: Width, 250 mm; length, 120 feet. Ruling rational with all ranges on a decimal basis. Indexed for reference. Graduated steel scale provides for any necessary correction of calibration. Two-position writing plate, 15° or 40° from vertical.

Chart Drive: Forward drive recording, reverse drive re-

cording, magnetic brake eliminating coasting when stopped and free clutch position with separate provision for rapid non-synchronous drive.

Recording speeds of $\frac{1}{3}$, $\frac{1}{2}$, 1, $1\frac{1}{2}$, 2, $2\frac{3}{4}$, 4, 8, and 12 inches per minute, selected by interchange of two gears on end of chassis.

Free clutch or neutral drive at the rate of approximately 20 feet per minute in either direction for rapid scanning of recorded information, chart reroll, or chart positioning.

Recording either by automatic take-up on roll or with free end chart and tear off.

Synchronous switching outlet for automatic synchronization of external devices with recording.

Pen Speed: 1 second full scale. Other speeds can be provided on special order with change of motors.

Bridge: Special Sargent specification. Provision for coupled transmitting potentiometer for output to integrating circuits, etc.

Damping: Dynamics controlled with single panel knob adjustment of amplifier gain.

Dimensions: Width, 21½ inches; depth, 13 inches; height, 24 inches; weight, about 75 pounds.

S-72150 RECORDER — Potentiometric, Sargent Complete with two S-72165 chart rolls; two each S-72175 pens; red, blue and green; one S-72176 wet ink pen, input cable assembly; synchronous switch cable assembly; plastic dust cover; spare ring for take-up mechanism; spare pen drive cable assembly; and fuses. For operation from 115 volt, A.C. single phase, 60 cycle circuits..... **\$1725.00**

SARGENT

SCIENTIFIC LABORATORY INSTRUMENTS • APPARATUS • SUPPLIES • CHEMICALS

E. H. SARGENT & COMPANY, 4647 W. FOSTER, CHICAGO 30, ILLINOIS
DETROIT 4, MICH. • DALLAS 35, TEXAS • BIRMINGHAM 4, ALA. • SPRINGFIELD, N. J.

The Electrochemical Society

Patron Members

Aluminum Co. of Canada, Ltd.,
Montreal, Que., Canada
International Nickel Co., Inc.,
New York, N. Y.
Olin Mathieson Chemical Corp.,
Niagara Falls, N. Y.
Industrial Chemicals Div., Research
and Development Dept.
Union Carbide Corp.
Divisions:
Electro Metallurgical Co.,
New York, N. Y.
National Carbon Co., New York, N. Y.
Westinghouse Electric Corp., Pittsburgh, Pa.

Sustaining Members

Air Reduction Co., Inc.
New York, N. Y.
Ajax Electro Metallurgical Corp.,
Philadelphia, Pa.
Allied Chemical & Dye Corp.
General Chemical Div., Morristown, N. J.
Solvay Process Div., Syracuse, N. Y.
(3 memberships)
Alloy Steel Products Co., Inc., Linden, N. J.
Aluminum Co. of America,
New Kensington, Pa.
American Machine & Foundry Co.,
Raleigh, N. C.
American Metal Co., Ltd.,
New York, N. Y.
American Potash & Chemical Corp.,
Los Angeles, Calif. (2 memberships)
American Zinc Co. of Illinois,
East St. Louis, Ill.
American Zinc, Lead & Smelting Co.,
St. Louis, Mo.
American Zinc Oxide Co., Columbus, Ohio
M. Ames Chemical Works, Inc.,
Glens Falls, N. Y.
Auto City Plating Company Foundation,
Detroit, Mich.
Bart Manufacturing Co., Bellville, N. J.
Bell Telephone Laboratories, Inc.
New York, N. Y. (2 memberships)
Bethlehem Steel Co., Bethlehem, Pa.
(2 memberships)
Boeing Airplane Co., Seattle, Wash.
Burgess Battery Co., Freeport, Ill.
(4 memberships)

C & D Batteries, Inc., Conshohocken, Pa.
Canadian Industries Ltd., Montreal, Que.,
Canada
Carborundum Co., Niagara Falls, N. Y.
Catalyst Research Corp., Baltimore, Md.
Chrysler Corp., Detroit, Mich.
Ciba Pharmaceutical Products, Inc., Summit,
N. J.
Columbian Carbon Co., New York, N. Y.
Columbia-Southern Chemical Corp.,
Pittsburgh, Pa.
Consolidated Mining & Smelting Co. of
Canada, Ltd., Trail, B. C., Canada
(2 memberships)
Continental Can Co., Inc., Chicago, Ill.
Cooper Metallurgical Associates, Cleveland,
Ohio
Corning Glass Works, Corning, N. Y.
Crane Co., Chicago, Ill.
Diamond Alkali Co., Painesville, Ohio
(2 memberships)
Dow Chemical Co., Midland, Mich.
Wilbur B. Driver Co., Newark, N. J.
(2 memberships)
E. I. du Pont de Nemours & Co., Inc.,
Wilmington, Del.
Eagle-Picher Co., Chemical Div., Joplin, Mo.
Eastman Kodak Co., Rochester, N. Y.
Electric Auto-Lite Co., Toledo, Ohio
Electric Storage Battery Co.,
Philadelphia, Pa.
Englehard Industries, Inc., Newark, N. J.
(2 memberships)
The Eppley Laboratory, Inc., Newport, R. I.
(2 memberships)
Erie Resistor Corp., Erie, Pa.
Fairchild Semiconductor Corp., Palo Alto,
Calif.
Federal Telecommunication Laboratories,
Nutley, N. J.
Food Machinery & Chemical Corp.
Becco Chemical Div., Buffalo, N. Y.
Westvaco Chlor-Alkali Div., South
Charleston, W. Va.
Ford Motor Co., Dearborn, Mich.
General Electric Co., Schenectady, N. Y.
Chemistry & Chemical Engineering
Component, General Engineering
Laboratory
Chemistry Research Dept.

(Sustaining Members cont'd)

General Electric Co. (cont'd)

- Metallurgy & Ceramics Research Dept.
General Motors Corp.
Brown-Lipe-Chapin Div., Syracuse, N. Y.
(2 memberships)
Guide Lamp Div., Anderson, Ind.
Research Laboratories Div., Detroit, Mich.
General Transistor Corp., Jamaica, N. Y.
Gillette Safety Razor Co., Boston, Mass.
Gould-National Batteries, Inc., Depew, N. Y.
Grace Electronic Chemicals, Inc.,
Baltimore, Md.
Great Lakes Carbon Corp., New York, N. Y.
Hanson-Van Winkle-Munning Co.,
Matawan, N. J. (3 memberships)
Harshaw Chemical Co., Cleveland, Ohio
(2 memberships)
Hercules Powder Co., Wilmington, Del.
Hoffman Electronics Corp., Evanston, Ill.
Hooker Electrochemical Co., Niagara
Falls, N. Y. (3 memberships)
Houdaille-Hershey Corp., Detroit, Mich.
Hughes Aircraft Co., Culver City, Calif.
International Business Machines Corp.,
Poughkeepsie, N. Y.
International Minerals & Chemical
Corp., Chicago, Ill.
Jones & Laughlin Steel Corp.,
Pittsburgh, Pa.
K. W. Battery Co., Skokie, Ill.
Kaiser Aluminum & Chemical Corp.
Chemical Research Dept.,
Permanente, Calif.
Div. of Metallurgical Research,
Spokane, Wash.
Kennecott Copper Corp., New York, N. Y.
Keokuk Electro-Metals Co., Keokuk, Iowa
Libbey-Owens-Ford Glass Co., Toledo, Ohio
P. R. Mallory & Co., Indianapolis, Ind.
McGean Chemical Co., Cleveland, Ohio
Merck & Co., Inc., Rahway, N. J.
Metal & Thermit Corp., Detroit, Mich.
Metals and Controls Corp., Attleboro, Mass.
Minnesota Mining & Manufacturing Co.,
St. Paul, Minn.
Monsanto Chemical Co., St. Louis, Mo.
Motorola, Inc., Chicago, Ill.
National Cash Register Co., Dayton, Ohio
National Lead Co., New York, N. Y.
National Research Corp., Cambridge, Mass.
National Steel Corp., Weirton, W. Va.
Northern Electric Co., Montreal, Que.,
Canada
Norton Co., Worcester, Mass.
Olin Mathieson Chemical Corp.,
Niagara Falls, N. Y.
High Energy Fuels Organization
(2 memberships)
Pennsalt Chemicals Corp.,
Philadelphia, Pa.
Phelps Dodge Refining Corp., Maspeth, N. Y.
Philips Laboratories, Inc., Irvington-on-
Hudson, N. Y.
Pittsburgh Metallurgical Co., Inc.,
Niagara Falls, N. Y.
Poor & Co., Promat Div., Waukegan, Ill.
Potash Co. of America,
Carlsbad, N. Mex.
Radio Corp. of America, Harrison, N. J.
Ray-O-Vac Co., Madison, Wis.
Raytheon Manufacturing Co.,
Waltham, Mass.
Reynolds Metals Co., Richmond, Va.
(2 memberships)
Schering Foundation, Inc., Bloomfield, N. J.
Shawinigan Chemicals Ltd., Montreal, Que.,
Canada
Speer Carbon Co.
International Graphite & Electrode
Div., St. Marys, Pa. (2 memberships)
Sprague Electric Co., North Adams, Mass.
Stackpole Carbon Co., St. Marys, Pa.
(2 memberships)
Stauffer Chemical Co., Henderson, Nev.,
and New York, N. Y. (2 memberships)
Sumner Chemical Co., Div. of
Miles Laboratories, Inc., Elkhart, Ind.
Sylvania Electric Products Inc., Bayside,
N. Y. (2 memberships)
Sarkes Tarzian, Inc., Bloomington, Ind.
Tennessee Products & Chemical Corp.,
Nashville, Tenn.
Texas Instruments, Inc., Dallas, Texas
Titanium Metals Corp., of America,
Henderson, Nev.
Udylite Corp., Detroit, Mich.
(4 memberships)
Universal-Cyclops Steel Corp.,
Bridgeville, Pa.
Upjohn Co., Kalamazoo, Mich.
Victor Chemical Works, Chicago, Ill.
Wagner Brothers, Inc., Detroit, Mich.
Western Electric Co., Inc., Chicago, Ill.
Wyandotte Chemicals Corp.,
Wyandotte, Mich.
Yardney Electric Corp., New York, N. Y.

How to make rust-and-scale removal an exact science: For more than 20 years, Enthone has studied metal finishing problems and developed specialized solutions. Among the rust and scale removal compounds perfected by Enthone research and proved in the field, are the Alka-Deox[®] series of alkaline materials which electrolytically or non-electrolytically remove rust and scale from steel, cast or malleable iron; Enthol[®] 42, a solvent acid cleaner for steel, zinc, aluminum and other metals; and Actane[®] 70, a replacement for hydrofluoric acid as a dispersing agent in acid pickles to remove colloidal and siliceous films from metals. Write us about your special oxide removal problems. Chances are we have the answer in stock. Enthone, Inc., 442 Elm Street, New Haven 11, Connecticut.



ENTHONE, INC. IS A SUBSIDIARY OF AMERICAN SMELTING AND REFINING COMPANY

ENTHONE